DOCTOR OF PHILOSOPHY

Development and critical assessment of a holistic optimisation tool for automotive components

Gong, Shuai

Award date:
2018

Awarding institution:
Coventry University

Development and Critical Assessment of a Holistic Optimisation Tool for Automotive Components

By

Shuai Gong

January 2018

A thesis submitted in partial fulfilment of the University's requirements for the Degree of Doctor of Philosophy

Acknowledgement

This PhD thesis represents not only a four-year research work but also a lifetime memory. Within this special memory,

I would like to thank my enthusiastic supervisor Dr. Jesper Christensen who has taught me consciously or unconsciously. I really appreciate his tremendous academic support. It has always been an honour for me to be his PhD student.

I want to send my gratitude to Steve Poote who has been supported me all the time. I am grateful to him for the opportunity to teach the laboratory and tutorial sessions.

Special and sincere gratitude goes to Dr. Christophe Bastien, especially for sharing his incredible academic experience, and for being a dedicated mentor.

Special mention goes to Dr. Glenn Miles, Dr. Bartosz Nowak for helping me with the fantastic lab session. To Dr. Mohamed Laradi for sharing his PhD experience and guidance. And to Alexis Wilson and Maninder Sehmi for sharing great research ideas.

Finally, but not the least, I want to thank my great parents and my lovely wife who has been consistently support me. A very special gratitude to my unborn little daughter for not only giving my PhD a wonderful ending but also offering me a precious beginning as a Dad!

Abstract

Optimisation is key to the improvement of most engineering products. Although the concepts of optimisation date back thousands of years, Computer Aided Engineering (CAE) based optimisation has only been widely developed over the past twenty years or so. Most conventional optimisation algorithms focus on a single application with a single goal (objective); for example, minimising the mass of a vehicle crash structure, or maximising the profit margin of a specific product. Although these objectives are different in nature they relate to the same product; and most often also indirectly influence each other, making the individual optimisation “less efficient”. Multi-objective optimisation algorithms do exist; but multi-objective and multi-disciplinary algorithms are neither well developed nor well understood. The overarching research question for this PhD study is: How to optimise an engineering product from a holistic viewpoint? The ideology of holistic optimisation is to obtain the ideal product by determining the optimum “compromise” between a number of indirectly linked aspects, such as structural performance and manufacturing costs. The ultimate aim, and the original contribution to knowledge of this PhD is to create a holistic optimisation algorithm / tool able to cater for the above. This will include aspects such as material selection, manufacturing methods, structural performance, end of life attributes, life cycle assessment, product cost, CO_2 equivalence, etc. The approach is to utilise a parametric model to analyse and optimise the overall “performance” of the product. Two different approaches to holistic optimisation will be evaluated: parallel and sequential. The ideology of the parallel approach is to optimise the aspects independently of each other. The sequential approach optimises the aspects sequentially with varying priorities.

Abbreviations

AAT	All at A Time
ABC	Absolute Criterion
ACO	Ant Colony Optimisation
CAE	Computer Aided Engineering
COFV	Change of Objective Function Value
DMOP	Dynamic Multi-Objective Problem
EOL	End of Life
GA	Genetic Algorithm
GOFVC	Global Objective Function Value Change
GSV	Global Spread Values
GT	General Trends
HC	Hand-Calculations
HOS1	Holistic Optimisation Study 1
HOS2	Holistic Optimisation Study 2
ICE	Individual Criterion Evaluation
INC	Incremental Criterion
LCA	Life Cycle Assessment
LOFVC	Local Objective Function Value Change
LSR	Least Squares Regression
LSV	Local Spread Values
MII	Multi Inner Iterations
MAT	Materials
MOEA	Multi-Objective Evolutionary Algorithm
MOGA	Multi-Objective Genetic Algorithm
MOP	Multi-Objective Problem
MOOP	Multi-Objective Optimisation Problem
MSP	Mean Squares Percent
NPGA	Niche Pareto Genetic Algorithm

NSGA	Non - inferior Sorting Genetic Algorithm
OAT	One at A Time
OMS	Optimisation Module Sequence
PAES	Pareto Archives Evolutionary Strategy
PAR	Parallel Optimisation
PESA	Pareto Envelope Selection Algorithm
QFD	Quality Function Deployment
RLV	Relative Length of Vector
SEQ	Sequential Optimisation
SII	Single Inner Iteration
SM	STRUCTURAL Module
TAT	Two at A Time
TS	Tabu Search
TSP	Travel Salesman Problem
VEGA	Vector Evaluated Genetic Algorithms

Table of Figures

Table List

Contents

1 Introduction

In the past, most engineering products were produced to make profits without considering energy economy or environmental protection as a serious issue. Moreover, manufacturers always ensured that they had the most attractive products so that they could have the biggest share of the local or global market. However, the environmental impact caused by engineering products has drawn the attention of researchers and governments. Manufacturers have been asked to start to further optimise their products in terms of reducing their environmental impact. Manufacturers in the 21st century are asked to make sustainable products due to the worsening issue of global warming. Although engineers have developed products for decades, industries in the whole world are still facing several crucial problems that need to be solved as soon as possible (Zhang et al. 2007). Nowadays, optimisation is the key to improving most engineering products. Most conventional optimisation algorithms focus on a single application with a single goal (objective); for example, minimising the mass of a vehicle crash structure, or maximising the profit margin of a specific product. Although these objectives are different in nature, they relate to the same product and most often also indirectly influence each other, making individual optimisation 'less efficient'. Multi-objective optimisation algorithms do exist; but multi-objective and multi-disciplinary algorithms are neither well developed nor well understood. The overarching research question for this PhD study is: How to optimise an engineering product from a holistic viewpoint? The ideology of holistic optimisation is to obtain an ideal product by determining the optimum 'compromise' between a number of indirectly linked aspects, such as structural performance and manufacturing costs. The ultimate aim and the original contribution to knowledge of this PhD is to create a holistic optimisation algorithm / tool able to cater for the above. This will include aspects such as material selection, manufacturing methods, structural performance, end of life attributes, life cycle assessment, product cost and CO_2 equivalence. The approach is to utilise a parametric model to analyse / optimise the overall 'performance' of a product. Two different approaches to holistic optimisation will be evaluated: parallel and sequential. The ideology of the parallel approach is to optimise the aspects independently of each other and simultaneously. The sequential approach optimises the aspects sequentially, with varying priorities.

This thesis contains following chapters:

- Literature Review
- Methodology
- Holistic Optimisation Study 1 (HOS1) – Side Impact Beam
- Holistic Optimisation Study 2 (HOS2) – Lower Engine Mount
- Design of Experiments (DOE)
- Discussion
- Conclusion

There are two main sections in the literature review chapter. The first section studies the aspects of an engineering product such as material selection, manufacturing methods, structural performance, end of life attributes and cost. The objective of the first section is to understand the whole life of a product starting with its raw materials and ending with its disposal. Details such as procedures and techniques of each aspect are reviewed and studied in order to find out their general inputs and outputs. From the inputs and outputs, the relationships between aspects are found and further analysed in the methodology chapter. These new directly/ indirectly linked aspects will be used to create the parametric model to analyse/ optimise the overall 'performance' of the product.

The second section in chapter 2 reviews both classic and advanced techniques of multi-objective optimisation. The aim of this section is to understand how to handle multi-objective optimisations and the differences between multi-objective optimisation and holistic optimisation. The literature review provides a basic understanding of both the product aspects and multi-objective optimisation techniques for the holistic optimisation tool to be created in the third chapter.

The third chapter contains the methodology of holistic optimisation studies. In this chapter, aspects of the products studied in the literature review are further analysed with the Quality Function Deployment (QFD) method from the first section. The QFD is defined as a procedure to convert customers' requirements to engineering characteristics of a product. With the help of the QFD method, relationships between aspects become clearer and more accurate. Aspects of the product are further categorised into the following major areas such as material selection, structural performance, CO_2 footprint and transportation. The approach for holistic optimisation in the second section is to utilise a parametric model to analyse and optimise the overall 'performance' of the product. This parametric model contains three fundamental modules:

1. The STRUCTURAL module analyses and optimises the structural performance of the product.
2. The COST module analyses and optimises the cost of the product in aspects such as material, manufacture, transportation and EOL.
3. The CO2 module analyses and optimises the CO_2 footprint of the product in aspects such as processing raw materials, manufacturing the product, transportation and EOL.

All three modules are created with PowerShell which is a Windows based programme language. The STRUCTURAL module uses the existing optimisation solver, HyperMesh, to analyse and optimise the structural performance of the product's CAD model. The COST module and CO2 module have the same four phases: Material phase, Manufacture phase, Transportation phase and End of Life phase. These two modules analyse and optimise the cost and CO_2 footprint of the product in these four phases.

The last section of the methodology contains three main subsections which introduce the types of holistic optimisations, the design of the case study and the evaluation methods. In this research, there are two types of holistic optimisations – Sequential (SEQ) and Parallel (PAR). Each type of holistic optimisation consists of the three individual modules: STRUCTURAL, COST and CO2. According to the optimisation module sequences (OMS), there are 6 OMS for SEQ and 1 OMS for PAR. In order to find out how the iteration loops influence the results of the 7 OMS, two types of the iteration loops are applied to these 7 OMS: Single-Inner Iteration loop (SII) and Multi-Inner Iteration loops (MII). The case studies are designed to study the 'performance' of the 7 OMS. The case studies will look at varying 1 – 2 parameters at a time and extract the general trends from the evaluations. There are 33 case studies for each of the 7 OMS. Each case study contains a number of models based on the change of the input parameters – 203 models in total for 33 case studies in each OMS. Three evaluation methods are introduced in this section to evaluate the results of the 7 OMS: Individual Criterion Evaluation (ICE), Absolute Criterion (ABC) and INC (Incremental Criterion). The ICE method will assess the summation of the 'performance' of each individual module. The ABC method will assess the

‘Global Distance’ between each result and the absolute optimum solution. The INC method will assess the ‘Local Distance’ between the results of the initial iteration and the final iteration. Both ‘Global Distance’ and ‘Local Distance’ indicate the idea of the magnitude of a vector.

Chapters 4 and 5 contain two different Holistic Optimisation Studies (HOS). In Chapter 4, a side impact beam of a vehicle will be studied. A lower engine mount will be investigated in Chapter 5. The basic framework of both chapters will be the same, beginning by introducing the setup of each HOS, respectively. The optimisation results will be evaluated by three methods: Individual Criterion Evaluation (ICE), Absolute Criterion (ABC) and INC (Incremental Criterion). The aim of the evaluation is to find out the general trends of the results in order to analyse the performance of each of the 7 OMS. Following the evaluations, a detailed analysis is applied to the results in each of the three individual modules based on two perspectives: Objective function values and Sensitivity. The purpose of this further analysis is to find out how the three individual modules/ input parameter(s) influence the performance of the holistic optimisation.

Chapter 6 contains the Design of Experiments (DOE). A DOE method is to find out the relationship between input variables/ parameters influencing the process and the output of the process. The main idea of this chapter is to use a DOE method to get a response surface of the results by allowing ‘all’ parameters at a time to change. This is different from what has been done in Chapters 4 and 5, as the analysis of the results in those two chapters are based on another viewpoint. The application of the DOE for the two HOS also will be introduced in this chapter. The purpose of is to give readers a general idea of determining the “best” Optimisation Module Sequence (OMS) with the DOE based optimisation.

The final chapter contains a comprehensive conclusion for the overall research.

2 Literature Review

There are two main sections in this chapter. The first section studies the aspects of an engineering product such as material selection, manufacturing methods, structural performance, end of life attributes and cost. The objective of the first section is to understand the whole life of a product starting with its raw materials and ending with its disposal. Details such as procedures and techniques of each aspect are reviewed and studied in order to find out their general inputs and outputs. The second section of this chapter is to review both classic and advanced techniques of multi-objective optimisation. The aim of this section is to understand how to handle multi-objective optimisations and the differences between multi-objective optimisation and holistic optimisation. The literature review provides a basic understanding of both the product aspects and the multi-objective optimisation techniques for the holistic optimisation tool to be created.

2.1 Literature review of product aspects

The core of this research is to optimise an engineering product from a holistic viewpoint. The first step is to study major aspects of an engineering product such as life cycle assessment, end-of-life, structural optimisation and materials. These aspects are simply illustrated with a mind map in Figure 1. In this research, an automotive product is studied as the initial case. The aim of this literature review is to study major aspects of engineering products and determine their inputs and outputs for further optimisation. The following sections of the literature review will focus on major aspects of automobiles. The Material Selection section reviews the conventional materials used for automobiles. The Manufacturing Methods section reviews methods such as cast components, frame-joining and painting. The Structural Performance section reviews structural optimisation methods, mainly focusing on CAE based on optimisations such as size, shape and topology. The End of Life section reviews the potential disposal methods of end-of-life engineering products. The Life Cycle Assessment (LCA) section reviews the procedures of LCA and the physical product's life cycle. The Disassembly section reviews methods to disassemble engineering products when they reach the end of their lives. The cost section reviews the methods of calculating the product's costs in its life cycle, such as material cost, manufacturing cost and transportation cost.

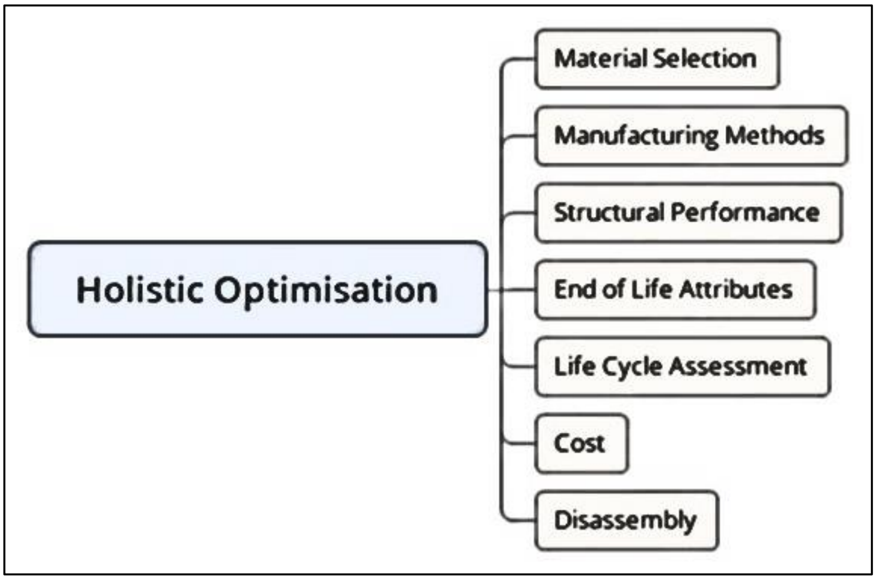

Figure 1: Mind Map of the Research

2.1.1 Material Selection

Each of the materials has unique mechanical properties such as yield strength and tensile elasticity (i.e. Young's Modulus) (Sakundarini et al. 2013). Therefore, product designers should understand the properties of the materials that are required in their products.

In automotive design, materials can be categorised for car bodies, engine components, powertrain components, chassis and the future direction of automotive materials (Cantor et al. 2007). This research will mainly focus on materials for automotive bodies. Table 1 outlines the history of automotive body materials (Cantor et al. 2007):

Table 1: History of materials for automotive bodies

Time	Developments	Comments/ Reasons
The 1950s and 1960s	Technologies of mass production. Deep drawing steel sheets (the 1950s). Anti-corrosive steel sheets (the 1960s).	Require more vehicles. Require high performance and reliability.
The 1970s and 1980s	Technology of low fuel consumption---high-strength steel sheets.	Due to two oil crises.
1990s	Technologies of automotive weight reduction---aluminium alloy sheets.	Safety and environmental issues.

Based on research by Tempelman (2011) and books by Davies (2003) and Cantor et al. (2007), the material candidates used for automotive bodies are listed:

- Steel
- Aluminium
- Magnesium
- Polymers
- Composites

The advantages and disadvantages of these materials are outlined in Table 2:

Table 2: Advantages and disadvantages of materials used for automotive bodies (Davies 2003)

<table>
<tr><th colspan="3">Materials</th><th>Advantages</th><th>Disadvantages</th></tr>
<tr><td colspan="3">Steel</td><td>• Low cost
• Corrosion resistance if coated with zinc
• Easy to form
• Easy to join
• Recyclable
• Energy absorption
• Consistency of supply</td><td>• High density
• Corrosion without coating</td></tr>
<tr><td colspan="3">Aluminium</td><td>• Low density
• Corrosion resistance
• Recyclable
• Strong supply base</td><td>• High cost
• Formability is poorer than that of steel
• Harder to be welded than steel</td></tr>
<tr><td colspan="3">Magnesium</td><td>• Low density
• Thin cast is feasible
• Possible to integrate components in casting</td><td>• Casting only
• High cost</td></tr>
<tr><td rowspan="3">Polymers</td><td colspan="2">Thermosets</td><td>• Low sensitivity to temperature
• Higher scratch resistant than thermoplastics</td><td>• Low toughness
• Low strain at fracture
• Difficult to be recycled</td></tr>
<tr><td rowspan="2">Thermoplastics</td><td>Amorphous</td><td>• Relatively dimensionally stable
• Low mould shrinkage</td><td>• Poor wear abrasion
• Poor fatigue resistance</td></tr>
<tr><td>Crystalline varieties</td><td>• Good wear resistance
• Good fatigue resistance</td><td>• Difficult to adhesive bond
• High creep</td></tr>
<tr><td colspan="3">Composites</td><td>• Low density
• Good strength to weight ratio
• Properties can be potentially controlled</td><td>• High cost
• Difficult to recycle</td></tr>
</table>

Selecting material candidates based on their advantages and disadvantages is essential for designers. However, the automotive materials should also be selected by considering sustainability, recyclability, lightweight, manufacturability and end-of-life disposal (Tempelman 2011; Sakundarini et al. 2013; Mayyas 2013). Moreover, properties (mechanical and physical) and cost should be considered during the design stage (Davies 2003). Information in Figure 2 gives designers a basic idea of the selection criteria to choose materials that are used in automotive body structure.

Material	Design parameters					Ease of manufacturing* ('process chain')			Environmental** 'friendliness'		Cost
Criteria	YS MPa	UTS MPa	A_{80} min%	E.Mod GPa	D g/cc	Forming	Joining	Paint	CO_2 + emissions	Disposal (ELV)	Forming steel = 1
1. Forming grade steel EN 10130 DCO4 + Z	140 min	270 min	40	210	7.87	8	9	9	7	9	1.0
2. HSS EN 10292 H300YD + Z	300 min	400 min	26	210	7.87	6	8	9	8	8.5	1.1
3. UHSS – martensitic	1050–1250	1350–1550	5	210	7.87	4	7	9	8	8.5	1.5
4. Aluminium 5xxx	110 min	240 min	23	69	2.69	6	5	8	9	9	4.0
5. Aluminium 6xxx	120 min	250 min	24	69	2.69	6	5	8	9	9	5.0
6. Magnesium sheet	160 min	240 min	7	45	1.75	4	4	7	9.5	6	4.0
7. Titanium sheet	880 min	924 min	5	110	4.50	6	5	7	9	6	60.0
8. GRP	950	400–1800	<2.0	40	1.95	8	7	8	8	5	8.0
9. Carbon fibre composite	1100	1200–2250	<2.0	120–250	1.60–1.90	8	7	8	9	5	50.0+

*Based on range 1 = difficult to process, 10 = few production problems
**Ease with which prevailing legislation can be met: 10 = without difficulty, 1 = extensive development required

Figure 2: Selection criteria to choose materials (Davies 2003)

According to the reviews, the criteria used in the selection of materials can be further summarised:

- Physical properties of materials
- Mechanical properties of materials
- Recyclability of materials
- Manufacturability of materials
- Life cycle assessment
- End-of-life disposal
- CO2 emissions
- Cost

2.1.2 Manufacturing Methods

Knowledge of manufacturing is necessary for optimising a vehicle, as it provides the idea of manufacturability. Manufacturability will affect the cost, shape, ability to join and functionality of a product (Omar 2011). In other words, it tells designers whether their designs can be manufactured or not.

Manufacturing systems and processes are simply reviewed in this section. Omar (2011) stated that automotive manufacturing activities are normally analysed at manufacturing system and process levels. Moreover, there are three aspects normally studied at the manufacturing system level:

- The production line
    1. Machinery
    2. Material handling equipment
    3. Labour resources
- The transformational aspect
    1. Convert raw materials into semi-finished or finished products
    2. Include casting, stamping, welding, painting, etc.
- The procedural aspect

The procedure aspect can also be divided into two different levels:

- The strategic level
- The operational level

The volume, type and operating conditions of products will be decided at the strategic level. The operational level includes activities such as production planning, process planning, scheduling, implementation and control.

Automotive manufacturing was simply categorised Omar (2011) and Cantor et al. (2007):

- Processes of Stamping and Forming
- Processes of Joining and Welding
- Processes of Casting
- Processes of Painting
- Final Assembly

2.1.2.1 Processes of stamping and forming

Formability is a very important factor that can affect a final vehicle's shell shape, its performance and its geometry (Omar 2011). Stamping is defined as a process that transforms a sheet metal blank into a useful product (Omar 2011; Mallick 2010). A stamping die is used for forming the sheet metal by applying stresses beyond the yield strength of the metal (Groover & Mikell 1939). The challenges of this process are its high costs and time-consumption.

2.1.2.2 Processes of joining and welding

Tang (2010) stated that the body-in-white assembly was one of the most important manufacturing operations of automotive manufacturing. Its basis is to join the formed sheet metals. Joining was defined as one of the major issues of design and manufacturing (Mallick 2010). The developments of joining can also reduce the cost of automotive manufacturing and improve sustainability. However, the developed joining methods still have challenges due to new materials being applied to automobiles (Cantor et al. 2007).

2.1.2.3 Processes of casting

According to Cantor et al. (2007), cast iron still plays an important role in the foundry sector although its share of the market has started to decline. Aluminium has started to take the place of iron as many manufacturers have developed aluminium vehicles. Research has pointed out the advantages of the casting processes (Cantor et al. 2007; Mallick 2010):

- Design flexibility
- Reduce the number of components
- Reduce the cost of assembly
- Reduce the number of equipment

The disadvantages are also outlined below by Cantor et al. (2007):

- Large cast factor (as large as 10)
- Filling issue of casting
- Issue of reliability (porosity)
- High scrap rates

2.1.2.4 Processes of Painting

Omar (2011) stated that painting is not just a process to make the final look of the vehicle but also improves resistance to corrosion. The basic processes are outlined below (Omar 2011):

- Immersion coating processes
- Paint curing process
- Under-body Sealant, PVC and Wax Applications
- Painting spray booth operations

2.1.2.5 Final assembly

Final assembly is very straight forward and demonstrates that the interior and exterior components are assembled. The basics of final assembly are outlined (Omar 2011):

- Installation of the trim assembly
- Installation of the chassis
- Final assembly and test area

Based on the review of manufacturing systems and processes, the technologies applied in these processes are outlined in Table 3 (Omar 2011; Cantor et al. 2007; Mallick 2010; Tang 2010):

Table 3: Manufacturing Technologies

Forming	**Cast**
• Sheet metal forming processes 1) Stamping 2) Sheet hydroforming 3) Superplastic forming • Bulk metal forming processes 1) Forging 2) Extrusion • Promising metal forming processes for automotive applications 1) Warm forming 2) Tube hydroforming 3) Electromagnetic forming	• Sand casting • Lost foam casting • High-pressure die casting • Low-pressure casting systems • Gravity permanent mould systems • Squeeze casting • Semi-solid casting systems
Joining	**Painting**
• Friction stir welding • Laser welding • Structural adhesive • Resistance Spot Welding • Gas Metal Arc Welding • Mechanical joining and bonding • Self-Piercing Riveting • Clinching • Bonding	• Spray paint • Waterborne paint • Powder coating

The general manufacturing methods have been reviewed in this subsection. The next subsection will simply go through the structural performance of a product; and how to optimise the structure of the product.

2.1.3 Structural Performance

According to Browne (2013), the earliest structural optimisation was studied by Michell (1904). Structural optimisation has been studied for more than a century since then (Balling et al. 2006). Based on the review of research done on structural optimisation, its history is outlined in Table 4 (Browne, 2013):

Table 4: History of structural optimisation

Year	Researcher	Work
1965	R. L. Fox and L. A. Schmit	Use FE methods with computers
1985	M. Save, W. Prager and W. H. Warner	Optimality Criteria
1989	M. P. Bendsøe	Optimal shape design
1904	A. G. M. Michell	Derived formula for structural optimisation
2004	M. Burger, B. Hackl and W. Ring	Scheme for hole insertion with level-set approach
2010	X. Qi, S. Tielin and Y. W. Michael	Minimise the frequency of a structure with a level-set method
2010	V. J. Challis	MATLAB code for topology optimisation with level-set approach
2010	P. Wei, M. Y. Wang and X. Xing	Optimise structural analysis with LEVEL-SET
2011	P. Dunning	Level-set based on topology optimisation

Structural optimisation normally consists of three main sub-problems (Balling et al. 2006): the size optimisation, the shape optimisation and the topology optimisation. Typically, the aim of size optimisation is to optimise the thickness distribution of for example, the truss structure, so as to either minimise or maximise the physical quantities such as deflection or peak stress (Bendsøe 2003). The design variables in size optimisation have limitations due to the cross-section area and properties of structural members (Balling et al. 2006). Differing from the goal of size optimisation, shape optimisation is used to achieve an optimal shape of the domain of the design model. For example, the coordinates of joints on a skeletal structure can be defined as this. Moreover, the domain is also the design variable of the shape optimisation (Bendsøe 2003; Balling et al. 2006). The purpose of topology optimisation is to find out the optimum layout of the design model within a given region (Bendsøe 2003). For example, the topology optimisation may remove some members of the structure and set up new locations for the other members and keep the connectivity of the domain.

According to Balling et al. (2006), genetic algorithms can handle continuous and discrete variables. Therefore, they are quite popular among researchers working in the area of structural optimisation. Literatures using genetic algorithms to optimise structures are outlined below:

Table 5: Structural optimisation using genetic algorithms

Researchers and year	**Research area with genetic algorithms**
• D. E Goldberg; M. P. Samtani (1986) • C. Y Lin; P. Hajela (1992) • S. Rajeev; C. Krishnamoorthy (1992) • M. Ohsaki (1995) • S. Wu; P. Chow (1995)	Optimise size with fixed shape and topology
• S. Wu; P. Chow (1995) • C. K. Soh; J. Yang (1996)	Optimise size and shape with fixed topology
• P. Hajela; E. Lee; C. Lin (1993) • J. Sakamoto; J. Oda (eds.) (1993)	Optimise size and topology with fixed shape
• D. E. Grierson; W. H. Pak (1993) • S. D. Rajan (1995) • S. M. Shrestha; J. Ghaboussi (1998)	Optimise both size, shape and topology

The inputs and outputs of size, shape and topology optimisation are summarised in Table 6. Characteristics of optimisations can be visualised using CAD models. The optimised CAD model can also be used in the manufacturing process.

Table 6: Inputs and outputs of structural optimisations

	Inputs	**Outputs**
Size optimisation	• Algorithms • Mesh generation • Definition of loads • Boundary conditions • Thickness variable (mainly) • Setup of optimisation	• Interpretation of results • CAD model • Optimised thickness of the design model
Shape optimisation	• Algorithms • Mesh generation • Definition of loads • Boundary conditions • Shape variable (mainly) • Setup of optimisation	• Interpretation of results • CAD model • Optimised distribution of shape based reinforcements
Topology optimisation	• Algorithms • Mesh generation • Definition of loads • Boundary conditions • Density variable (mainly) • Setup of optimisation	• Interpretation of results • CAD model • Ideal layout of materials

2.1.4 End-of-life Attributes

According to the research of Mat Saman and Blount (2006), issues of environment and automotive sustainability have become a global concern due to there being a great number of vehicles in the world. Environmental burdens and the disposal of end-of-life vehicles are related (Konz, 2009). End-of-life vehicles, known as the ELVs, are defined in two groups. One group represents vehicles that normally reach the end of their useful life and are going to be disposed of; another represents vehicles that accidentally reach their end-of-life but have some parts that can be reused directly (Mat Saman & Blount, 2006). Traditionally, these kinds of non-functioning vehicles will have a common procedure to their end-of-life (Konz, 2009):

- Valuable components removed by dismantlers
- Remaining parts will be delivered to the shredder and milled into chunks

Lee et al. (2001) stated that there are many choices for dealing with ELVs such as reuse, remanufacturing, recycling and landfill. When ELVs are reused, remanufactured and recycled, a process is shown, defined by Mathieux et al. (2008) as recoverability. Gerrard and Kandlikar (2007) illustrated the recovery hierarchy with Figure 3. Amelia et al. (2009) also agreed with Gerrard and Kandlikar (2007) that reuse is the priority option in recovery. Remanufacturing, in the second hierarchy, happens when there is no option for the ELVs to be directly reused. In this case, the ELVs or their components will need some additional procedures to work on either their original or some other pattern or form (Go et al. 2011). Östlin et al. (2009) defined reprocessing or upgrading a product in an industrial process as remanufacturing. The purpose of remanufacturing is to provide a second life for the product instead of incinerating it (Zwolinski et al. 2006). Recycling, described in the research of Lambert and Gupta (2005), is defined as a process that extracts the material from its original forms and recreates it as a brand-new product. Energy recovery is the last stage to squeeze useful parts from the waste before dumping it in landfill (Mat Saman and Blount, 2006).

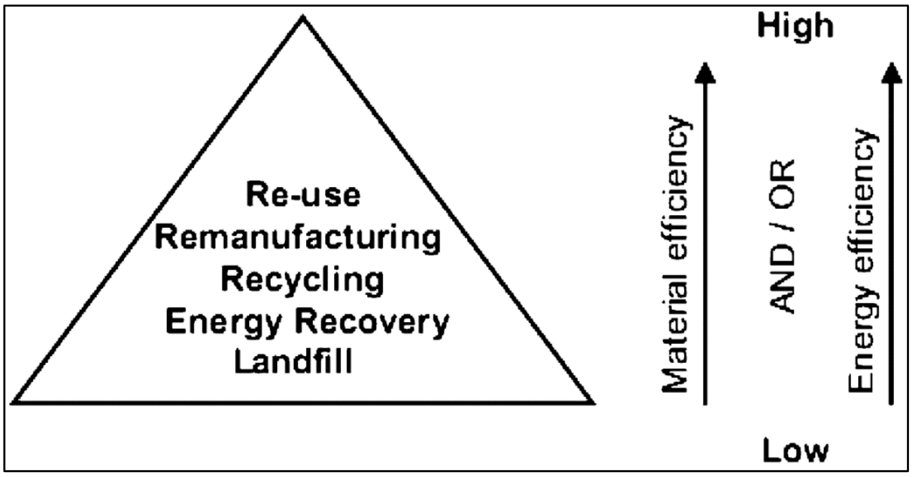

Figure 3: The recovery stages and priority (Gerrard & Kandlikar, 2007)

Lee et al. (2001) stated that choosing an end-of-life option depends on what kind of objective was required: minimise the impact on the environment or maximise the profit. They also provided some definitions of the EOL options:

- The EOL product or component can be reused in two ways: directly used or indirectly used.
- Components with 4Rs (retaining serviceable, replaceable, reworked and refurbishing usable) can be remanufactured.
- Recycling (primary) demonstrates that materials can still be used in the same way after reprocessing, or as a high-level product.
- Recycling (secondary) demonstrates that materials can only be used as a 'low' value product after reprocessing.
- Energy recovery can be used, for example incinerating the end-of-life product to produce heat or electricity
- The waste material will be put into landfill when there are no more options for recovery. It should be the last choice for an EOL product due to damage to the environment.
- Materials such as toxic materials that cannot normally be dealt with require expert methods.

A guideline was made by Lee et al. (2001) based on the component level. It is used to provide appropriate EOL options for the components.

Table 7: The guidelines for selecting EOL options for components (Lee et al., 2001)

Materials for the product	Recommended End-of-life options	Comments or alternative options
Metal without alloys	Primary recycling	The mechanical properties are not changed
Metal with alloys	Secondary recycling or landfill	The alloys can affect the mechanical properties of the major material
Polymeric	Primary recycling	• Secondary recycling • Incineration
Ceramic	Secondary recycling or landfill	
Elastomer or composite	• Secondary recycling • incineration	landfill
Toxic or hazardous materials	Special Approach	

There are no decisions made for components to be reused or remanufactured in the guidelines (Table 7), as the manufacturing processes and conditions of the end-of-life components are unpredictable. Therefore, human intervention is required to make the decision to reuse or remanufacture (Lee et al. 2001).

Inputs and outputs according to the review of ELVs are outlined in Table 8:

Table 8: Inputs and outputs of end-of-life vehicles

Inputs	End-of-life options	Outputs
• End-of-life Products • Energy • Cost • Other resources	• Disassembly • Cleaning or Refurbishment • Remanufacturing • Recovery • Reassembly • Recycle/Waste management	• New Products • Profits/ Costs • Export • Wastes • Other releases

Automotive designers who consider ELVs can provide a safe and efficient way to recycle, reuse or remanufacture the components (Mat Saman & Blount, 2008). Based on the current environmental issues caused by automobiles, more legislation or directives could be set to require or even force the manufacturers to consider ELVs. Therefore, it is necessary to consider the concept of ELVs in the optimisation design of automobiles.

2.1.5 Life Cycle Assessment

According to Pennington et al. (2004) and Sundin (2004), the definition of life cycle assessment is described as an approach used to explain the impact on the environment associated with the complete life cycle of a product. A definition of life cycle assessment based on ISO 14040 (Anon. 2006) is described as a methodology used in a manufacturing process or production that can evaluate the state of the environment. The full life cycle that represents the start-to-end process of products will be considered in the assessment. Henrikke Baumann and Anne-Marie Tillman (2004) described the life cycle of a product as a process starting with the extraction of its raw materials and ending with its 'grave'. They demonstrated their definition of LCA with the figure displayed below.

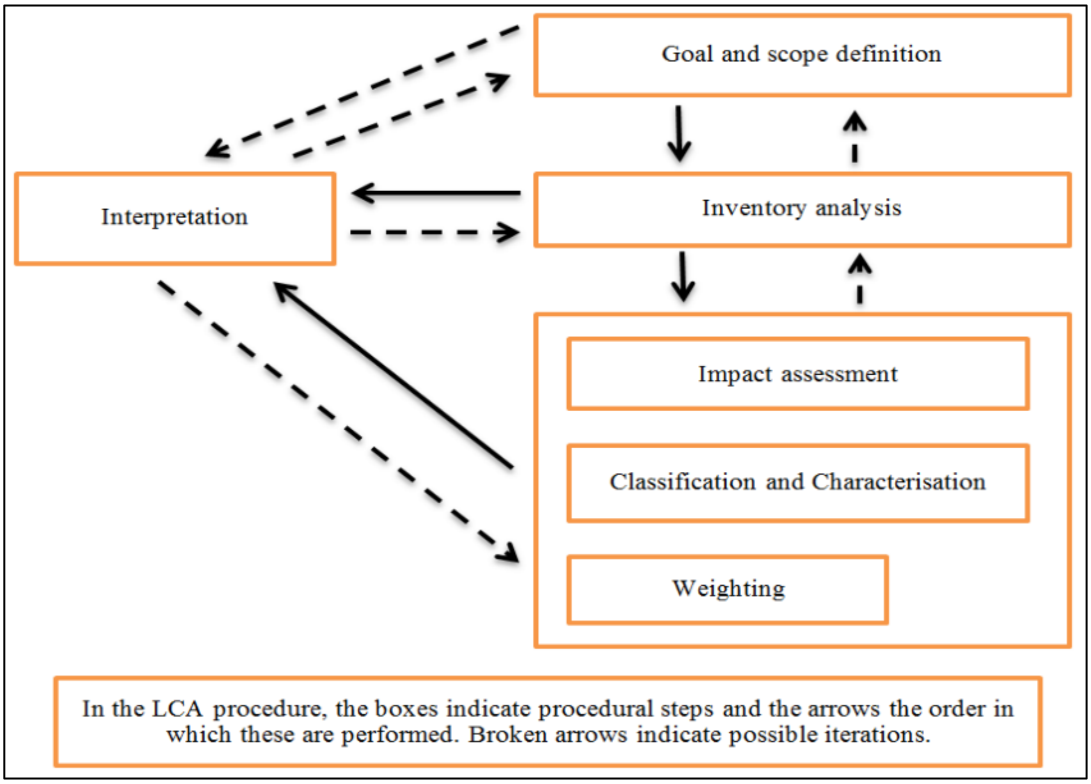

Figure 4: The LCA procedure (Baumann & Tillman, 2004)

Sundin (2004) stated that there are four stages in LCA: the use of raw materials, manufacturing products, actual application and disposal. All stages are illustrated in Figure 5. However, there is another stage, that of transportation as stated by Ashby (2009). At the use stage, the energy can be treated as a measurement of the environmental burden.

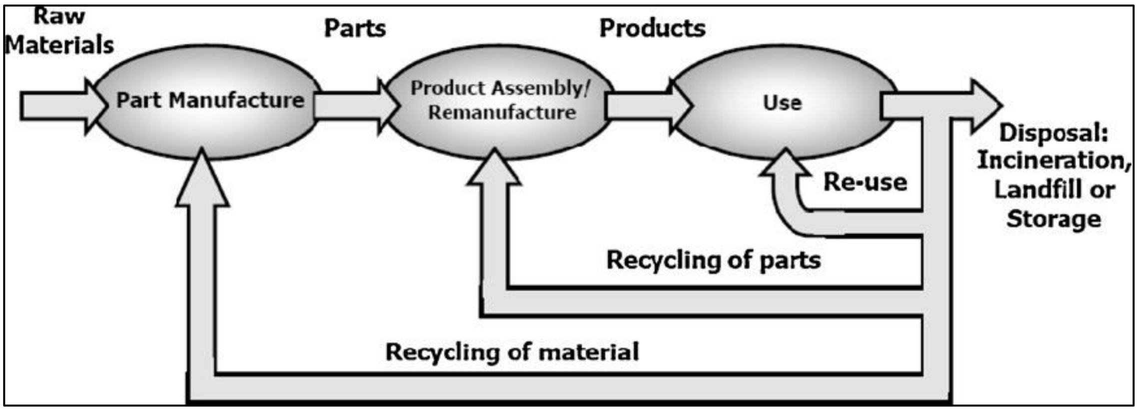

Figure 5: The physical product life cycle (Sundin, 2004)

LCA was described as a very important tool in the ISO 14000 series (Koffler et al. 2008). According to Pennington et al. (2004) and Koffler et al. (2008), the study of the life cycle assessment typically consists of four phases:

- The phase of aim and scope
- The phase of record analysis
- The phase of environmental impact evaluation
- The phase of interpretation

The aim and scope phase of the LCA study must clearly and consistently define the purpose, motivation, procedures and functional units etc., of the intended application (Koffler et al. 2008; Baumann & Tillman 2004). The second phase of LCA is based on the first phase and focuses on the data collection. Typically, bar charts will be used to present the results of the inventory analysis. The third phase of LCA, also known as the life cycle impact assessment, is used to analyse the results of both phase one and phase two, as so to evaluate the environmental impact. In the interpretation phase, the raw results from the previous phases are refined. Based on the refined results, the last phase can then reach a conclusion or make recommendations (Baumann & Tillman 2004).

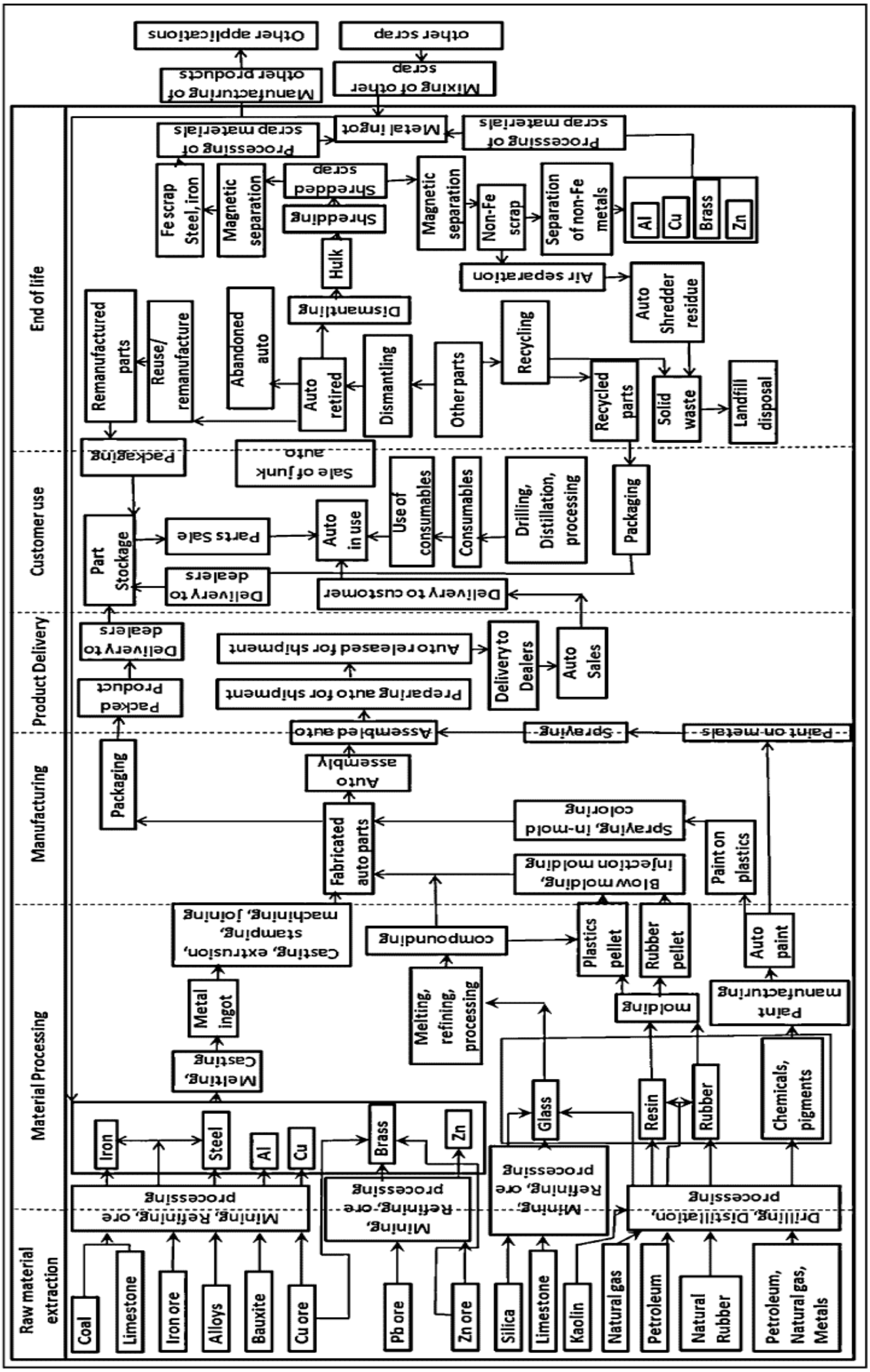

Figure 6: Automobiles analysed with LCA (Mildenberger & Khare, 2000)

Figure 6 shows the details of automobiles analysed with LCA from its raw materials to its end-of-life. In this figure, proper materials were extracted from raw materials and refined to be manufactured. Components of products were manufactured and assembled in the manufacturing process. The full assembled products were on sale to customers for use. After their useful life, products were sent to the EOL scenarios. This is the ideal life cycle of a vehicle. However, the challenges of using LCA are also illustrated in Figure 6. Omar (2011) summarised that the variety and variations of materials, durations, processing methods and ways of disposal could increase the difficulty of applying LCA to vehicles. Moreover, the range of the automotive life cycle (vehicle degradation) in different countries can affect the implementation of LCA. According to research in 2000 (Mildenberger & Khar, 2000), the total lifetime of vehicles in developing countries is about 45 years while the number in developed countries is 25 to 35 years.

Based on the review of LCA, the inputs and outputs are outlined in Table 9 below:

Table 9: Inputs and outputs of the LCA (Mallick 2010: 311)

Inputs		**Outputs**
• Raw Material • Energy • Water • Other resources	• Raw material acquisition • Material manufacture • Product Fabrication • Filling/ packaging/ distribution • Use/ reuse/ maintenance • Recycle/ Waste Management	• Atmospheric emissions • Waterborne waste • Solid wastes • Co-products/ By-products • Other releases

As the concern about environmental impact increases, the application of life cycle assessment to product development becomes popular. Based on the literature review it can be found that researchers have spent a great amount of time on LCA. Researchers have also proposed some LCA-based approaches that will be introduced in the methodology chapter. Baumann and Tillman (2004) even stated that the LCA based approaches could bring a holistic environmental perspective to the product design. Therefore, the life cycle assessment is an important tool for achieving the sustainability of vehicle design and contributing to holistic optimisation in this research.

2.1.6 Disassembly

In the past, automobile design was mainly developed for functionality, cost and manufacturability but rarely with respect to the environment (Ilgin and Gupta, 2010). Today, the impact on the environment caused by the disposal of vehicles is the major issue that all automotive manufacturers in the world are facing (Nunes and Bennett, 2008). Tseng et al. (2008) stated that reducing the impact on the environment and increasing the use of resources are very important for designers to keep in mind. Many countries such as Japan, the USA, etc., have set laws that require producers to recycle or recover vehicles that have reached the end of their useful lives. Go et al. (2010) stated that a certain level of disassembly is required to make sure that the end-of-life products can be disassembled easily. Before recycling any part of the ELVS, the disassembly of the vehicle must be applied in the first place (Feri Afrinaldi et al. 2008). The most efficient way of recycling a vehicle is to disassemble every single component. However, it would seem impossible to do this due to the high operational costs of this kind of disassembly (Feri Afrinaldi et. al. 2008). Therefore, a well-organised process to disassemble automotive components is required (Desai & Mital, 2003; 2005).

According to Gupta & McLean's research (1996), there are four groups of researches in the study of disassembly:

- Easy to operate product disassembly (disassemble ability)
- Processes planning of product disassembly
- Design and apply the disassembly system
- Operational issues in the disassembly process

They also stated that the improvement of disassembly could be developed in two aspects:

- Design for disassembly (a constructional system in the product design phase
- Disassembly sequence planning, also known as DSP, to plan and optimise the sequence of product disassembly.

Design for Disassembly (DFD) is defined as a design approach and guideline to improve disassembly for maintaining products and handling EOL (Takeuchi & Saitou, 2005). Back in the mid-1980s, automotive manufacturers started to increase the study of design for disassembly, such as BMW, that provided funding for investigation (Kroll & Hanft, 1998).

Table 10 demonstrates the outputs of some major studies that were previously undertaken by researchers in the area of DFD.

Table 10: Outputs of previous research (Go, et al. 2010)

Researchers	**Years**	**Outputs**
J.F. Scheuring, B. Bras and K. M. Lee	1994	Guidelines for the design of disassembly
T. Dowie-Bhamra	2000	1) Developed the guidelines of disassembly for recycling, reuse and remanufacturing 2) Pointed out three factors that need to be considered by designers
S.G. Lee, S.W. Lye and M.K. Khoo	2001	Proposed the guideline for end-of-life disassembly
R. Bogue	2007	Demonstrated the design rules of design for disassembly

The factors pointed out in Dowie-Bhamra's research are (Go et al. 2010):

- The material selection and the use of those selected materials
- The design of components and the structural design of products

- The fastener selection

The design guidelines for disassembly proposed by Robert Bogue (2007) are:

- Reduce the material used for making products.
- Improve the efficiency of energy used in the manufacturing process.
- Use more reused components.
- Use more recycled components.

The design rules of DFD in Bogue's research (2007) are summarised in Table 11:

Table 11: DFD design rules (Bogue 2007)

Factors affecting the disassembly process	Guides to improve disassembly
Product structure	Create a modular design Minimise the component count Optimise component standardisation Minimise product variants
Materials	Minimise the use of different materials Use recyclable materials Eliminate toxic or hazardous materials
Fasteners, joints and connections	Minimise the number of joints and connections Make joints visible and accessible, eliminate hidden joints Use joints that are easy to disassemble Mark non-obvious joints Use fasteners rather than adhesives
Characteristics of components for disassembly	Good accessibility Low weight Robust, minimise fragile parts Non hazardous Preferably unpainted
Disassembly conditions	Design for automated disassembly Eliminate the need for specialised disassembly procedures DFD with simple and standard tools

Takeuchi and Saitou (2005) stated that design for disassembly is a method for the recycling, reuse and remanufacturing of end of life products. However, a certain level of disassembly is required for an EOL product to achieve the best results. Therefore, it is necessary for the disassembly sequence to be well planned. According to Kongar and Gupta (2006), an ideal disassembly sequence is quite important for obtaining an efficient process. Gungor and Gupta (1997) defined disassembly sequence planning (DSP) as a series of steps that starts with disassembling the product and ends with a status in which each part of the product is disassembled. To find the ideal sequence of disassembly, many methods and algorithms were proposed. The approaches and algorithms used for the disassembly sequence will be reviewed and discussed in the methodology chapter.

Based on the research on designs for disassembly and design sequence planning, Table 12 summarises the inputs and outputs of automotive disassembly as outlined below:

Table 12: The inputs and outputs of automotive disassembly

Inputs	Outputs
• CAD Model • End-of-life assembly • Disassembly sequences • Algorithms • Labour • Other resources	• Ease of disassembly • Ease of remanufacturing • Ease of reuse • Ease of recycling • Less cost/ time

An appropriate disassembly is crucial to improve the life cycle of products not only at the use and maintenance stage but also at the EOL stage and the 3 'Rs' (Giudice & Fargione 2007), which are known as 'reuse, reduce and recycle' (Takeuchi and Saitou 2005). Therefore, optimised disassembly makes a very important contribution to the automotive optimisation.

2.1.7 Cost

As the automotive market is competitive, automotive industries need to improve the quality of their products, reduce the time for developing them and control their costs (Roy et al. 2011). The definition of cost based on the product design engineer's perspective is the total cost of the product. The total cost can then be estimated as the sum of the three other viewpoints of cost (Tseng et al. 2008):

- The cost of materials
- The cost of manufacturing
- The cost of assembly

To improve the accuracy of estimating the cost, Roy et al. (2011) stated that cost estimation would require data and information. How to define good information was researched by Souchoroukov (2004). The research also stated that users needed to know:

- Why choose this information?
- Is there any limitation in using the information?
- How and where to access the information?

According to Roy et al. (2008), multiple information sources are available, and can be used to make cost estimations:

- Accounting databases
- Professional and reference material
- Knowledge
- Similar work done previously

However, it is challenging to make the decision when suppliers are involved.
Court et al. (1993) and Roy et al. (2001) identified the categories of information:

- Internal
- External

- Personal
- Cost drivers

As cost estimation is difficult work in automotive industries, the estimation is normally performed by the technical cost specialists and the most experienced engineers (Aderoba, 1997). Börjesson (1994) suggested that estimators need a quantitative way to estimate the cost based on the actual data instead of making assumptions: 'Unfortunately, there is usually little quantitative information to be used for the analysis of cost,' (Roy et al. 2011:695).

A table of cost elements performed in the research of Roy et al. (2011) can be used to provide data and information for the estimation of cost (Table 13).

Table 13: Cost elements (Roy et al. 2011)

Raw materials	**Parts from out sources**
Cost of Materials	Profits of Recovered scrap
Cost in industries 1. Direct cost of human source 2. Indirect cost of human source 3. Cost of equipment	
Cost from other sources 1. Cost of researching, designing and developing 2. EOL cost 3. Logistics cost 4. The cost of managing, selling, market analysing, etc.	

As the environmental impact has become a global concern, the end-of-life of a vehicle is one of the main research topics in automotive industries. Along with the ELVs, end-of-life value has also become a concern for manufacturers. This is simply because the EOL may cause discontinuing production, develop a new product which addresses the current market requirement, responsibility of the disposal for exist products, etc. Lee et al. (2001) proposed the following methods to calculate the end-of-life economic value:

1. Reuse value = Cost of component − Miscellaneous cost (1)
2. Remanufacture value = Cost of component − Remanufacture cost − Miscellaneous cost (2)
3. Primary recycle value = (Weight of component × Market value of material) − Miscellaneous cost (3)
4. Secondary recycle value = (Weight of component × Scrap value of material) − Miscellaneous cost (4)
5. Incinerate value = (Energy produced × Unit cost of energy) − Miscellaneous cost (5)
6. Landfill cost = − (Weight of component × Cost of landfill) − Miscellaneous cost (6)
7. Special handling cost = − (Weight of component × Cost of special handling) – Miscellaneous cost (7)
8. Miscellaneous cost = Collection cost + Processing cost (8)

Figure 7: Methods for calculating the economic value of EOL (Lee et al. 2001)

They also provided formulas to calculate the cost of the end-of-life retirement of a product:

Total time for product retirement = Time to collect the product from the user + Labour time to disassemble product + Time to reuse, remanufacture, recycle, or landfill the components (11)

Disassembly cost = (Labour to disassemble product × Labour rate) + Tooling costs + Material costs + Overhead costs (12)

Net recoverable cost = end-of-life economic value (see Section 2.2) − Disassembly cost (13)

Figure 8: Formulas to calculate the cost of the end-of-life retirement of a product (Lee et al. 2001)

The total cost was further discussed by Witik et al. (2011). They proposed a life-cycle cost model for the automotive industries. There are four aspects that can be considered: materials, manufacture, vehicle use and end of life treatments. Based on the information considered in the reviews above, the inputs and outputs of automotive costs are outlined in Table 14 based on the cost model from Witik et al. (2011):

Table 14: Inputs and outputs of cost

Inputs		**Outputs (overall cost)**
• Materials quantities & cost • Power cost • Plant cost • Labour cost • Reject rates • Scrap quantities • Production time • Assembly cost • Cycle times • Tool costs • Machine cost • Painting cost	Materials and manufacture	• Cost segmentation • Cost volume curves • Sensitivity analysis
• Fuel cost • Lifetime	Vehicle use	Total use cost
• Disassembly cost • Transport cost • Incineration cost • Landfill cost • Scrap cost	End of life	Cost segmentation of EOL

2.1.8 Discussion

Connections between these aspects can be found in the tables that summarised the inputs and outputs of each aspect and the information in the literature review. For example, according to Table 13 and Table 14, it is easy to find connections between costs and other the aspects. As the connections are found, a general idea of holistic optimisation is formed. The idea is to create a holistic optimisation tool that can provide a multi-perspective view of optimisation. The core of this tool, as mentioned before, is holistic optimisation. Branches such as LCA, EOL and disassembly will provide necessary information and support to the core. A draft flowchart is illustrated in Figure 9.

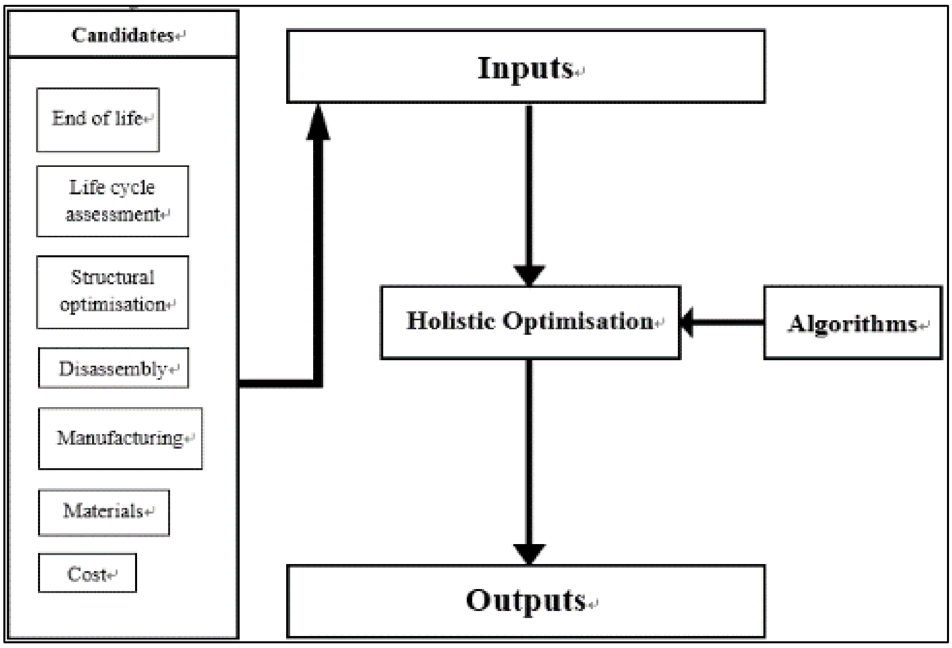

Figure 9: The draft flowchart of holistic optimisation

As optimisation with a single perspective or view is not considered in this research, the inputs in the flowchart could be any combination of the candidates/ aspects. This is similar to a multi-objective optimisation. However, the major challenge in this optimisation is how to make sure the selected candidates/ aspects work together with the relationship found in the literature review. Therefore, a good understanding of multi-objective optimisation is critical for this research. The next section contains the techniques for handling multi-objective optimisations.

2.2 The literature review of the optimisation algorithm

The pursuit of the best goal is the ideal of human beings, and optimisation is the science of selecting the 'best' decisions from many possibilities. In many areas of life such as industrial and agricultural production, transportation, finance, trade, energy, communication, national defence and scientific research, optimisation is widespread and has a very important application value, so it has become a difficulty and a great demand for academic research. The classical optimisation algorithms include the simplex method, the ellipsoid algorithm, the interior point method, etc. Intelligent algorithms are algorithms that emulate certain rules and systems by nature, and these new intelligent optimisation algorithms will provide new solutions for optimisation problems. The algorithms have been further studied and widely applied in various fields, and the problems of complex, multi-objective optimisation and holistic optimisation have become the focus of research.

This section will firstly introduce the basic understanding of the phrase "optimisation", i.e. the general principles, techniques and methods, etc. The second and third parts of this section are to compares and summarises multi-objective optimisation and holistic optimisation by analysing their characteristics and general algorithms. Then a final subsection will summarise the reviews of the optimisations.

2.2.1 General Introduction to Optimisation

The purpose of this subsection is to introduce the optimisation based on the general principles, techniques and methods. Before implemented the in-depth discussion of the optimisation, firstly should be done is to know what "optimisation" is and why optimisation. Generally speaking, optimisation is a process which optimises a set of objectives to achieve the most "efficiency" or the best "performance". For instance, the optimisation of a certain structure indicates a process that makes the structure performs at its most "efficient" (Christensen, J., Bastien, C., 2016). It also should be noted that the "structure" in the example could also be replaced by things such as an organisation or a supply chain management. In order to define the optimisation problem, the structural optimisation as an example will be used throughout the remainder of this subsection.

There are some basic factors of the optimisation problem: an objective, design variables and constraints. The objective of a structural optimisation shows which part of the structure will be optimised, e.g. the mass or the vonMises stress from a Finite Element Analysis. The design variables represent the parameters which affect the optimum solution for the optimisation. For structural optimisation, the design variables could be the geometry of the structure, the mechanical properties of the input material, the load/ force acts on the structure, etc. The constraints added to the optimisation can reduce the number of solutions to the optimisation problem.

To demonstrate how the optimisation problem is solved, the flowcharts of two general optimisation methods are illustrated in Figure 10. Both methods contain a number of self-constrained step-by-step actions, but terminate at a different point: for algorithms, the loop in Figure 10 will terminate when iterations reach the pre-configured number; for the iterative method, the loop will terminate based on the convergence criterion (Christensen, J., Bastien, C., 2016).

Figure 10: Optimisation methods (Christensen, J., Bastien, C., 2016)

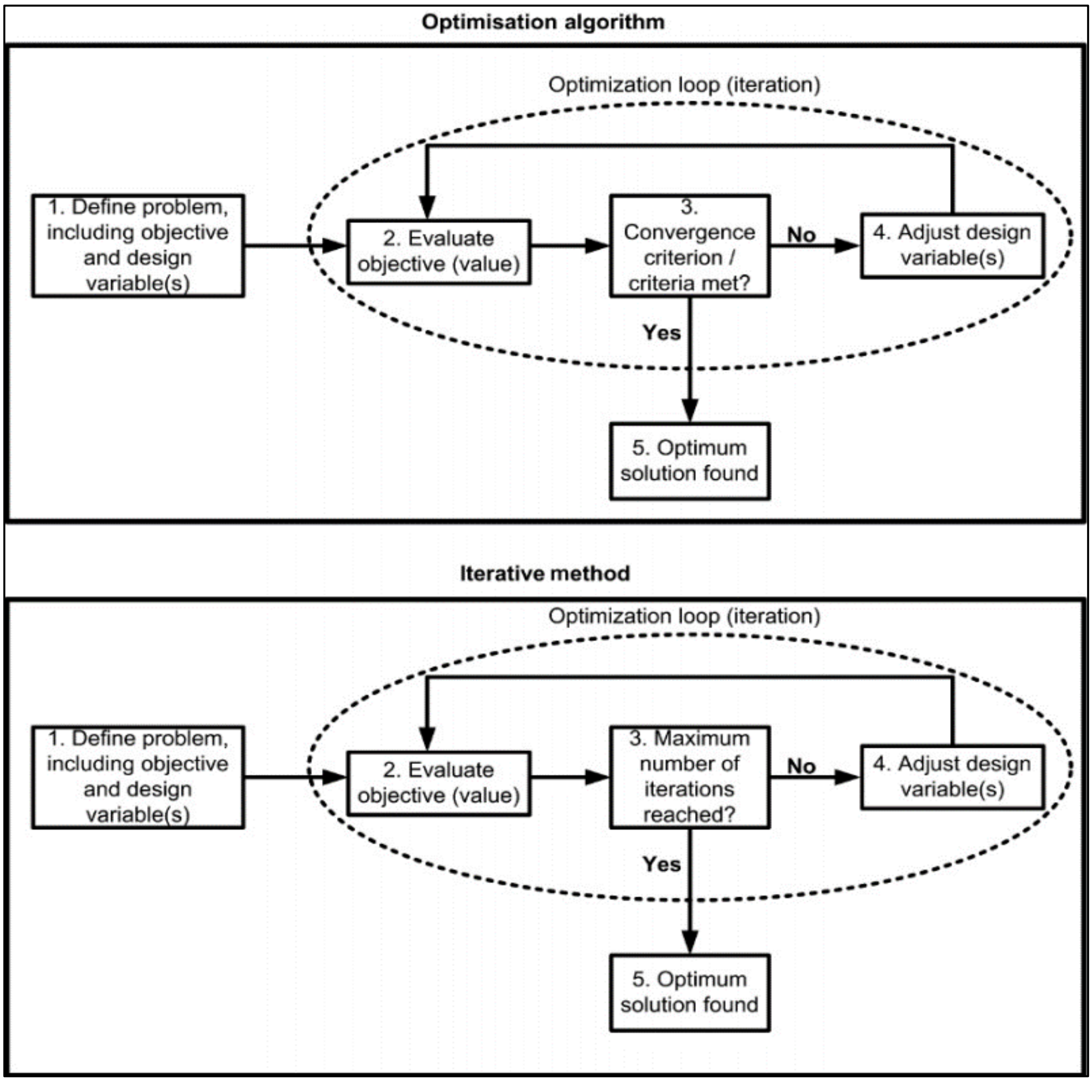

The methods defined above represent a single-objective optimisation. It should be noted that the multi-objective optimisations do exist in some other cases. To further explain the optimisation method, the optimisation problem is expressed by an objective function mathematically, i.e. equation(2.1).

$$f(x) = x^2 - 4 \tag{2.1}$$

Assuming that the objective of this optimisation problem is to minimise the function f of the variable x. The solution to the objective function is obviously obtained when x equals to 0. However, if x equals to 0 is ignored, then the solution will be changed accordingly. The new solution to the problem should be 2 and -2. The two cases above-indicated two types of optimisation problems: constrained optimisation problem and unconstrained optimisation problem. The constrained optimisation problem is the case that the x equals to 0 was ignored. This is a constraint which applied to the design variable x directly. There is, of course, the case where the constraint is not applied to the design variable directly. For instance, if the objective of an optimisation problem is to maximise the displacement of a bar within the maximum stress of the material. Apparently, the stress is a function of the radius of the cross-section of the bar. However, the displacement is not a direct function of the stress. Therefore, the constraint (i.e. maximum stress) is not directly applied to the design variable, the radius. Based on the example described above, a new equation can be created to express this optimisation problem:

$$\begin{aligned} &\min(f(x)) \mid x > 0 \wedge x \in \mathrm{Z} \\ &Subject\ to: \sigma \le \sigma_{\max} \wedge d \ge d_{\min} \end{aligned} \tag{2.2}$$

The equation represents an optimisation problem of a bar. The radius of the cross-section is the design variable x. The radius should be an integer which is larger than zero. The displacement ($d_{\min}$) represents the minimum displacement could be a direct constraint to the design variable; while the maximum stress ($\sigma_{\max}$) represents the indirect constraint. As defined previously, the constraints will help the optimisation to obtain the optimum solution efficiently by reducing the number of potential solutions. In fact, many optimisation problems are constrained optimisation problems. For instance, the structural optimisation might be subject to the constraints such as manufacturing methods, mechanical properties of the material, cost, etc.

The multi-objective optimisation problem can also be expressed by the mathematical method. However, this will make a much more complex optimisation process. To simply demonstrate a multi-objective problem, the equation (2.3) is created as follows:

$$\begin{aligned} &\min\left[f_1(x), f_2(x) \ldots f_n(x) \right] \mid n > 1 \\ &Subject\ to: C \in (a\ number\ of\ \ constraints) \end{aligned} \tag{2.3}$$

Equation (2.3) simply indicates that a multi-objective problem consists of multiple objective functions. Such a problem could be, for instance, reducing the cost while maximising the performance of a vehicle. Sometimes the multiple objectives have conflicts. The optimum solution of this type of problem will be a "compromised" solution as the optimum solution on one target may be the worst for another. Further details of the multi-objective optimisation will be discussed in the next subsection subsequently.

2.2.2 The Multi-objective optimisation

The natural planning and design process for human transformation reflects the basic principle of 'maximising efficiency and minimising costs' (Christensen, Bastien, 2016). 'Maximise efficiency, minimise costs' is essentially a multi-objective problem (MOP). Single target optimisation refers to a situation with only one function to optimise. MOPs on the contrary present more than one objective function. In fact, as the targets cannot be compared and are often contradictory in a MOP, it is usually difficult to make each of the sub-goals achieve the best at the same time. Because of the fact that a solution which is optimal for one target may be the worst for another, a MOP is often an equilibrium solution, as well as a Pareto optimal solution. Since the 1960s, many scholars have begun to study multi-objective optimisation problems and have made important contributions to this area, but it is generally recognised at home and abroad that France Pareto is the pioneer of this field, so multi-objective optimisation has his name.

The way to obtain an optimal solution to these MOPs when there are many conflicting goals, has always been the focus of engineering and science academics' attention. The Vector Evaluated Genetic Algorithms (VEGA) (Fonseca & Fleming 1993) was first put forward by Schaffer in 1985. It was the first algorithm that used an evolutionary algorithm to solve multi-objective problems, but VEGA was essentially a weighted method. After that, many kinds of MOA have appeared. The development phase of the multi-objective evolutionary algorithm (MOEA) can be summarised as follows (Horn, Nafpliotis & Goldberg 1994).

The slow development period from 1985 to 1994: This stage of the algorithm includes the non-Pareto method and the Pareto method. The non-Pareto method does not directly utilise the basic concept of Pareto optimisation, which is efficient and easy to implement, but it cannot produce Pareto for some parts of the optimal front end. The Pareto method uses non-inferior ordering and selection to estimate the entire population to the Pareto optimal front end. The representative algorithms for this period are: Vector Evaluation Genetic Algorithm (VEGA), Multi-Objective Evolutionary Algorithm (MOEA), Niche Pareto Genetic Algorithm (NPGA) and Non-Inferior Sorting Genetic Algorithm (NSGA) (Srinivas & Deb 1994).

The rapid development period from 1994 to 2003: Since Zitzler and Thieler proposed the intensity of the Pareto evolutionary algorithm (SPEA) in 1999 (Zitzler & Thiele 1999), scholars started to combine external files and populations into their MOEA. The elite retention strategy became the basic steps of the two-stage MOEA design and the efficiency of the algorithm search had also been significantly improved. The representative algorithms for this stage are: NSGA II (Deb et al. 2002), Pareto Archives Evolutionary Strategy (PAES), Pareto Envelope Selection Algorithm (PESA) and SPEA II.

The comprehensive development period from 2003 to the present: The research of the forefront of the multi-objective evolutionary algorithm field has come into a new stage of development (Knowles & Corne, 2000). Various new concepts, mechanisms and strategies are being introduced into MOGA, which greatly promotes the efficiency of the algorithm. Some new examples have been introduced into multi-objective optimisation fields such as particle swarm optimisation, the ant colony algorithm and distribution estimation algorithms. At the same time, the research on high-dimensional multi-objective optimisation problems (MOOP) and dynamic multi-objective optimisation problems (DMOP) has also made some preliminary progress.

2.2.2.1 The Traditional Algorithm

The traditional multi-objective optimisation method requires the decision maker to determine the weights according to the decision-making needs and then merge the various objective functions into a single objective function in the weighting method. The common multi-objective optimisations are the weighted sum method, the constraint method, the linear programming method, etc.

2.2.2.1.1 The Weighted sum method

The weighted sum method refers to the method that transforms the MOP into the overall goal of the optimisation problem by establishing a linear combination of each objective function (Cohon, 1978). Suppose the new objective function is $p(x)$

$$p(x) = \sum_{i=1}^{m} w_i f_i \ (x) \tag{2.4}$$

Where,

w_i is the weight coefficient, and there is $\sum_{i=1}^{m} w_i = 1$.

The relatively important degree of every target function determines the size of the weight coefficient for the decision maker. This method not only requires scholars to have a more thorough understanding of the objective function of a multi-objective problem, but also it is subjective.

2.2.2.1.2 The Constraint method

The constraint method is not limited to optimising the Pareto optimal front-end protrusions. Generally, in a MOOP, there are often n decision-making variables, k objective functions and m constraints, while the constraint method picks one of the k multi-objective optimisation functions as the object function. The remaining m-1 objective functions are transformed into constraints:

$$\max \& \min \quad y = f(x) = f_h(x) \quad | \quad s.t.\ e_i(x) = f_i(x) \geq \varepsilon_i \quad (1 \leq i \leq k, i \neq h)$$

The parameter ε_i requires artificial adjustment of the lower bound, in order to find the Pareto optimal solution. However, in the case where the message of each object in a multi-objective problem is not clear, the determination of the parameter value ε_i may not be able to affect the accuracy of the optimisation.

2.2.2.1.3 Linear programming method

The linear programming method (Jeffrey & Deepak 2002) obtains the ideal optimal value f_i* of the sub-objective function (which can be adjusted automatically according to requirements), and then normalise and sum according to the following formula to establish a unified objective function:

$$F(x) = \sum_{i=1}^{N} \left[\frac{f_i(x) - f_i^*}{f_i^*} \right]^2 \tag{2.5}$$

The key to this method is to select the ideal value fi * of each sub-objective function. It is usually necessary to establish a unified objective function based on a certain experience, or a single objective function to optimise the solution.

2.2.2.1.4 Summary

The traditional method is basically followed by the method of seeking single objective function optimisation. For large-scale optimisation problems, these multi-purpose
standard optimisation methods are rarely used. Their defects are mainly manifested in the following aspects:

1. the choice of weight coefficient is often strongly subjective; the optimisation results are not ideal enough;
2. the optimisation target is only the weighted sum of each target, the optimisation speed of each target is not operational;
3. it can only get to an optimal solution in the end, there is no alternative to the program;
4. the relationship between the various objective functions through the decision variables are interrelated, the topology is very complex;
5. different natures of the targets have a different dimension, which is difficult to compare.

2.2.2.2 The Evolutionary Algorithm

In view of the shortcomings of the traditional optimisation methods in solving MOOP, researchers abandoned the multi-objective optimisation methods which have been mentioned above and actively studied new methods of dealing with multi-objective problems. The multi-objective evolutionary algorithm can deal with large scale search in parallel at the same time and bring about multiple so-called ‘Pareto optimal solutions’ during single-wheel optimisations, solving the limitations of the traditional optimisation methods. There are many unsatisfactory areas in the early evolutionary algorithm. With the deepening study of evolutionary algorithms, a number of new algorithms are proposed.

2.2.2.2.1 The Genetic algorithm

The heuristic thought of the genetic algorithm (GA) originated from Darwin's evolution theory and Mendel's genetics theory. It is based on ‘survival of the fittest’, and other natural evolutionary rules to search and solve the problem. Through the natural selection of the ‘survival of the fittest’, the high value of the genetic structure is preserved (Wang & Jang 2000). For many problems that are difficult to solve with mathematical methods, especially MOOP, GA puts forward a new possibility to solve them. GA expresses the solution of the problem as a chromosome, thus forming a group of chromosomes. According to the principle of ‘survival of the fittest’, through natural selection, gene crossover and mutation, the descendants that are more suitable for the environment will be produced, that is, the final convergence to an individual that adapts to the environment. The Figure 11 shows the basic flow chart of GA.

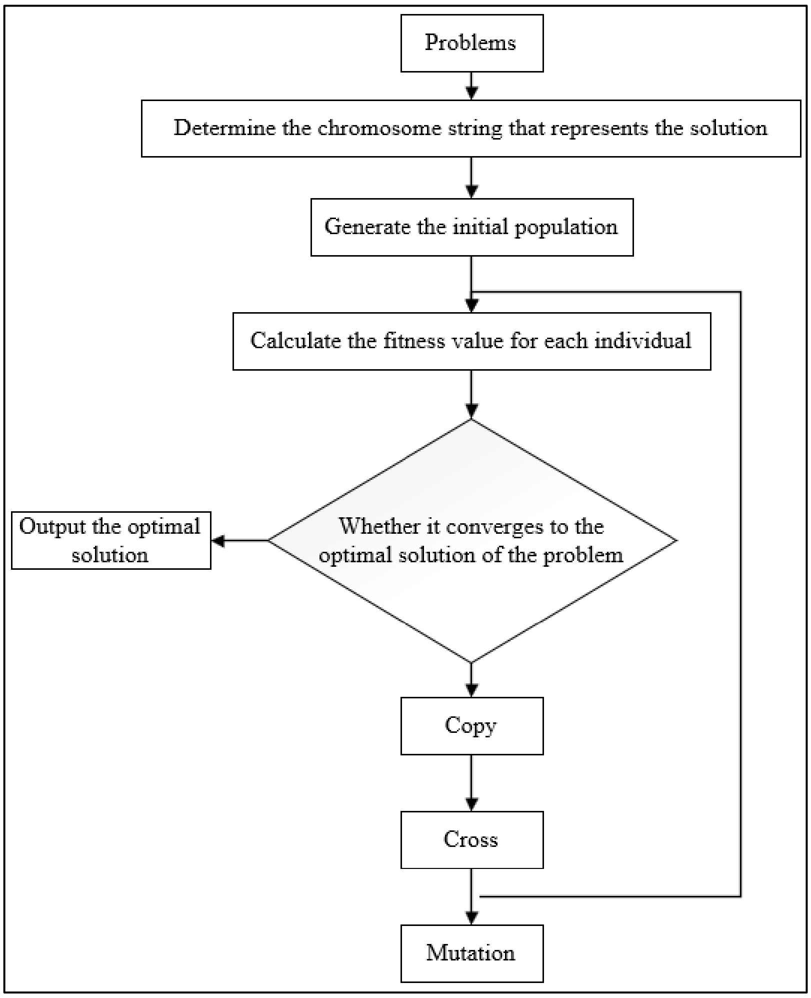

Figure 11: Basic flowchart of GA

2.2.2.2.2 Ant Colony Optimisation

In 1991, the Italian scholar Dorigo and two other scientists put forward a new evolutionary algorithm: Ant Colony Optimisation (ACO). It is based on population and simulates ant colony foraging behaviour. Its principle is a positive feedback mechanism (also called an enhanced learning system) and its convergence path is as follows: increase in the number of ants on the optimal path → increase in the pheromone intensity → increase in the choosing probability of the ants coming later →increase in the number of the ants on the best path.

It is a general-purpose stochastic optimisation method that absorbs the behaviour of ants (intrinsic search mechanism) using artificial ant simulations (also known as ant systems) to solve problems, but artificial ants are never a simple simulation of real ants: artificial ants have a certain memory; artificial ants are not completely blind; artificial ants' living time and space is discrete. It is a distributed optimisation method, not only for the current serial computer, but also fit for parallel computers in the future (Du & Swamy 2016).

Although the theory of the ant colony algorithm has not been studied for long, the preliminary studies have shown that it has a great advantage in solving complex optimisation problems, especially after the first international ant anatomy was held in 1998 in Brussels, Belgium. The International Symposium on Ant Optimisation is now held every two years. This indicates that the study of the ant colony algorithm has been widely supported by the international community. With the progress of multi-objective optimisation, the prospect of holistic optimisation becomes more and more attractive. The details of the holistic optimisation algorithms will be discussed in the next subsection.

2.2.3 Holistic Optimisation Algorithms

The optimisation problem exists in many fields in real life. The optimisation method is important in carrying out modelling and analysis when an actual problem is studied. Many of the optimisation models abstracted in the process of analysing a problem can be attributed to the holistic solution, so the holistic optimisation method is of wide concern.

As early as the 1960s, studies began on the problem that is now known as holistic optimisation, but at that time the focus was mainly on the linear programming and nonlinear programming of localised numerical algorithms, until in the 1970s, collections of papers on holistic optimisation began to appear. After years of development, holistic optimisation has grown into an independent branch of the field of optimisation, which is one of the important methods to model and analyse practical problems.

The problem of holistic optimisation research is the holistic optimal solution of a multi-variable nonlinear function over a certain constraint region and the method of constructing that solution (Casado & Martinez, 2001). Since it is possible to have multiple local optimal that are different from the holistic optimal solution to the problem, these problems cannot be solved by means of the classical local optimisation method, especially as there is no good holistic judgment criterion at present, which makes holistic optimisation research very challenging.

However, in the last two or three decades, holistic optimisation has made rapid development in many fields at a noteworthy rate. Many new holistic optimisation theories and algorithms are being effectively applied to the difficult situations encountered in science and production, recently emerging holistic optimisation methods have been successfully applied to production and design issues as a powerful tool.

Nowadays, as information technology is developing at a fast speed, holistic optimisation's application in fields of economic models, fixed costs, finance, network, transportation, molecular biology and environmental engineering is becoming increasingly wider (Csendes, 2001). Many of the advances in science, economics, and engineering rely on numerical techniques to compute the corresponding holistic optimal solutions. Therefore, the holistic optimisation theory and methods deserve an in-depth study.

In general, the existing methods of solving holistic optimisation problems are divided into two categories according to their convergence properties: the deterministic method and the stochastic method. The deterministic method can produce a finite or infinite order sequence to converge to the global best solution by using the analytic nature of the problem, such as the interval method, the branch and bound method, the filling function method, the penalty function method, the integral level set method, primitive dual methods, etc. Convexity, monotonicity, isometric continuity, density, surface constants, level sets, etc. are often referred to as the holistic nature of these analytic properties. This method searches for local minima based on a deterministic strategy and attempts to combine these local minima to achieve a holistic optimal point (Sun & Wang 2014). The random method uses the probability mechanism to describe iterative processes, such as GA, the evolutionary strategy method, etc. These are commonly used stochastic algorithms. This method has the advantages of a low requirement of objective function, wider and easier achievement, good stability and other prominent features.

In the following subsubsections, five optimisation algorithms will be introduced. The first two algorithms are the typical deterministic optimisation algorithms; the other three are the stochastic optimisation algorithms.

2.2.3.1 The Interval algorithm

R.E. Moore proposed the concept of the interval algorithm in the late 1950s. He abandoned the floating point approximation method of real number, proposing that a real number r should be expressed on a computer with an interval $r = \left[\underline{r}, \bar{r}\right]$, $\bar{r}$ and $\underline{r}$, and that both can be accurately expressed by computer, and $\underline{r} \leq r \leq \bar{r}$.

Although the interval algorithm is intended to calculate the reliability of the results, it was soon found to have a wider range of applications. Due to the collection properties of the interval itself, the collection operations between the intervals can easily be carried out for the study of interval mathematics derived from the interval analysis of this modern mathematical branch. This branch defines the theoretical basis of many new computational methods based on the interval algorithm (Markót, Fernández, Casado & Csendes, 2006). These new computational methods can reliably solve some problems which may be difficult to solve in traditional ways, such as solving nonlinear equations' all numerical solutions in a given region, the overall optimisation and other issues. In addition, many of the computational parameters are expressed in terms of intervals in practice, and it is easy to include them in calculations using the interval algorithm. This means the interval algorithm has had some success in financial risk control, rocket nozzle force, nuclear magnetic resonance machine design and robot applications.

2.2.3.2 The Branch and Bound algorithm

The Branch and bound algorithm is an important way to deal with optimisation problems (also known as integer programming). It is applied in many optimisation problems, such as integer programming, total extreme value problem of non-convex function, minimal problem of piece-wise function and feasible set complex problem optimisation issues. The main thought of the branch and bound algorithm is to separate one complicated problem and turn it into several small individual problems, while each sub-problem can continue to decompose until the sub-problem can no longer be decomposed or cannot produce the best answer. The process of decomposing a problem into a sub-problem according to different characteristics of each of them is called 'branch'. The branch-and-bound method uses the depth-first method as the basis for the branch decision and estimates the upper bound or the lower bound of the target F value that can be achieved at each branch node and compares the estimate with the best score that has been recognised. It is possible to improve the efficiency of branch decision making by the early withdrawal or deletion of decision paths where it is not possible to exceed the best score which has been recognised.

The branch and bound algorithm considered by holistic optimisation is:

$$\min_{x \in S} f(x),$$

In this case, $x \subset R^n$, S is a compact set, the function $f: R^n \to R$ is continuous on S, and the branch and bound method is one of the main algorithms of holistic optimisation. The most important characteristics of branch and bound can also be generalised by dividing the feasible domain gradually and adding the monotonically decreasing higher boundary of the optimal solution and the monotonically increasing lower boundary sequence. When the upper and lower bounds are equal or the difference between the upper and lower bounds meets the wrong requirement, the iteration is terminated, and the holistic optimal solution is obtained; otherwise the iteration continues.

According to the process of segmentation and the selection of the upper and lower bounds, the method of branching and delimiting can be divided into two categories, one is to combine the tangent plane process with the branch and bound technology and the other is to use the objective function approximation process. The Branch and drop method is widely used in optimisation models of integer programming and nonlinear programming. An increasing number of scientists and scholars are searching for new ways and new methods.

2.2.3.3 The Simulate Anneal Arithmetic

The simulated annealing algorithm is a general probability algorithm. It is usually used in searching the best approaches of a problem in a huge searching scope (Fang, Liu & Chen 2014). S. Kirkpatrick and his partners first came by the simulated annealing algorithm in 1983. Vern and Yacute had also invented this algorithm independently in 1985. It is one of the effective methods to deal with TSP problems.

Its name comes from the proper term 'annealing' from metallurgy. Annealing is to heat the material and then cool at a specific rate in order to raise the volume of the grains and to decrease flaws in the lattice. The atoms in the material will remain in the local minimum value of the location, in heating so that the energy becomes larger and the atoms will leave their original position and randomly move to other locations. Annealing is slow at the time of cooling, making the atoms more likely to find a lower position than originally. The principle of simulated annealing is also similar to the principle of metal annealing. With the process of controlling the parameters of the cooling schedule, the algorithm is used to reduce the temperature of the control parameter from t to zero, and finally get the holistic finest solution to the relative optimisation problem.

2.2.3.4 Tabu Search

The Tabu algorithm is a mate-heuristic random search algorithm. It starts from an initial feasible solution and selects a set of specific search directions as a 'temptation' to choose to move up to a specific target function (Glover 1989). For the purpose of not stepping into a local optimum, the TS search uses a flexible 'memory' technology. The optimisation process has been carried out to record and select and to guide the next search direction, which is the establishment of the Tabu table. This is to avoid searching the points that have already been searched and to 'forgive' some of the 'taboo' of the fine state through the 'contempt' criteria and then ensure the effective exploration of diversification to achieve the ultimate holistic optimisation. In recent years, the TS algorithm has been researched more and more in the holistic optimisation of function.

One essential component of TS is to make a mark at the local optimum that it has first searched and to try to keep away from these marks as much as possible in the further iterative searches (rather than absolutely prohibiting the loop), so as to ensure that different effective search paths are explored. The TS algorithm has a flexible memory function and 'contempt' criteria. In the search process it can receive a poor solution and can avoid the non-comprehensive solution during the calculation, turning to those solutions in the space of other areas. Thereby, the probability of obtaining a better optimal solution is increased. However, the most puzzling drawback of TS is that the convergence of the algorithm and the convergence rate of the theoretical research is still not perfect and is waiting to be improved.

2.2.3.5 The Genetic Algorithm

The Genetic algorithm is a computational model that simulates both Darwin's genetic selection and the biological evolution process of natural elimination. It simulates the natural evolutionary process to search the best method for solving problems. It was first invented by Michigan University Professor J. Holland in 1975. The genetic algorithm is an adaptive artificial intelligence technology that simulates the problem of biological evolutionary process and mechanism solving. Its core idea stems from the basic understanding of 'survival of the fittest'. The process of biological evolution in this natural law is itself a natural, parallel occurrence and a stable optimisation process. The goal of this optimisation process is adaptability to an environment. The biological population achieves the purpose of evolution through 'survival of the fittest' and genetic variation. If the problem waiting to be solved is described as the holistic optimisation of a target function, the basic method of solving the problem is to interpret the target function to be optimised as the adaptation of the biological population to the environment and to optimise the variable to the individual, starting from the current population, using the appropriate replication, hybridisation, mutation and selection operations to generate a new population; and to repeat this process until the required population or the required evolution time is obtained. Based on natural selection and genetic mechanism, GA has been applied in practice in the optimisation of machine learning, automatic program generation and knowledge based maintenance of expert systems since the mid-1980s.

2.2.4 Summary

The optimisation methods/ algorithms were reviewed in this section. The optimisation problem generally means getting the best method of solving a series of objective functions through a certain optimisation program (Deb 2014). When there is only one objective function, it is called single-objective optimisation, otherwise it is known as MOP if the number of functions is two or more. The best answer is calculated out of a set of equilibrium solutions in general (Pareto equalisation). The problem of holistic optimisation research is the holistic optimal solution of a multi-variable nonlinear function over a certain constraint region and the method of constructing the holistic optimal solution (Ravi, Liu & Chakradhar 2014). Since it is possible to have multiple local optimal in a holistic optimisation problem and as they are different from the holistic optimal solution of the problem, these problems cannot be solved by means of the classical local optimisation method.

The purpose of multi-objective optimisation looks for a balanced optimal solution among a set of target functions (Deb 2001). The multi-objective optimisation algorithm comes down to two categories: the traditional optimisation algorithm and the intelligent optimisation algorithm. The traditional optimisation algorithms include the weighting method, constraint method and linear programming method (Deb, Thiele, Laumanns & Zitzler, 2002). The intelligent optimisation algorithm includes evolutionary algorithm (EA), Particle Swarm Optimisation (PSO), Ant Colony Algorithm (ACO), etc.

As for the holistic optimisation algorithms, they can be separated according to their convergence properties into two categories: deterministic methods and random methods. The deterministic method can use the analytic nature of the problem to produce a finite or infinite order sequence to converge to the holistic optimal solution, such as the interval method, the branch and bound method, the filling function method, the penalty function method, the integral level set method, the primitive dual method, etc. The random method class uses the probability mechanism to describe the iterative process, such as the random inflow method, the genetic algorithm, the simulated annealing algorithm, the evolutionary strategy method, the Tabu search algorithm, etc., which are commonly used stochastic algorithms. They have low requirements to objective function properties, a wide range of applications, easy achievement, good stability and other prominent features.

With the progress of multi-objective optimisation, the prospect of holistic optimisation becomes more and more attractive. Imaging an optimisation tool not only addresses the structural challenge but also finds the most "efficient" ways to manufacture, transport, assemble and disassemble from a CO_2 equivalent emissions perspective. Such a holistic optimisation would be a very interesting development in the optimisation domain.

This research aims to create a holistic optimisation tool/ algorithm to deal with the conflicts between different variables when solving multi-objective problems. The complexity of these problems can sometimes only be solved by numerical methods (Askar & Tiwari 2009). The key is to turn a multi-objective function into one, so that it can be solved through the 'single' objective ways. This is also the challenge for holistic optimisation to reach the optimum 'compromise'. The following chapter contains the methodology of holistic optimisation.

3 Methodology

In this chapter, the major aspects indicated in the literature review will be further studied by a Quality Function Deployment (QFD). Within the QFD, connections between different aspects will be discussed. According to the links found in QFD, the parameters of aspects are further categorised into three groups as the basis of the three individual modules: STRUCTURAL module, COST module and CO2 module. The integration of these three modules will form two general types of holistic optimisations: Sequential (SEQ) and Parallel (PAR). This chapter consists of 5 sections. The first section is to use QFD to further analyse the major aspects of the product and summarise the relationships between different aspects. The second section contains the setup of the three individual modules. The third section will introduce the integration of the three modules and the 'structure' of the two types of holistic optimisations. The fourth section contains the design of the case study which indicates how the holistic optimisations will be studied. The fifth section gives the evaluation methods which will demonstrate the methods for evaluating the results of the optimisations.

3.1 Further Analysis of the Aspects – QFD

Quality Function Deployment (QFD) was developed in Japan to introduce statistical quality control (Brief 2012). Nowadays, QFD is used to help the designer understand the customer's requirements and transform these requirements into engineering characteristics. The QFD diagram, also called the House of Quality, consists of five sections as illustrated in Figure 12.

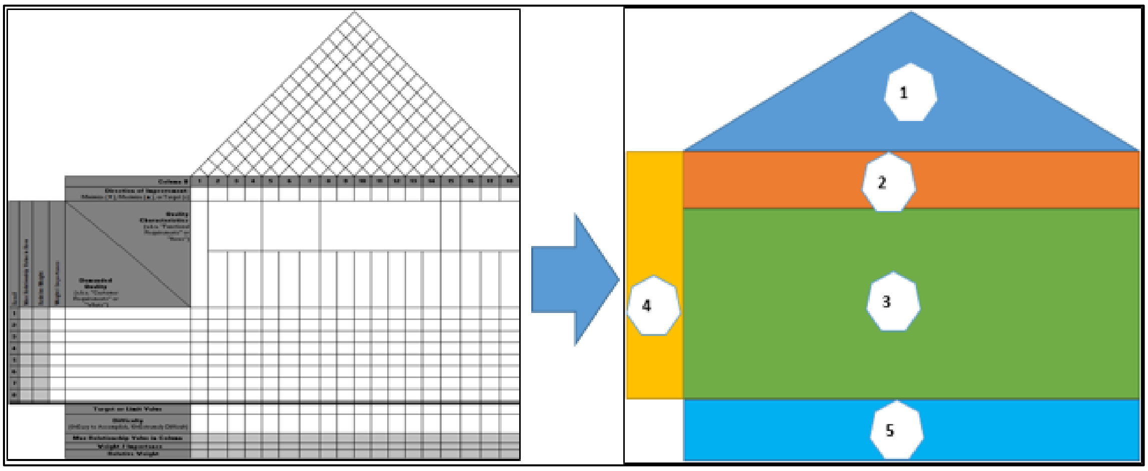

Figure 12: House of Quality

1. The roof matrix contains the co-relationships between the technical requirements. The relationships could reinforce each other or conflict.
2. Technical requirements located under the roof matrix represent the transformed customer requirements.
3. The relationship matrix section determines how well each technical requirement satisfies costumer requirements.
4. The customer's requirements are listed on the left side of the House representing 'what customers want from the product'.
5. The target values block under the relation matrix has three aspects: weights, benchmark and target value. The weights are used to rank the importance of each requirement. The

benchmark value is used to make the comparison. The target value is the ultimate value of the requirements (Rowley 2017).

To further understand the relationship between the aspects found in the literature review, the QFD method is applied in this study (Appendix A). As the QFD diagram is only used to find out the relationships of the aspects, therefore, there are no other products to be compared. All weight/ importance factors are made as assumptions that can be changed in future work. The customer requirements are: lightweight, safe, reduce CO_2 emission, reduce manufacturing time, reduce assembly/ disassembly time, recyclable and reduce cost. Several function requirements are listed in the QFD diagram to achieve these customer requirements: mass of the materials, design efficiency, structural optimisation, end-of-life options, life cycle assessment and cost. The correlation matrix in the roof is explained by the following points:

1. The mass of material has a positive correlation with size optimisation and topology optimisation. The mass of material is the major objective of the optimisation process.
2. The mass of material has a strong positive correlation with CO_2 equivalent, material cost, manufacturing cost and end of life cost. For example, the heavier vehicle can generate more CO_2 emissions. If the mass of one single material is increasing, it demonstrates that more materials are used. Meanwhile, the material cost, the manufacturing cost and the end of life cost will increase.
3. Design for manufacturing (DFM) can be used to control the manufacturing time, processes and costs. Therefore, it has a strong positive correlation with remanufacturing and manufacturing costs. As CO_2 emissions can also be found in manufacturing processes, the DFM has a positive correlation with the CO_2 equivalent.
4. Design for assembly and disassembly (DFA/ DFD) has a strong positive correlation as they can both improve the design efficiency. Normally, when a product is easy to assemble, it will be easy to disassemble as well.
5. Design for disassembly has a correlation with the special handling of the end of life and the end of life cost. Special handling may be required in the disassembly if for example, the disassembly contains toxicity. As the DFD will affect the efficiency of the implementation of the end-of-life options, it will therefore affect the end of life cost.
6. All end of life options will affect the end of life cost. Therefore, the options have a strong correlation with the end of life cost.
7. Energy recovery incinerates the end of life products to produce heat and electricity. The more the energy recovery from the end of life products, the less the products are going to be reused, remanufactured or recycled. Therefore, reuse, remanufacture and recycle have a negative correlation with energy recovery.
8. Landfill has a negative correlation with reuse, remanufacture, recycle and energy recovery, because when the reuse, remanufacture, recycle, and energy recovery options

are improved, the waste material put into landfill will reduce.

9. The processes of some of the end of life options may generate CO_2. Therefore, options such as remanufacture, recycle (primary/ secondary), and energy recovery has a correlation with the CO_2 equivalent.

The relationship of the aspects in the relationship matrix is straightforward. The relationship matrix can be explained by the following points:

1. 'Lightweight' has a strong relationship with the mass of materials, structural optimisation, CO_2 equivalent and cost. The material and structural optimisation can optimise the mass of the product. On the other hand, 'lightweight' can reduce the CO_2 equivalent and cost respectively.
2. 'Safety' has a strong relationship with the structural optimisation and the special handling of the end-of-life options. Structural optimisation can provide the load path of the structure and the method to optimise the safety of the structure. To protect the operator, special handling is required in some specific end-of-life cases. For example, if the end-of-life product contains toxicity, special handling will be required.
3. To 'reduce manufacturing time, assembly and disassembly' and improve design efficiency is necessary. Therefore, they have a strong relationship with design efficiency.
4. 'Recyclable' has a strong relationship with material, some of the end-of-life options and the end-of-life cost. If 'recyclable' is required, at least one recyclable material should be selected for the product. The end-of-life options such as reuse, remanufacture, primary-recycle and secondary-recycle can recycle the useful materials from the end-of-life product. On the other hand, any end-of-life product that can be applied to those options is recyclable. Meanwhile, such products also increase the end-of-life costs.
5. As the cost of the product consists of three aspects (material cost, manufacturing cost and end-of-life cost), 'reduce cost' has a strong relationship with the mass of materials, design efficiency and these three major aspects. It also has a moderate relationship with the other aspects except for the CO_2 equivalent. The reduction of the CO_2 equivalent will increase the cost.

Further study of the product based on the QFD has indicated the relationship between different aspects of the product as defined above. The discovered direct/ indirect links between those aspects will be the foundation of the holistic optimisation programme, i.e. the three individual modules. The basic setup of the three modules will be defined in the next section.

3.2 Parametric Modules

The parametric modules are the foundation of the holistic optimisation program. The three modules are created using a Windows system based scripting language, PowerShell. In this section, three individual optimisation modules will be demonstrated. The internal structure of each module will be built based on the relationship between the different aspects found in the literature review.

3.2.1 Structural Module (STRUCTURAL)

The structural optimisation module is programmed in PowerShell. This module is to optimise the product structure in terms of material selection, component volume, etc. The basic information of the module is tabulated as follows:

Table 15: Structural Optimisation

<table>
<tr><td rowspan="6">Inputs</td><td rowspan="5">FE model</td><td>Component geometry</td></tr>
<tr><td>Geometry constraints</td></tr>
<tr><td>Structural performance requirements (e.g. max stress, displacement etc.)</td></tr>
<tr><td>MAT (properties)</td></tr>
<tr><td>Boundary Conditions</td></tr>
<tr><td>Optimisation</td><td>MAT (read from / written to FE file)</td></tr>
<tr><td rowspan="2">Constraints</td><td colspan="2">MAT type (Isotropic linear elastic materials)</td></tr>
<tr><td colspan="2">Yield Stress of the MAT</td></tr>
<tr><td rowspan="4">Outputs</td><td colspan="2">Optimum geometry</td></tr>
<tr><td colspan="2">(Max) displacement</td></tr>
<tr><td colspan="2">(Max) Von Mises Stress</td></tr>
<tr><td colspan="2">Component volume</td></tr>
</table>

The idea of the structural optimisation module is to change inputs in PowerShell and optimise a beam by sizing optimisation in HyperMesh. To achieve this aim, three functions are created to extract major outputs from HyperMesh. The 'Mass' function aims to extract the mass of a beam from the '.out' file. The 'Max_displacement' and 'Max_VM_stress' functions aim to extract the maximum displacement and the Von Mises stress from the '.html' file. The outputs from the initial beam analysis will be the benchmark of the optimisation. Once the objective of the optimisation is decided, the relevant inputs will be the design variables. For instance, if the objective is to minimise the mass of the beam by decreasing the thickness, the value of the thickness will vary for each optimisation iteration. In each iteration, the new thickness will be exported to replace the old data in the '.fem' file. This file works associated with the 'OptiStruct' solver of the HyperMesh. The structural optimisation module will call the 'OptiStruct' to run the analysis for the updated '.fem' file. The iteration finishes when the new outputs are extracted and compared with the target value. The iteration is repeated to form the optimisation loop until the target value is achieved. To find the objective function value, the Gradient Descent Method (GDM) and Line search algorithm are applied in this module. The GDM method normally focuses on the convex and concave functions to find the minimum and maximum solutions. The differentiation of the function is used to obtain the objective function value. Therefore, the gradient of the function should be determined first (Christensen, Bastien, 2016).

$$\nabla f(x) = f'(x) \tag{3.1}$$

When the gradient is equal to zero, the minimum or maximum solution can be obtained. In the structural optimisation module, there is a function of deflection regarding the thickness as indicated in Equation (3.2).

$$f(T) = \frac{5wL^4}{384E} \times \frac{204}{2929 \times T^4} \tag{3.2}$$

Where,

w, the uniformly distributed force (N/m)

L, the length of the beam (m)

E, the Young's Modulus of the material (GPa)

T, the thickness of the beam (mm)

Equation (3.2) is expressed based on the calculation in Appendix B. The function of deflection should have a roughly plotted graph like Figure 13. As the value of thickness cannot be zero, the maximum deflection will be found when the value of thickness is infinitely close to zero. As required by the GDM method, the gradient of the deflection function is indicated in Equation (3.3).

$$f'(T) = -4T^{-5} \tag{3.3}$$

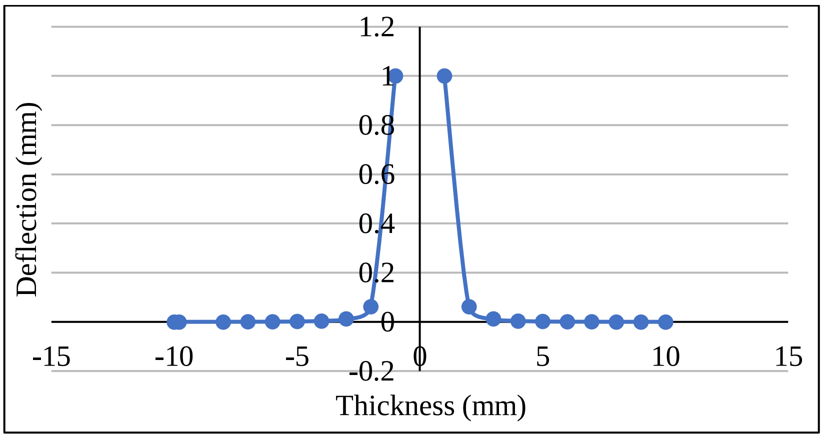

Figure 13: Roughly Plotted Graph of the Deflection Function

To obtain the maximum value of the function, the thickness must move towards zero. Therefore, the search direction must be $-\nabla f(T_0)$. More solutions can be found if using the GMD method to update the value of the thickness. Thus, a new Equation (3.4) is indicated:

$$T_{i+1} = T_i - SF \times \nabla f(T_i) \,|\, i \geq 0 \tag{3.4}$$

Where,

SF, the scale factor which represents the time step size between iterations

i, the iteration numbers.

The scale factor should be less than 1.0 (Christensen, Bastien, 2016). If the value is too large, the outputs will become divergent and unstable. If the value is too small, the computation time of the optimisation will be increased dramatically. Therefore, an appropriate value of the scale factor is necessary. To find the appropriate scale factor a line search algorithm is used, for instance, to minimise the mass of the beam by reducing the thickness. As the thickness reduces, the deflection will increase. Therefore, it gives a function expressed as Equation (3.2). The value of thickness starts with 3.0 millimetres. Three values of scale factors are selected: 0.1, 0.5 and 1.0. The constraints of this optimisation are the yield stress of the material and the minimum thickness. The material used in this optimisation is high strength steel with a 470 MPa yield stress. The minimum thickness is assumed as 1.3 millimetres (Cline & Shapiro 2000). The outputs of this example are tabulated in Table 16. The optimisation with the three scale factors gives similar results. However, optimisation with scale factor = 0.1 spends too much time to converge the result. Although the time spent on factor = 0.5 is twice the time spent on factor = 1.0, to keep the stability of the GDM, the appropriate value of the scale factor should be 0.5.

Table 16: Scale factor Convergence

SF	Iteration	Thickness (mm)	Max Displacement (mm)	Mass(kg)	Time (s)
0.1	293	1.7	18	0.4	877
0.5	60	1.6	19	0.4	180
1	30	1.6	19	0.4	90

In this case, the GMD applied to the thickness is indicated by Equation (3.5).

$$T_{i+1} = T_i - 0.5 \times 4 \times T_i^{-5} \tag{3.5}$$

The basic idea of the STRUCTURAL module has been introduced in this subsection. In the following two subsections, two similar modules will be introduced respectively. The COST module will be introduced subsequently in the next subsection.

3.2.2 Cost Module (COST)

The major information of this module is tabulated in Table 17. Its aim is to optimise the total cost of the product in terms of material cost, manufacturing cost, transportation cost, etc. The initial cost estimation will give a benchmark to the cost optimisation. It is also known as the maximum cost allowance of the product.

Table 17: Cost Optimisation

Inputs		MAT (Price)
		Volume (per unit)
		Total amount of CO_2 per unit produced (from CO_2 estimator)
	Initially defined user-defined inputs	Total production quantity
		Recycled material used per unit produced (%)
		Amount of material removed per unit produced during manufacturing (%)
		Manufacturing country (Address)
		Destination of delivery (Address)
		Production rate (units / hour)
		Maximum component cost per unit
		Packaging dimensions (per unit for transportation)
		Ratio of CO_2 to total manufacturing cost per unit (%)
Constraint		Maximum component cost per unit (£)
Outputs		Current cost (optimum for transport cost)
		Suggest alternative MAT (lower £)
		Suggest min. number of units produced (to lower £/unit)
		Suggest different volume (lower £/unit)
		Suggest % of recycled material (lower £/unit)
		Transport method

3.2.2.1 Material Phase

Analysis level: the task in this level is to estimate the initial material cost. The material cost consists of two parts: the cost of virgin material and the cost of the recycled content (%). When the 'recycled content' is equal to 0, it means the virgin material is 100% produced from the raw material. However, if the 'recycled content' is 100, it demonstrates that all materials used are recycled materials. The costs are found as indicated in Equations (3.6) and (3.7).

$$\mathrm{C}_{virgin} = \frac{C_{material}}{(1-R_f)+R_f \times f_{rm}} \times Mass \qquad (3.6)$$

Where,

C_{virgin}, the cost of material (GBP)

$C_{material}$, the price of the raw material (GBP/kg)

R_f, the recycle fraction (0 – 100%)

f_{rm}, the price of the recycled material as fraction of virgin price (Metal Ferrous = 0.93; Non-ferrous = 0.65)

Mass, the mass of the single product or products (kg)

$$C_{grade} = ((1-R_c)\times C_{virgin} + R_c \times C_{virgin} \times f_{rm})\times Mass \quad (3.7)$$

Where,

C_{grade}, the cost of user-defined recycled content (GBP)

R_c, the recycled content (%)

Some materials will be removed during the manufacturing process. The real mass of the material needs to be adjusted. Therefore, a factor needs to be applied to the cost of the material.

$$M_{cf} = \frac{1}{1-removed\%} \quad (3.8)$$

Where,

$removed\%$, the material removed during manufacturing process (%)

M_{cf}, the mass correction factor

The actual material cost now can be found as indicated in the Equation (3.6).

$$C_{total\_material} = \frac{C_{grade}\times M_{cf}}{f_p} - (\frac{M_{cfw}}{f_p} - 1)\times C_{virgin} \times f_{sm} \quad (3.9)$$

Where,

$C_{total\_material}$, the total material cost (GBP)

f_p, the material utilisation fraction, ≈ 1.0

M_{cfw}, the recycle material = M_{cf}, otherwise = 0

f_{sm}, the value of manufacturing scrap as a fraction of the virgin price (Metal Ferrous = 0.49; Non-ferrous = 0.31)

Optimisation level: the task in this level is to optimise the cost either by using the cheaper material or reducing the mass. Reducing the mass of the product is the link to structural optimisation.

3.2.2.2 Manufacture Phase

As the manufacturing location of the product should be decided, the task of this phase is to estimate the cost instead of optimising it. The overhead cost, the tooling cost and the labour cost are the major parts of the Manufacturing cost. However, due to the lack of data, the tooling cost cannot be calculated. The overhead cost is calculated based on the user defined manufacturing location by Equation (3.10). Assuming that the electricity cost is the only overhead cost considered in this phase. The labour cost is part of the cost of the secondary process and is calculated in Equation (3.11). (CES EduPack 2016*)*. The total manufacturing cost is the sum of the overhead cost and the labour cost.

$$C_{overhead} = \frac{1}{\mathrm{P\_}Rate} \times \frac{C_{E\_in\_specified\_country}}{C_{E\_in\_USA}} \times Overhead\_Rate_{USA} \times N_{\mathrm{Pr}oducts} \quad (3.10)$$

Where,

$C_{overhead}$, the total overhead cost (GBP)

$\mathrm{P\_}Rate$, the production rate (units/hr) (Assumption needed)

$C_{E\_in\_specified\_country}$, the cost of electricity in user-defined country (GBP/MJ)

$C_{E\_in\_USA}$, the cost of electricity in the USA = 0.0192 (GBP/MJ)

$Overhead\_Rate_{USA}$, the overhead rate in the USA = 96 (GBP/hr)

$N_{\mathrm{Pr}oducts}$, the number of product(s) (unit) (Assumption needed)

$$C_{labour} = C_{labour\_in\_specified\_country} \times Time \quad (3.11)$$

Where,

C_{labour}, the total labour cost (GBP)

$C_{labour\_in\_specifie\_country}$, the labour cost in the user defined country (GBP)

Time, the hours of labour (hrs). (Assumption needed)

3.2.2.3 Transport Phase

The ideal of the transport phase at the analysis level is to estimate the cost of transport. The cost of transport consists of some aspects such as air freight, ocean freight, truck freight and rail freight. The cost also depends on the distance travelled from the start location to the destination. The start location and the destination are defined by the users. To improve the accuracy of the address, the program works with Google Application Programming Interfaces (APIs). The API key is required for the program to access Google Maps. Once the locations are decided, the program can detect in which continent are the locations. Different transport options will be listed based on the result of the detection. The program has a function to search the closest depot (e.g. airport) around the defined locations (Figure 14) The type of the depot must be identical for both locations so that the distance can be worked out easily. The method for estimating the travel distance is to calculate three sections as expressed in Figure 15:

1. distance from the start location to depot 1which is the closest to the location
2. distance from depot1 to depot 2 which is the closest to the destination
3. distance from depot 2 to the destination.

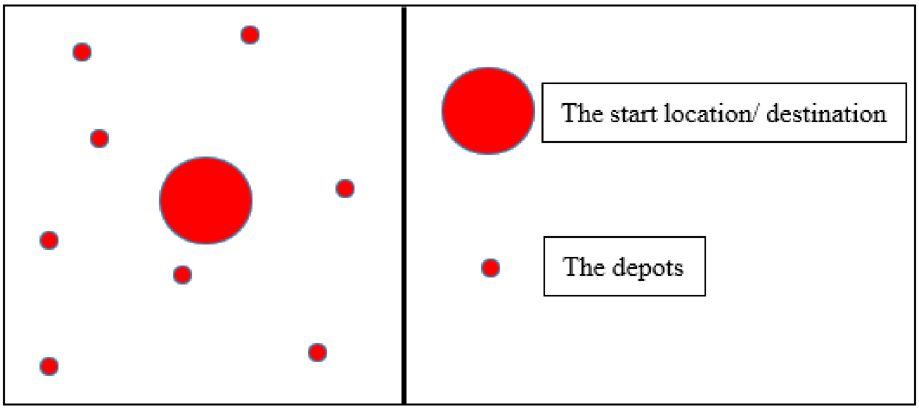

Figure 14: The depots around the locations

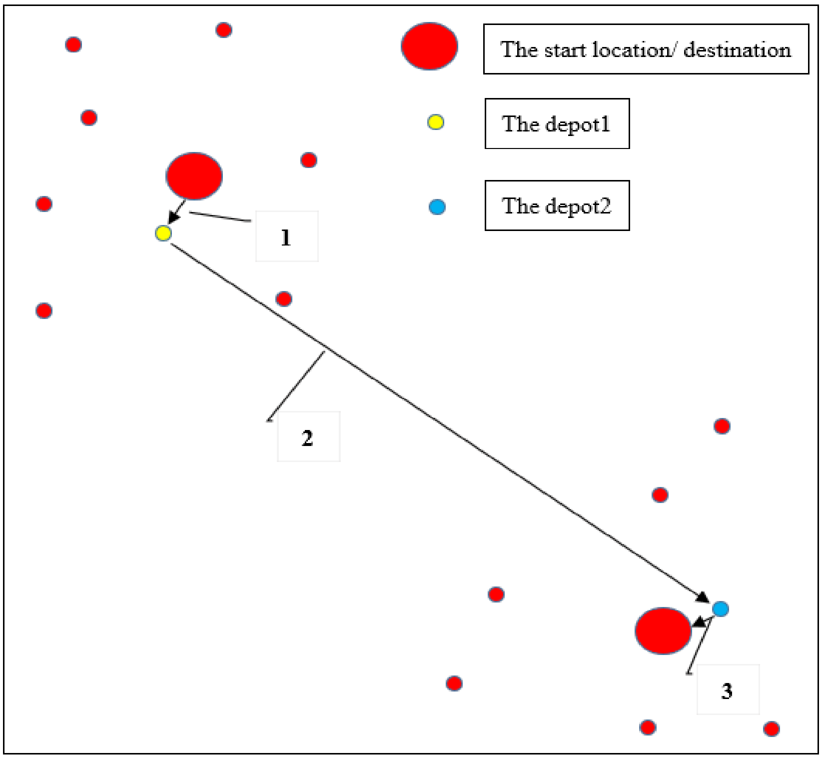

Figure 15: The travel direction and distance

As depot 1 and 2 are very close to the defined locations, the transport method is assumed to be truck freight. In this case, the actual travel route is planned and calculated in Google Maps. Thus, travel distance 1 and 3 can be found. The calculation of distance 2 in Figure 15 is more complicated than the first. For instance, the two depots are on the same continent considering the truck travel distance. If the two depots have a relatively short distance, distance 2 will be calculated based on the actual route planned in Google Maps. If the distance between two depots is significantly long so that Google Maps cannot even plan the route, distance 2 will be calculated as the direct distance (on earth) between the two depots. Similar cases happen when two depots are on different continents. The direct distance between two points on earth is found as indicated in the Haversine formula (3.12) (Veness, C.,2016).

$$a = \sin^2(\Delta\varphi/2) + \cos\varphi_1 \times \cos\varphi_2 \times \sin^2(\Delta\lambda/2)$$
$$c = 2 \times \text{atan2}(\sqrt{a}, \sqrt{(1-a)})$$
$$d = R \times c \tag{3.12}$$

Where,

φ , the latitude of the location

λ , the longitude of the location

R , the radius of the earth, roughly equals to 6371km

d , the distance between two locations

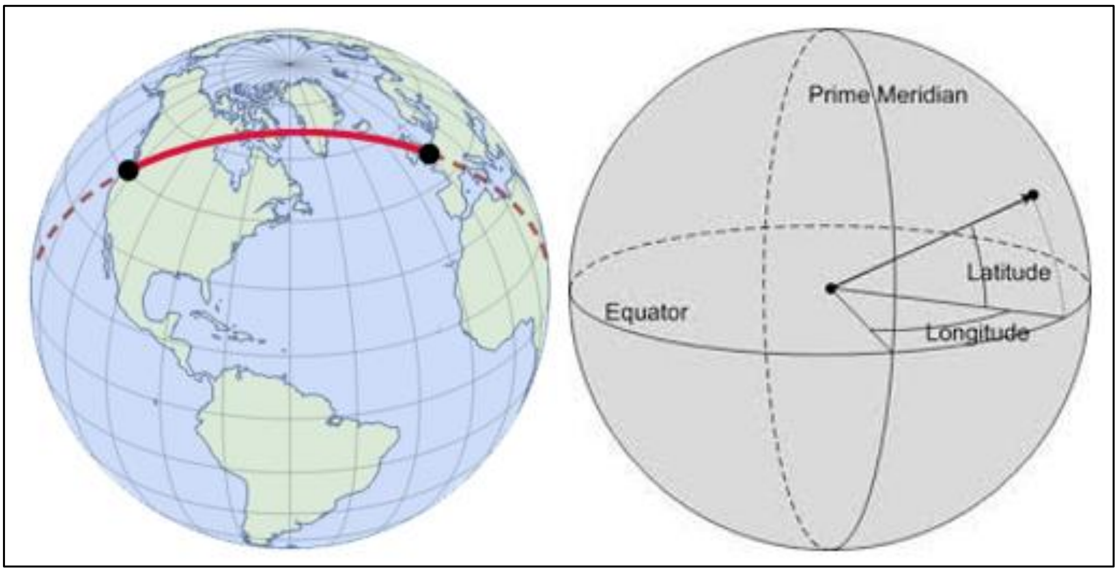

Figure 16: Distance on the Earth (Couture & Jada 2016)

The total distance equals the sum of the three sections in Figure 15. However, the total transport cost needs to be calculated with caution as the freight in the second section could be varied. Therefore, a set of logical rules for the transport is pre-setup for the second section. The program will calculate the cost for the three sections based on the logical rules and compare the total transport cost to select the cheapest combination. The transport cost is determined as indicated in Equation (3.13) (CES EduPack, 2016).

$$M_v = MH \times ML \times MW \times CMD$$
$$C_{trans} = T_1 \times TMASS \times (T_2 + T_3 \times \text{Distance}) \tag{3.13}$$

Where,

M_v, Volumetric Weight (kg)

MH, Maximum height of the packaging (m)

ML, Maximum length of the packaging (m)

MW, Maximum width of the packaging (m)

CMD, Critical min. density

C_{trans}, Transport Cost (GBP)

TMASS, Total Mass (kg)

MASS, Mass (per unit/ component/ product), (kg).

If $MASS > M_v$ $\quad$ $TMASS = MASS \times Qty$,

otherwise $TMASS = M_v \times Qty$

T_1, Correction Factor (%)

T_2, Fixed Cost (GBP/kg/m)

T_3, Variable Cost (GBP/kg/m)

SD, Switch Distance (m)

Distance (d), Distance travelled – if d>SD then d=d, otherwise d=SD (m)

3.2.2.4 End of Life Phase

For the end of life phase, only the cost of disposal is considered. The cost of the end of life potentials is not calculated due to a lack of information. The cost of disposal does not contain any taxes required for disposal in a landfill. The disposal cost is given by (CES EduPack 2016):

$$C_{disposal} = CollectionEnergy \times CollectionFactor \times Mass \tag{3.14}$$

Where,

$C_{disposal}$, Disposal Cost (GBP/kg)

Collection Energy, Energy of collection = 0.2 (MJ/kg)

Collection Factor, Cost conversion factor for collection 0.0205 (GBP/ MJ)

CO_2 Phase

In this phase, the cost of the CO_2 will be calculated based on CO_2 emissions in the material phase, manufacturing phase, transport phase and the end of life phase. According to the EU Emission Trading System (EU ETS), the allowance is about £5.20 per tonne of CO_2 footprint (Ec.europa.eu. 2016). Therefore, the cost of the CO_2 emissions can be found as indicated in Equation (3.15).

$$C_{CO_2} = OneAllowance \times CO_{2\_Total} \tag{3.15}$$

Where,

C_{CO_2}, the cost of the CO2 footprint (GBP)

$OneAllowance$, the price of one tonne CO2 footprint (GBP/tonne)

CO_{2_Total}, the total amount of CO2 emission (tonne)

3.2.3 CO_2 Module (CO2)

CO_2 emissions are of significant concern to industrialists and manufacturers. They are keen to reduce CO_2 emissions to comply with the relevant regulations such as those from the EU Commission. According to the EU ETS, each company/ industry will have a CO_2 emissions allowance. The CO_2 estimation is the function of this module at the analysis level. The CO2 module optimises the CO_2 footprint of the product in terms of material, manufacturing, transportation, etc.

Table 18: CO_2 Optimisation

Inputs	MAT (CO_2, Energy)	
	Volume (per unit)	
	Total amount of cost per unit produced (from the cost estimator)	
	Initially defined user-defined inputs	Total production quantity
		Recycled material used per unit produced (%)
		Amount of material removed per unit produced during manufacturing (%)
		Manufacturing country (Address)
		Destination of delivery (Address)
		Production rate (units / hour)
		Maximum component CO_2 per unit
		Packaging dimensions (per unit for transportation)
Constraint		Maximum component cost per unit (£)
Outputs		Current CO_2 (optimum for transport CO_2)
		Suggest alternative MAT (lower £)
		Suggest min. number of units produced (to lower £/unit)
		Suggest different volume (lower £/unit)
		Suggest % of recycled material (lower £/unit)
		Transport method

3.2.3.1 Material Phase

The CO_2 emission in this phase consists of two parts: the CO_2 footprint of the recycled content and the recycling of the manufacturing waste. The CO_2 emission of the two parts can be found as indicated in Equations (3.16) and (3.17) (CES EduPack 2016).

$$CO_{2\_grade} = ((1-R_f)\times CO_{2\_\mathrm{Primary}} + R_f \times CO_{2\_\mathrm{recycling}})\times Mass \tag{3.16}$$

Where,

R_f, the recycle fraction (0 – 100%)

$CO_{2\_\mathrm{recycling}}$, the CO_2 footprint, recycling (kg/kg)

CO_{2_Primary}, the CO_2 footprint, primary production (kg/kg)

Mass, the mass of a single product or products (kg)

CO_{2_grade}, the CO_2 footprint of the recycled content (kg)

$$CO_{2\_waste\_recycling} = (CO_{2\_recycling} - CO_{2\_grade})\times Mass \tag{3.17}$$

Where,

$CO_{2\_waste\_recycling}$, the CO_2 footprint of the manufacturing waste recycling (kg)

Hence, the total material CO_2 footprint can be found as indicated in Equation (3.18).

$$CO_{2\_material\_total} = CO_{2\_grade} \times M_{cf} + CO_{2\_waste\_recycling} \times (M_{cf} - 1) \tag{3.18}$$

3.2.3.2 Manufacture Phase

Based on the literature review, the side impact beam is made with the rolling form process. In this case, the CO_2 emission is from that process, and the value is calculated with Equation (3.19) (CES EduPack*,* 2016).

$$CO_{2\_Manufacture} = (CO_{2\_\mathrm{Primary}} \times M_{cf} + CO_{2\_\mathrm{Rolling\_Form}} \times (M_{cf} - 1)) \times Mass \tag{3.19}$$

Where,

$CO_{2\_Manufacture}$, the CO_2 footprint of the manufacturing product (kg)

$CO_{2\_\mathrm{Rolling\_Form}}$, the CO_2 footprint of the rolling form process (kg/kg)

Mass, the mass of a single product or products (kg)

3.2.3.3 Transport Phase

The CO_2 footprint in this phase depends on the actual distance travelled and the freight method used. The calculation of the distance uses the same method as the cost optimisation module. The total transport CO_2 footprint is indicated by Equation (3.20).

$$CO_{2\_trans} = H_{trans} \times TMASS \times CO_{2\_trans\_method} \times \mathrm{Distance} \tag{3.20}$$

Where,

CO_{2_trans}, the total CO_2 footprint of the transport phase (kg)

H_{trans}, the available transport option and associated energy (MJ/kg/m)

$TMASS$, the total mass of product(s) (kg)

$CO_{2\_trans\_method}$, the available transport option and the associated CO_2 footprint (kg/MJ)

Distance (d), Distance travelled (m)

3.2.3.4 End of Life Phase

Products are collected and sorted when they reach the end of their lives. The disposal of CO_2 emissions depends on the end of life options. The common Equation (3.21) is defined as:

$$H_{disposal} = (H_c + H_{ps} + H_{ss}) \times \%\text{recovered} + \text{H}_c \times (1 - \%\text{recovered})$$
$$CO_{2\_disposal} = \alpha \times H_{disposal} \times Mass \qquad (3.21)$$

Where,

% recovered, the material recovered from disposal, assuming 100% in this study

H_c, Embodied energy, collection (MJ/kg)

H_{ps}, Embodied energy, primary sorting (MJ/kg)

H_{ss}, Embodied energy, secondary sorting (MJ/kg)

α, kg (CO_2)/MJ = 0.07

$H_{disposal}$, Energy of collection (MJ/kg)

Mass, the mass of a single product or products (kg)

$CO_{2\_disposal}$, CO_2 footprint of collection (kg)

Table 19: Summary of Energies Associated with End of Life Options (CES EduPack, 2016)

	Collection Energy H_c (MJ/kg)	Primary Sorting Energy H_{ps} (MJ/kg)	Secondary Sorting Energy H_{ss} (MJ/kg)
Comminution	0.2	0.3	-
Reprocess	0.2	0.3	-
Recycle	0.2	-	0.5
Remanufacture	0.2	-	-

The CO_2 emission of each end of life attribute is calculated based on the data in Table 19. After collecting and sorting, the product will be processed in the available end of life option. The total CO_2 emission in each option is found as indicated in the following equations.

- For Comminution:

$$\text{CO}_{2\_\text{CommninutionDisposal}} = (H_c + H_{ps}) \times \%\text{recovered} \times \text{Mass} \times \alpha$$
$$\text{CO}_{2\_\text{Comminution}} = \text{CO}_{2\_\text{CommninutionDisposal}} + (-0.1 \times \%\text{recovered}) \times \text{Mass} \times \alpha \qquad (3.22)$$

Where,

$\text{CO}_{2\_\text{CommninutionDisposal}}$, the disposal CO_2 footprint of the comminution (kg)

Mass, the mass of a single product or products (kg)

$\text{CO}_{2\_\text{Comminution}}$, the total CO_2 footprint of the comminution (kg)

- For Reprocess:

$$\text{CO}_{2\_\text{ReprocessDisposal}} = (H_c + H_{ps}) \times \%\text{recovered} \times \text{Mass} \times \alpha$$
$$\text{CO}_{2\_\text{Reprocess}} = \text{CO}_{2\_\text{ReprocessDisposal}} + (\text{CO}_{2\_\text{recycling}} - \text{CO}_{2\_\text{primary\_production}}) \times \text{Mass} \times \beta \qquad (3.23)$$

Where,

$\text{CO}_{2\_\text{ReprocessDisposal}}$, the disposal CO_2 footprint of the reprocess (kg)

$\text{CO}_{2\_\text{recycling}}$, the CO_2 footprint of recycling (kg/kg)

$CO_{2\_primary\_production}$, the CO_2 footprint of primary production (kg/kg)

β , the reprocess factor for metal = 0.5

$CO_{2\_Reprocess}$, the total CO_2 footprint of the reprocess (kg)

- For Recycle:

$$\begin{aligned} CO_{2\_Recycle\_Disposal} &= (H_c + H_{ss}) \times \%\text{recovered} \times \text{Mass} \times \alpha \\ CO_{2\_Recycle} &= CO_{2\_Recycle\_Disposal} + (CO_{2\_recycling} - CO_{2\_primary\_production}) \times \text{Mass} \end{aligned} \tag{3.24}$$

Where,

$CO_{2\_Recycle\_Disposal}$, the disposal CO_2 footprint of the recycle process (kg)

$CO_{2\_Recycle}$, the total CO_2 footprint of the recycle process (kg)

- For Remanufacture:

$$\begin{aligned} CO_{2\_Remanufacture\_Disposal} &= H_c \times \%\text{recovered} \times \text{Mass} \times \alpha \\ CO_{2\_Remanufacture} &= CO_{2\_Remanufacture\_Disposal} + CO_{Re\text{-}work} \times \text{Mass} \times \alpha \end{aligned} \tag{3.25}$$

Where,

$CO_{2\_Remanufacture\_Disposal}$, the disposal CO_2 footprint of the remanufacture (kg)

$CO_{Re\text{-}work}$, the CO_2 footprint of the re-work process (kg/kg)

$CO_{2\_Remanufacture}$, the total CO_2 footprint of the remanufacture process (kg)

- For reuse and landfill, both options have no further processes required. Therefore, there is no more additional energy or environment impact. In this case, both options are not considered in this module.

3.3 Module Validation and Verification

The three parametric modules defined in the previous section will subsequently be used to create the holistic optimisation programmes. Before this is done the development, programming and initial validation/verification of the individual modules will be discussed in this section. Firstly, a database is required for running the three parametric modules. This database contains a number of parameters which will be used as the inputs for the relevant calculations defined in section 3.2. In this study, the database was created for two specific components; a side impact beam and a lower engine mount, as shall be introduced in Chapter 4 and Chapter 5. It is envisaged that the database may be extended at a later stage to cater for other scenarios. The database files are illustrated in Figure 17. The three modules will extract the relevant parameters from the individual files during the optimisation process.

1	CitiesAndCountries.csv
2	countriesandcontinents.csv
3	Materials.csv
4	OverheadCost.csv
5	LabourCost.csv
6	TransportEnergy.csv
7	TransportFactor.csv

Figure 17: The database for the three parametric modules

Files 1 and 2 in Figure 17 contains the parameters for calculating the travel distances used in the COST and the CO2 modules. The end-user must select two locations from the list of cities/ countries as the location of production and the final destination which will be used to calculates the travel distance. File 3 contains the material data, e.g. volumetric mass density, Young's Modulus etc. The STRUCTURAL module will utilise this data along with the FE model in HyperMesh to optimise the geometry of the product. File 3, 'Materials.csv', will also be utilised in the COST module and CO2 modules. Files 4 and 5 contain the overhead cost and labour cost of the countries listed in files 1 and 2. These two types of costs are used during the manufacturing cost calculations in the COST module. The data in files 6 and 7 are used to calculate the cost and CO_2 of the transportation phase in both the COST and CO2 modules respectively.

Using the database files, the coding and initial verification of the three individual modules will be presented in the following three subsections.

3.3.1 STRUCTURAL Module

For the STRUCTURAL module, the core is to optimise the structure of a component/ product using size-optimisation. As discussed in subsection 3.2.1, size optimisation can be completed using HyperMesh. The drawback of using this commercial solver is that it is not possible to alter input materials automatically. Therefore, the STRUCTURAL module used PowerShell to extract data of materials from the database and input data into HyperMesh for optimisation. After optimisation, the programme created in PowerShell will read the results from the '.out file' of HyperMesh for further analysis. The STRUCTURAL module is divided into three distinct phases:

1. Data input (pre-processing)
2. HyperMesh (optimisation)
3. Results reading (post-processing)

Figure 18 represents a simplified flowchart of the three phases of the STRUCTURAL module. In phase 1 the material data, e.g. Young's Modulus, is read from the database files in Figure 17 and input into the Optistruct FE file.

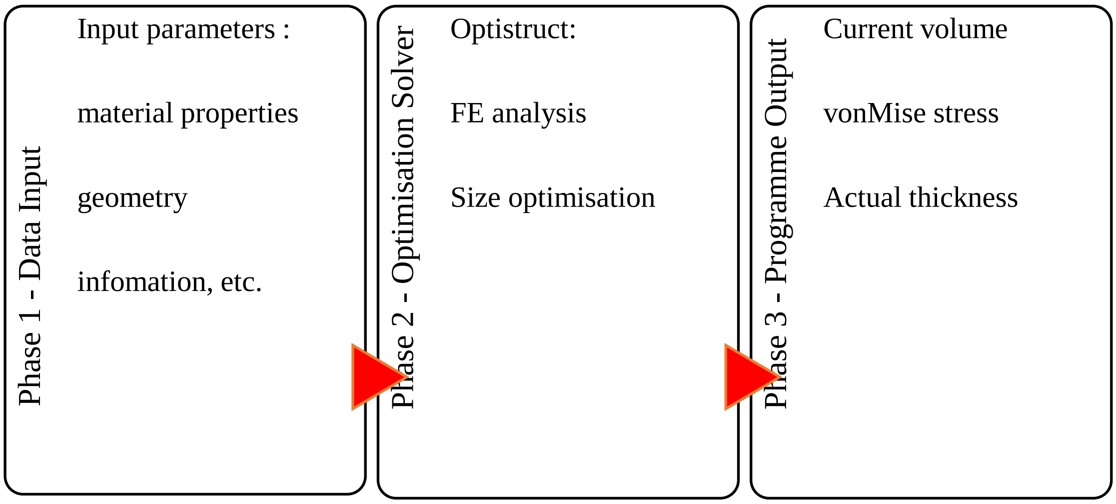

Figure 18: Simple Flowchart of STRUCTURAL Module

In the second phase of the STRUCTURAL module, the optimisation solver, Optistruct, optimises the FE model created based on the user-defined optimisation criteria including objective and constraints as outlined in Table 15.

The third phase of the STRUCTURAL module reads and processes the following data from the Optistruct output files:

1. Current component volume
2. Maximum Von Mises stress
3. Current component thickness

As the “central” phase of the STRUCTURAL module is the commercial FE solver Optistruct it is rational to assume that the calculations from the solver will be accurately provided, the input FE model is set up appropriately and correctly. The verification of the STRUCTURAL Module (SM), therefore, focused on ensuring that the changes to input (phase 1, Figure 18) and reading outputs (phase 3, Figure 18) are correct. The focus of the verification process was therefore done by comparing results to Hand-Calculations (HC) of a simply supported beam subjected to a uniformly distributed load. The objective is to optimise the volume of the structure by minimising the thickness. The thickness of this beam can also be calculated with the equation (3.2). The cross-section of the beam and corresponding calculations are detailed in Appendix B. Table 20 contains the numerical data from the STRUCTURAL Module (SM) and Hand-Calculations (HC) of the simply-supported beam using 11 different input materials from the database.

Table 20: Example of the Validation based on the Simplistic Database

Material	Component Thickness			Maximum Von Mises Stress			Average Difference
	SM	HCs	Difference	SM	HCs	Difference	
High Alloy Steel AcerMet100	1.30	1.31	0.8%	319	319	0.0%	0.4%
Medium Alloy Steel AMS6485	1.30	1.31	0.8%	319	319	0.0%	0.4%
Low Alloy Steel AISI4620	1.30	1.31	0.8%	319	319	0.0%	0.4%
Low Carbon Steel AISI1010	1.32	1.32	0.0%	315	314	0.3%	0.2%
Medium Carbon Steel AISI1080	1.30	1.31	0.8%	319	319	0.0%	0.4%
High Carbon Steel AISI1144	1.30	1.30	0.0%	319	319	0.0%	0.0%
High Strength Steel S550MC	1.30	1.30	0.0%	319	319	0.0%	0.0%
Structural Steel S275N	1.55	1.55	0.0%	273	274	0.4%	0.2%
Aluminium 5182H34	1.42	1.41	0.7%	295	294	0.3%	0.5%
Aluminium 6111T62	1.30	1.30	0.0%	319	320	0.3%	0.2%
Aluminium 6063T5	1.30	1.30	0.0%	125	124	0.8%	0.4%
Average Difference			0.4%			0.2%	0.3%

As Table 20 reveals, the maximum difference between HCs and the SM is 0.8% with average differences of no more than 0.4%. These values are of such low magnitude to successfully verify the outputs of the structural module.

3.3.2 COST Module

In this subsection, the setup and programming of the COST module based on the equations in subsection 3.2.2 will be introduced. The COST module considers four aspects:

1. Material
2. Manufacturing
3. Transport
4. End of life

The validation method used for each of the four aspects was the same as the one used for the STRUCTURAL module namely hand calculations, based on the simply supported beam in Appendix B. As there were four aspects of the COST module, the validation was applied to each aspect individually. In the validation of each aspect, there were three variations for the input parameters. The aim is to find out whether the module provides correct outputs as a function of input parameter variation.

For validation of the first parameter, the input material was varied. The results of both the COST module and hand calculations are summarised in Table 21.

Table 21: Validation of Material Aspect for COST Module

Input Material	Cost (GBP/unit)		
	COST Module	Hand calculations	Difference
HighAlloySteelAcerMet100	0.140	0.141	0.20%
HighStrengthSteelS550MC	0.144	0.142	1.37%
Aluminum6111T62	0.146	0.147	0.26%
Average difference			0.61%

As listed in Table 21, the maximum difference found is 1.37% with an average difference of 0.61%. It is found that the difference between COST module and hand calculations is less than 2%. Therefore, the programme of the material aspect for COST module was correctly created.

For manufacturing and transport aspects, both aspects were influenced by the country of production and destination. For manufacturing, the country of production will influence the overhead cost and labour cost, i.e. both costs are part of the manufacturing cost. For transport, the two locations will influence the travel distance, transportation method, etc. The results were summarised in Table 22.

Table 22: Validation of Manufacturing and Transport for COST Module

Country of production - Destination	Manufacturing (GBP/unit)		
	COST Module	Hand calculations	Difference
Coventry, USA - Coventry, UK	0.16	0.16	0.00%
Shanghai, China - Coventry, UK	0.01	0.01	0.00%
Tokyo, Japan - Coventry, UK	0.01	0.01	0.00%
Average			0.00%
Country of production - Destination	Transport (GBP/unit)		
	COST Module	Hand calculations	Difference
Coventry, USA - Coventry, UK	0.29	0.29	0.64%
Shanghai, China - Coventry, UK	0.19	0.19	0.81%
Tokyo, Japan - Coventry, UK	0.48	0.48	0.03%
Average			0.49%

By observing Table 22, it is found that the outputs between COST module and hand calculations have no difference. The maximum difference for transport is 0.81% with an average difference of 0.49%. The differences for both manufacturing and transport are low magnitude which indicates that programmes for both manufacturing and transport were correctly designed. For the end of life, the results are summarised in Table 23.

Table 23: Validation of End of Life for COST Module

Input Material	End of life (GBP/unit)		
	COST Module	Hand calculations	Difference
HighAlloySteelAcerMet100	0.05	0.05	0.00%
HighStrengthSteelS550MC	0.05	0.05	0.00%
Aluminum6111T62	0.05	0.05	0.00%

The difference between COST module and hand calculation is 0. This is not a surprise as the cost of this aspect was calculated based on the disposal option only (consists of two constants as demonstrated in subsection 3.2.2).

3.3.3 CO2 Module

The validation method for CO2 module used hand calculation based on the equations defined in subsection 3.2.3. Similar to the COST module, the CO2 module also contains four aspects:

1. Material
2. Manufacturing
3. Transport
4. End of life

The basic setup of the validation method for each aspect is also similar to the COST module. For material, the results of both hand calculations and CO2 module were summarised in Table 24. By observing Table 24, the maximum difference of CO_2 footprint between CO2 module and hand calculations is 0.85% (low magnitude) with an average difference of 0.33%. This indicates the programme of material aspect for CO2 module was accurately created.

Table 24: Validation of Material Aspect for CO2 Module

Input Material	CO_2 (kg/unit)		
	CO2 Module	Hand calculations	Difference
HighAlloySteelAcerMet100	1.18	1.17	0.85%
HighStrengthSteelS550MC	0.84	0.84	0.00%
Aluminum6111T62	4.24	4.23	0.14%
Average			0.33%

Different from the COST module, the manufacturing part of the CO2 module is influenced by the material. The results are summarised in Table 25. From Table 25, it is found that the maximum difference of results between the CO2 module and hand calculation is 0.33% with an average difference of 0.24%. This verifies the CO_2 footprint of manufacturing part for the CO2 module.

Table 25: Validation of Manufacturing Aspect for CO2 Module

Input Material	Manufacturing (kg/unit)		
	CO2 Module	Hand calculations	Difference
HighAlloySteelAcerMet100	1.360	1.365	0.33%
HighStrengthSteelS550MC	0.960	0.959	0.14%
Aluminum6111T62	4.830	4.842	0.24%
Average			0.24%

The CO_2 footprint for transport part of the CO2 module is still influenced by the travel distance, i.e. country of production and destination. The corresponding outputs for CO2 module and hand calculations are summarised in Table 26. The maximum difference in results between CO2 module and hand calculations is 0.67% with an average difference of 0.26% as illustrated in Table 26. This indicates that the transport part was correctly created and the outputs of this part have been verified.

Table 26: Validation of Transport Aspect for CO2 Module

Country of production - Destination	Transport (kg/unit)		
	CO2 Module	Hand calculations	Difference
Coventry, USA - Coventry, UK	0.69	0.69	0.67%
Shanghai, China - Coventry, UK	1.12	1.12	0.09%
Tokyo, Japan - Coventry, UK	1.16	1.16	0.02%
Average			0.26%

The CO_2 footprint of the end of life aspect was related to the material. Therefore, the validation was based on the variation of materials. The results are summarised in Table 27. In Table 27, the results of both CO2 module and hand calculations are negative values as the end of life process was to save CO_2 footprint. The maximum difference in results between the CO2 module and hand calculations is 0.27% with an average difference of 0.18%. Both values are very small which indicates the output of this part for CO2 module was verified successfully.

Table 27: Validation of End of Life Aspect for CO2 Module

Input Material	End of life (kg/unit)		
	CO2 Module	Hand calculations	Difference
HighAlloySteelAcerMet100	-0.940	-0.943	0.27%
HighStrengthSteelS550MC	-0.660	-0.661	0.19%
Aluminum6111T62	-3.620	-3.617	0.07%
Average			0.18%

Within this section, the three parametric modules were validated by the hand calculations. It was found that the difference in results between each module and corresponding hand calculations was very small, i.e. the maximum difference is less than 2%. The low magnitude of the differences indicates that the three modules were verified successfully. The validated modules were subsequently used to form the creation of the holistic optimisation programmes as shall be discussed in the next section.

3.4 General Types of Holistic Optimisation

Two general types of holistic optimisation algorithms are introduced in this section: Sequential (SEQ) and Parallel (PAR). Each type of the optimisation contains three modules as defined in section 3.2. The first sub-section will introduce the SEQ optimisation. The second sub-section will introduce the PAR optimisation. The last sub-section contains two general types of iteration loops for both SEQ and PAR optimisations.

3.4.1 Sequential Optimisation (SEQ)

The idea of an SEQ optimisation is to optimisation CO2, COST and STRUCTURAL modules sequentially. The flowchart in Figure 19 shows one example of SEQ optimisation sequences.

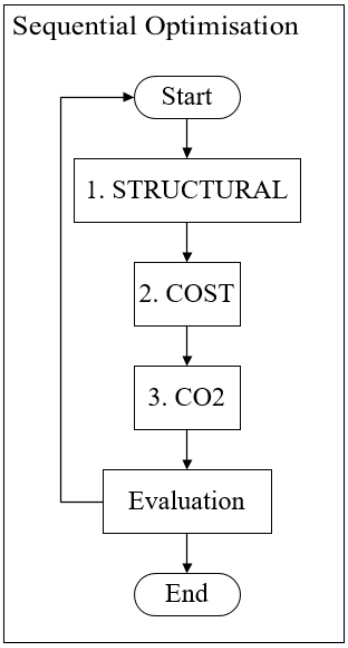

Figure 19: Simple Flowchart of SEQ Optimisation

The sequence of SEQ optimisation is a permutation problem which tries to find out the method to arrange the position of the three modules. If there are n elements that need to be arranged, it will have $n!$ arrangements. It's the factorial (Singh, K., 2011). The equation is expressed in Equation (3.26).

$$n! = 1 \times 2 \times 3 \times 4 \times \cdots \times (n-1) \times n \tag{3.26}$$

The number of sequences for COST, CO2 and STRUCTURAL modules is found by:

$$3! = 1 \times 2 \times 3 = 6 \tag{3.27}$$

All 6 Optimisation Module Sequences (OMS) are defined in Table 28. Each module has the same possibility to be optimised at each position (1, 2 and 3) in Figure 19.

Table 28: Sequences of Three Modules

OMS 1	OMS 2	OMS 3
COST	COST	CO2
CO2	STRUCTURAL	COST
STRUCTURAL	CO2	STRUCTURAL
OMS 4	**OMS 5**	**OMS 6**
CO2	STRUCTURAL	STRUCTURAL
STRUCTURAL	COST	CO2
COST	CO2	COST

The 5th sequence in Table 28 is the SEQ optimisation in Figure 19 and its simplified flowchart is illustrated in Figure 20. The first three steps (1 - 3) represent Finite Element analysis in the STRUCTURAL module, outputs such as the optimum geometry, current maximum displacement, current volume, etc., are calculated. The information from the STRUCTURAL module will be pass to the COST module (Step 4 - 6) for further optimisation. The initial cost per unit will be calculated and compared with the constraint limit. The program will detect if the criterion has been met. If yes, the outputs will be passed to the CO2 module. If not, the program will further optimise the product using an alternative material, a new production quantity or a new percentage of recycled material. After the further optimisation, the current outputs will be passed to the CO2 module. In the CO2 module (Steps 7 - 9), the current CO_2 footprint per unit is calculated and compared with the constraint limit. The objective function value will then be evaluated (Step 10). If the criterion has been met, the optimisation will end (Step 11). If not, the program will further check if the maximum iteration has been met (Step 12). If the current iteration has met its upper limit, then the optimisation will stop and output the current solution. If the solution does not meet the criterion and the current iteration does not meet its upper limit, a new iteration will start (Step 12-1).

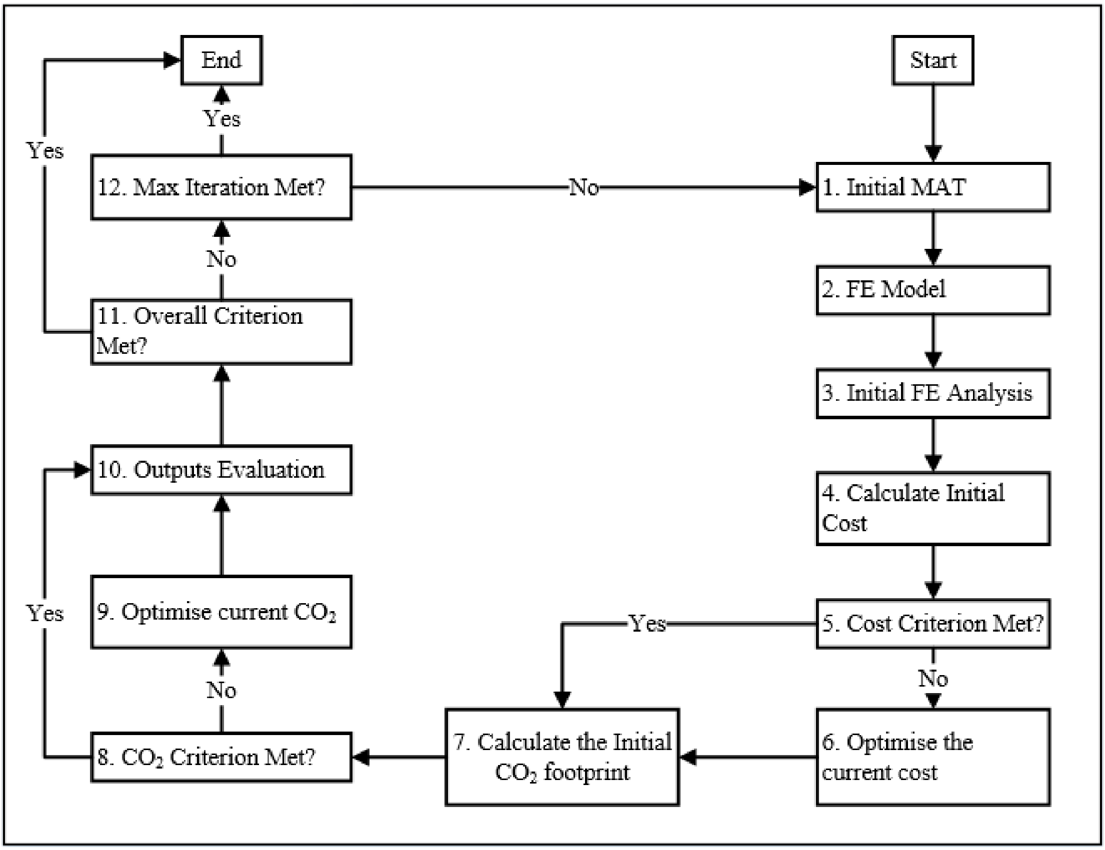

Figure 20: The simplified flowchart of an SEQ optimisation

3.4.2 Parallel Optimisation (PAR)

The PAR optimisation optimises the COST, CO2 and STRUCTURAL modules simultaneously and independently as illustrated in Figure 21.

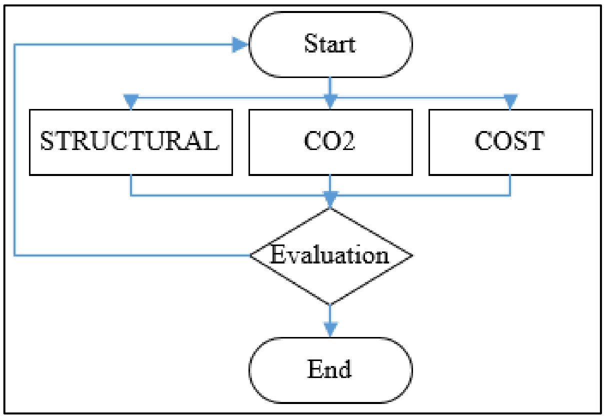

Figure 21 Simple flowchart of PAR optimisation

A detailed flowchart is illustrated in Figure 22 to show how the PAR optimisation works. In Figure 22, the **horizontal** box represents each major **Step** in the flowchart while the **vertical** box represents the optimisation **Route** or path starting with a different module.

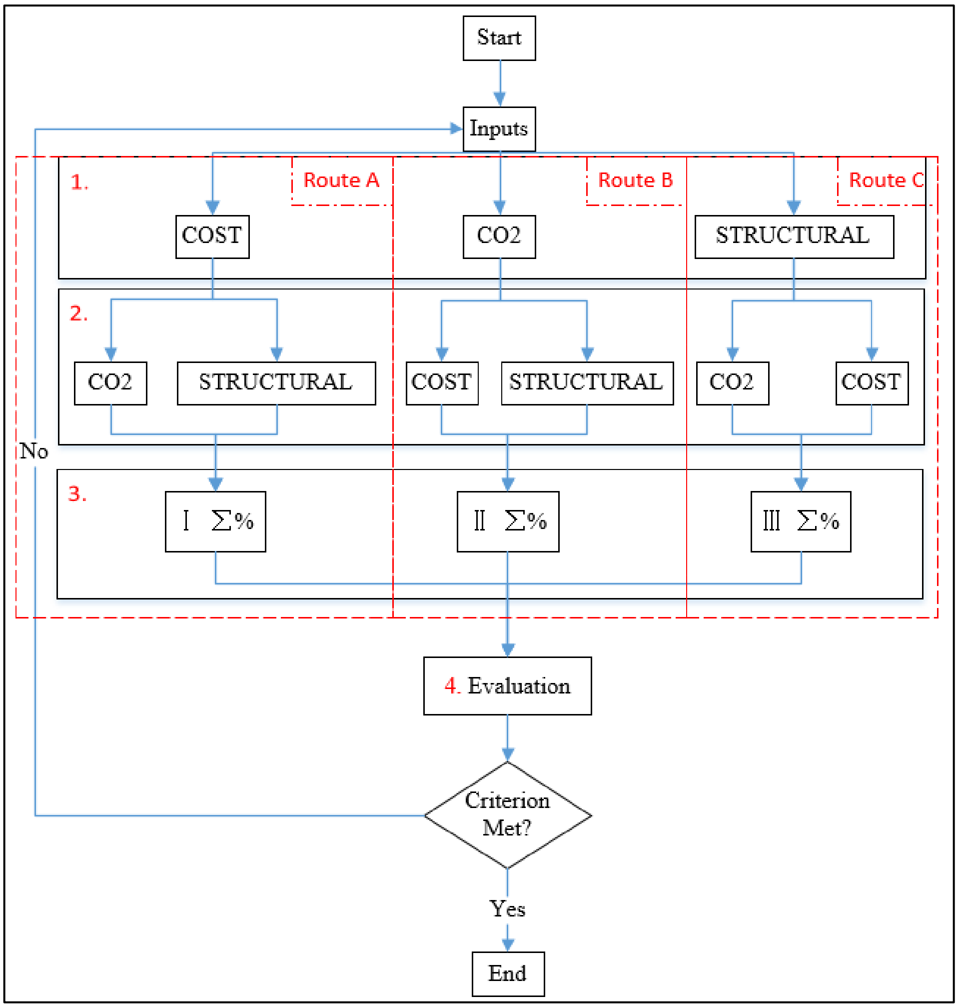

Figure 22: The detailed flowchart of PAR optimisation

When the three modules are optimised simultaneously and independently, the output of each module may have a conflict(s). For instance, in Figure 22 the output of the COST module shows Low Carbon Steel gives optimum cost, the output of CO2 shows Aluminium gives optimum CO_2 and the output of STRUCTURAL shows Titanium gives optimum volume (Step 1). To determine which material is the best for 'Holistic', the program will use each material as input for the other two modules (Step 2). For example, the Low Carbon Steel from the COST module will be put into the CO2 and STRUCTURAL modules to estimate the CO_2 footprint and volume. The same procedure is also used in the other two routes. Now, each route should have one objective function value from Step 1 and two estimations from Step 2 as illustrated in Table 29.

Table 29: Conflict solving in PAR optimisation

Route	**A**	**B**	**C**
Start Modules	**COST**	**CO2**	**STRUCTURAL**
Step 1	optimum cost	optimum CO_2	optimum volume
Material	Low Carbon Steel	Aluminium	Titanium
Step 2	estimated CO_2	estimated cost	estimated cost
	estimated volume	estimated volume	estimated CO_2

Both objective function value and estimations in each route will be compared with the initial cost, CO_2 and volume to find out the differences. The summation of differences in each route represents how much the objective has been improved based on different materials (Step 3).

Table 30: Individual evaluation example - PAR

Route	**A**	**B**	**C**
Step 3	30% cost improvement	30% CO2 improvement	30% volume improvement
	12% CO2 improvement	20% cost improvement	5% cost improvement
	15% volume improvement	15% volume improvement	50% CO2 improvement
Sum	57% improvement	65% improvement	85% improvement

There are three summations as tabulated in Table 30. In Table 30, it is found that route C made the most improvement (85%) with Titanium (Step 4). Therefore, the output of each module in route C is selected as the current solution. If the current solution does not meet the criterion and the current iteration does not reach the max. iteration number, the optimisation will go to the next iteration. If the current solution has met the criterion or the current iteration reaches the max. iteration number, the optimisation will terminate.

3.4.3 Iteration Loops of Optimisations

There are two different setups for the iteration loops: Single Inner Iteration (SII) and Multi-Inner Iterations (MII). The SII is very straightforward in that each optimisation will only run one inner iteration in each module. On the other hand, the MII will run multiple inner iterations in each module. Naturally, the MII optimisation will produce a better optimum solution than the SII optimisation as more iterations leads to further optimisation. However, if the first iteration has already produced the optimum, MII and SII will make no difference. The MII and SII loops will be applied to both the SEQ and PAR optimisations. The aim of setting different iteration loops is to find out if there is any huge difference between the results accordingly. Furthermore, analysis of the two types of iteration loops can potentially improve the accuracy for users to set up the appropriate iteration number and reduce the CPU time for optimisations.

3.5 Design of the Case Study

To define the most efficient method for holistic optimisation, a series of case studies has been designed. The overall purpose of case studies is to determine the general trends of the optimisations, identify pitfalls, pros and cons, etc. The first sub-section introduces major parameters analysed in the case studies. The second sub-section introduces the setup of the case studies.

3.5.1 Influential Parameters

Case studies are used to find out how parameter(s) variation influences the objective function value of each optimisation. Input parameters that can influence the objective function value are considered as potentially sensitive parameters. The eight influential parameters are tabulated in Table 31. The parameters will be analysed one at a time (OAT) and two at a time (TAT). The OAT method will assess the sensitivity of the individual parameter while the TAT method will assess the sensitivity of a combo of two parameters.

Table 31: Potential sensitive parameters

1. Geometry	2. Production Quantity	3. Recycled Content (%)	4. Maximum component cost (GBP/unit)
5. Maximum component CO_2 (kg/unit)	6. Travel Distance (km)	7. Labour Cost (GBP/hr)	8. Overhead cost (GBP/MJ)

- The geometry represents the 'core' of a product. The variation of the geometry will influence the results of the structural optimisation for the product. It is assumed that there are three different initial geometries of the product for the studies in the next two chapters. It should be noted that the geometry is considered as a single "variable" of the optimisation in this research. This indicates that the three initial geometries represent the variations of a variable which contains the original, variation 1 and variation 2. How the variation of the geometry influences optimum solutions will be found out in the next two chapters subsequently.
- The production quantity represents the total number of products. It is set up to 400 initially. As a discrete parameter, it will apply a 100% increment to the previous quantity: 800 (400+400), 1600 (800+800) and 3200 (1600+1600).
- The recycled content represents how much recycled material is added to the product. If the value of recycled content is zero, then the product is fully made of virgin material. If the value is 100%, then product is fully made of recycled material. Based on Equations (3.7) and (3.16), different levels of recycled content lead to a different level of cost spent on the product and CO_2 released to the atmosphere. The value of the recycled content is increased from 10% to 90% with a constant increment of 20%.
- The maximum cost and the maximum CO_2 are the two constraint limits of the optimisation. Obviously, these two limits relate to the COST and CO2 modules. The initial value of maximum cost and CO_2 are 10 GBP/ unit and 1.5 kg/ unit. To find out how these two constraint limits influence the optimisation results, the cost limit will decrease from 10 GBP/ unit to 2 GBP/ unit with a constant decrement of 2 GBP/ unit. The initial CO_2 limit will decrease by 2/3 (1.0 kg/unit) and 1/3 (0.5 kg/unit).
- Travel distance represents the total distance between the country of production and the destination. The equations to calculate travel distances can be found in section 3.2.2.3. The travel distance relates to both the COST and CO2 modules as it influences the

transportation cost and the CO_2 footprint. To find out how the travel distance influences the optimum solution, the case study contains three types of distances including the extreme cases: the longest, the medium and the shortest distances. The extreme cases are used to find out the fluctuation/ spread (max-min) between the optimisation results of the extreme points. If the fluctuation/ spread is very small, the optimisation result is not sensitive to the travel distance. If the fluctuation/ spread is large, the optimisation result is sensitive to the travel distance.

- The labour cost and overhead cost are part of the manufacturing costs relating to the COST module. The labour cost represents the local labour cost in the country of production. The overhead cost represents the electricity cost in the country of production. The labour cost and overhead cost also use the extreme cases (i.e. the lowest to the medium and the highest) to analyse their sensitivity. The ideology of the extreme cases is defined the same as the travel distance.

3.5.2 The Case Study Setup

A list of 33 case studies has been set up to assess the sensitivity of the parameters tabulated in Table 31. The case studies are tabulated and attached in Appendix – C. An example of the first case study is indicated in Table 32. In this table, models 1 – 3 represent the variation of a parameter (Geometry). This case study analyses how the change in geometry influences the optimisation result. The case study list is used for both the SEQ and PAR optimisations.

Table 32: Example of the first case study

Case Study No.	**1**		
Model No.	**1**	**2**	**3**
Geometry	a	b	c
Production Quantity	400	400	400
Recycled Content (%)	10	10	10
Maximum component cost (GBP/unit)	10	10	10
Maximum component CO_2 (kg/unit)	1.5	1.5	1.5
Travel Distance (km)	Long	Long	Long
Labour Cost (GBP/hr)	Medium	Medium	Medium
Overhead cost (GBP/MJ)	Medium	Medium	Medium

The case study list consists of two parts: the analysis of influential individual parameters and the analysis of influential multiple parameters. The idea to assess the most influential individual parameter is to change One parameter at A Time (OAT) while fixing the value of the other parameters. As defined in Table 31, there are eight major influential parameters. To assess the most influential individual parameter, each of the eight parameters requires an individual case study using the OAT method. The first 8 case studies are individual parameter analyses with the OAT method. The method is used in the second part to analyse Two parameters at A Time (TAT). This analysis required a matrix to work out every possible combination of these two parameters defined in Table 31. As the change of travel distance will influence extreme cases for both labour costs and overhead costs simultaneously, these three parameters therefore will not have combinations in multiple parameters analysis. The matrix of the parameters then becomes 5 x 8 instead of 8 x 8 as indicated in Table 33.

Table 33 Combination matrix of parameters

Parameters	Geometry	Production Quantity	Recycled Content (%)	Max cost (GBP/unit)	Max CO2 (kg/unit)
Geometry					
Production Quantity	9				
Recycled Content (%)	10	16			
Max cost (GBP/unit)	11	17	22		
Max CO2 (kg/unit)	12	18	23	27	
Travel Distance	13	19	24	28	31
Labour Cost (GBP/hr)	14	20	25	29	32
Overhead cost (GBP/MJ)	15	21	26	30	33

In Table 33, the numbers from 9 to 33 represent case studies of the multiple parameters analysis. According to the variations of each parameter in the case studies (i.e. as defined in 3.5.1), the total model number is 203. The case study setup for each optimisation is 33 case studies containing 203 models. The case studies and corresponding parameters analysed in each case study are summarised in a table in Appendix – D.

3.6 Evaluation of Objective Function Values

This section will discuss the evaluation of the results for each optimisation. Three methods are introduced in this section: Individual Criterion Evaluation (ICE), Absolute Criterion (ABC) and INC (Incremental Criterion). The ICE method is used to assess the performance of the three modules after optimisation. The percentage difference between the inputs and outputs of each module is calculated to represent their individual contribution to a holistic optimisation. The summation of their contributions is used to assess the improvement to the overall objective. The ABC method and INC method will use the magnitude of a 3D vector to assess the objective function value of each optimisation. Each objective function value represents a point that consists of outputs from the three modules: STRUCTURAL, COST and CO2. The output of each module represents the coordinate of a 3D vector: X, Y, Z. The basic idea of both methods is to calculate magnitudes of 3D vectors to assess solutions for the optimisations. The magnitude of each vector in the ABC method measures the distance between the origin point 'O' and each objective function value. This distance is called Global Distance. Magnitude calculated in the INC method is used to measure the distance between the objective function values of the initial iteration and the final iteration. Distance measured in the INC method is called Local Distance. The following three subsections are used to introduce the three evaluation methods respectively.

3.6.1 Individual Criterion Evaluation (ICE)

In the ICE approach, programs will collect the output from each module and work out the percentage difference between the inputs and outputs. The calculation of percentage difference is expressed in Equation (3.28), and the brackets contain the calculation for each module. For instance, the first brackets contain the percentage difference of the STRUCTURAL module.

$$F(s) = (\frac{Volume_0 - Volume_i}{Volume_0} \times 100\%) + (\frac{CO_{2_0} - CO_{2i}}{CO_{2_0}} \times 100\%) + (\frac{\mathrm{Cost}_0 - \mathrm{Cost}_i}{\mathrm{Cost}_0} \times 100\%) \tag{3.28}$$

Where,

$Volume_0$ is the initial volume calculated from the STRUCTURAL module.

$Volume_i$ is the volume of the current iteration.

CO_{2_0} is the initial CO_2 footprint calculated from CO2 module.

CO_{2i} is the CO_2 footprint of the current iteration.

Cost_0 is the initial cost calculated from COST module.

Cost_i is the cost of the current iteration.

i is the iteration number from 1 to 'n', n is the maximum limit of the iteration.

The holistic optimisation in this research is to minimise the overall objective. The ideal output of each iteration should be smaller than the input. Therefore, a positive percentage difference of each module represents an improvement to the objective. On the contrary, a negative percentage difference of each module represents a setback. The summation of the three modules' percentage differences represents the performance of each iteration. To define the converged iteration of the optimisation, the summations are contrasted. The converged iteration should have the highest summation which represents the outputs of the three modules in this iteration from the objective function value of the optimisation. Such a summation is also called the 'converged' summation. Each model in each case study has its converged summation. Those summations are further analysed in each case study to study the parameter variation: the highest is highlighted with a red colour; the lowest is highlighted with a green colour as illustrated in Table 34. Model 1 in Table 34 has the highest summation, meaning that the parameter variation in model 1 has made the most improvement to the overall objective. Because of this, the objective function value of model 1 is the best solution in case study 1. Due to different types of optimisations, ICE in SEQ optimisations and PAR optimisations is slightly different.

Table 34: Summations in Case Study 1 – ICE

Case Study No.	Model	Summation
1	1	94%
	2	24%
	3	39%

3.6.1.1 ICE in SEQ Optimisation

In SEQ optimisation, each iteration only has one summation due to its typical optimisation sequence, as in the example illustrated in Figure 19. In Table 35. P1, P2 and P3 represent the percentage difference of each module. A positive percentage difference of each module represents an improvement to the objective. On the contrary, a negative percentage difference of each module represents a setback. The summation of each iteration is the add-up of P1, P2 and P3. SEQ optimisation stops when the converged summation is found.

Table 35: ICE in SEQ optimisation (Optimisation sequence from left to right)

Name	**Volume_mm3**	**CO_2 kg/Unit**	**Cost GBP/Unit**	**Summation**
Inputs	A	B	C	
Objective function values	a	b	c	
Difference	$P1 = \frac{(A-a)}{A} \text{x } 100\%$	$P2 = \frac{(B-b)}{B} \text{x } 100\%$	$P3 = \frac{(C-c)}{C} \text{x } 100\%$	$\sum = P1 + P2 + P3$

3.6.1.2 ICE in PAR Optimisation

The three modules are optimised simultaneously in PAR optimisation as mentioned previously. Each route has a converged summation as illustrated in Table 36. The ICE method in PAR optimisation will compare three converged summations, and the highest one represents the route that has the objective function value of the PAR optimisation. That summation is the final converged summation of the PAR optimisation.

Table 36: ICE in PAR optimisation (Optimisation sequence from top to bottom)

Route	A	B	C
Name	**Volume_mm3**	**CO_2 kg/Unit**	**Cost GBP/Unit**
Inputs	A1, B1, C1	A2, B2, C2	A3, B3, C3
Objective function values	a1, b1, c1	a2, b2, c2	a3, b3, c3
Percentage Difference	$P1 = \frac{(A1 - a1)}{A1} x\,100\%$	$P1 = \frac{(A2 - a2)}{A2} x\,100\%$	$P1 = \frac{(A3 - a3)}{A3} x\,100\%$
	$P2 = \frac{(B1 - b1)}{B1} x\,100\%$	$P2 = \frac{(B2 - b2)}{B2} x\,100\%$	$P2 = \frac{(B3 - b3)}{B3} x\,100\%$
	$P3 = \frac{(C1 - c1)}{C1} x\,100\%$	$P3 = \frac{(C2 - c2)}{C2} x\,100\%$	$P3 = \frac{(C3 - c3)}{C3} x\,100\%$
Sum	$\sum 1 = P1 + P2 + P3$	$\sum 2 = P1 + P2 + P3$	$\sum 3 = P1 + P2 + P3$

3.6.2 Absolute Criterion (ABC)

As results from each module have different ranges, the ABC requires that all outputs of STRUCTURAL, COST and CO2 modules be normalised into [0,1]. The normalised outputs from three modules can be used as coordinates for a 3D plot. The data normalisation (Dodge 2006) is expressed in Equation (3.29).

$$x' = \frac{x - x_{\min}}{x_{\max} - x_{\min}} \tag{3.29}$$

Where,

x is the current value.

$x_{\min}$ is the minimum value.

$x_{\max}$ is the maximum value.

A simple example is indicated in Table 37 to further explain Equation (3.29). The example shows how to do data normalisation for volume. In Table 37, the maximum value is highlighted with a red colour while the minimum value is highlighted with a green colour.

Table 37: Example of data normalisation

Case Study No.	Model	Volume_mm3
1	1	42265
	2	47547
	3	42068

Based on Equation (3.29), the normalised volume value for model 1 should be:

$$\frac{x - x_{min}}{x_{max} - x_{min}} = \frac{42265.6 - 42068.3}{47547.6 - 42068.3} \approx 0.036 \tag{3.30}$$

Replace volume values in Table 37 by the normalised data; and the new table is indicated below.

Table 38: The normalised data

Case Study No.	Model	Volume_mm3
1	1	0.04
	2	1
	3	0

The ABC evaluation method uses a 3D plot to evaluate the solution of each optimisation. Each objective function value consists of the results of the three modules. The results are normalised volume, CO_2 and cost. A solution of each optimisation is considered as a point of the plot, for instance, A = (X, Y, Z). The three axes X, Y and Z represent normalised volume, CO_2 and cost. One example of a plot is illustrated in Figure 23. The coloured points represent solutions of case studies. As the optimisation in this research is to minimise the objective, the ideal outputs of each module should therefore be smaller than the inputs. In this case, '0' represents the extreme output of each module. Therefore, the 'O' point (0, 0, 0) represents the extreme outputs of the COST, CO2 and STRUCTURAL modules, i.e. the absolute optimum solution. It also represents the extreme objective function value of the optimisation.

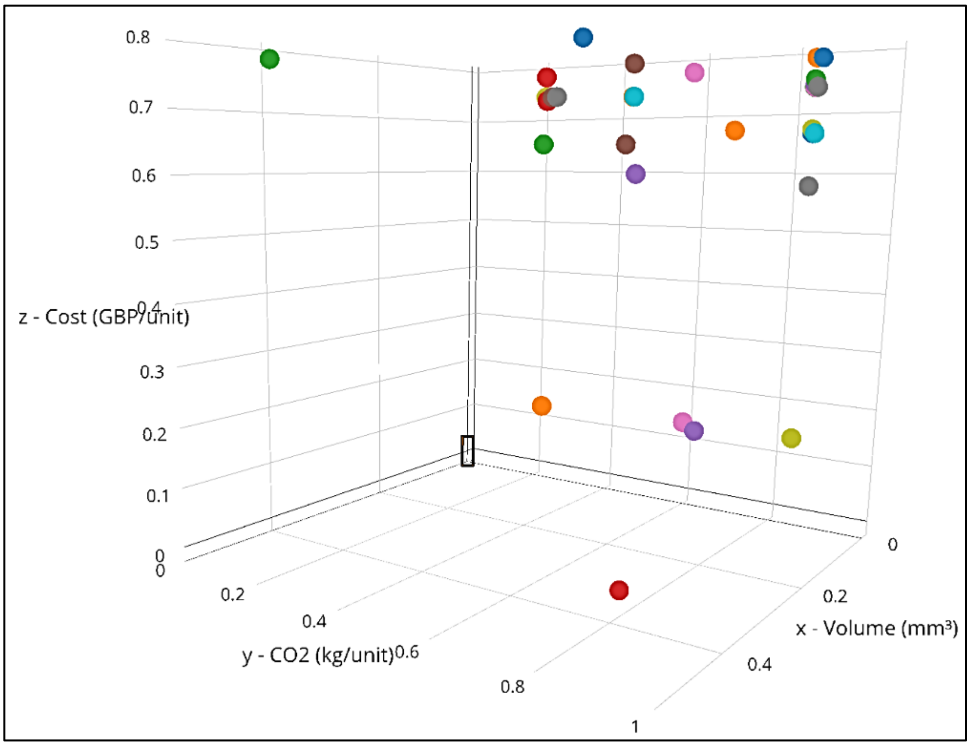

Figure 23: Example of the 3D scatter plot

In the ABC evaluation method, instead of comparing optimisation results with summations, the magnitude of the vector is used to compare the objectives of each optimisation. Vectors start with the point ‘O’ and end with each objective function value. The idea is to calculate the magnitude of the vector between the origin point ‘O’ and each objective function value. The magnitude of the vector is calculated using Equation (3.31). This magnitude is called the ‘Global Distance’. As the ‘O’ point (0, 0, 0) represents the extreme objective function value, therefore the shortest Global Distance represents the objective function value that is closest to the extreme objective function value (the closer is the better). One example of Global Distance is illustrated in Figure 24. Figure 24 contians an X-Y plane of the 3D coordinate system. There are two objective function values of case study 1 (Red) and 2 (Green). The Global Distance is calculated with Equation (3.31). If Global Distance of case study 1 is shorter than the Global Distance of case study two as illustrated in Figure 24, the objective function value of case study one should be better than the solution of case study 2.

$$\left|\overrightarrow{OA}\right| = \sqrt{X^2 + Y^2 + Z^2} \tag{3.31}$$

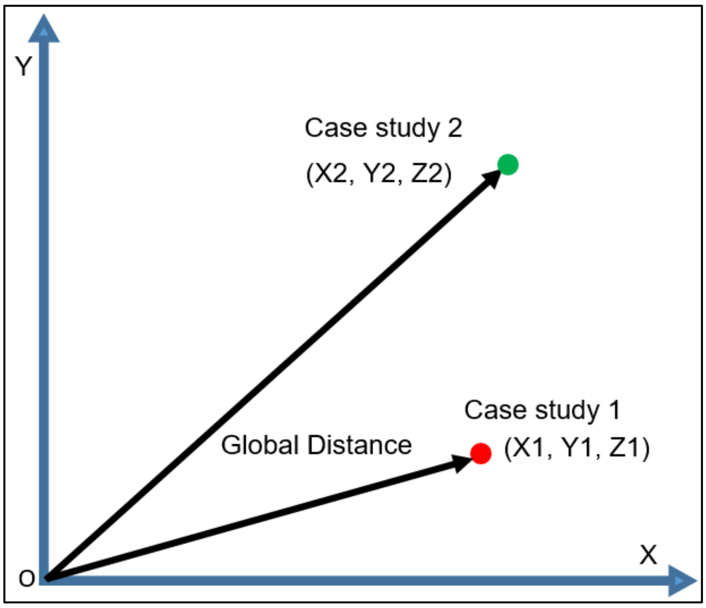

Figure 24: Example of Global Distance (2D)

The ABC evaluation method is applied to the models in each case study to analyse the influence of parameter variations. The Global Distance in each case study is further categorised into four types of distances: max., min., average and median. The max. and min. distances are used to analyse the fluctuation of solutions in each case study and find out the sensitivity of the parameters. The average and median distances are used to find out the general trends of different setups of optimisations. The magnitude of vector method cannot only apply to 3D problems (3 outputs) but also to N-dimensional problems. One drawback of this Global Distance is that two of the Global Distances may have a similar value. Because of this, the sensitivity of parameter variation will be difficult to find out. Therefore, a more detailed version of the distance between the solutions is required.

3.6.3 The Incremental Criterion (INC)

Similar to ABC, the INC will also use 3D coordinates to calculate the distance (vector magnitude), the difference being that INC evaluates the 'Local Distance' between results of the initial iteration and the final iteration as illustrated in Figure 25. Figure 25 contains an X-Y plane of the 3D coordinate system. The magnitude of the 'Green' vector represents the Local Distance between A and B. If A = (X, Y, Z) represents the final objective function value (I_n) of Model 1 and B = (x, y, z) represents the initial objective function value (I_0), the magnitude of the vector $\overrightarrow{BA}$ will be given by:

$$\left|\overrightarrow{BA}\right| = \sqrt{(X-x)^2 + (Y-y)^2 + (Z-z)^2} \tag{3.32}$$

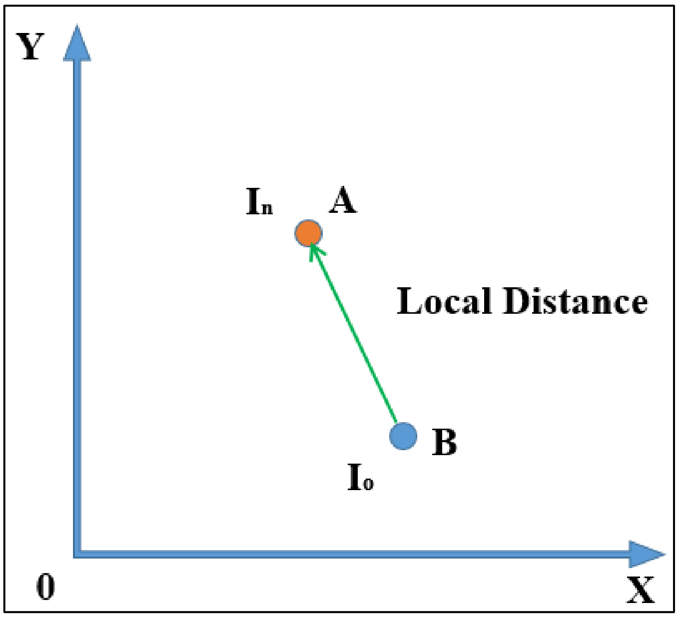

Figure 25: Example of Local Distance (2D)

In the following two chapters, two Holistic Optimisation Studies will be implemented. The results of the 7 OMS for each product will be assessed by the three evaluation methods defined in section 3.6; and the general trends for further comparison and analysis will be extracted.

4 Holistic Optimisation Study 1 (HOS1) – Side Impact Beam

The first Holistic Optimisation Study (HOS) is created in this chapter. For the HOS 1, a side impact beam of the vehicle will be analysed within the FEA solver and optimised by the 7 Optimisation Module Sequences (OMS) as defined in section 3.3, i.e. 6 Sequential and 1 Parallel holistic optimisations. It should be noted that the two types of iteration loops will be applied to the 7 OMS, i.e. Single Inner Iteration (SII) and Multi-Inner Iterations (MII). In this case, the SII optimisations and MII optimisations will be compared based on the objective function values and the CPU time. The results of the 7 OMS will be evaluated depending on which iteration type has the 'outperformance'. For either SII or MII, each of the 7 OMS contains 203 models leading to 1,421 individual models in total. The results of the 7 OMS will then be evaluated by the three evaluation methods defined in section 3.6: Individual Criterion Evaluation (ICE), Absolute Criterion (ABC) and INC (Incremental Criterion). The extracted general trends from each evaluation will be analysed and compared. The first section of this chapter will introduce the setup of HOS 1. The second section contains the comparison of the two types of iteration loops. The third to fifth sections will evaluate the results of the 7 OMS based on ICE, ABC and INC respectively. In each of sections 3 – 5, the evaluated results of the 7 OMS will be analysed based on four aspects: average, minimum, maximum objective function value change and average spread. The analysis of section 4.3 will go through all four aspects and summarise the trends accordingly. Sections 4.4 and 4.5 only contains the results based on the maximum change of objective function values. The analyses and summaries for the rest three aspects can be found from Appendix – E **(ABC)** and Appendix – F **(INC)** respectively. The final section will be the comparison of the general trends extracted from sections 3 – 5.

4.1 Setup of Holistic Optimisation Study 1

In this section, the setup of HOS 1 will be introduced within four subsections: a brief background of the side impact beam, load cases for initial analysis, FEA model for STRUCTURAL module and the design of the case study for HOS 1.

4.1.1 Brief background of the side impact beam

A side-door impact beam is studied in Holistic Optimisation Study 1. The side impact beam is the reinforcement structure on the door panel which aims to provide protection to passengers during a side impact. Its general position is illustrated in Figure 26.

Figure 26: The location of the side-door impact beam (Winter 2013)

Assuming that the side impact beam is a simply supported beam (Figure 27), the beam is constrained on both ends, and the load acts on the top of the beam. As the side impact is not a point force acting on the beam, another assumption is made that the load is assumed as a uniformly distributed force (N/m).

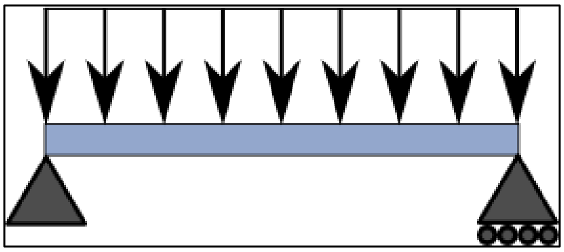

Figure 27: The Simply Supported Beam – 2D (learnt engineer 2014)

The material used for side impact beam requires high strength and high toughness. Materials with such properties can absorb more energy during the impact and have less deformation. As the weight reduction of the engineering product is of importance to the manufacturers, especially for automobiles, 'lightweight' is one more requirement for selecting the material (Lim & Lee 2002). The conventional material for manufacturing automotive components is the metal (e.g. steel). The side impact beam is manufactured using the rolling form method (Sturrus, Lewis and Johnson 1992). Based on the requirements, a list of metals is selected from the CES EduPack 2016 in Table 39.

Table 39: Material list (CES EduPack 2016)

MAT Names	MAT code	Density (kg/m^3)	Young's Modulus (GPa)	Yield Strength (MPa)	Poisson's Ratio	Price (£/kg)
High Alloy Steel	Acer Met 100	7900	203	1790	0.3	24.3
Medium Alloy Steel	AMS 6585	7900	218	1660	0.37	15.5
Low Alloy Steel	AISI 4620	7900	212	410	0.3	0.7
Low Carbon Steel	AISI 1010	7900	215	315	0.3	0.4
Medium Carbon Steel	AISI 1080	7900	215	650	0.3	0.4
High Carbon Steel	AISI 1144	7900	215	470	0.3	0.4
High Strength Steel	S 550 MC	7900	221	650	0.3	0.4
Structural Steel	S 275 N	7900	221	275	0.32	0.4
Aluminium	5182 H34	2700	72	297	0.34	1.78
Aluminium	6111 T62	2740	70	336	0.34	1.8
Aluminium	6063 T5	2710	70	125	0.34	1.78

4.1.2 Load cases and initial FEA

According to the side impact beam illustrated in Figure 26, its cross-section is considered to be shaped as illustrated in Figure 28. The length of the beam is from 508 millimetres to 1397 millimetres (Wilson, Shapiro & Cline 1989). The thickness of the beam is from 1.3 millimetres to 3.0 millimetres (Cline & Shapiro 2000). The width of the beam is about 40 millimetres (Lim & Lee 2002). The dimensions a, b and c can be varied to change the geometry of the cross-section of the beam. It should be noted that the change in these dimensions must comply with the constraint limits defined above.

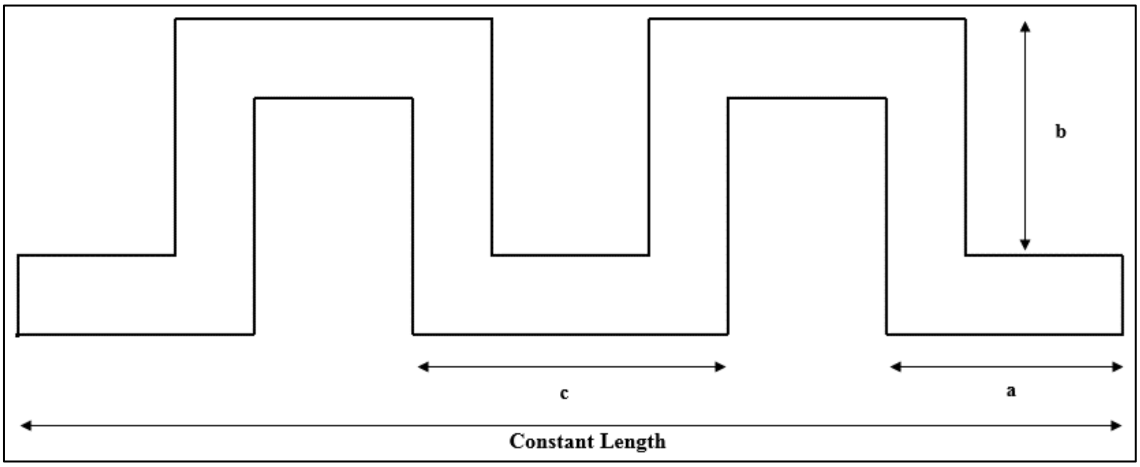

Figure 28: Cross section of the beam

The purpose of this subsection is to analyse the structural performance of the side impact beam with an initial FE analysis. The 2D model of the side impact beam is created in HyperMesh as illustrated in Figure 29.

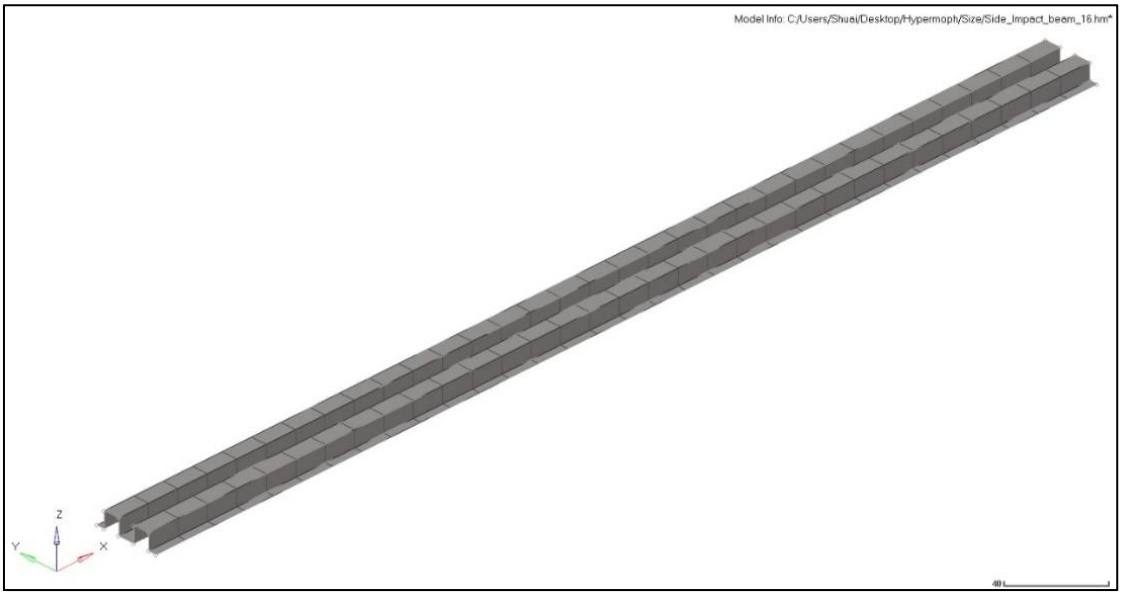

Figure 29: 2D Beam model in HyperMesh

The initial material used in HyperMesh is the default material (steel). The initial thickness of the beam was 3.0 millimetres which is also the maximum thickness of a side impact beam as defined in subsection 4.1.1. As the side impact beam is considered as a simply supported beam in this study, two types of the constraints are applied to the two ends of the beam respectively, i.e. pin support and roller support (Figure 27). The pin support demonstrates that one end of the FEA model needs to be fully constrained. The roller support demonstrates that the other end of the beam is not allowed to move in Z-direction. In HyperMesh, there are 6 degrees of freedoms (DOF). DOFs 1-3 demonstrate the node translation in the X, Y and Z directions and DOFs 4-6 demonstrate the node rotation in the X, Y and Z directions (Thota 2016). Therefore, all DOFs are fully constrained at the pin-supported end, as illustrated in Figure 30. Only DOF 3 is constrained for the roller-supported end, as illustrated in Figure 31.

Figure 30: Fully constrained end

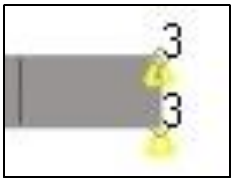

Figure 31: Not fully constrained end

The load applied to the 2D side impact beam is not a point load as defined in subsection 4.1.1. Due to the limitations in analysing an actual side impact beam, the maximum load for such a beam is assumed to be 2000N. A 2000N uniformly distributed force acting on the top of the beam is illustrated in Figure 32 and Figure 33.

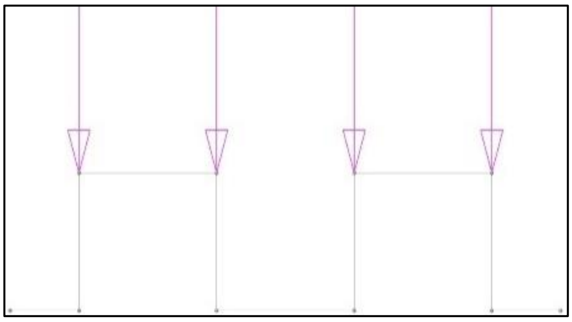

Figure 32: Load applied to the beam (side view)

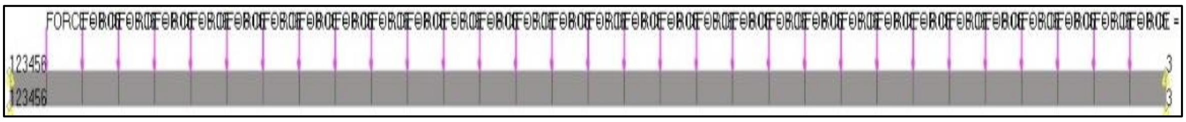

Figure 33: Load applied to the beam (front view)

By running the initial FEA test for this side impact beam, the detailed results are illustrated in Figure 34 and Figure 35. The displacement results in Figure 34 show that the maximum displacement is obtained at the middle of the beam. This is not a surprise as the middle part has no support, i.e. no external force against the distributed load. The maximum displacement is about 1.57 mm which is not a large deflection of the beam. On the other hand, the maximum vonMises stress in Figure 35 is found at the fully constrained end of the beam; the reason being that the stress of the fully constrained end consists of stress from three directions, X, Y and Z instead of the single Z-direction stress at the other end. The maximum vonMises is about 158 MPa which is lower than the minimum yield strength of steel defined in Figure 33, i.e. Structural Steel (275 MPa).

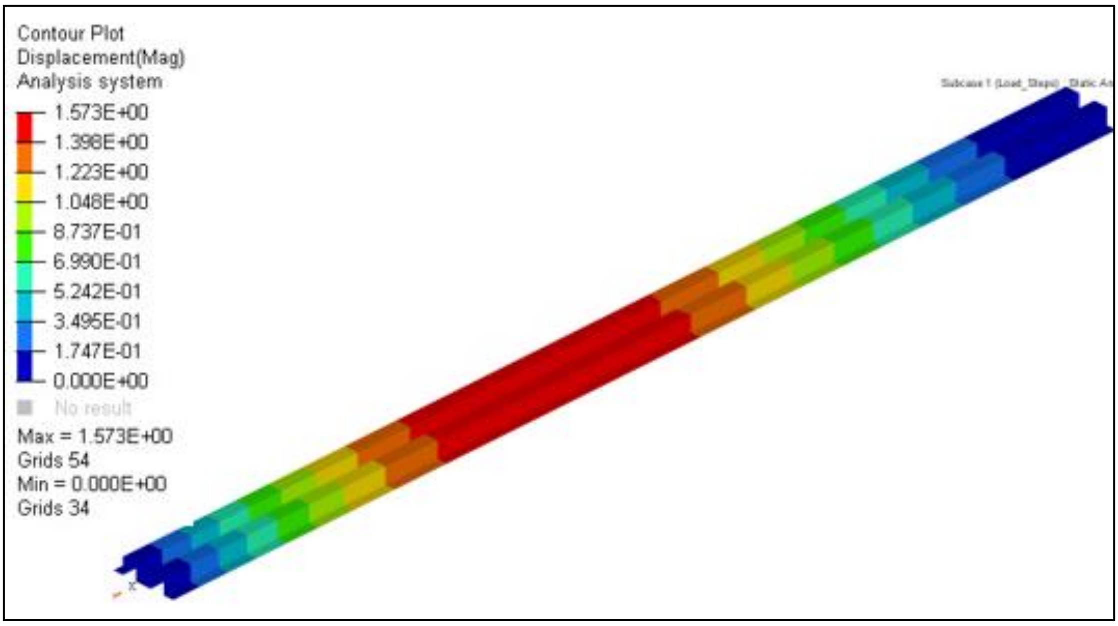

Figure 34: Displacement results of the side impact beam

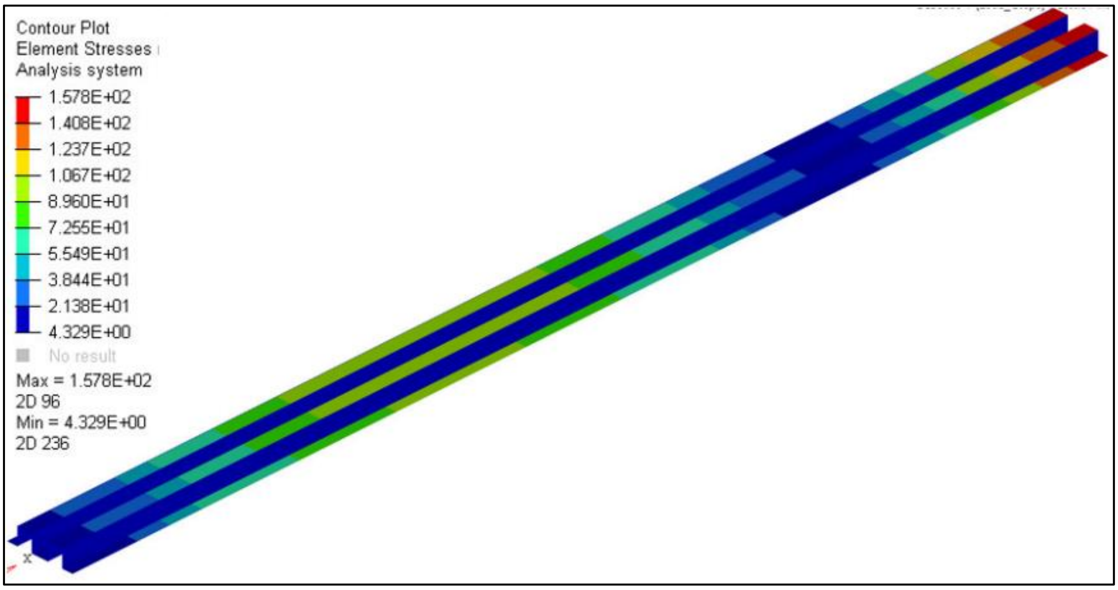

Figure 35: Stress results of the side impact beam

The results of the initial FEA test are within the permissible limits of the yield strength of the material. However, it should be noted that this FEA test is not based on a real side impact but on an estimated static force. The ultimate aim is to use the tested FEA model for the optimisation modules.

4.1.3 FEA models for the STRUCTURAL module

The setup of the FEA model is adopted as the results of the analysis are within the permissible limits. The FEA model of the beam is then considered to be used for the structural optimisation in the STRUCTURAL module. As defined in subsection 3.2.1, the optimisation method used in the STRUCTURAL module is sizing optimisation. The aim of implementing this optimisation method for the beam is to achieve minimum volume by minimising its thickness. As defined in subsection 3.5.1, there will be three geometries for the product in order to study how the change of geometry influences the optimum solution. The length and width of the beam will be the constant values, but the dimensions of the cross-section defined in Figure 28 will be changed to vary the geometry of the beam. The three cross-sections of the beam are illustrated in Table 40. For convenience, the detailed dimensions of the cross-section are tabulated in Table 40 as well.

Table 40: Initial cross-sections of the beam geometry

Cross-sections		Dimension a	Dimension b	Dimension c
1	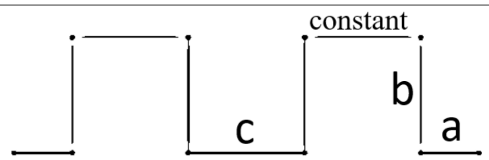	5cm	8cm	8cm
2	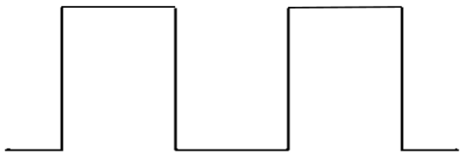	4cm	10cm	8cm
3	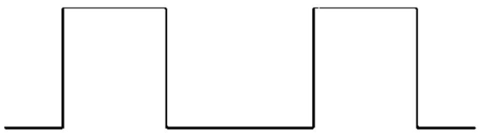	4cm	8cm	10cm

Based on the cross-sections defined in Table 40, the initial geometries of the beam are created. The initial volume of each of the three beams is determined within HyperMesh. The initial cost and CO_2 footprint of the beams are calculated based on the equations defined in subsection 3.2.2 and 3.2.3. The manufacturing method is the rolling form, the initial country of production is the UK (Coventry) and the destination is Coventry (Connecticut, the USA). The measured initial volumes and calculated cost and CO_2 footprint are summarised in Table 41.

Table 41: Initial values of the side impact beam

Beam	Initial Volume (mm^3)	Initial CO_2 per unit (kg)	Initial Cost per unit (£)
1	97536	0.84	0.72
2	109725	0.94	0.74
3	97536	0.84	0.72

It should be noted that the variation of the initial geometry is used to find out how the change of geometry influences the optimum solution. Although the initial volume of Beams 1 and 3 is the same, the geometry of the two beams is different based on the cross-sections defined in Table 40

4.1.4 Case study definitions of Holistic Optimisation Study 1

The design of the case studies for HOS 1 is the same as the case studies defined in subsection 3.5.2. There are 7 Optimisation Module Sequences (OMS) including 6 Sequential (SEQ) optimisations and one Parallel (PAR) optimisation. There are 203 optimisation models for each of the 7 OMS leading to 1,421 models in total. As defined in subsection 3.5.2, the first 8 case studies for each of the 7 OMS will be the study of 8 individual parameters: geometry, recycled content, production quantity, maximum component cost, maximum component CO_2, travel distance, labour cost and overhead cost. This is also called the One at A Time method (OAT). The other 25 case studies will investigate the combinations of two of the individual parameters. This is also known as the Two at A Time method (TAT). Therefore, there are 33 case studies for each of the 7 OMS leading to 231 case studies in total.

4.2 Comparison of SII and MII Optimisations

After running the case studies for the 7 OMS with both the SII and MII loops, the results of the two optimisation iteration types will be compared in this section. The performance of the two iteration types will be assessed from two aspects: objective function values and CPU time. The first section will be the investigation of the objective function values.

4.2.1 Comparison of the objective function values

The results of the 7 OMS with both SII and MII will be assessed in this subsection. The average Change of Objective Function Value (**COFV**) for each of the 7 OMS is calculated by Equation (4.1). In order to compare the 'performance' of the two types of iteration loops, the average COFV for each of the 7 OMS with both MII and SII loops are summarised in Table 42.

$$Average\ COFV = \frac{\sum_{i=1}^{203} \mathrm{Result}_{Model\_i}}{203} \tag{4.1}$$

Table 42: Average objective function value change for each OMS – HOS 1

Evaluation methods	Iteration types	OMS						
		SEQ1	SEQ2	SEQ3	SEQ4	SEQ5	SEQ6	PAR
ICE	SII	199%	97%	204%	99%	215%	101%	166%
	MII	206%	111%	211%	106%	223%	108%	183%
ABC	SII	0.36	0.82	0.32	0.83	0.17	0.79	0.62
	MII	0.35	0.81	0.31	0.83	0.15	0.79	0.50
INC	SII	1.52	1.10	1.54	1.51	1.61	1.61	1.45
	MII	1.53	1.13	1.55	1.51	1.63	1.61	1.48

For the ICE method, a larger COFV represents a better optimum solution. In Table 42, it is easy to find out that the average COFV of each of the 7 OMS-MII is larger than the average COFVs of the corresponding 7 OMS-SII. The differences between the two corresponding OMS are 7% for the minimum and 17% for the maximum. This indicates that the results of the 7 OMS-MII outperform the results of the 7 OMS-SII.

For the ABC method, the COFV represents the ‘distance’ between each result and the absolute optimum solution (defined in subsection 3.6.2). The shorter the ‘distance’ the better, i.e. the result is much closer to the absolute optimum solution. In Table 42, the average COFV of each of the 7 OMS-SII is equal to or larger than the values of the corresponding 7 OMS-MII. The difference between the corresponding SEQ OMS is very small, i.e. the maximum is 0.02 and the minimum is 0. This indicates that the 6 SEQ OMS with MII and SII loops have nearly the same performance within the ABC evaluation. On the other hand, the difference between two corresponding PAR OMS is relatively large at 0.12 (about 20%). This indicates that the PAR OMS show more sensitivity in the ABC method. This is also evidenced in the ICE method as PAR OMS also have the largest difference within the ICE evaluation, i.e. 17%. From the overview of the ‘performance’ for the 7 OMS-MII (SII) evaluated by the ABC method, the 7 OMS-MII slightly outperform the 7 OMS-SII. For the INC method, the COFV represents the ‘distance’ between the result of the initial iteration and the result of the final iteration. Therefore, the longer the ‘distance’, the better. By observing Table 42, the values of the 7 OMS-MII are equal to or larger than the values of the 7 OMS-SII. The maximum difference between the values of the corresponding OMS is 0.03. This indicates that the difference of the ‘performance’ between the 7 OMS-MII and the corresponding 7 OMS-SII is nearly the same based on the INC method. According to the findings in Table 42, it can be concluded that the average COFV of each of the 7 OMS-MII outperforms the corresponding 7 OMS-SII based on the three evaluation methods. The CPU time of each of the 7 OMS-MII (SII) will be discussed in the next subsection, as another part for assessing the overall performance of the 7 OMS-MII (SII).

4.2.2 Comparison of the CPU time

The CPU time assessed in this subsection represents the time for running 203 models of each of the 7 OMS-MII (SII). The CPU time for the OMS is summarised in Table 43. It is found that the CPU time for each of the 7 OMS-MII is higher than the CPU time for each of the 7 OMS-SII. However, this is not a surprise as more iteration loops consume more CPU time.

Table 43: The CPU time of each OMS – HOS 1

Iteration types	CPU time (mins.) of the 7 OMS						
	SEQ1	SEQ2	SEQ3	SEQ4	SEQ5	SEQ6	PAR
SII	335	442	341	431	367	377	368
MII	369	444	366	447	399	419	376

In order to find out if there is any trend that can be found from the CPU time of each model, the average CPU time for each OMS across the 203 models is calculated. The values are summarised in Table 44.

Table 44: The average CPU time of each model for each OMS – HOS 1

Iteration types	Average CPU time (s) of each model for each OMS						
	SEQ1	SEQ2	SEQ3	SEQ4	SEQ5	SEQ6	PAR
SII	99	131	101	127	108	111	109
MII	109	131	108	132	118	124	111

In Table 44, it is found that the average CPU time of each model for the corresponding OMS is very close, i.e. the maximum difference is 13s at SEQ6. This indicates that CPU-time 'performance' of the 7 OMS-MII is close to the 'performance' of the 7 OMS-SII. However, the 7 OMS-MII have a larger change of objective function values than the 7 OMS-SII. Therefore, the overall performance of the 7 OMS-MII outperforms the 7 OMS-SII. In this case, the three evaluation methods will be applied to assess the results of the 7 OMS-MII in the following sections.

4.3 ICE results of Holistic Optimisation Study 1

A figure with clustered column graphs for each model is initially considered to analyse the general trends of 7 OMS-MII with the Individual Criterion Evaluation (ICE) method. The clustered column graph in Figure 36 contains the results of the three models contained in case study one (subsection 3.5.2). In Figure 36, each model has 7 columns representing the results of the 7 corresponding OMS. The X-axis contains the model number; whereas the Y-axis contains the change of objective function values. Please note that the number of iterations for each model may vary.

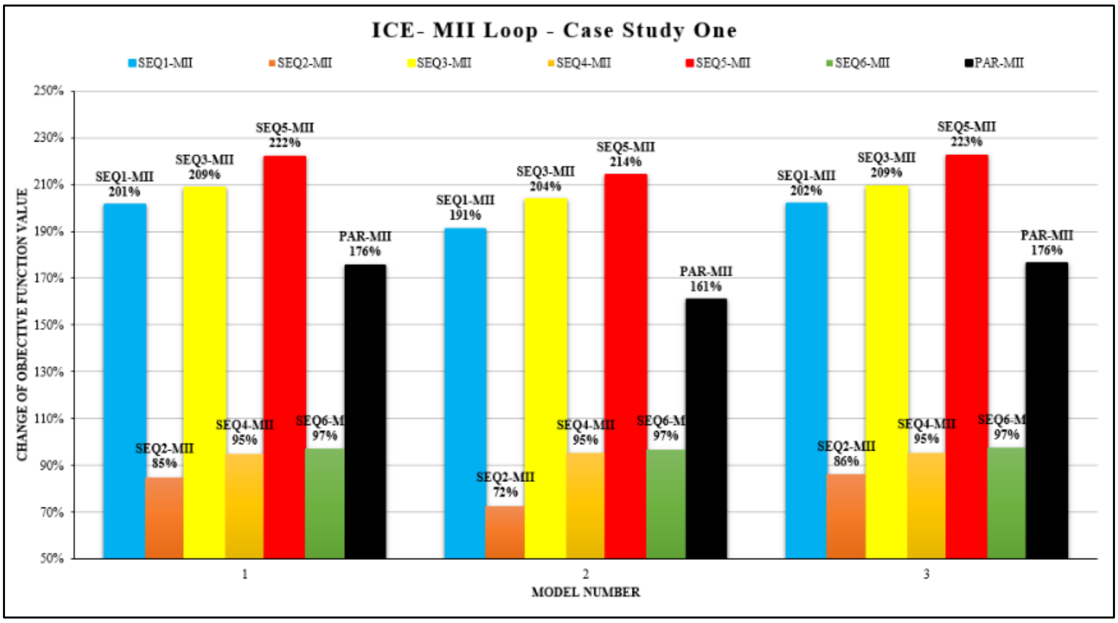

Figure 36: Results of case study one for the 7 OMS-MII – ICE

In Figure 36, it is easy to assess the 'performance' of individual models for each of the 7 OMS with the data labelled at the top of each column. However, to obtain a general overview, the chart would have to contain 1,421 results representing the 203 models and the combination of ICE and MII which would make it very difficult to identify general trends. It was therefore chosen to plot the individual results as single points in a figure and utilise linear lines to connect the individual points. Consequently, it is possible to more clearly identify general trends for each of the 7 OMS as well as enabling direct comparison between the different OMS. As a result, Figure 37 is plotted. According to the definition of the ICE method in subsection 3.6.1, more Changes of Objective Function Value (COFV) will produce better results. Figure 37 shows that the results of SEQ5-MII are nearly consistently higher than the results of the other 6 OMS. This indicates that the SEQ5-MII outperforms the other OMS based on the ICE method. On the other hand, the results of SEQ2-MII, SEQ4-MII and SEQ6-MII are nearly consistently lower than the results of the other OMS. This indicates that those three OMS underperform the other four OMS based on the ICE method. To further investigate the general trends of the 7 OMS-MII, the average, maximum and minimum COFV across the 203 models for each of the 7 OMS will be analysed in subsection 4.3.1, 4.3.2 and 4.3.3 respectively. The sensitivity analysis of the results for the 7 OMS will then be analysed in subsection 4.3.4. Finally, the overall general trends of the 7 OMS will be summarised in the subsection 4.3.5.

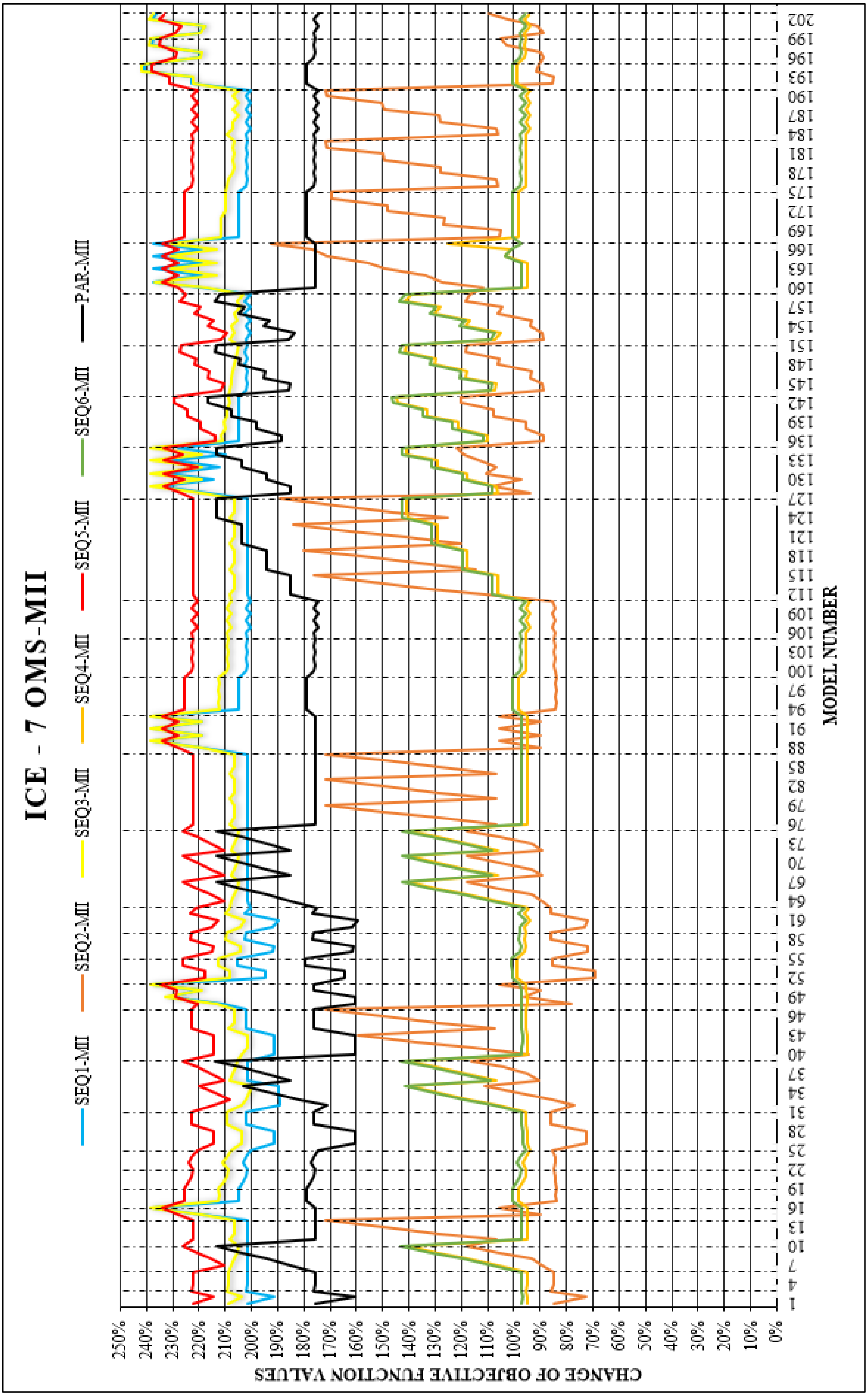

Figure 37: Results of the 7 OMS – ICE method – HOS 1

4.3.1 Results based on the average change of objective function values

The average change of objective function values (COFV) across the 203 models of each of the 7 OMS will be assessed in this subsection. The calculation method of the average COFV has been defined by Equation (4.1). The 7 OMS are ranked from the highest average COFV to the lowest average COFV in Table 45.

Table 45: The ranked 7 OMS based on the average COFV – ICE – HOS 1

Rank	OMS	Objective function value changes (Average – ICE)
1	SEQ5-MII	223%
2	SEQ3-MII	211%
3	SEQ1-MII	206%
4	PAR-MII	183%
5	SEQ2-MII	110%
6	SEQ6-MII	108%
7	SEQ4-MII	106%

From Table 45, the 7 OMS can be categorised into three groups based on the range of the average COFV:

HOS1-Avg-ICE 1. The first group labelled Group A contains the Sequential (SEQ) OMS SEQ1-MII, SEQ3-MII and SEQ5-MII. The majority of the COFV for the models in these three OMS are between 200% and 225%.

HOS1-Avg-ICE 2. Group B contains the SEQ2-MII, SEQ4-MII and SEQ6-MII. The majority of the COFV for the models in SEQ2-MII, SEQ4-MII and SEQ6-MII are between 100% and 110%.

HOS1-Avg-ICE 3. Group C contains the single Parallel (PAR) OMS, PAR-MII. The majority of the COFV for the models in the PAR are between 110% and 200%.

These three groups are defined in Table 46, which for convenience also contains the specific OMS order and the range of average COFV.

Table 46: The 7 OMS grouped by the range of average COFV – ICE – HOS 1

Group A				
OMS Name	**SEQ1-MII**	**SEQ3-MII**	**SEQ5-MII**	**Range of objective function value change**
Module Sequence	STRUCTURAL	COST	COST	**200% - 225%**
	COST	CO2	STRUCTURAL	
	CO2	STRUCTURAL	CO2	
Group B				
OMS Name	**SEQ2-MII**	**SEQ4-MII**	**SEQ6-MII**	**100% - 110%**
Module Sequence	STRUCTURAL	CO2	CO2	
	CO2	COST	STRUCTURAL	
	COST	STRUCTURAL	COST	
Group C				
OMS Name	**PAR-MII**			**110% - 200%**
Module Sequence	Parallel			

As illustrated in Table 46, the following trends are found:

HOS1-Avg-ICE 4. The change of objective function value for each model in Group A is constantly higher than the values of the corresponding models in Group B.

HOS1-Avg-ICE 5. The majority of models in Group C have higher values than the corresponding models in Group B; excluding model 1 and model 167.

HOS1-Avg-ICE 6. Evidenced by Figure 37, the graphs of the OMS in Group A and Group C display ‘fewer’ and ‘lower’ fluctuations (as a function of the model number) when compared to those of Group B. This for example is the case between models 112 and 127. This indicates that the OMS in Group B are more sensitive to the change of input parameters than the other two groups: MII-A and MII-C. Consequently, it is suggested that the OMS of Group A and Group C represent more ‘stable’ or ‘robust’ OMS than those of Group B.

HOS1-Avg-ICE 7. As the OMS of Group A and C are ‘higher’ and more ‘stable’ than those of Group B, the OMS in these two groups therefore are more ‘interesting’.

At this point it should however be noted that these observations are based on a limited number of models. It should also be noted that at this stage there has been no direct evaluation of the results feasibility such as manufacturing constraints, apart from those built into the individual optimisation modules as defined in section 3.2.

HOS1-Avg-ICE 8. Comparing the OMS of SEQ optimisations in Table 46, it is found that the optimisations in Group A always optimise the COST module before the CO2 module. Meanwhile, the COST module in Group B is always optimised after the CO2 module. The ‘priority’ i.e. the module sequence order. may explain why Group A consistently outperforms Group B. However, there is no priority for the modules in Group C as the three modules are optimised simultaneously and independently in the PAR OMS.

HOS1-Avg-ICE 9. The graphs of SEQ4-MII and SEQ6-MII in Figure 37 are nearly identical apart from models 164 to 167. The average COFV between SEQ4-MII and SEQ6-MII is less than 2%. This indicates the ‘performance’ of these two OMS is almost the same; i.e. the module sequence did not influence the objective function value significantly in SEQ4-MII and SEQ6-MII.

HOS1-Avg-ICE 10. The largest spread value, defined as the difference between the maximum and minimum y-values for each individual ‘function line’ differs significantly for each group. In Group A it is 51%, in Group B it is 124% and in Group C it is 57%. The different spreads of each group are related to the sensitivity of the parameter(s). The sensitivity analysis of the parameter(s) will be analysed in sub-section 4.3.4. Before this is done, the next step will be to analyse the general trends of the 7 OMS based on the maximum and minimum COFV.

4.3.2 Results based on the maximum change of objective function values

The maximum COFV represents the maximum value of the 203 COFV (i.e. from the 203 models) for each of the 7 OMS. There are 7 maximum COFV in total for the 7 OMS as defined in Table 47. The 7 OMS are ranked from the highest maximum COFV to the lowest in Table 47.

Table 47: The ranked 7 OMS based on the maximum COFV – ICE – HOS 1

Rank	OMS	Objective function value changes (Maximum – ICE)
1	SEQ3-MII	242%
2	SEQ1-MII	241%
3	SEQ5-MII	238%
4	PAR-MII	217%
5	SEQ2-MII	193%
6	SEQ6-MII	147%
7	SEQ4-MII	145%

The following trends are found in Table 47:

HOS1-Max-ICE 1. SEQ1-MII, SEQ3-MII and SEQ5-MII outperform the other OMS as their maximum COFV is larger than the values of the other OMS, i.e. the largest spread between SEQ3-MII and SEQ4-MII is nearly 100%. This indicates that the specific OMS order of the top three OMS is better than the OMS orders of the others.

HOS1-Max-ICE 2. The 7 OMS can still be categorised into three groups as defined in subsection 4.3.1. The trends found in each group are that SEQ1, 3 and 5 always optimise the COST module before the CO2 module. Meanwhile, the COST module in SEQ2, 4 and 6 is always optimised after the CO2 module. This is the same trend as demonstrated in HOS1-Avg-ICE 8.

HOS1-Max-ICE 3. The PAR-MII is still in the middle between the SEQ1, 3, 5 and SEQ2, 4, 6. This is the same trend as defined in subsection 4.3.1, i.e. HOS1-Avg-ICE 4.

The general trends found in this subsection are nearly the same as the trends observed in subsection 4.3.1. To further study the trends of the 7 OMS, the minimum COFV of each of the

7 OMS are investigated in the next subsection.

4.3.3 Results based on the minimum change of objective function values

The minimum COFV of each of the 7 OMS represents the minimum value of the 203 models in each OMS. The 7 minimum COFV are summarised in Table 48. The 7 OMS are ranked from the highest minimum COFV to the lowest in Table 48.

Table 48: The ranked 7 OMS based on the minimum COFV – ICE – HOS 1

Rank	OMS	Objective function value changes (Minimum – ICE)
1	SEQ5-MII	208%
2	SEQ3-MII	200%
3	SEQ1-MII	189%
4	PAR-MII	159%
5	SEQ6-MII	96%
6	SEQ4-MII	94%
7	SEQ2-MII	69%

According to Table 48, the general trends of the 7 OMS are summarised as follows:

HOS1-Min-ICE 1. The 7 OMS can be categorised into the same groups as defined in subsection 4.3.1.

HOS1-Min-ICE 2. The top three ranked OMS are also the same as discovered in subsection 4.3.1 and subsection 4.3.2, i.e. SEQ1-MII, SEQ3-MII and SEQ5-MII. This indicates that the OMS orders of these three OMS produced better results than the other OMS, i.e. the largest spread between SEQ5-MII and SEQ2-MII is significantly huge – 139%.

HOS1-Min-ICE 3. The top three OMS always optimise the COST module before the CO2 module. On the other hand, the COST module in SEQ2, 4 and 6 is always optimised after the CO2 module. This is the same trend as demonstrated in HOS1-Avg-ICE 8.

Based the objective function value change, the general trends found in subsection 4.3.1, 4.3.2 and 4.3.3 are nearly the same. Before summarising the overall general trends of the 7 OMS, the sensitivity trend(s) will be studied in the next subsection.

4.3.4 Results based on the average spreads of objective function value change

In this subsection, the average spreads of the COFV for each of the 7 OMS will be studied. The average spread of each of the 7 OMS is calculated by Equation (4.2).

$$Average\,Spread = \frac{\sum_{i=1}^{33}(\text{CaseStudyResult}_{Max\_i} - \text{CaseStudyResult}_{Min\_i})}{33} \qquad (4.2)$$

The calculated average spreads for the 7 OMS are summarised in Table 49. The 7 OMS are ranked from the highest spread to the lowest spread in Table 49.

Table 49: The average spreads of the 7 OMS – ICE – HOS 1

Rank	OMS	Average Spreads – ICE
1	SEQ5-MII	7%
2	SEQ1-MII	8%
3	SEQ3-MII	8%
4	SEQ6-MII	9%
5	SEQ4-MII	10%
6	PAR-MII	11%
7	SEQ2-MII	29%

By observing Table 49, the following trends are found:

HOS1-ASp-ICE 1. The results of SEQ5-MII are more stable than those of the other 6 OMS as SEQ5-MII has the lowest average spread value.

HOS1-ASp-ICE 2. The results of SEQ2-MII are less stable than other OMS, as SEQ2-MII has the largest average spread value.

HOS1-ASp-ICE 3. Although the 7 OMS have different average spreads, the average spreads of the OMS ranked from 1st to 6th are very close; i.e. the difference between them is 4%. This indicates that the results of the 7 OMS, apart from SEQ2-MII, have similar sensitivity to the change of input parameter(s).

HOS1-ASp-ICE 4. For the 6 SEQ optimisation programmes, SEQ1-MII, SEQ3-MII and SEQ5-MII have lower average spreads than SEQ2-MII, SEQ4-MII and SEQ6-MII. It is suggested that the results of SEQ1-MII, SEQ3-MII and SEQ5-MII are more stable than the results of the other three SEQ optimisation programmes. This also indicates that the results of the OMS will be less sensitive if the OMS optimise the COST module before the CO2 module.

The average, maximum and minimum COFV and the average spreads of each of the 7 OMS have been investigated respectively; and the general trends were extracted from the investigations. The next subsection will compare and summarise the general trends of the 7 OMS based on the ICE method.

4.3.5 Summary of the general trends – ICE – HOS 1

According to the general trends discovered in each subsection of section 4.3, the General Trends (GT) of the 7 OMS are summarised as follows:

HOS1-GT-ICE 1. The 7 OMS are categorised into three groups based on overall performance. As defined in subsection 4.3.1, Group A contains SEQ1-

MII, SEQ3-MII and SEQ5-MII; Group B contains SEQ2-MII, SEQ4-MII and SEQ6-MII; Group C contains PAR-MII.

HOS1-GT-ICE 2. The three OMS in Group A are suggested to be more stable than those in Groups B and C. This is evidenced by the general trends found in subsections 4.3.1, 4.3.2, 4.3.3 and 4.3.4.

HOS1-GT-ICE 3. For the OMS in Groups A and B, SEQ1-MII, SEQ3-MII and SEQ5-MII in Group A always optimise the COST module before the CO2 module; while the OMS in Group B always optimise the CO2 module before the COST module. This is suggested to be the reason why the OMS in Group A outperform those in Group B.

HOS1-GT-ICE 4. The SEQ5-MII is the most stable of the OMS while SEQ2-MII is the least stable, as evidenced by HOS1-ASp-ICE 1 and HOS1-ASp-ICE 2 in subsection 4.3.4. Even though SEQ2-MII is the most sensitive of the 7 OMS however it can be considered to be indifferent; simply because the SEQ2-MII objective function value changes are consistently lower than SEQ1-MII, SEQ3-MII, SEQ5-MII and PAR-MII.

HOS1-GT-ICE 5. The performance of SEQ4-MII and SEQ6-MII is nearly the same, which indicates that the two specific OMS orders might have same optimisation 'effectiveness'. This is evidenced by Table 45, Table 47, Table 48 and Table 49.

HOS1-GT-ICE 6. The PAR-MII of Group C is always ranked in the middle of the two groups of SEQ optimisation programmes. This is evidenced by Table 45, Table 47 and Table 48. Apart from SEQ2-MII, the results of PAR-MII are less stable than the other SEQ optimisation programmes.

The general trends summarised above are observed by evaluating the results of the 7 OMS with the ICE method. To verify the trends of the 7 OMS, the results will be evaluated by the ABC and INC method in the next two sections respectively.

4.4 The ABC results of Holistic Optimisation Study 1

The results of the 7 OMS will be studied by the Absolute Criterion (ABC) method to extract the general trends. To obtain a general overview of the results, the individual results of each of the 7 OMS are plotted as single points in a figure and linear lines are utilised to connect the points. As a result, Figure 38 is created. However, the 7 continuous lines for the 7 OMS in Figure 38 are 'interlaced' and unable to find out trends directly. Therefore, the results of the 7 OMS will be studied from some specific perspectives in this section. The basic setup of this section is the same as the setup of section 4.3. The study of the results of the 7 OMS consists of 4 subsections:

- Subsection 4.4.1, Results based on the maximum change of the objective function values
- Subsection 9.1.1 in Appendix – E, Results based on the average change of the objective function values
- Subsection 9.1.2 in Appendix – E, Results based on the minimum change of the objective function values
- Subsection 9.1.3 in Appendix – E, Results based on the average spreads of objective function value change
- Subsection 9.1.4 contains the summary of section 4.4.

The definition of the ABC method in subsection 3.6.2 demonstrated that the idea of the ABC evaluation method is to calculate the distance between each result and the absolute optimum solution. The shorter the distance the better, as a shorter distance means the result is closer to the absolute optimum solution. This distance, namely 'Global Distance', also represents the change of the objective function value (COFV). Therefore, a smaller COFV in this section indicates a shorter distance/ a better result. The maximum COFV of each of the 7 OMS will first be studied in Subsection 4.4.1.

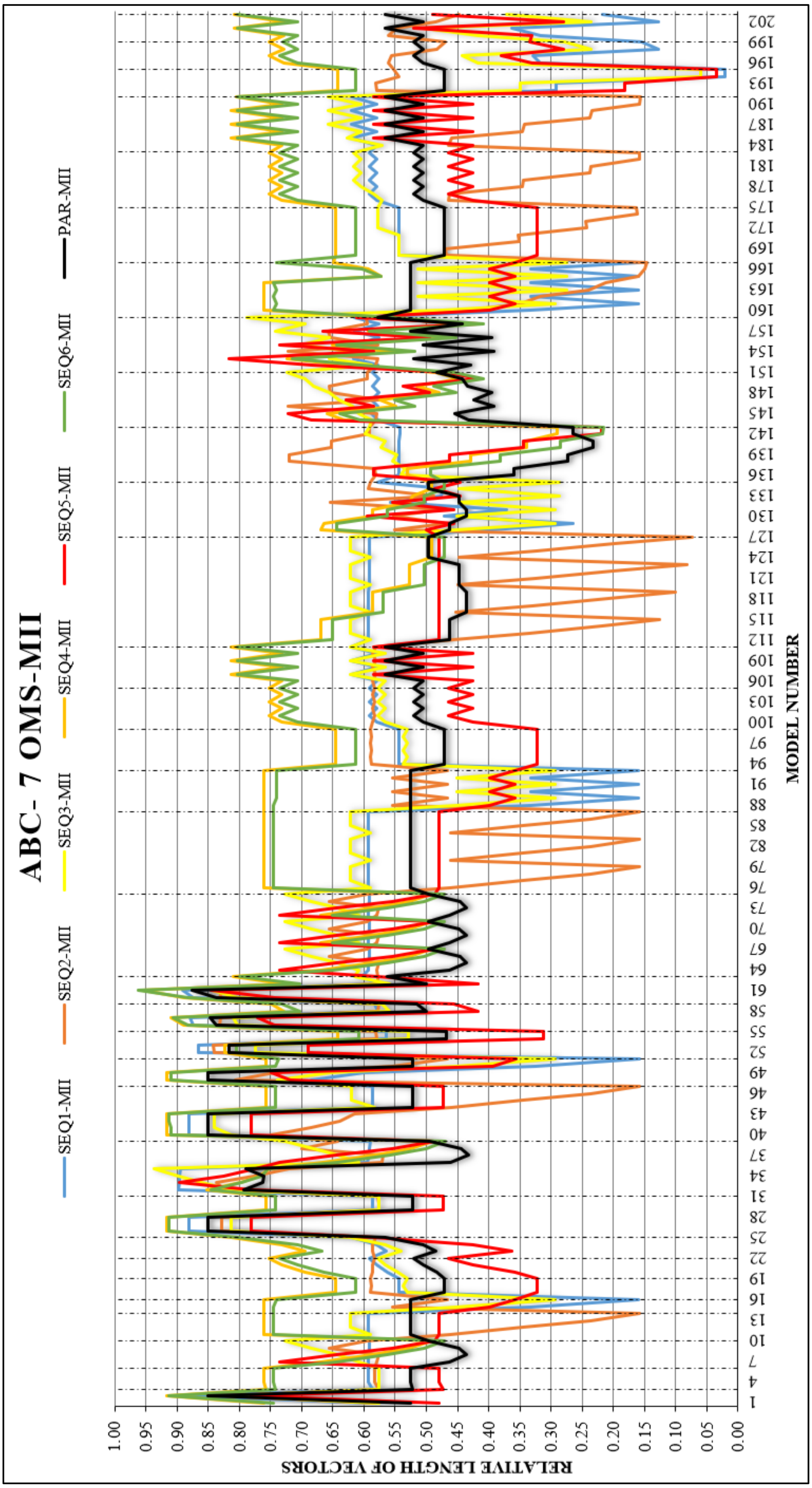

Figure 38: Results of the 7 OMS – ABC method – HOS 1

4.4.1 Results based on the maximum change of the objective function values

As defined in subsection 4.3.1, the maximum COFV is the maximum value of the 203 COFVs for each of the 7 OMS. The 7 OMS are ranked based on the 7-corresponding maximum COFVs as illustrated in Table 50.

Table 50: The ranked 7 OMS based on the maximum COFV – ABC – HOS 1

Rank	OMS	Objective function value changes (Maximum – ABC)
1	SEQ5-MII	0.29
2	SEQ3-MII	0.37
3	SEQ1-MII	0.48
4	PAR-MII	0.77
5	SEQ6-MII	1.00
6	SEQ4-MII	1.03
7	SEQ2-MII	1.08

Table 50 shows the following trends of the 7 OMS:

HOS1-Max-ABC 1. The 7 OMS can be categorised into 3 Groups based on the range of the maximum COFV of each OMS. The three groups are the same as the groups defined in Table 116 although the ranking of the bottom three OMS is slightly different.

HOS1-Max-ABC 2. SEQ1-MII, SEQ3-MII and SEQ5-MII have a smaller maximum COFV than the other OMS. It indicates that the results of these three OMS are closer to the absolute optimum solution than the results of the other OMS.

HOS1-Max-ABC 3. SEQ1-MII, SEQ3-MII and SEQ5-M optimise the COST module before the CO2 module compared to the OMS orders of the other OMS. This trend is also found in section 4.3. It is also suggested that this is the reason SEQ1-MII, SEQ3-MII and SEQ5-MII outperform SEQ2-MII, SEQ4-MII and SEQ6-MII.

HOS1-Max-ABC 4. SEQ5-MII has the smallest maximum COFV while SEQ2-MII has the largest maximum COFV. This indicates that the results of SEQ5-MII outperform the other 6 OMS while the results of SEQ2-MII underperform the other OMS.

HOS1-Max-ABC 5. The PAR-MII has a ‘medium’ level performance which is same as discovered in section 4.3.

4.5 INC results of Holistic Optimisation Study 1

In this section the results of the 7 OMS will be studied by the Incremental Criterion (INC) method; and the general trends will be extracted. To obtain a general overview of the results, the individual results of each of the 7 OMS are plotted as single points in a figure and linear lines are utilised to connect the points. As a result, Figure 39 is created. As the definition of the INC method in subsection 3.6.3 demonstrated, the idea is to calculate the 'distance' between the results of the initial and the final iteration. For this distance, namely 'Local Distance', the larger is the better. The 'Local Distance' also represents the COFV in this section. The 7 continuous lines for the 7 OMS in Figure 39 are 'interlaced' and only one trend is clearly found directly from the figure. The graph of SEQ2-MII in Figure 39 is nearly consistently lower than the graphs of the other OMS. This indicates that the results of SEQ2-MII underperform the results of the other OMS. To obtain more trends of the 7 OMS, the results will be studied from several specific perspectives in this section. The basic setup of this section is the same as that of section 4.3. The study of the results of the 7 OMS consists of 4 subsections:

- Subsection 4.5.1, Results based on the maximum change of the objective function values
- Subsection 9.1.5 in Appendix – F, Results based on the average change of the objective function values
- Subsection 9.1.6 in Appendix – F, Results based on the minimum change of the objective function values
- Subsection 9.1.7 in Appendix – F, Results based on the average spreads of objective function value change
- Subsection 9.1.8 contains the summary of section 4.5.

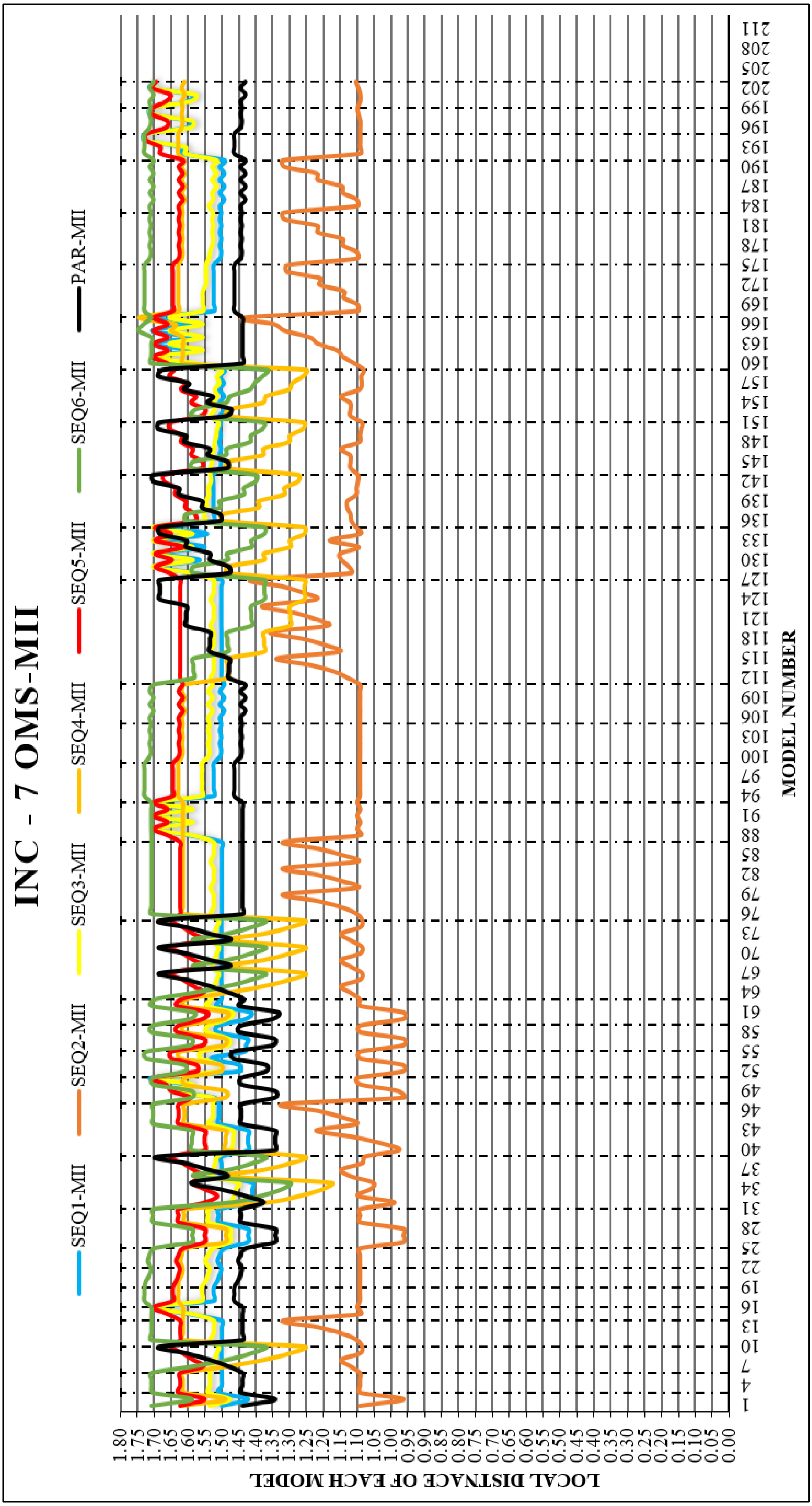

Figure 39: Results of the 7 OMS – INC method – HOS 1

4.5.1 Results based on the maximum change of the objective function values

The maximum COFV is the maximum value of the 203 COFV for the 203 models in each OMS. The 7 OMS are ranked from 1st to 7th based on the maximum COFV, as illustrated in Table 51.

Table 51: The ranked 7 OMS based on the maximum COFV – INC – HOS1

Rank	OMS	Objective function value changes (Maximum – INC)
1	SEQ4-MII	1.74
2	SEQ6-MII	1.74
3	SEQ1-MII	1.73
4	SEQ3-MII	1.72
5	SEQ5-MII	1.72
6	PAR-MII	1.70
7	SEQ2-MII	1.43

Based on the ranking of the 7 OMS illustrated in Table 51, several trends are found as follows:

HOS1-Max-INC 1. SEQ2-MII is ranked 7th. This indicates that SEQ2-MII underperforms the other OMS based on the maximum COFV.

HOS1-Max-INC 2. The maximum COFV of the OMS ranked from 1st to 6th has very close values, i.e. the difference of the maximum COFV between the OMS ranked 1st and 6th is only 0.04. This indicates that those 6 OMS have a similar performance based on the maximum COFV.

HOS1-Max-INC 3. SEQ4-MII is now ranked 1st while the SEQ5-MII is ranked 6th. However, the maximum COFV of these two OMS have a very small difference, i.e. 0.04 as defined in HOS1-Max-INC 2. Therefore, the trend found here is considered to be indifferent as there is no significant difference between the two OMS.

4.6 Detailed Analysis of the Holistic Optimisation Study 1

Some of the general trends have been discovered in the previous sections by using the three evaluation methods:

- Individual Criterion Evaluation (ICE) method
- Absolute Criterion (ABC) method
- Incremental Criterion (INC) method.

In this section, these three methods will be used again but mainly to focus on the performance of the three individual modules: STRUCTURAL, COST and CO2. The analysis consists of two perspectives:

- Perspective of the objective function values
- Perspective of the sensitivity

The performance of the 7 OMS based on the three evaluation methods will be the 'Global' performance. The performance of the three individual modules will be the 'Local' performance. The 'Local' performance based on the two perspectives will be discussed in two subsections respectively.

4.6.1 Perspective of the objective function values – HOS 1

Firstly, the performance of the 7 individual OMS based on three evaluation methods are summarised and ranked according to their efficiency in Table 52. In Table 52, the 7 OMS are ranked in descending order according to the average Global Objective Function Value Change (GOFVC) of each of them.

Table 52: Ranked 7 OMS based on the average GOFVC – HOS 1

Rank	ICE		ABC		INC	
	OMS	GOFVC	OMS	GOFVC	OMS	GOFVC
1	SEQ5-MII	223%	SEQ5-MII	0.15	SEQ5-MII	1.63
2	SEQ3-MII	211%	SEQ3-MII	0.31	SEQ6-MII	1.61
3	SEQ1-MII	206%	SEQ1-MII	0.35	SEQ3-MII	1.55
4	PAR-MII	183%	PAR-MII	0.50	SEQ1-MII	1.53
5	SEQ2-MII	110%	SEQ6-MII	0.79	SEQ4-MII	1.51
6	SEQ6-MII	108%	SEQ2-MII	0.81	PAR-MII	1.48
7	SEQ4-MII	106%	SEQ4-MII	0.83	SEQ2-MII	1.13
Difference (%) Between Rank 1st and 7th		110%		441%		44%

The individual ranking in Table 52 of the 7 OMS is slightly different and a number of noteworthy trends are found as follows:

HOS1-G1. The average GOFVC of SEQ5-MII consistently outperforms all the other OMS. It can be seen that for the three evaluation methods, 'outperformance' is significant as the difference between ranking 1 and ranking 7 is 110% for ICE, 441% for ABC and 44% for INC. It is found that the 'outperformance' of SEQ5-MII illustrated by the ABC method is more noticeable. The reason could be that the three evaluation methods are different in nature or that the ABC evaluation method may be more appropriate to analyse the 7 OMS.

HOS1-G2. According to Table 45 in subsection 4.3.1, the 6 SEQ optimisation programmes are categorised into two groups based on the specific position of the COST and CO2 module during the optimisation. This is also the reason that SEQ1-MII, SEQ3-MII and SEQ5-MII are always ranked top in each column of Table 52, apart from SEQ6-MII in the INC column. Although SEQ6-MII is ranked 2nd in the INC column, the overall performance of SEQ1-MII (3rd), SEQ3-MII (4th) and SEQ5-MII (1st) still outperforms SEQ2-MII

(7^{th}), SEQ4-MII (5^{th}) and SEQ6-MII (2^{nd}).

HOS1-G3. Apart from the ranking of SEQ6-MII in the INC column of Table 52, the OMS that optimise the COST module before the CO2 module will be ranked higher. This is evidenced by the OMS orders in Table 45, Table 115 and the rankings in Table 52.

To find out how the three individual modules 'help' SEQ5-MII to be ranked 1^{st}, the average GOFVCs of the 7 OMS in the ICE, ABC and INC columns of Table 52 are 'decomposed' into 'Local' Objective Function Values Change (LOFVC). The LOFVCs of the 7 OMS based on the three evaluation methods will be studied in the following subsubsections respectively.

4.6.1.1 ICE – LOFVC – HOS 1

The new rankings of the 7 OMS based on the performance of each module are illustrated in Table 53. The 7 'Local' Objective Function Values Change (LOFVC) of each module are ranked from the largest to the smallest.

Table 53: The LOFVC of each module based on the ICE method – HOS 1

Rank	OMS	LOFVC (STRUCTURAL)	OMS	LOFVC (CO2)	OMS	LOFVC (COST)
1	SEQ1-MII	56%	SEQ5-MII	73%	SEQ5-MII	94%
2	SEQ2-MII	56%	SEQ3-MII	62%	SEQ3-MII	93%
3	SEQ3-MII	56%	SEQ1-MII	59%	PAR-MII	93%
4	SEQ4-MII	56%	PAR-MII	34%	SEQ1-MII	91%
5	SEQ5-MII	56%	SEQ2-MII	29%	SEQ6-MII	37%
6	SEQ6-MII	56%	SEQ4-MII	14%	SEQ4-MII	35%
7	PAR-MII	56%	SEQ6-MII	14%	SEQ2-MII	26%
Difference Between Rank 1^{st} and 7^{th}		0		59.11%		67.58%

The trends observed from Table 53 are as follows:

HOS1-LOFVC-ICE1. The LOFVC in the STRUCTURAL module of the 7 OMS is the same. This indicates the performance of the STRUCTURAL module across the 7 OMS is the same.

HOS1-LOFVC-ICE2. SEQ5-MII outperforms all the other OMS in both the CO2 and the COST columns of Table 53. This indicates the reason why SEQ5-MII is consistently ranked 1^{st} in Table 52.

HOS1-LOFVC-ICE3. The difference in the LOFVC between the OMS ranked 1^{st} and 7^{th} for both the COST and the CO2 column is significant large, i.e. for CO2 it is 59.11% and for COST it is 67.58%. This indicates that the variation of the 'Global' performance for each of the 7 OMS is related to their 'Local' performance in the CO2 and the COST modules.

HOS1-LOFVC-ICE4. SEQ1-MII, SEQ3-MII and SEQ5-MII consistently outperform SEQ2-MII, SEQ4-MII and SEQ6-MII in both the COST and the CO2 column. This also verifies the trend defined in HOS1-G2 in subsection 4.6.1.

4.6.1.2 ABC – LOFVC – HOS 1

The objective function value change of the 7 MOS based on the ABC method are also 'decomposed' into individual objective function value changes for each module. The rankings of the 7 OMS according to the local objective function value changes (LOFVC) are tabulated in Table 54.

Table 54: The LOFVC of each module based on ABC method – HOS 1

Rank	OMS	LOFVC (STRUCTURAL)	OMS	LOFVC (CO2)	OMS	LOFVC (COST)
1	SEQ1-MII	0.01	SEQ5-MII	0.14	SEQ5-MII	0.03
2	SEQ2-MII	0.01	SEQ3-MII	0.30	SEQ3-MII	0.04
3	SEQ3-MII	0.01	SEQ2-MII	0.32	PAR-MII	0.04
4	SEQ4-MII	0.01	SEQ1-MII	0.34	SEQ1-MII	0.05
5	SEQ5-MII	0.01	PAR-MII	0.49	SEQ6-MII	0.06
6	SEQ6-MII	0.01	SEQ4-MII	0.78	SEQ4-MII	0.24
7	PAR-MII	0.01	SEQ6-MII	0.78	SEQ2-MII	0.69
Difference Between Rank 1st and 7th		0		0.64		0.66

The trends discovered in Table 54 are as follows:

HOS1-LOFVC-ABC1. The LOFVC in the STRUCTURAL module of the 7 OMS is the same. This indicates the performance of the STRUCTURAL module across the 7 OMS is the same.

HOS1-LOFVC-ABC2. SEQ5-MII outperforms all other OMS in both the CO2 and the COST columns of Table 54. This indicates the reason why SEQ5-MII is consistently ranked 1st in Table 52.

HOS1-LOFVC-ABC3. The difference in the LOFVC between the OMS ranked 1st and 7th for both the COST and the CO2 column is significantly large, i.e. for CO2 it is 0.64 and for COST it is 0.66. This indicates that the variation of the 'Global' performance for each of the 7 OMS is related to their 'Local' performance in the CO2 and COST modules.

HOS1-LOFVC-ABC4. Although SEQ2-MII in the CO2 column is ranked 3rd, it will not change the fact that the overall performance of SEQ1-MII, SEQ3-MII and SEQ5-MII outperforms SEQ2-MII, SEQ4-MII and SEQ6-MII in Table 52.

4.6.1.3 INC – LOFVC – HOS 1

The previous two subsections have similar trends for the 7 OMS in each of the individual modules. This subsection will further investigate the trends by ranking the 7 OMS based on their individual module performance assessed by the INC method. The ranking of the 7 OMS for each module is tabulated in Table 55.

Table 55: The LOFVC of each module based on the INC method – HOS 1

Rank	OMS	LOFVC (STRUCTURAL)	OMS	LOFVC (CO2)	OMS	LOFVC (COST)
1	SEQ1-MII	0.99	SEQ5-MII	0.86	SEQ5-MII	0.97
2	SEQ2-MII	0.99	SEQ3-MII	0.70	SEQ3-MII	0.96
3	SEQ3-MII	0.99	SEQ2-MII	0.68	PAR-MII	0.96
4	SEQ4-MII	0.99	SEQ1-MII	0.66	SEQ1-MII	0.95
5	SEQ5-MII	0.99	PAR-MII	0.51	SEQ6-MII	0.94
6	SEQ6-MII	0.99	SEQ4-MII	0.22	SEQ4-MII	0.76
7	PAR-MII	0.99	SEQ6-MII	0.22	SEQ2-MII	0.31
Difference Between Rank 1st and 7th		0		0.64		0.66

The trends discovered in Table 55 are as follows:

HOS1-LOFVC-INC1. The LOFVC in the STRUCTURAL module of the 7 OMS is the same. This indicates the performance of the STRUCTURAL module across the 7 OMS is the same.

HOS1-LOFVC-INC2. SEQ5-MII outperforms all other OMS in both the CO2 and the COST columns of Table 55. This indicates the reason why SEQ5-MII is consistently ranked 1st in Table 52.

HOS1-LOFVC-INC3. The difference in the LOFVC between the OMS ranked 1st and 7th for both the COST and the CO2 column is significant large, i.e. for CO2 it is 0.64 and for COST it is 0.66. This indicates that the variation of the 'Global' performance for each of the 7 OMS is related to their 'Local' performance in the CO2 and COST modules.

HOS1-LOFVC-INC4. Although SEQ2-MII is ranked 3rd in the CO2 column, it will not change the fact that the overall performance of SEQ1-MII, SEQ3-MII and SEQ5-MII outperforms SEQ2-MII, SEQ4-MII and SEQ6-MII in Table 52.

The general trends listed in subsections 4.6.1.1, 4.6.1.2 and 4.6.1.3 will be compared and summarised in section 0. Before this is done, the results of the three modules across the 7 OMS will be further studied from the perspective of sensitivity.

4.6.2 Perspective of Sensitivity – HOS 1

In addition to the ranking of the 7 OMS based on the objective function value changes in Table 52, the ranking of the 7 OMS based on their sensitivity performance is summarised and ranked in Table 56.

Table 56: Ranked 7 OMS based on the Global Spread Values (GSV) – HOS 2

Rank	ICE		ABC		INC	
	OMS	GSV	OMS	GSV	OMS	GSV
1	SEQ5-MII	7%	SEQ3-MII	0.06	SEQ5-MII	0.05
2	SEQ1-MII	8%	SEQ5-MII	0.06	SEQ1-MII	0.05
3	SEQ3-MII	8%	SEQ1-MII	0.06	SEQ3-MII	0.05
4	SEQ6-MII	9%	PAR-MII	0.13	PAR-MII	0.08
5	SEQ4-MII	10%	SEQ4-MII	0.15	SEQ6-MII	0.08
6	PAR-MII	11%	SEQ6-MII	0.18	SEQ4-MII	0.09
7	SEQ2-MII	29%	SEQ2-MII	0.22	SEQ2-MII	0.10

The 7 OMS are ranked from the lowest to the highest sensitivity. The following trends are found from Table 56:

HOS1-GSV1. The spread between the OMS ranking 1st and 7th is significantly large in each evaluation method. For ICE, the spread is 22%; for ABC, the spread is 0.16; for INC, the spread is 0.05. This indicates that the results of the 7 OMS have significantly different sensitivity performances in each evaluation method although some of the OMS have same GSV in each evaluation method; i.e. SEQ1-MII, SEQ3-MII and SEQ5-MII have same GSV in both the ABC and the INC column.

HOS1-GSV2. The top three ranked SEQ optimisation programmes have smaller values than the bottom three. This indicates that the results of SEQ2-MII, SEQ4-MII and SEQ6-MII are more sensitive to the change of the parameters than SEQ1-MII, SEQ3-MII and SEQ5-MII. It is suggested that the results of SEQ1-MII, SEQ3-MII and SEQ5-MII are considered to be more stable.

HOS1-GSV3. The top three ranked SEQ optimisation programmes optimised the COST module before the CO2 module while the bottom three optimised the CO2 module before the COST module. This is evidenced by the OMS orders in Table 46. This could be the reason that SEQ1-MII, SEQ3-MII and SEQ5-MII are ranked higher than SEQ2-MII, SEQ4-MII and SEQ6-MII based on the sensitivity analysis.

In order to find out how the three individual modules influence the ranking of the 7 OMS based on their sensitivity performance, the global spread values (**GSV**) in ICE, ABC and INC are 'decomposed' into the local spread values (**LSV**) of the three individual modules respectively.

The LSV of the 7 OMS for each module based on each evaluation method will be investigated in the following subsections.

4.6.2.1 ICE – LSV – HOS 1

In order to assess the sensitivity performance of the 7 OMS in the three individual modules, a table containing the local spread values (LSV) of each module across the 7 OMS was created (Table 57). The local spread values of the 7 OMS based on the ICE method are ranked from the lowest to the highest in Table 57.

Table 57: The local spread values of each module based on the ICE method – HOS 1

Rank	OMS	LSV (STRUCTURAL)	OMS	LSV (CO2)	OMS	LSV (COST)
1	SEQ1-MII	1%	SEQ5-MII	5%	SEQ5-MII	1%
2	SEQ2-MII	1%	SEQ3-MII	5%	SEQ6-MII	1%
3	SEQ3-MII	1%	SEQ1-MII	6%	SEQ1-MII	1%
4	SEQ4-MII	1%	SEQ6-MII	10%	SEQ3-MII	1%
5	SEQ5-MII	1%	SEQ4-MII	10%	PAR-MII	1%
6	SEQ6-MII	1%	PAR-MII	10%	SEQ4-MII	2%
7	PAR-MII	1%	SEQ2-MII	15%	SEQ2-MII	34%
Average		1%		9%		6%

The following trends are discovered:

HOS1-LSV-ICE1. The results of the STRUCTURAL module are less sensitive to the change of parameters, as this module has the lowest average LSV (1%) than the other two (9% for CO2 and 6% for COST). This also indicates that the performance of the 7 OMS in the STRUCTURAL module is more stable than their performance in other modules. On the other hand, the results of the 7 OMS in the CO2 module are more sensitive to the change of parameters.

HOS1-LSV-ICE2. The STRUCTURAL module has the same performance across the 7 OMS, as the LSV is the same.

HOS1-LSV-ICE3. SEQ2-MII is ranked 7th in both the CO2 and the COST columns in Table 57. This indicates that the results of SEQ2-MII are more sensitive to the change of the input parameter(s).

HOS1-LSV-ICE4. The results of SEQ5-MII are more stable than all the other OMS as SEQ5-MII has the lowest LSV across the three modules.

HOS1-LSV-ICE5. Apart from SEQ2-MII, all the other OMS in the COST column have nearly the same LSV. This indicates that the results of those OMS have nearly the same sensitivity to the change of input parameter(s).

In addition to the sensitivity analysis of the results of the 7 OMS in each module, the spreads of the 33 case studies for each of the 7 OMS are also investigated. The 33 case studies of each OMS consist of two types of sensitivity analysis:

- One at A Time (OAT), how the change of a single parameter influences the optimisation result.
- Two at A Time (TAT), how the change of two parameters influences the optimisation result.

The two types of methods were defined in subsection 3.5.2. OAT analyses the case studies 1 – 8; while TAT analyses case studies 9 – 33. The spreads of the 33 case studies are then ranked in Table 58. The following trends are found in Table 58:

HOS1-LSV-ICE6. For OAT, the single parameter of case study 5 is the most influential parameter for SEQ1-MII and SEQ3-MII, i.e. the Maximum component CO_2. The single parameter of case study 4 is the most influential parameter for SEQ2-MII, i.e. Maximum component cost. The single parameter of case study 3 is the most influential parameter for SEQ4-MII, SEQ5-MII, SEQ6-MII and PAR-MII, i.e. Recycled content.

HOS1-LSV-ICE7. For TAT, the two parameters of case study 12 are the most influential parameters for SEQ1-MII and SEQ3-MII, i.e. Geometry and Maximum component CO_2. The two parameters of case study 27 are the most influential parameters for SEQ2-MII, i.e. Maximum component CO_2 and Maximum component cost. The two parameters of case study 26 are the most influential parameters for SEQ4-MII and SEQ6-MII, i.e. Recycled content and Overhead Cost. The two parameters of case study 10 are the most influential parameters for SEQ5-MII and PAR-MII, i.e. Geometry and Recycled content.

The results of the three modules for the 7 OMS will be analysed based on the ABC evaluation method in the next subsubsection. The similar analysis as in this subsubsection will also be implemented in the next subsubsection, to compare/ verify the general trends discovered above.

Table 58: Spread of each case study for the 7 OMS by the ICE method – HOS1

Methods	Rank	Case Study No.	SEQ1-MII	Case Study No.	SEQ2-MII	Case Study No.	SEQ3-MII	Case Study No.	SEQ4-MII	Case Study No.	SEQ5-MII	Case Study No.	SEQ6-MII	Case Study No.	PAR-MII
OAT	1	5	18%	4	65%	5	20%	3	34%	3	16%	3	35%	3	28%
	2	1	11%	3	29%	1	6%	8	3%	1	8%	8	3%	1	16%
	3	8	3%	5	16%	8	4%	7	1%	5	6%	7	1%	8	3%
	4	7	2%	1	14%	3	3%	1	0%	8	3%	1	1%	7	2%
	5	3	0%	7	1%	4	2%	2	0%	7	2%	5	0%	4	0%
	6	6	0%	6	0%	7	2%	4	0%	2	0%	2	0%	2	0%
	7	2	0%	2	0%	6	0%	5	0%	4	0%	4	0%	6	0%
	8	4	0%	8	0%	2	0%	6	0%	6	0%	6	0%	5	0%
TAT	1	12	27%	27	81%	12	25%	26	36%	10	18%	26	36%	10	42%
	2	23	25%	22	78%	27	24%	10	35%	26	18%	10	35%	26	30%
	3	33	20%	11	78%	33	22%	25	35%	25	16%	25	35%	25	29%
	4	32	19%	30	66%	32	20%	16	35%	16	16%	24	35%	16	28%
	5	18	18%	29	66%	23	20%	22	35%	24	16%	16	34%	23	28%
	6	27	18%	17	65%	18	20%	23	35%	12	14%	22	34%	22	28%
	7	31	18%	28	65%	31	20%	24	35%	23	13%	23	34%	24	28%
	8	15	13%	10	39%	10	8%	27	30%	15	10%	27	7%	15	18%
	9	10	12%	24	32%	15	8%	15	2%	14	9%	15	3%	14	16%
	10	14	11%	25	30%	11	7%	21	2%	9	8%	21	2%	12	16%
	11	13	11%	26	30%	14	6%	30	2%	11	8%	30	2%	13	16%
	12	9	11%	16	29%	9	6%	33	2%	13	8%	33	2%	9	16%
	13	11	11%	23	28%	26	5%	14	1%	33	8%	14	1%	11	16%
	14	26	2%	12	27%	13	5%	32	1%	32	7%	20	1%	21	2%
	15	21	2%	33	20%	30	4%	20	1%	18	6%	29	1%	30	2%
	16	30	2%	13	17%	25	4%	29	1%	27	6%	32	1%	33	2%
	17	25	1%	32	16%	24	3%	9	0%	31	6%	9	1%	29	1%
	18	20	1%	18	16%	16	3%	11	0%	21	2%	11	1%	32	1%
	19	29	1%	14	14%	29	3%	12	0%	30	2%	12	1%	20	1%
	20	22	0%	15	14%	21	2%	13	0%	20	1%	13	1%	18	0%
	21	24	0%	9	14%	17	2%	17	0%	29	1%	18	0%	17	0%
	22	16	0%	31	7%	22	2%	18	0%	17	0%	17	0%	28	0%
	23	19	0%	21	1%	28	2%	19	0%	19	0%	19	0%	19	0%
	24	28	0%	20	0%	20	1%	28	0%	22	0%	28	0%	31	0%
	25	17	0%	19	0%	19	0%	31	0%	28	0%	31	0%	27	0%

4.6.2.2 ABC – LSV – HOS 1

In this subsection, the rankings of the 7 OMS in each module based the ABC method will be studied and discussed. The rankings of the 7 OMS for the individual modules are tabulated in Table 59.

Table 59: The local spread values of each module based on the ABC method – HOS 1

Rank	OMS	LSV (STRUCTURAL)	OMS	LSV (CO2)	OMS	LSV (COST)
1	SEQ1-MII	0.02	SEQ5-MII	0.06	SEQ5-MII	0.01
2	SEQ2-MII	0.02	SEQ3-MII	0.06	SEQ6-MII	0.01
3	SEQ3-MII	0.02	SEQ1-MII	0.07	SEQ1-MII	0.01
4	SEQ4-MII	0.02	PAR-MII	0.15	SEQ3-MII	0.01
5	SEQ5-MII	0.02	SEQ6-MII	0.19	SEQ4-MII	0.01
6	SEQ6-MII	0.02	SEQ4-MII	0.19	PAR-MII	0.01
7	PAR-MII	0.02	SEQ2-MII	0.19	SEQ2-MII	0.31
Average		0.02		0.13		0.05

The following trends are discovered from Table 59:

HOS1-LSV-ABC1. The results of the STRUCTURAL module are less sensitive to the change of parameters as this module has the lowest average LSV (0.02) than the other two (0.011 for CO2 and 0.13 for COST). This also indicates that the performance of the 7 OMS in the STRUCTURAL module is more stable than their performance in the other modules. On the other hand, the results of the 7 OMS in the CO2 module are more sensitive to the change of parameters.

HOS1-LSV-ABC2. The STRUCTURAL module has the same performance across the 7 OMS, as the LSV of the 7 OMS is the same. The same trend can be found in the COST module as the LSV of the OMS (apart from SEQ2-MII) is the same.

HOS1-LSV-ABC3. SEQ2-MII is ranked 7th in both the CO2 and the COST columns of Table 59. This indicates that the results of SEQ2-MII are more sensitive to the change of the input parameter(s) than all the other OMS.

HOS1-LSV-ABC4. Apart from SEQ2-MII, all the other OMS in the COST column have nearly the same LSV. This indicates that the results of those OMS have nearly the same sensitivity to the change of input parameter(s).

HOS1-LSV-ABC5. The 'Global' sensitivity of the results for the 7 OMS is more related to the 'Local' sensitivity performance of the CO2 module. This is because almost all the OMS in the STRUCTURAL and COST module have the same LSV respectively.

HOS1-LSV-ABC6. The results of SEQ5-MII are more stable than all other OMS, as SEQ5-MII has the lowest LSV across the three modules.

Similar to the subsection 4.6.1.1, the spreads of the 33 case studies are also studied in this subsection based on the ABC evaluation method. The 33 case studies are then ranked in Table 60.

A few trends are found from Table 60:

HOS1-LSV-ABC7. For OAT, the single parameter of case study 5 is the most influential parameter for SEQ1-MII and SEQ3-MII, i.e. the Maximum component CO_2. The single parameter of case study 4 is the most influential parameter for SEQ2-MII, i.e. Maximum component cost. The single parameter of case study 3 is the most influential parameter for SEQ4-MII, SEQ5-MII, SEQ6-MII and PAR-MII, i.e. Recycled content.

HOS1-LSV-ABC8. For TAT, the two parameters of case study 23 are the most influential parameters for SEQ1-MII, i.e. Recycled content and Maximum component CO_2. The two parameters of case study 22 are the most influential parameters for SEQ2-MII, i.e. Recycled content and Maximum component cost. The two parameters of case study 27 are the most influential parameters for SEQ3-MII, i.e. Maximum component CO_2 and Maximum component cost. The two parameters of case study 24 are the most influential parameters for SEQ4-MII, SEQ5-MII and SEQ6-MII, i.e. Recycled content and Travel distance. The two parameters of case study 10 are the most influential parameters for PAR-MII, i.e. Geometry and Recycled content.

The general trends of the sensitivity analysis for the 7 OMS in this subsubsection are quite similar to those in subsubsection 4.6.2.1. The overall trends of the sensitivity analysis will be summarised in section 4.7. Before this is done, the average spread of each case study for the 7 OMS will be studied based on the INC method in the next subsubsection.

Table 60: Spread of each case study for the 7 OMS by the ABC method – HOS1

Methods	Rank	Case Study No.	SEQ1-MII	Case Study No.	SEQ2-MII	Case Study No.	SEQ3-MII	Case Study No.	SEQ4-MII	Case Study No.	SEQ5-MII	Case Study No.	SEQ6-MII	Case Study No.	PAR-MII
OAT	1	5	0.17	4	0.51	5	0.18	3	0.54	3	0.18	3	0.66	3	0.39
	2	1	0.09	3	0.27	4	0.02	1	0.10	1	0.06	1	0.10	1	0.15
	3	8	0.00	5	0.14	1	0.01	8	0.01	5	0.06	7	0.01	8	0.00
	4	7	0.00	1	0.03	8	0.01	7	0.01	8	0.01	8	0.00	7	0.00
	5	6	0.00	7	0.00	3	0.01	2	0.00	7	0.00	5	0.00	4	0.00
	6	3	0.00	6	0.00	6	0.00	4	0.00	2	0.00	2	0.00	2	0.00
	7	2	0.00	2	0.00	7	0.00	5	0.00	4	0.00	4	0.00	5	0.00
	8	4	0.00	8	0.00	2	0.00	6	0.00	6	0.00	6	0.00	6	0.00
TAT	1	23	0.23	22	0.60	27	0.25	24	0.56	24	0.18	24	0.68	10	0.52
	2	12	0.22	11	0.54	31	0.21	26	0.55	26	0.18	26	0.66	24	0.42
	3	31	0.20	27	0.52	12	0.20	25	0.55	25	0.18	25	0.66	26	0.40
	4	33	0.18	30	0.51	33	0.19	16	0.54	10	0.18	10	0.66	25	0.40
	5	32	0.18	29	0.51	32	0.19	22	0.54	16	0.18	16	0.66	16	0.39
	6	18	0.17	28	0.51	23	0.18	23	0.54	23	0.12	22	0.66	23	0.39
	7	27	0.17	17	0.51	18	0.18	10	0.54	12	0.11	23	0.66	22	0.39
	8	10	0.08	10	0.32	11	0.03	15	0.10	31	0.07	15	0.10	15	0.15
	9	15	0.07	24	0.29	30	0.02	14	0.09	33	0.07	14	0.10	14	0.15
	10	14	0.07	25	0.29	29	0.02	13	0.09	32	0.06	13	0.10	13	0.15
	11	13	0.07	26	0.29	28	0.02	9	0.09	15	0.06	11	0.10	12	0.15
	12	9	0.07	16	0.27	17	0.02	11	0.09	14	0.06	12	0.10	11	0.15
	13	11	0.07	23	0.24	22	0.02	12	0.09	13	0.06	9	0.10	9	0.15
	14	26	0.00	33	0.18	15	0.02	27	0.03	9	0.06	27	0.00	21	0.00
	15	21	0.00	12	0.16	9	0.01	21	0.00	11	0.06	21	0.00	30	0.00
	16	30	0.00	32	0.14	14	0.01	30	0.00	18	0.06	30	0.00	33	0.00
	17	25	0.00	18	0.14	10	0.01	33	0.00	27	0.06	33	0.00	29	0.00
	18	20	0.00	13	0.06	26	0.01	32	0.00	21	0.01	20	0.00	32	0.00
	19	29	0.00	31	0.06	24	0.01	20	0.00	30	0.01	29	0.00	20	0.00
	20	22	0.00	14	0.04	25	0.01	29	0.00	20	0.00	32	0.00	18	0.00
	21	16	0.00	15	0.04	13	0.01	17	0.00	29	0.00	18	0.00	17	0.00
	22	24	0.00	9	0.04	16	0.01	18	0.00	17	0.00	17	0.00	28	0.00
	23	19	0.00	21	0.01	19	0.00	19	0.00	19	0.00	19	0.00	19	0.00
	24	28	0.00	20	0.00	21	0.00	28	0.00	22	0.00	28	0.00	31	0.00
	25	17	0.00	19	0.00	20	0.00	31	0.00	28	0.00	31	0.00	27	0.00

4.6.2.3 INC – LSV – HOS 1

In order to see if the trends of the 7 OMS in each module are similar based on the INC method, the 7 OMS are ranked according to their sensitivity performance in each module. The rankings are tabulated in Table 61.

Table 61: The local spread values of each module based on the INC method – HOS 1

Rank	OMS	LSV (STRUCTURAL)	OMS	LSV (CO2)	OMS	LSV (COST)
1	SEQ1-MII	0.02	SEQ5-MII	0.06	SEQ5-MII	0.01
2	SEQ2-MII	0.02	SEQ3-MII	0.06	SEQ6-MII	0.01
3	SEQ3-MII	0.02	SEQ1-MII	0.07	SEQ1-MII	0.01
4	SEQ4-MII	0.02	PAR-MII	0.15	SEQ3-MII	0.01
5	SEQ5-MII	0.02	SEQ6-MII	0.19	SEQ4-MII	0.01
6	SEQ6-MII	0.02	SEQ4-MII	0.19	PAR-MII	0.01
7	PAR-MII	0.02	SEQ2-MII	0.19	SEQ2-MII	0.31
Average		0.02		0.13		0.05

The following trends are discovered:

HOS1-LSV-INC1. The results of the STRUCTURAL module are less sensitive to the change of parameters, as this module has the lowest average LSV (0.02) than the other two modules (0.13 for CO2 and 0.05 for COST). This also indicates that the performance of the 7 OMS in the STRUCTURAL module is more stable than their performance in other modules. On the other hand, the results of the 7 OMS in the CO2 module are more sensitive to the change of parameters.

HOS1-LSV-INC2. The STRUCTURAL module has the same performance across the 7 OMS, as the LSV is the same. The same trend can be found in the COST module as the LSV of the OMS (apart from SEQ2-MII) is the same.

HOS1-LSV-INC3. SEQ2-MII is ranked 7th in both the CO2 and the COST columns of Table 61. This indicates that the results of SEQ2-MII are more sensitive to the change of the input parameter(s) than all the other OMS.

HOS1-LSV-INC4. Apart from SEQ2-MII, all the other OMS in the COST column have nearly the same LSV. This indicates that the results of those OMS have nearly the same sensitivity to the change of input parameter(s).

HOS1-LSV-INC5. The ‘Global’ sensitivity of the results for the 7 OMS is more related to the ‘Local’ sensitivity performance of the CO2 module. This is because almost all the OMS in the STRUCTURAL and COST modules have the same LSV respectively.

HOS1-LSV-INC6. The results of SEQ5-MII are more stable than all the other OMS as the SEQ5-MII has the lowest LSV across the three modules.

The spreads of the 33 case studies are also studied in this subsection based on the INC evaluation method. The 33 case studies are then ranked in Table 62. The following trends are found in Table 62:

HOS1-LSV-INC7. For OAT, the single parameter of case study 5 is the most influential parameter for SEQ1-MII and SEQ3-MII, i.e. the Maximum component CO_2. The single parameter of case study 4 is the most influential parameter for SEQ2-MII, i.e. Maximum component cost. The single parameter of case study 3 is the most influential parameter for SEQ4-MII, SEQ5-MII, SEQ6-MII and PAR-MII, i.e. Recycled content.

HOS1-LSV-INC8. For TAT, the two parameters of case study 12 are the most influential parameters for SEQ1-MII and SEQ3-MII, i.e. Geometry and Maximum component CO_2. The two parameters of case study 11are the most influential parameters for SEQ2-MII, i.e. Geometry and Maximum component cost. Two parameters of case study 10 are the most influential parameters for SEQ4-MII, SEQ5-MII, SEQ6-MII and PAR-MII, i.e. Geometry and Recycled content.

The general trends of the 7 OMS based on the three evaluation methods for the HOS1 will be summarised in the next section.

Table 62: Spread of each case study for the 7 OMS by the INC method – HOS1

Methods	Rank	Case Study No.	SEQ1-MII	Case Study No.	SEQ2-MII	Case Study No.	SEQ3-MII	Case Study No.	SEQ4-MII	Case Study No.	SEQ5-MII	Case Study No.	SEQ6-MII	Case Study No.	PAR-MII
OAT	1	5	0.11	4	0.22	5	0.12	3	0.23	3	0.09	3	0.21	3	0.20
	2	1	0.09	1	0.13	1	0.06	1	0.13	1	0.08	1	0.12	1	0.10
	3	8	0.02	3	0.06	8	0.02	8	0.01	5	0.04	8	0.02	8	0.02
	4	7	0.01	5	0.01	3	0.02	7	0.01	8	0.02	7	0.01	7	0.01
	5	3	0.00	7	0.00	7	0.01	2	0.00	7	0.01	5	0.00	4	0.00
	6	6	0.00	6	0.00	4	0.01	4	0.00	2	0.00	2	0.00	2	0.00
	7	2	0.00	2	0.00	6	0.00	5	0.00	4	0.00	4	0.00	6	0.00
	8	4	0.00	8	0.00	2	0.00	6	0.00	6	0.00	6	0.00	5	0.00
TAT	1	12	0.19	11	0.34	12	0.18	10	0.30	10	0.14	10	0.28	10	0.31
	2	23	0.15	27	0.33	27	0.14	26	0.24	12	0.11	26	0.22	26	0.22
	3	33	0.12	22	0.28	33	0.13	25	0.23	26	0.11	25	0.21	25	0.21
	4	32	0.12	30	0.22	32	0.12	23	0.23	25	0.10	23	0.21	16	0.20
	5	18	0.11	29	0.22	23	0.12	16	0.23	16	0.09	16	0.21	23	0.20
	6	27	0.11	17	0.22	18	0.12	22	0.23	24	0.09	22	0.21	22	0.20
	7	31	0.11	28	0.21	31	0.12	24	0.22	15	0.09	24	0.21	24	0.20
	8	13	0.10	10	0.16	10	0.08	27	0.13	23	0.08	15	0.13	15	0.12
	9	15	0.10	12	0.14	15	0.08	15	0.13	14	0.08	14	0.12	14	0.11
	10	10	0.09	15	0.13	11	0.07	14	0.12	9	0.08	9	0.12	12	0.10
	11	14	0.09	9	0.13	14	0.06	9	0.12	11	0.08	11	0.12	9	0.10
	12	9	0.09	14	0.13	9	0.06	11	0.12	13	0.07	12	0.12	11	0.10
	13	11	0.09	13	0.13	13	0.06	12	0.12	33	0.05	13	0.11	13	0.10
	14	26	0.01	23	0.09	26	0.03	13	0.12	32	0.04	27	0.04	21	0.01
	15	21	0.01	26	0.07	25	0.02	33	0.01	18	0.04	21	0.01	30	0.01
	16	30	0.01	16	0.06	30	0.02	21	0.01	27	0.04	30	0.01	33	0.01
	17	25	0.00	25	0.06	24	0.02	30	0.01	31	0.04	33	0.01	29	0.00
	18	20	0.00	24	0.03	16	0.02	32	0.00	21	0.01	20	0.00	32	0.00
	19	29	0.00	33	0.01	21	0.01	20	0.00	30	0.01	29	0.00	20	0.00
	20	22	0.00	18	0.01	29	0.01	29	0.00	20	0.00	32	0.00	18	0.00
	21	24	0.00	32	0.01	17	0.01	17	0.00	29	0.00	18	0.00	17	0.00
	22	16	0.00	31	0.00	22	0.01	18	0.00	17	0.00	17	0.00	28	0.00
	23	19	0.00	21	0.00	28	0.01	19	0.00	19	0.00	19	0.00	19	0.00
	24	28	0.00	20	0.00	20	0.00	28	0.00	22	0.00	28	0.00	31	0.00
	25	17	0.00	19	0.00	19	0.00	31	0.00	28	0.00	31	0.00	27	0.00

4.7 Summary of Holistic Optimisation Study 1

After applying a series of analyses to the results of the 7 OMS-MII for the side impact beam in this chapter, the overall general trends are extracted and summarised as follows:

HOS1-1. According to Table 42, the average COFV of each of the 7 OMS-MII outperforms the 7 corresponding OMS-SII based on the three evaluation methods. According to Table 43 and Table 44, the average CPU time of the 203 models for each OMS-MII is nearly the same as the average CPU time of the 203 models for each corresponding OMS-SII. The trends above proved that the 7 OMS-MII outperform the 7 OMS-SII based on the three evaluation methods and CPU time comparison.

HOS1-2. SEQ5-MII is suggested to be the best OMS as it is more stable than all the others.

HOS1-3. The 6 SEQ optimisation programmes can be categorised into two main groups as defined in Table 46 of subsection 4.3.1. The overall performance of the group that contains SEQ1-MII, SEQ3-MII and SEQ5-MII is better than the group of OMS including SEQ2-MII, SEQ4-MII and SEQ6-MII. This is also explained by the difference in the OMS orders between the two groups of SEQ optimisation programmes. SEQ1-MII, SEQ3-MII and SEQ5-MII always optimise the COST module before the CO2 module; while SEQ2-MII, SEQ4-MII and SEQ6-MII always optimise the CO2 module before the COST module. This is evidenced by HOS1-GT-ICE1, HOS1-GT-ICE3, HOS1-GT-ABC1, HOS1-GT-ABC3, HOS1-GT-INC1 and HOS1-GT-INC3.

HOS1-4. The PAR-MII is always ranked 4th or lower, based on the three evaluation methods. Furthermore, the results of PAR-MII are more sensitive to the change of the input parameters. Therefore, the performance of the PAR-MII can be considered to be indifferent; simply because the COFV of the PAR-MII is consistently lower than SEQ1-MII, SEQ3-MII and SEQ5-MII.

HOS1-5. The performance of the STRUCTURAL module across the 7 OMS is the same. This is evidenced by the trends of HOS1-LOFVC-ICE1, HOS1-LOFVC-ABC1 and HOS1-LOFVC-INC1.

HOS1-6. The ‘Global’ performance for each of the 7 OMS is related to their ‘Local’ performance in the CO2 and COST modules. This is evidenced by the trends of HOS1-LOFVC-ICE3, HOS1-LOFVC-ABC3 and HOS1-LOFVC-INC3.

HOS1-7. The results of the 7 OMS in the CO2 module are more sensitive to the change of parameters. This is evidenced by HOS1-LSV-ICE1, HOS1-LSV-ABC1 and

HOS1-LSV-INC1.

HOS1-8. The results of the STRUCTURAL module are very stable as they have a constant LSV based on the three evaluation methods. This is evidenced by the trends of HOS1-LSV-ICE2, HOS1-LSV-ABC2 and HOS1-LSV-INC2.

HOS1-9. For the sensitivity analysis based on OAT, the single parameter of case study 5 is the most influential parameter for SEQ1-MII and SEQ3-MII, i.e. the Maximum component CO_2. The single parameter of case study 4 is the most influential parameter for SEQ2-MII, i.e. Maximum component cost. The single parameter of case study 3 is the most influential parameter for SEQ4-MII, SEQ5-MII, SEQ6-MII and PAR-MII, i.e. Recycled content.

HOS1-10. For sensitivity analysis based on TAT, the two most influential parameters for each of the 7 OMS are different based on the three evaluation methods. However, the high-frequency influential parameters for each OMS based on the three evaluation methods are same as the most influential parameters summarised in HOS1-9; i.e. the Maximum component CO_2, Maximum component cost, Recycled content. This indicates that the results of the 7 OMS are more sensitive to the change of these three parameters.

HOS1-11. Another top-ranked influential parameter is the geometry. This is not a surprise as the geometry is the basis of the product structure which can directly influence the structural optimisation.

It should be noted that the general trends summarised above are based on the holistic optimisation of a side impact beam. In order to compare and verify the trends based on another product, a lower engine mount will be studied in the next chapter, as Holistic Optimisation Study 2 (HOS2).

5 Holistic Optimisation Study 2 (HOS2) – Lower Engine Mount

In the previous study (Holistic Optimisation Study 1), a simple side impact beam was optimised by 6 sequential and one parallel holistic optimisations; the 7 Optimisation Module Sequences (OMS). Each of the 7 OMS contained 203 models leading to 1,421 optimisation models in total. The results of the models were evaluated by three approaches: the Individual Criterion Evaluation (ICE) method, the Absolute Criterion (ABC) method and the Incremental Criterion (INC) method. The findings such as the general trends of the 7 optimisation module sequences (OMS) for Holistic Optimisation Study 1 were analysed and compared in the previous chapter as well. In this chapter, another Holistic Optimisation Study (HOS2) is implemented. Holistic Optimisation Study 2 will optimise a Lower Engine Mount with the same approaches as were used in Holistic Optimisation Study 1. It has been proved that under same conditions (e.g. assumptions, limitations, etc.), the 7 OMS with Multi-Inner Iteration (MII) loops outperform those with Single-Inner Iteration (SII) loop. Therefore, the lower engine mount will be optimised by the 7 OMS with Multi-Inner Iteration (MII) loops in this chapter. The first section will introduce the basic setup of Holistic Optimisation Study 2. Sections 5.2, 5.3 and 5.4 will analyse and evaluate the results of Holistic Optimisation Study 2 with ICE, ABC and INC respectively. Section 5.5 will generate a further analysis for the three individual modules based on the two perspective views: objective function values and sensitivity analysis. The last section will be the summary of this chapter.

5.1 Setup of Holistic Optimisation Study 2

In this section, a different component will be analysed. A lower engine mount was chosen for HOS2 which has a different manufacturing method (casting) from the roll forming method used in HOS1. Furthermore, the setup of HOS2 is similar to that of HOS1. It indicates that there will be 203 models for each of the 7 OMS leading to 1,421 studies in total. The detailed definition of the case study is demonstrated in subsection 5.1.4.

5.1.1 Brief background of the lower engine mount

The engine mounts of a vehicle are designed to firmly hold the powertrain components and bear the inertial load, etc. The lower engine mount analysed in this Holistic Optimisation Study 2 is used for the engine of a student formula car. As the Formula Society of Automotive Engineers (FSAE) car is a high-performance vehicle, the correct positioning and geometry are therefore important for the design of the engine mount. The location of the lower engine mount in the

FSAE car is illustrated in Figure 40. The lower engine mounts are bolted onto a large outer bracket (Metal) and the engine bracket (Black). The original material used for this lower engine mount is aluminium and it is manufactured by machining. However, the machining methods are not compatible with the calculations in the COST module as they have no 'Cost Modelling' information in the CES EduPack. Therefore, the machining methods are not considered in this Holistic Optimisation Study 2. The alternative method selected in the CES EduPack is casting.

Figure 40: The location of the engine mount (FSAE car) – HOS 2

The materials used for this lower engine mount are selected based on the casting method and are listed in Table 63.

Table 63: Material Selection for the Lower Engine Mount – HOS 2 (CES EduPack)

MAT Names	Density (kg/m^3)	Young's Modulus (GPa)	Yield Strength (MPa)	Poisson's Ratio	Price (£/kg)
Cast Iron Grey	7250	138	420	0.28	0.34
Cast Al. Alloy	2900	89	330	0.36	1.59
Cast Magnesium Alloy	1870	47	215	0.31	2.21
Stainless Steel	8100	210	1000	0.275	4.61

The material and manufacturing method for the lower engine mount have been introduced. In order to check its structural performance, the load cases will be calculated, and the structural analysis will be produced in the next subsection.

5.1.2 Load cases and initial FEA

The purpose of this subsection is to analyse the structural performance of the lower engine mount within the FEA solver under a certain load case. Before applying any FEA analysis to the engine mount model, the load cases around the engine mounts must be calculated. According to the information provided by the FSAE team, the load cases around the full engine block are illustrated in Figure 41. The meaning of each symbol is summarised in Table 64:

Table 64: Symbols of parameters used for calculating the forces

Symbol Names	Meaning	Values
F_A	$Force\ through\ top\ engine\ mount\ (N)$	
F_B	$Force\ through\ lower\ engine\ mount\ (N)$	
FoS	$Factor\ of\ Safety$	1.2
S_1	$Distance\ in\ Z\ from\ drive\ sprocket\ to\ the\ lower\ engine\ mount\ hole\ (m)$	0.11
S_2	$Distance\ in\ Z\ from\ drive\ sprocket\ to\ the\ upper\ engine\ mount\ hole\ (m)$	0.15
S_3	$Distance\ between\ the\ engine\ mount\ locations\ (m)$	0.258

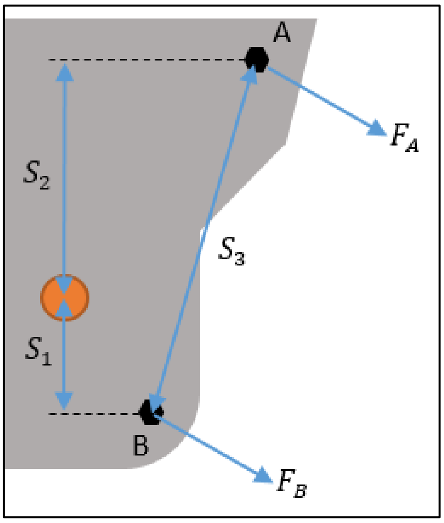

Figure 41: Schematic to assist the engine mount load calculations (Coventry University FSAE team 2016-2017)

The FSAE car is assumed to be pulled away from still, which gives the largest torque, i.e. the worst-case scenario. The force through the chain (Orange circle) in Figure 41 is given as 4351.4N. The force through the lower engine mount is calculated by the following equation from the FSAE team,

$$F_B = \left(\frac{F_{Chain} \times S_2}{S_3}\right) \times FoS = 3035.9N \tag{5.1}$$

The initial setup of the lower engine mount for the FEA analysis is illustrated in Figure 42. The red arrow shows the force acting on the lower engine mount and the green triangles show the constraints. The initial material for this model is Cast Iron Grey from Table 63.

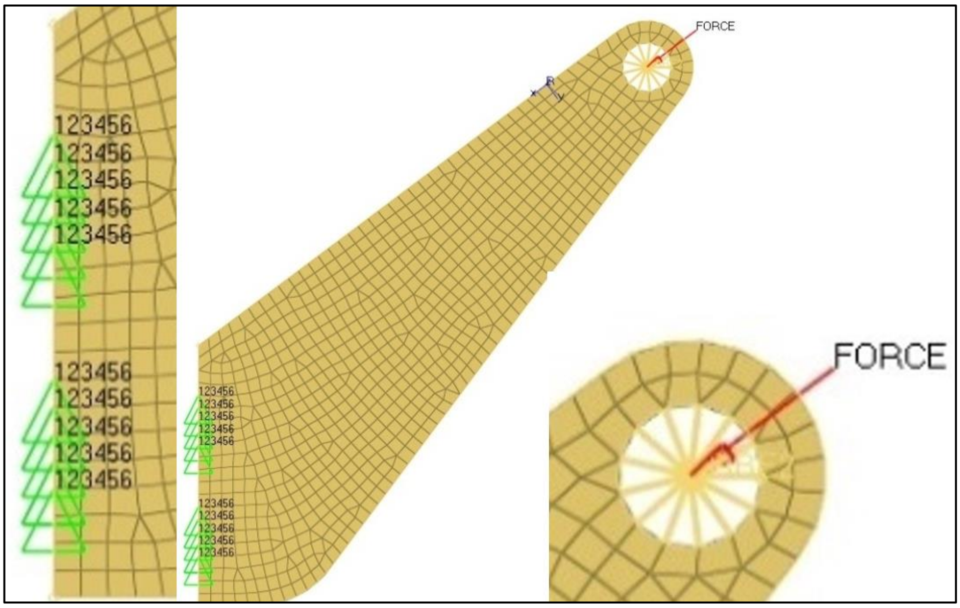

Figure 42: Initial setup of the Lower Engine Mount for the initial FEA analysis

Due to limitations in actually casting the engine mount, its initial thickness is assumed to be 7mm. But according to some resources (e.g. Mrt-Casting 2017 and CES EduPack 2017), the thickness can be cast as low as 3-5mm but with a poor surface quality. After running the initial FEA test for this engine mount model, the detailed results are illustrated in Figure 43 and Figure 44. In Figure 44, it is found that the maximum displacement is obtained where the force acted on. The maximum vonMises stress is found at the top constrained edge due to the bending caused by the force in Figure 42.

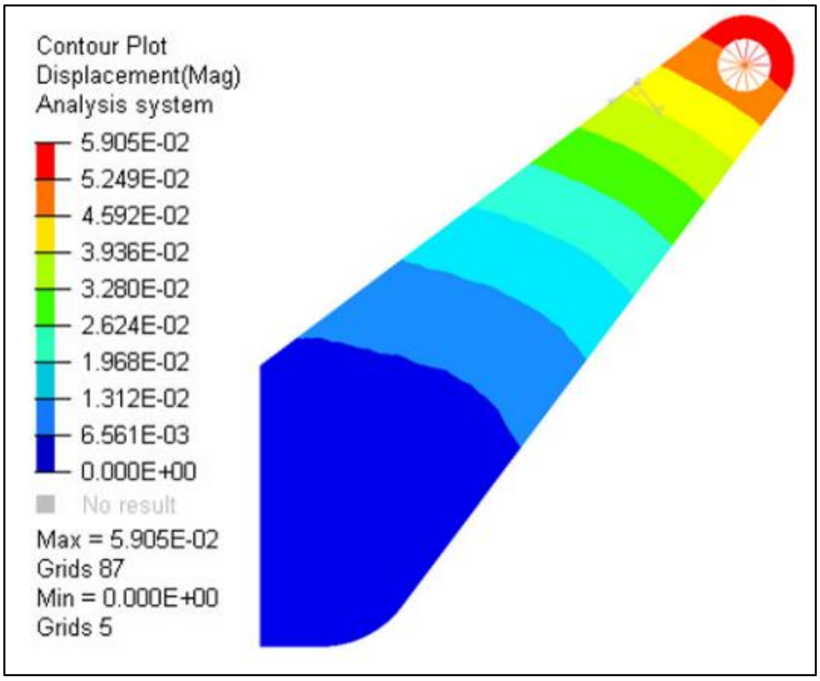

Figure 43: Displacement results of the engine mount

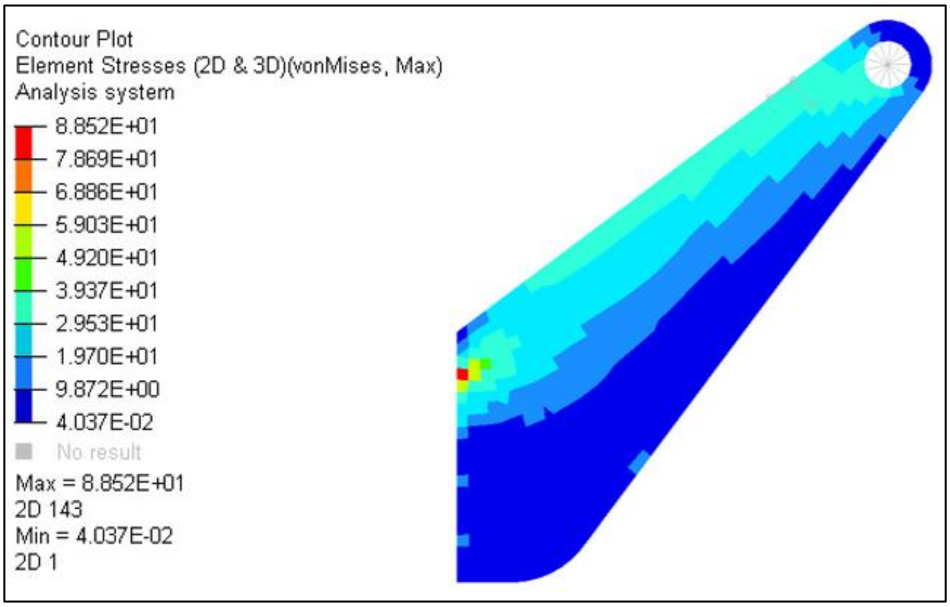

Figure 44: vonMises stress results of the engine mount

The maximum displacement and maximum vonMises stress are obtained: 0.06 mm and 88.5 MPa. The maximum displacement is very small which indicates that the engine mount has barely moved under 3035.9N. The maximum vonMises stress does not exceed the yield strength of the cast iron. A similar analysis was also done for the model with different materials in Table 63. The results of each FEA analysis are within the permissible limits such as the yield strength of each material.

5.1.3 FEA models for the STRUCTURAL module

After the initial FEA analysis of the engine mount, the setup of the model is adoptable as the results of the analysis are within the permissible limits. The model is then considered for use in the STRUCTURAL module. As defined in Holistic Optimisation Study 1, the optimisation method used in the STRUCTURAL module is sizing. This type of optimisation is used to optimise the thickness, width and length of a certain part. The distribution of the vonMises stress in Figure 44 shows that most of the lower engine mount is under low stress between 0.04 MPa and 39.37 MPa (much lower than the permissible limit). This indicates that the material in the low-stress area defined above can be removed without affecting the structural performance of the engine mount. This is an optimisation process which is similar to topology optimisation. The ideology of topology optimisation is to optimise the product by the re-layout of its material within certain constraints. By following the concept of topology optimisation, five extra holes are added to the original CAD model (A) within the low-stress area, e.g. CAD model B and C as illustrated in Figure 45. The five extra holes have the same radius. The pin-hole of each model keeps the same size. By increasing or decreasing the size of the extra holes simultaneously, the model can have different layouts of the material; i.e. the original model is achieved when the size of the extra holes is 0.

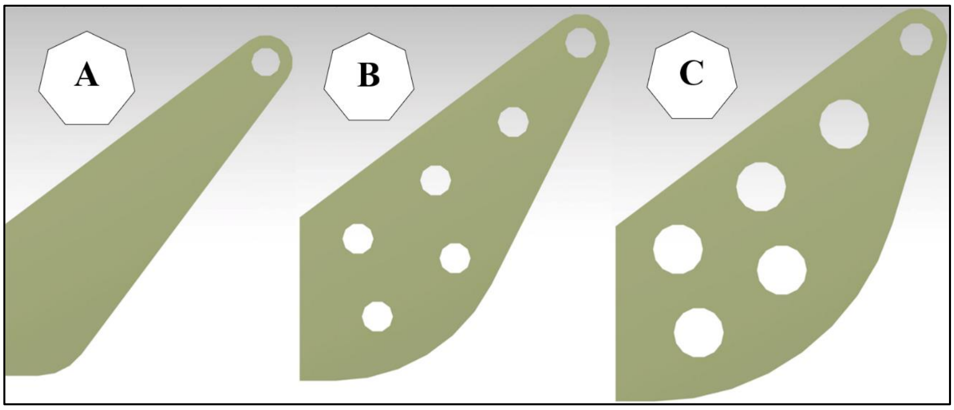

Figure 45: 2D CAD models of the lower engine mount – Holistic Optimisation Study 2

The three models in Figure 45 will be used in the STRUCTURAL module, and their major dimensions are illustrated in Figure 46. Based on Figure 46, the radius of the Pin-hole is 4 mm which is a constant value for all three models illustrated in Figure 45. The radius of the extra 5 holes and the bottom curves for model A, B and C are tabulated in Figure 46 respectively.

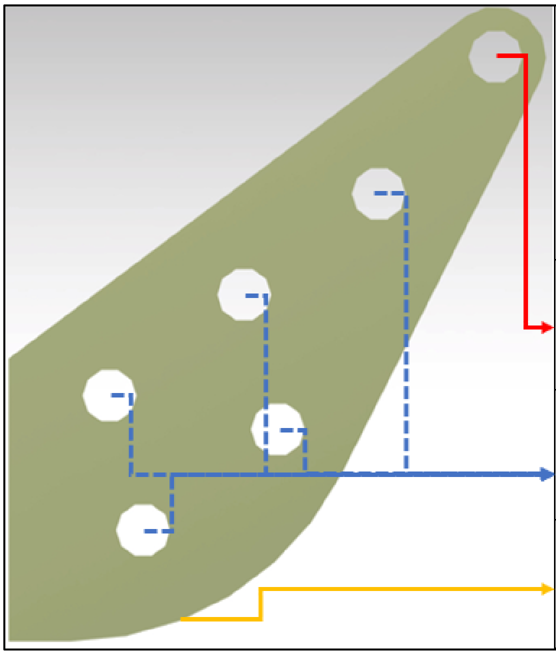

Name	Model		
	A	B	C
Pin-Hole	r = 4mm		
Extra Holes	0	r = 4mm	r = 6mm
Bottom Curve	R = 15mm	R = 45mm	R = 60mm

Figure 46: Initial dimensions of the three models for the STRUCTURAL module

As the three models for the engine mount have been set up, the initial values of the engine mount are then measured/ calculated through HyperMesh, Initial Cost calculator and Initial CO_2 calculator. The initial volumes of the three models are measured within HyperMesh. Their initial costs and CO_2 footprints are calculated based on the equations defined in subsection 3.2.2

and 3.2.3. The manufacturing method is casting, the initial country of production is the UK (Coventry) and the destination is Coventry (in Connecticut, the USA). The measured volumes, the calculated cost and the CO_2 footprint are tabulated in Table 65.

Table 65: Initial values of the lower engine mount

Model	Initial Volume (mm³)	Initial CO_2 per unit (kg)	Initial Cost per unit (£)
A	44570.5	0.82	0.73
B	51595.7	0.94	0.76
C	53795.8	0.98	0.76

5.1.4 Case study definition of Holistic Optimisation Study 2

The initial input models have been setup for the three modules for the holistic optimisation. The major influential parameters were defined in subsection 3.5.1, e.g. production quantity, travel distance, recycled content, etc. In this Holistic Optimisation Study 2, there will be 203 studies for each of the 7 OMS leading to 1,421 studies in total. The 203 studies can be categorised into 33 case studies and each case study will investigate how the change of input parameter(s) influences the optimum solutions. As defined in subsection 3.5.2, the first 8 case studies will investigate One parameter At a Time (OAT) and the rest of the 25 case studies will investigate Two parameters At a Time (TAT). The results of the 203 models for each of the 7 OMS will then be evaluated by the Individual Criterion Evaluation (ICE) method, the Absolute Criterion (ABC) method and the Incremental Criterion (INC) method in section 5.2, 5.3 and 5.4 respectively.

5.2 ICE results of Holistic Optimisation Study 2

The general trends of the 7 OMS will be analysed and compared by the Individual Criterion Evaluation (ICE) method in this section. To achieve this, 203 models defined in subsection 4.2.2 will be optimised using all 7 OMS leading to a total of 1,421 optimisation results. Each result was plotted as a single point in a figure and linear lines were utilised to connect individual points. The plotted and connected results of the 7 OMS are illustrated in Figure 47.

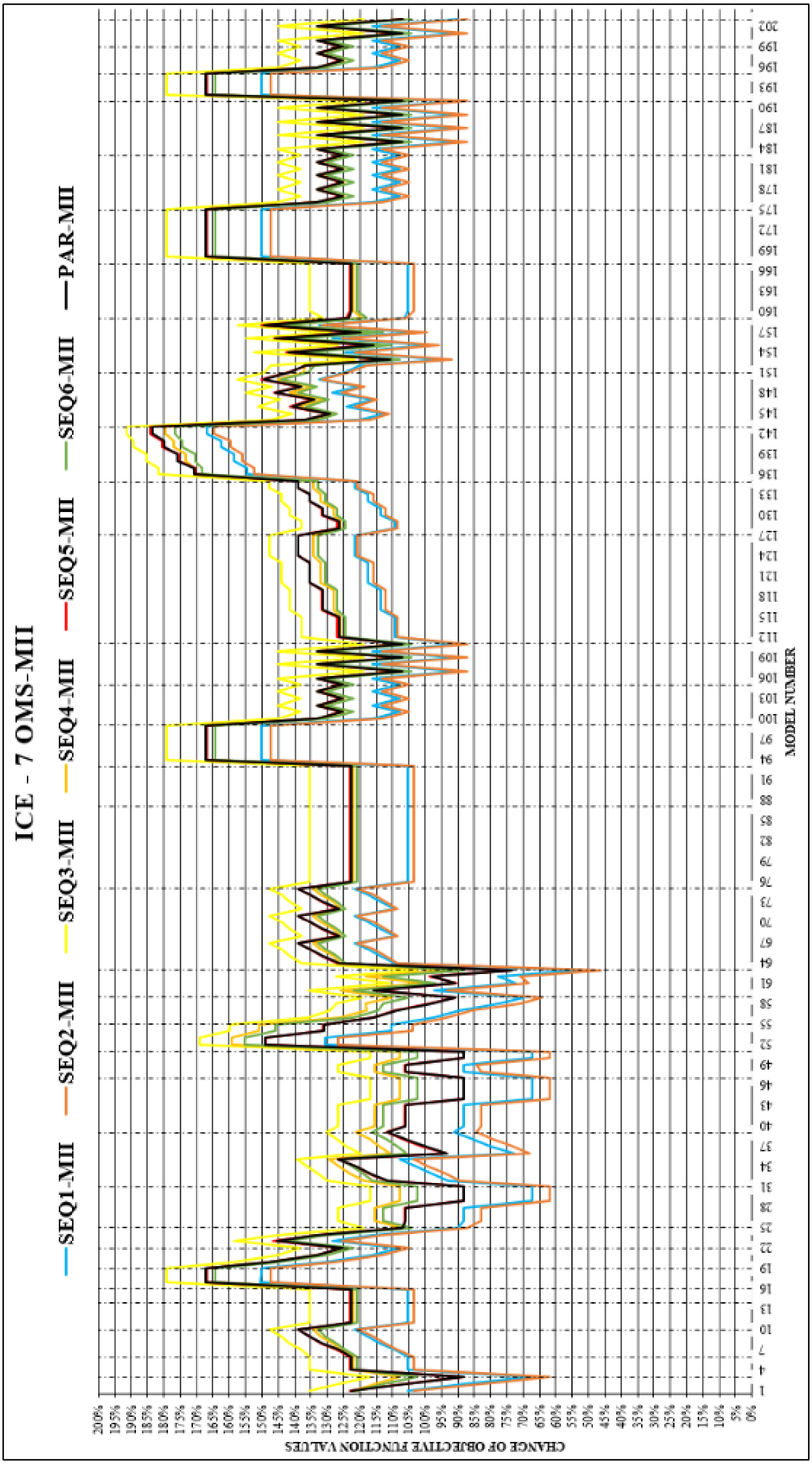

Figure 47: The results of the 7 OMS (ICE – Holistic Optimisation Study 2)

According to the definition of the ICE method (in subsection 4.3.1), more Changes of Objective Function Value (COFV) will produce better optimisation results. Figure 47 shows that the results of SEQ2-MII are consistently lower than the results of the other OMS. This indicates that the SEQ2-MII underperforms them as it has fewer changes of the objective function values. On the other hand, the results of SEQ3-MII are consistently higher than the results of the other OMS. Therefore, it is suggested that SEQ3-MII outperforms them based on the ICE evaluation method. In order to investigate the trends of the 7 OMS, the average, maximum and minimum change of objective function values across the 203 models for each of the 7 OMS will be analysed in subsection 5.2.1, 5.2.2 and 5.2.3 respectively. The sensitivity of the results of the 203 models for each of the 7 OMS will be assessed in subsection 5.2.4. The general trends of the ICE results for the 7 OMS will be summarised in subsection 5.2.5.

5.2.1 Results based on the average change of objective function values

The average change of objective function value (**COFV**) across the 203 models for each of the 7 OMS is analysed in this subsection. The average change of objective function value for each of the OMS is calculated based on Equation (4.1). The 7 OMS are ranked in Table 66 from the highest average objective function value change to the lowest.

Table 66: The ranked 7 OMS based on average COFV – ICE (HOS 2)

Rank	OMS	Objective function value changes (Average – ICE)
1	SEQ3-MII	143%
2	SEQ4-MII	131%
3	SEQ5-MII	130%
4	PAR-MII	129%
5	SEQ6-MII	129%
6	SEQ1-MII	112%
7	SEQ2-MII	109%

According to the ranking of the 7 OMS in Table 66, following trends are found:

HOS2-Avg-ICE 1. The PAR-MII is ranked in the middle of the SEQ optimisation programmes, however it has the same objective function value change as SEQ6-MII. This indicates that the performance of the PAR-MII and SEQ6-MII is the same.

HOS2-Avg-ICE 2. The 6 SEQ optimisation programmes can be categorised into three groups based on the OMS order. These three groups are defined in Table 67, which for convenience also contains the specific OMS order and the range of objective function value change.

Table 67: Average COFV grouped by OMS – HOS 2

Group	OMS name	Optimisation Module Sequence (OMS)			Average COFV (ICE)
		1	2	3	
G	SEQ1-MII	STRUCTURAL	COST	CO2	112%
	SEQ2-MII	STRUCTURAL	CO2	COST	109%
H	SEQ3-MII	COST	CO2	STRUCTURAL	143%
	SEQ4-MII	CO2	COST	STRUCTURAL	131%
I	SEQ5-MII	COST	STRUCTURAL	CO2	130%
	SEQ6-MII	CO2	STRUCTURAL	COST	129%

In Table 67, the following trends are found:

HOS2-Avg-ICE 3. The average objective function value change of SEQ3-MII and SEQ4-MII are higher than the other four SEQ optimisation programmes. This indicates that the late optimisation position of the STRUCTURAL module will benefit the average change of objective function value.

HOS2-Avg-ICE 4. If the position of the STRUCTURAL module is the same, the OMS benefits from optimising the COST module before the CO2 module, i.e. SEQ1-MII (112%) outperforms SEQ2-MII (109%).

5.2.2 Results based on the maximum change of objective function values

As previously defined in section 5.2, there are 203 models for each of the 7 OMS. The maximum change of objective function value of the 203 models is also the maximum value for each of the 7 OMS. The maximum objective function value change for each of the 7 OMS is tabulated in Table 68.

Table 68: The ranked 7 OMS based on maximum COFV – ICE (HOS 2)

Rank	OMS	Objective function value changes (Maximum – ICE)
1	SEQ3-MII	192%
2	SEQ5-MII	184%
3	PAR-MII	184%
4	SEQ4-MII	179%
5	SEQ6-MII	177%
6	SEQ1-MII	167%
7	SEQ2-MII	164%

In Table 68, the following trends are found:

HOS2-Max-ICE 1. SEQ3-MII has the best maximum change of objective function values. It indicates that SEQ3-MII outperforms the other 6 OMS in comparison to the extreme (maximum) results across the 7 OMS.

HOS2-Max-ICE 2. SEQ2-MII is still ranked at the bottom compared to its ranking in Table 66.

HOS2-Max-ICE 3. The PAR-MII however is ranked top (3^{rd}) in Table 68 and it has the same maximum objective function value change as SEQ5-MII. By comparing the rankings of PAR-MII and SEQ5-MII in Table 66 and Table 68, it is found that these two OMS have nearly the same change of objective function values (i.e. a difference less than 1%).

Apart from the PAR-MII, the 6 SEQ optimisation programmes in this subsection cannot be categorised into same groups as those defined in Table 67 of subsection 5.2.1. However, a few trends are still found if they are grouped based on their specific OMS orders. The new groups are tabulated in Table 69.

Table 69: Maximum COFV grouped by OMS – HOS 2

Group	OMS name	Optimisation Module Sequence (OMS)			Maximum COFV (ICE)
		1	2	3	
J	SEQ1-MII	STRUCTURAL	COST	CO2	167%
	SEQ2-MII	STRUCTURAL	CO2	COST	164%
K	SEQ3-MII	COST	CO2	STRUCTURAL	192%
	SEQ5-MII	COST	STRUCTURAL	CO2	184%
L	SEQ4-MII	CO2	COST	STRUCTURAL	179%
	SEQ6-MII	CO2	STRUCTURAL	COST	177%

By observing Table 69, the following trends are found:

HOS2-Max-ICE 4. The OMS that optimised the STRUCTURAL module first always underperformed the OMS that optimised the other modules first, e.g. the OMS in Group J.

HOS2-Max-ICE 5. The results of OMS benefits from optimising the COST module first, e.g. the OMS in Group K.

HOS2-Max-ICE 6. If the COST/ CO2 module is optimised first, the results of the OMS will benefit from optimising the STRUCTURAL module late, e.g. the OMS in either Group K or Group L.

5.2.3 Results based on the minimum change of objective function values

Analogous to the definition of the maximum objective function value change, the minimum change of objective function value for each of the 7 OMS is apparently the lowest value of the 203 models. The minimum objective function value change for each of the 7 OMS is tabulated in Table 70.

Table 70: The ranked 7 OMS based on the minimum COFV – ICE (HOS 2)

Rank	OMS	Objective function value changes (Minimum – ICE)
1	SEQ3-MII	102%
2	SEQ4-MII	93%
3	SEQ6-MII	88%
4	SEQ5-MII	74%
5	PAR-MII	73%
6	SEQ1-MII	53%
7	SEQ2-MII	46%

The trends of the 7 OMS found in Table 70 are as follows:

HOS2-Min-ICE 1. SEQ3-MII still has the best minimum objective function value change. It indicates that SEQ3-MII outperforms the other 6 OMS in comparison to the extreme (minimum) results across the 7 OMS.

HOS2-Min-ICE 2. The PAR-MII is still ranked beside the SEQ5-MII which shows that the two OMS have very close performances based on the minimum objective function value change.

The 6 SEQ optimisation programmes can be categorised into three groups based on their OMS orders. The details of the three groups are summarised in Table 71.

Table 71: Minimum COFV grouped by OMS – Holistic Optimisation Study 2

Group	OMS name	Optimisation Module Sequence (OMS)			Minimum COFV (ICE)
		1	2	3	
M	SEQ1-MII	STRUCTURAL	COST	CO2	53%
	SEQ2-MII	STRUCTURAL	CO2	COST	46%
N	SEQ3-MII	COST	CO2	STRUCTURAL	102%
	SEQ4-MII	CO2	COST	STRUCTURAL	93%
O	SEQ5-MII	COST	STRUCTURAL	CO2	74%
	SEQ6-MII	CO2	STRUCTURAL	COST	88%

The following trends are found from Table 71:

HOS2-Min-ICE 3. The minimum objective function value change of SEQ3-MII and SEQ4-MII are higher than the other four SEQ optimisation programmes. This indicates that the late optimisation position for the STRUCTURAL module will benefit the average change of objective function value.

HOS2-Min-ICE 4. The SEQ1-MII and SEQ2-MII in Group M still underperform the other 4 OMS. This trend is same as was found in Table 67 and Table 69.

5.2.4 Results based on average spreads of objective function value change

In order to further study the general trends of the 7 OMS, the average value of the spreads of 33 case studies for each of the OMS has been calculated by Equation(4.2). The average spreads of the 7 OMS are ranked from the lowest to the highest in Table 72. The lower average spread demonstrates a lower sensitivity for the results of the OMS.

Table 72: The average spreads of the 7 OMS based on the ICE method (HOS 2)

Rank	OMS	Average Spreads (ICE)	Groups
1	SEQ4-MII	11%	Group P
2	SEQ3-MII	12%	
3	SEQ6-MII	12%	Group Q
4	SEQ5-MII	15%	
5	PAR-MII	15%	
6	SEQ1-MII	16%	Group R
7	SEQ2-MII	16%	

The following trends are found by observing Table 72:

HOS2-ASp-ICE 1. The results of SEQ4-MII have the lowest average spreads which indicates that the results of these OMS are less sensitive but more stable to the change of the input parameters than the other OMS.

HOS2-ASp-ICE 2. The results of SEQ1-MII and SEQ2-MII have relatively higher spreads (16%) which means that the results of these two OMS are more sensitive to the change of input parameters. However, the results of SEQ1-MII and SEQ2-MII are consistently lower than the other OMS as evidenced in Table 66, Table 68 and Table 70. Therefore, the high sensitivity of the results of those two OMS is considered to be uninterested.

HOS2-ASp-ICE 3. The spread between SEQ4-MII (Ranked 1st) and SEQ2-MII (Ranked 7th) is 5% which is an insignificant difference. It indicates that the results of the 7 OMS have a very close sensitivity performance.

HOS2-ASp-ICE 4. If the 6 SEQ optimisation programmes are categorised into the same groups as defined in Table 67 (or Table 69 or Table 71), the average spreads of the two OMS in each group (P, Q and R) will a have very small difference. This means that the difference in the sensitivity between the two OMS in each group is insignificant (less than 3%). This may also indicate that the position of the COST module and the CO2 module does not have a great influence on the results sensitivity in each group of OMS.

HOS2-ASp-ICE 5. It is suggested that optimising the STRUCTURAL module later than the other two modules gives lower sensitivity to the results of the OMS. This is evidenced by the ranking of SEQ3-MII and SEQ4-MII in Table 72 and their specific OMS order defined in Table 67 (or Table 69 or Table 71).

5.2.5 Summary of the general trends – ICE – HOS 2

The results of the 203 models of the 7 OMS are evaluated by the ICE method in this section. In order to find out the detailed trends, the average, maximum, minimum and spread values of the results across the 7 OMS were assessed in four subsections respectively. Each subsection obtained several general trends of the results for the 7 OMS. The General Trends (GT) based on the ICE evaluation method in those subsections are summarised as follows:

HOS2-GT-ICE1. SEQ2-MII underperforms the other OMS as its results (average, maximum and minimum) are consistently lower than those of the other OMS and its average spread is higher. This indicates that the results of SEQ2-MII are less stable and robust than the results of the other OMS. This is evidenced by its ranking in Table 66, Table 68, Table 70 and Table 72.

HOS2-GT-ICE2. The results (average, maximum/ minimum) of SEQ3-MII are consistently higher than the results of the other 6 OMS. Moreover, the results of SEQ3-MII have the lowest average spread value across the 7 OMS. Therefore, it is suggested that SEQ3-MII is more robust and stable than the other OMS based on the ICE evaluation method.

HOS2-GT-ICE3. The 6 SEQ optimisation programmes can be categorised into three groups based on the OMS order which is defined in Table 67, Table 69 and Table 71. SEQ1-MII and SEQ2-MII always underperform the other 4 OMS. It indicates that the results of the OMS will not benefit from optimising the STRUCTURAL module first.

HOS2-GT-ICE4. It is suggested that optimising the STRUCTURAL module later than the other two modules gives lower sensitivity to the results of the OMS.

HOS2-GT-ICE5. Optimising the STRUCTURAL module later than the other two modules gives lower sensitivity to the results of the OMS. This is evidenced by the ranking of SEQ3-MII and SEQ4-MII in Table 72 and their specific OMS order defined in Table 67.

HOS2-GT-ICE6. The results of PAR-MII and SEQ5-MII have nearly the same performance in the analysis of the average, maximum, minimum and spread values. This is also found in Figure 47 where the graphs of the two OMS are nearly identical.

5.3 ABC results of Holistic Optimisation Study 2

In order to find out the general trends of the 7 OMS from another viewpoint, the results are evaluated by the ABC method in this subsection. The results of the 7 OMS are illustrated in Figure 48. The definition of the ABC method in subsection 3.6.2 demonstrated that the idea is to calculate the distance between each result and the absolute optimum solution. The shorter distance is better, as a shorter distance means the result is closer to the absolute optimum solution. This distance, namely ‘Global Distance’, also represents the change of objective function value (COFV). Therefore, a smaller COFV in this section indicates a shorter distance/ a better result. In this case, Figure 48 shows that the graph of SEQ3-MII is consistently lower than the graphs of all the other OMS. This indicates that the results of SEQ3-MII outperform the results of all the other OMS based on the ABC evaluation. On the other hand, the graph of SEQ2-MII is consistently higher than the graphs of all the other OMS. This indicates that the results of SEQ2-MII underperform the results of all the other OMS. To further study the trends of the 7 OMS, the results of the 7 OMS will be further analysed by different methods in the following subsections respectively:

- Subsection 5.3.1, Results based on the average change of objective function values.
- Subsection 5.3.2, Results based on the maximum change of the objective function values.
- Subsection 5.3.3, Results based on the minimum change of the objective function values.
- Subsection 5.3.4, Results based on the average spreads of objective function value change.
- Final subsection contains the summary of section 5.3.

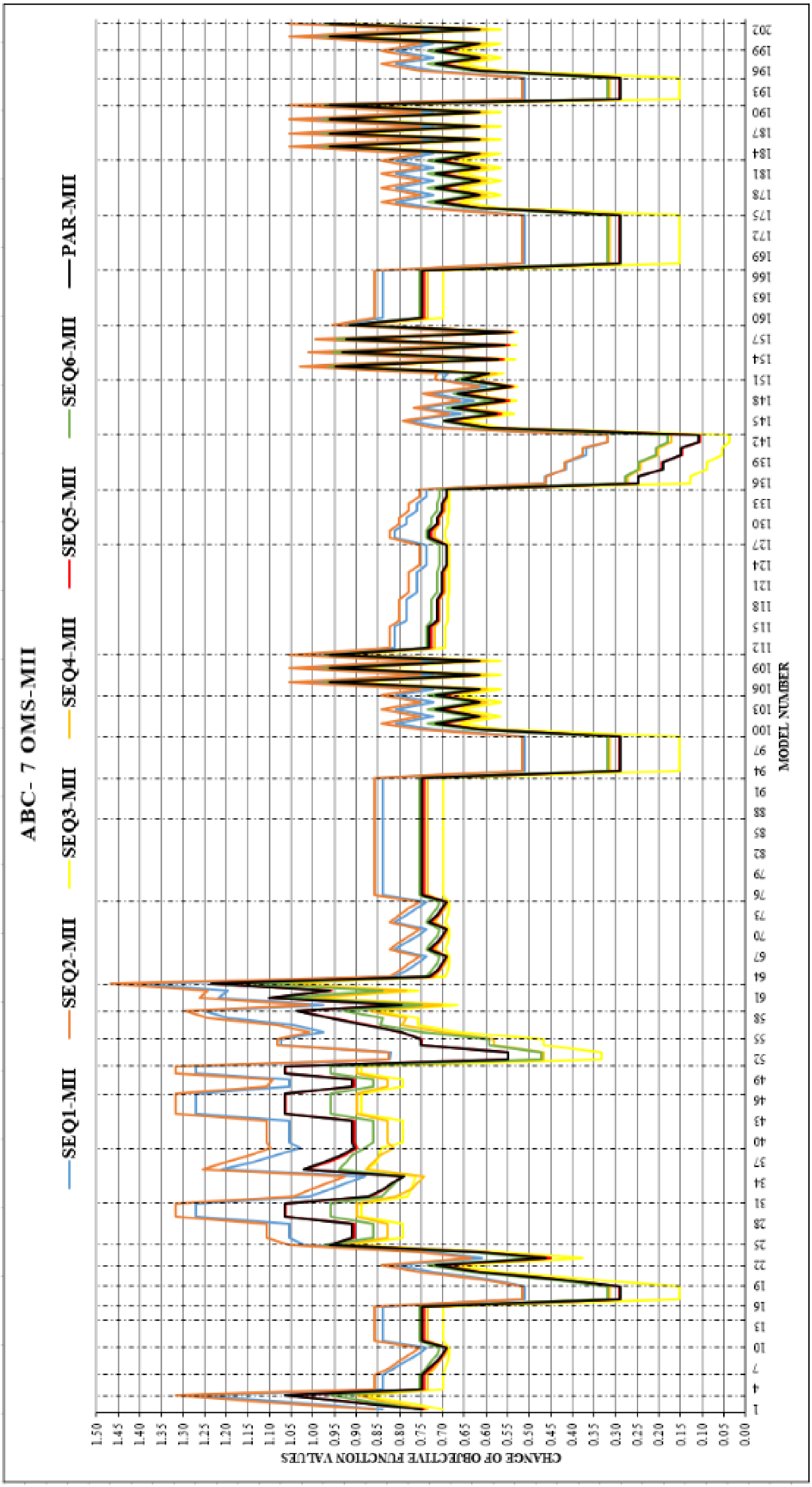

Figure 48: The results of the 7 OMS (ABC – Holistic Optimisation Study 2)

5.3.1 Results based on the average change of objective function values

The average COFV across the 203 models of each of the 7 OMS is calculated based on Equation (4.1). The 7 OMS are ranked from the lowest COFV to the highest average COFV in Table 73.

Table 73: The ranked 7 OMS based on the average COFV – ABC – HOS 2

Rank	OMS	Objective function value changes (Average – ABC)
1	SEQ3-MII	0.62
2	SEQ4-MII	0.67
3	SEQ5-MII	0.69
4	SEQ6-MII	0.69
5	PAR-MII	0.69
6	SEQ1-MII	0.81
7	SEQ2-MII	0.84

The following trends are observed from Table 73:

HOS2-Avg-ABC 1. The 6 SEQ optimisation programmes can be categorised into 3 Groups based on the range of the average COFV of each OMS. The three groups of OMS are tabulated in Table 74, which for convenience also contains the specific OMS order and the range of average COFV.

Table 74: The 7 OMS grouped by the range of average COFV – ABC -HOS 2

Group	OMS name	Optimisation Module Sequence (OMS)			Average COFV (ABC)
		1	2	3	
S	SEQ1-MII	STRUCTURAL	COST	CO2	0.81
	SEQ2-MII	STRUCTURAL	CO2	COST	0.84
T	SEQ3-MII	COST	CO2	STRUCTURAL	0.62
	SEQ4-MII	CO2	COST	STRUCTURAL	0.67
U	SEQ5-MII	COST	STRUCTURAL	CO2	0.69
	SEQ6-MII	CO2	STRUCTURAL	COST	0.69

HOS2-Avg-ABC 2. The average objective function value change of SEQ3-MII and SEQ4-MII are higher than the other four SEQ optimisation programmes. This indicates that the late optimisation position of the STRUCTURAL module will benefit the average change of objective function value.

HOS2-Avg-ABC 3. If the position of the STRUCTURAL module is the same, the OMS benefits from optimising the COST module before the CO2 module, i.e. SEQ1-MII (0.81) outperforms SEQ2-MII (0.84). It can be argued that SEQ5-MII and SEQ6-MII have the same value. However, SEQ5-MII is still ranked higher than SEQ6-MII based on their actual values which contain more than three significant numbers.

The general trends of the 7 OMS based on the average COFV are nearly the same as those found in subsection 5.3.1. To further analyse the trends of the 7 OMS based on the ABC method, the maximum COFV for each OMS is studied in the next subsection.

5.3.2 Results based on the maximum change of objective function values

As defined in subsection 4.3.1, the maximum COFV is the maximum value of the 203 COFVs for each of the 7 OMS. The 7 OMS are ranked based on the 7-corresponding maximum COFVs as illustrated in Table 75.

Table 75: The ranked 7 OMS based on the maximum COFV – ABC – HOS 2

Rank	OMS	Objective function value changes (Maximum – ABC)
1	SEQ4-MII	1.07
2	SEQ3-MII	1.08
3	SEQ6-MII	1.14
4	SEQ5-MII	1.23
5	PAR-MII	1.24
6	SEQ1-MII	1.40
7	SEQ2-MII	1.47

Table 75 shows the following trends of the 7 OMS:

HOS2-Max-ABC 1. SEQ3-MII and SEQ4-MII have nearly the same maximum change of objective function values, as the difference between the values is less than 1%. It indicates that the two OMS have the same performance based on the maximum COFV. Furthermore, SEQ3-MII and SEQ4-MII outperform all the other OMS as they are ranked top in Table 75.

HOS2-Max-ABC 2. SEQ2-MII is still ranked at the bottom compared to its ranking in Table 73. This indicates that SEQ2-MII underperforms all the other OMS based on both average and maximum COFV.

HOS2-Max-ABC 3. In comparing the rankings of PAR-MII and SEQ5-MII in Table 73 and Table 75, it is found that these two OMS have nearly the same COFV (i.e. a difference less than 1%).

5.3.3 Results based on the minimum change of objective function values

Similar to the maximum COFV, the minimum COFV is the minimum value of the 203 COFVs for each of the 7 OMS. The 7 OMS are ranked based on the minimum COFVs in Table 76, i.e. from the lowest to the highest.

Table 76: The ranked 7 OMS based on the minimum COFV – ABC – HOS 2

Rank	OMS	Objective function value changes (Minimum – ABC)
1	SEQ3-MII	0.04
2	SEQ5-MII	0.11
3	PAR-MII	0.11
4	SEQ4-MII	0.17
5	SEQ6-MII	0.18
6	SEQ2-MII	0.32
7	SEQ1-MII	0.32

The following trends are found from Table 76:

HOS2-Min-ABC 1. SEQ3-MII still has the best minimum objective function value change. It indicates that SEQ3-MII outperforms the other 6 OMS in the comparison of the extreme (minimum) results across the 7 OMS.

HOS2-Min-ABC 2. The PAR-MII (3rd) is still ranked beside the SEQ5-MII (2nd) which shows that the two OMS have a very close performance based on the minimum objective function value change.

The 6 SEQ optimisation programmes can be categorised into three groups based on their OMS orders. The details of the three groups are summarised in Table 77.

Table 77: Minimum COFV grouped by OMS – Holistic Optimisation Study 2

Group	OMS name	Optimisation Module Sequence (OMS)			Minimum COFV (ABC)
		1	2	3	
V	SEQ3-MII	COST	CO2	STRUCTURAL	0.04
	SEQ5-MII	COST	STRUCTURAL	CO2	0.11
W	SEQ4-MII	CO2	COST	STRUCTURAL	0.17
	SEQ6-MII	CO2	STRUCTURAL	COST	0.18
X	SEQ2-MII	STRUCTURAL	CO2	COST	0.32
	SEQ1-MII	STRUCTURAL	COST	CO2	0.32

The following trends are found from Table 77:

HOS2-Min-ABC 3. The minimum objective function value change of SEQ3-MII and SEQ5-MII are higher than the other four SEQ optimisation programmes. This indicates that optimising the COST module before the other two modules will benefit the minimum COFV.

HOS2-Min-ABC 4. SEQ1-MII and SEQ2-MII in Group X are still underperforming the other 4 OMS. This trend is same as what was found in Table 73 and Table 75.

5.3.4 Results based on average spreads of objective function value change

The average spread of COFV for each of the 7 OMS is calculated based on Equation (4.2) as defined in subsection 4.3.4. The 7 OMS are ranked based on the average spread of COFV in Table 78, i.e. from the lowest to the highest.

Table 78: The average spreads of the 7 OMS – ABC – HOS 2

Rank	OMS	Average Spreads – ABC	Groups
1	SEQ4-MII	0.12	W
2	SEQ6-MII	0.13	
3	SEQ3-MII	0.13	V
4	SEQ5-MII	0.15	
5	PAR-MII	0.15	
6	SEQ1-MII	0.16	X
7	SEQ2-MII	0.16	

The ranking of the 7 OMS in Table 78 shows the following trends:

HOS2-ASp-ABC 1. The results of SEQ4-MII have the lowest average spread which indicates that the results of this OMS are less sensitive but more stable to the change of the input parameters than the other OMS.

HOS2-ASp-ABC 2. The results of SEQ1-MII and SEQ2-MII have relatively higher spreads (0.16) which means that the results of these two OMS are more sensitive to the change of input parameters. Despite the high sensitivity of the results of SEQ1-MII and SEQ2-MII, the above trends can be considered to be indifferent as the COFV of SEQ1-MII and SEQ2-MII are consistently lower than all the other OMS.

HOS2-ASp-ABC 3. The spread between SEQ4-MII (Rank 1st) and SEQ2-MII (Rank 7th) is 0.04 which is an insignificant difference. It indicates that the results of the 7 OMS have a very close sensitivity performance.

HOS2-ASp-ABC 4. If the 6 SEQ optimisation programmes are categorised into the same groups as defined in Table 77, the average spread of the two OMS in each group (V, W and X) is insignificant (less than 0.02). This indicates that optimising the CO2 module before the other two modules gives lower sensitivity to the results for the specific group of OMS; i.e. SEQ4-MII and SEQ6-MII.

5.3.5 Summary of the general trends – ABC – HOS 2

The results of the 7 OMS are analysed based on the ABC method in this section. It is found that most of the general trends of the 7 OMS are same as the trends found in section 4.3. However, some are slightly different as the ABC method is different from the ICE method in nature. The General Trends of the 7 OMS based on the ABC method are summarised as follows:

HOS2-GT-ABC 1. The 7 OMS can be categorised into three groups based on the OMS orders and the COFV types. However, the trends based on the OMS orders are not found to be identical. This indicates the uniqueness of the OMS order for each of the 7 OMS.

HOS2-GT-ABC 2. SEQ1-MII and SEQ2-MII are consistently ranked 6th and 7th in the analysis of each subsection respectively. This indicates that SEQ1-MII and SEQ2-MII are less stable than all the other OMS based on the ABC evaluation.

HOS2-GT-ABC 3. SEQ3-MII and SEQ4-MII are suggested to be the best OMS in the ABC evaluation as they are more stable than all the others. This is evidenced by the rankings of the two OMS in Table 73, Table 75, Table

76 and Table 78.

HOS2-GT-ABC 4. The PAR-MII shows a consistent 'medium' performance in each analysis. This is evidenced by the ranking of PAR-MII in Table 73, Table 75, Table 76 and Table 78.

HOS2-GT-ABC 5. The results of PAR-MII and SEQ5-MII have nearly the same performance in the analysis of the average, maximum, minimum and spread values. This is also found in Figure 47 where the graphs of the two OMS are nearly identical.

As defined above, the general trends found in subsection 5.2.5 are similar to those listed above. The next section will continue to analyse the results of the 7 OMS based on the INC method. The extracted general trends will be compared with the trends discovered in this section and in section 5.2.

5.4 INC results of Holistic Optimisation Study 2

The previous two subsections analysed the general trends of the 7 OMS by the ICE and the ABC evaluation methods. In this subsection, the 7 OMS will be further assessed by the INC method in order to compare the findings from the previous evaluations. The results of the 7 OMS are illustrated in Figure 49. As the definition of the INC method in subsection 3.6.3 demonstrated, the idea is to calculate the 'distance' between the results of the initial and the final iteration. This distance, namely the 'Local Distance', is the larger the better. The 'Local Distance' also represents the COFV in this section. By observing Figure 49, it is found that the graph of SEQ3-MII is higher than all the other OMS. This indicates that the results of SEQ3-MII outperform the results of all the other OMS. The graph of SEQ2-MII however is consistently lower than the graphs of the other OMS. This indicates that the results of SEQ2-MII underperform the results of all the other OMS. In order to further analyse the trends of the 7 OMS based on the INC method, several detailed analyses will be implemented in the following subsections:

- Subsection 5.4.1, Results based on the average change of objective function values.
- Subsection 5.4.2, Results based on the maximum change of the objective function values.
- Subsection 5.4.3, Results based on the minimum change of the objective function values.
- Subsection 5.4.4, Results based on the average spreads of objective function value change.
- Final subsection contains the summary of section 5.4.

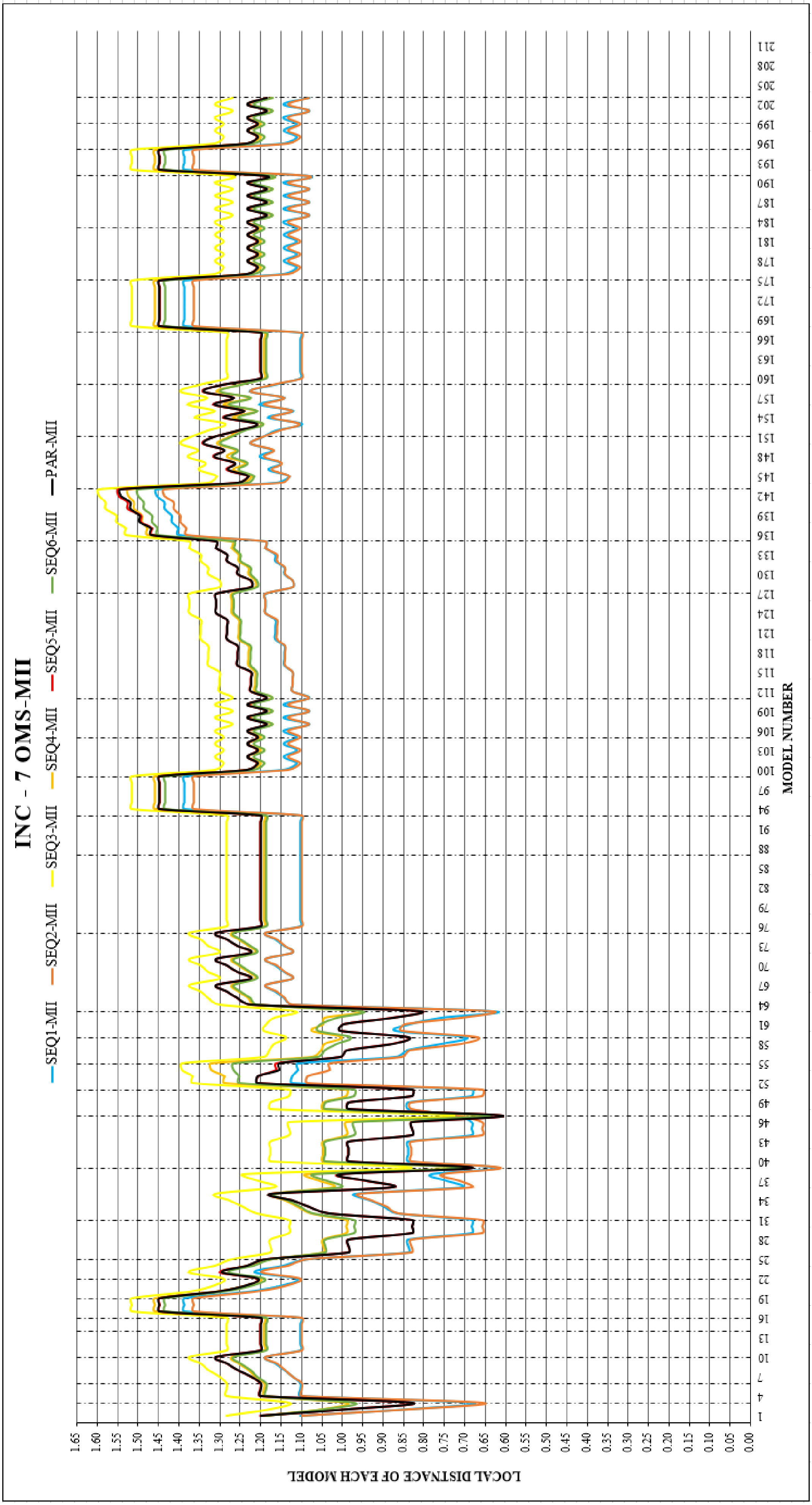

Figure 49: The results of the 7 OMS (INC – Holistic Optimisation Study 2)

5.4.1 Results based on the average change of objective function values

The average COFV of each of the 7 OMS based on the INC method is calculated by Equation(4.1). The 7 OMS are ranked based on the average COFV in Table 79, from the highest to the lowest.

Table 79: The ranked 7 OMS based on the average COFV – INC – HOS2

Rank	OMS	Objective function value changes (Average – INC)
1	SEQ3-MII	1.32
2	SEQ4-MII	1.22
3	SEQ5-MII	1.21
4	PAR-MII	1.21
5	SEQ6-MII	1.21
6	SEQ1-MII	1.11
7	SEQ2-MII	1.10

According to the ranking of the 7 OMS in Table 79, the following trends are found:

HOS2-Avg-INC 1. SEQ3-MII is ranked 1st which indicates it outperforms all the other OMS based on the average COFV analysis.

HOS2-Avg-INC 2. SEQ2-MII is ranked 7th. This indicates that SEQ2-MII underperforms the other OMS based on the average COFV.

HOS2-Avg-INC 3. The 6 SEQ optimisation programmes cannot be categorised into three groups as defined in subsection 5.3.1. The trends here will be the same as HOS2-Avg-ICE3.

HOS2-Avg-INC 4. The PAR-MII is ranked in the middle of the SEQ optimisation programmes, however it has the same objective function value change as SEQ6-MII. This indicates that the performance of the PAR-MII and SEQ6-MII is the same.

5.4.2 Results based on the maximum change of objective function values

The maximum COFV is the maximum value of the 203 COFV for the 203 models in each OMS. The 7 OMS are ranked from 1st to 7th based on the maximum COFV as illustrated in Table 80.

Table 80: The ranked 7 OMS based on the maximum COFV – INC – HOS2

Rank	OMS	Objective function value changes (Maximum – INC)
1	SEQ3-MII	1.60
2	SEQ5-MII	1.55
3	PAR-MII	1.55
4	SEQ4-MII	1.52
5	SEQ6-MII	1.50
6	SEQ1-MII	1.46
7	SEQ2-MII	1.43

Based on the ranking of the 7 OMS illustrated in Table 80, several trends are found as follows:

HOS2-Max-INC 1. SEQ3-MII has the best maximum change of objective function values. It indicates that SEQ3-MII outperforms the other 6 OMS in the comparison of the extreme (maximum) results across the 7 OMS.

HOS2-Max-INC 2. SEQ2-MII is still ranked at the bottom compared to its ranking in Table 79. This indicates SEQ2-MII underperforms all the other OMS.

HOS2-Max-INC 3. The PAR-MII however is ranked top (3^{rd}) in Table 80 and it has the same maximum objective function value change as SEQ5-MII. By comparing the ranking of PAR-MII and SEQ5-MII in Table 79 and Table 80, it is found that these two OMS have nearly the same change of objective function values (i.e. a difference less than 1%).

HOS2-Max-INC 4. The 6 SEQ optimisation programmes can be categorised into the same three groups as defined in Table 69. The trends based on the three groups of SEQ optimisation programmes are the same as those defined in HOS2-Max-ICE 4, HOS2-Max-ICE 5 and HOS2-Max-ICE 6.

5.4.3 Results based on the minimum change of objective function values

The minimum COFV of each OMS is summarised and ranked from the highest to the lowest in Table 81.

Table 81: The ranked 7 OMS based on the minimum COFV – INC – HOS2

Rank	OMS	Objective function value changes (Minimum – INC)
1	SEQ3-MII	0.72
2	SEQ4-MII	0.64
3	SEQ6-MII	0.64
4	SEQ1-MII	0.62
5	SEQ2-MII	0.61
6	PAR-MII	0.61
7	SEQ5-MII	0.61

The following trends are obtained from the Table 81:

HOS2-Min-INC 1. SEQ3-MII still has the best minimum objective function value change. It indicates that SEQ3-MII outperforms the other 6 OMS in comparison to the extreme (minimum) results across the 7 OMS.

HOS2-Min-INC 2. The difference in the minimum COFV between SEQ4-MII and SEQ5-MII is insignificant, i.e. 0.03. This indicates that the OMS ranked from 2^{nd} to 7^{th} have a similar performance based on the minimum COFV.

5.4.4 Results based on the average spreads of objective function value change

The average spread of the COFV for each of the 7 OMS is calculated by Equation (4.2). The 7 OMS are ranked in Table 82 based on the average spread, from the lowest to the highest.

Table 82: The average spreads of the 7 OMS – INC – HOS2

Rank	OMS	Average Spreads – INC
1	SEQ3-MII	0.11
2	SEQ5-MII	0.11
3	SEQ2-MII	0.12
4	SEQ6-MII	0.12
5	PAR-MII	0.12
6	SEQ1-MII	0.13
7	SEQ4-MII	0.13

The trends observed from Table 82 are summarised below:

HOS2-ASp-INC 1. SEQ3-MII and SEQ5-MII have the lowest average spread. It indicates that SEQ3-MII and SEQ5-MII are more stable than the other 6 OMS.

HOS2-ASp-INC 2. The PAR-MII has same value as SEQ2-MII and SEQ6-MII which indicates that the sensitivity results of these three OMS are the same. The same trend is also found between SEQ1-MII and SEQ4-MII.

HOS2-ASp-INC 3. The 6 SEQ optimisation programmes can be categorised based on their average spreads as illustrated in Table 83.

Table 83: 6 SEQ optimisation programmes grouped by average COFV – HOS 2

Group	OMS name	Optimisation Module Sequence (OMS)			Average Spreads (INC)
		1	2	3	
Y_1	SEQ3-MII	COST	CO2	STRUCTURAL	0.11
	SEQ5-MII	COST	STRUCTURAL	CO2	0.11
Y_2	SEQ6-MII	CO2	STRUCTURAL	COST	0.12
	SEQ2-MII	STRUCTURAL	CO2	COST	0.12
Y_3	SEQ1-MII	STRUCTURAL	COST	CO2	0.13
	SEQ4-MII	CO2	COST	STRUCTURAL	0.13

HOS2-ASp-INC 4. SEQ3-MII and SEQ5-MII optimise the COST module before the other two modules. This could be the reason why SEQ3-MII and SEQ5-MII are more stable than all the other OMS.

5.4.5 Summary of the general trends – INC – HOS 2

The overall general trends of the 7 OMS based on the INC method in this section are summarised as follows:

HOS2-GT-INC 1. SEQ2-MII is suggested to be the worst OMS based on the INC evaluation. Although the results of SEQ2-MII have a similar sensitivity to the results of the other OMS, its COFV is consistently lower ranked in subsection 5.4.1, 5.4.2 and 5.4.3.

HOS2-GT-INC 2. SEQ3-MII is suggested to be more stable than the other OMS. This is evidenced by the following general trends: HOS2-Avg-INC 1, HOS2-Max-INC 1, HOS2-Min-INC 1 and HOS2-ASp-INC 1.

HOS2-GT-INC 3. The PAR-MII shows different performance based on the analysis of different types of COFV. However, the overall COFV of PAR-MII in each subsection was not ranked at the top of the 7 OMS. Furthermore, it is ranked as one of the bottom three OMS in Table 82. Therefore, the PAR-MII is not considered to be a robust and stable OMS based on the INC method.

5.5 Detailed Analysis of Holistic Optimisation Study 2

In this chapter, the optimisation of a lower engine mount is investigated as Holistic Optimisation Study 2. The results of Holistic Optimisation Study 2 are assessed by three evaluation methods:

- Individual Criterion Evaluation (ICE) method
- Absolute Criterion (ABC) method
- Incremental Criterion (INC) method.

In this section, the findings from the three evaluation methods will be summarised and further investigated.

5.5.1 Perspective of Objective Function Values – HOS 2

Firstly, the performance of the 7 individual OMS based on the three evaluation methods are summarised and ranked in Table 84. In Table 84, the 7 OMS are ranked in descending order according to the average global objective function value change (**GOFVC**) of each OMS.

Table 84: Ranked 7 OMS based on the average GOFVC

Rank	ICE		ABC		INC	
	OMS	GOFVC	OMS	GOFVC	OMS	GOFVC
1	SEQ3-MII	143%	SEQ3-MII	0.62	SEQ3-MII	1.32
2	SEQ4-MII	131%	SEQ4-MII	0.67	SEQ4-MII	1.22
3	SEQ5-MII	130%	SEQ5-MII	0.69	SEQ5-MII	1.21
4	PAR-MII	129%	SEQ6-MII	0.69	PAR-MII	1.21
5	SEQ6-MII	129%	PAR-MII	0.69	SEQ6-MII	1.21
6	SEQ1-MII	112%	SEQ1-MII	0.81	SEQ1-MII	1.11
7	SEQ2-MII	109%	SEQ2-MII	0.84	SEQ2-MII	1.11
Difference (%) Between Rank 1st and 7th		31%		35%		19%

The individual ranking in Table 84 of the 7 OMS is almost identical across all three evaluation methods. Table 84 reveals a number of noteworthy trends:

HOS2-G1. The change of objective function value of SEQ2-MII consistently underperforms all the other OMS. It can be seen that for the ICE and ABC evaluation methods, the 'underperformance' is insignificant as the difference between ranking 6 and 7 is 3% (ICE) and 0.03 (ABC). For INC, the 'underperformance' is marginal as well, i.e. the objective function value change only differs after the third significant digit. However, the difference (%) between ranking 1 and ranking 7 for INC (19%) is low compared to those of ICE (31%) and ABC (35%).

HOS2-G2. According to Table 66 in subsection 5.2.1, the 6 SEQ optimisation programmes are categorised into three groups based on the specific position of the STRUCTURAL module during the optimisation. It was evidenced that a postposition of the STRUCTURAL module leads to a higher ranking. This is the reason that SEQ3-MII and SEQ4-MII are ranked top in each column of Table 84.

HOS2-G3. The OMS that optimise the COST module before the CO2 module will be ranked higher when the position of the STRUCTURAL module is fixed. This is evidenced by the OMS orders in Table 66 and the rankings in Table 84.

In order to find out how the three individual modules 'help' SEQ3-MII to be ranked first, the values in ICE, ABC and INC are 'decomposed' into the local objective function values change (**LOFVC**) of the three individual modules respectively.

5.5.1.1 ICE – LOFVC – HOS 2

The new rankings of the 7 OMS based on the performance of each module are tabulated in Table 85. The local changes of objective function values of each module are ranked from the highest to the lowest in Table 85.

Table 85: LOFVC of each module based on the ICE method – HOS 2

Rank	OMS	LOFVC (STRUCTURAL)	OMS	LOFVC (CO2)	OMS	LOFVC (COST)
1	SEQ1-MII	50.10%	SEQ3-MII	68.21%	SEQ1-MII	23.40%
2	SEQ2-MII	50.10%	SEQ5-MII	53.86%	SEQ4-MII	23.31%
3	SEQ3-MII	50.10%	PAR-MII	53.86%	SEQ3-MII	20.97%
4	SEQ4-MII	50.10%	SEQ4-MII	53.36%	SEQ5-MII	20.97%
5	SEQ5-MII	50.10%	SEQ6-MII	53.36%	SEQ6-MII	20.80%
6	SEQ6-MII	50.10%	SEQ1-MII	32.73%	PAR-MII	20.76%
7	PAR-MII	50.10%	SEQ2-MII	32.62%	SEQ2-MII	20.70%
Difference Between Rank 1st and 7th		0		35.59%		2.7%

The trends discovered in Table 85 are as follows:

HOS2-LOFVC-ICE1. The LOFVC in the STRUCTURAL module of the 7 OMS is the same. This indicates the performance of the STRUCTURAL module across the 7 OMS is the same.

HOS2-LOFVC-ICE2. The values of the CO2 column in Table 85 show that SEQ3-MII is ahead of the other OMS with a 14% difference compared with the OMS ranked in second place. As there is not much difference between the values of rankings 1 and 7 in the COST column (i.e. the max spread = 2.7%), it is suggested that the CO2 module made the most 'effort' in making SEQ3-MII be ranked first in Table 84.

HOS2-LOFVC-ICE3. SEQ2-MII has the same performance as the other OMS in the STRUCTURAL module. However, it underperforms the other OMS in both the CO2 and the COST module. This is why it is ranked the lowest in Table 84. Another reason could be the uniqueness of its specific OMS order.

HOS2-LOFVC-ICE4. SEQ1-MII is ranked first in the COST column which indicates that the specific OMS order of SEQ1-MII gives a better optimisation performance in the COST module though the difference compared to the other OMS is very small, i.e. the maximum spread is 2.7%.

5.5.1.2 ABC – LOFVC – HOS 2

The objective function value change of the 7 MOS based on the ABC method are also 'decomposed' into the individual objective function value change of each module. The rankings of the 7 OMS according to the local objective function value change (LOFVC) are tabulated in Table 86.

Table 86 LOFVC of each module based on the ABC method – HOS 2

Rank	OMS	LOFVC (STRUCTURAL)	OMS	LOFVC (CO2)	OMS	LOFVC (COST)
1	SEQ1-MII	0.06	SEQ3-MII	0.13	SEQ1-MII	0.55
2	SEQ2-MII	0.06	SEQ5-MII	0.29	SEQ4-MII	0.55
3	SEQ3-MII	0.06	PAR-MII	0.29	SEQ3-MII	0.58
4	SEQ4-MII	0.06	SEQ4-MII	0.30	SEQ5-MII	0.58
5	SEQ5-MII	0.06	SEQ6-MII	0.30	SEQ6-MII	0.58
6	SEQ6-MII	0.06	SEQ1-MII	0.54	PAR-MII	0.59
7	PAR-MII	0.06	SEQ2-MII	0.54	SEQ2-MII	0.59
Difference Between Rank 1st and 7th		0		0.41		0.04

The trends discovered in Table 86 are as follows:

HOS2-LOFVC-ABC1. The LOFVC in the STRUCTURAL module of the 7 OMS is the same. This indicates the performance of the STRUCTURAL module across the 7 OMS is the same.

HOS2-LOFVC-ABC2. The values of the CO2 column in Table 86 show that SEQ3-MII is ahead of the other OMS with a 0.41 difference compared with the OMS ranked in the 7th place. As there is not much difference between the values of rankings 1 and 7 in the COST column (i.e. the max spread = 0.04), it is suggested that the CO2 module made the most 'effort' in making SEQ3-MII be ranked first in Table 84.

HOS2-LOFVC-ABC3. SEQ2-MII has same performance as the other OMS in the STRUCTURAL module. However, it underperforms the other OMS in both the CO2 and the COST module. This is why it is ranked the lowest in Table 84. The uniqueness of the specific OMS order could be another reason for SEQ2-MII to be ranked the lowest.

HOS2-LOFVC-ABC4. SEQ1-MII is ranked first in the COST column. It shows that the order of this OMS is more efficient than other OMS in the COST module. However, the difference between the OMS ranked 1 and 7 is as small as 0.04. Therefore, this trend found in the COST module is considered to be indifferent.

Overall, the general trends discovered in this subsection are the same as those stated in ICE1-4 in subsection 5.5.1.2.

5.5.1.3 INC – LOFVC – HOS 2

The previous two subsections have discussed the rankings of the 7 OMS based on individual module performance. The trends found in both subsections are the same. This subsection will further investigate the trends by ranking the 7 OMS based on their individual module performance assessed by the INC method. The ranking of the 7 OMS for each module is tabulated in Table 87.

Table 87: LOFVC of each module based on the INC method – HOS 2

Rank	OMS	LOFVC (STRUCTURAL)	OMS	LOFVC (CO2)	OMS	LOFVC (COST)
1	SEQ1-MII	0.94	SEQ3-MII	0.84	SEQ1-MII	0.34
2	SEQ2-MII	0.94	SEQ5-MII	0.67	SEQ4-MII	0.33
3	SEQ3-MII	0.94	PAR-MII	0.67	SEQ3-MII	0.31
4	SEQ4-MII	0.94	SEQ4-MII	0.66	SEQ5-MII	0.31
5	SEQ5-MII	0.94	SEQ6-MII	0.66	SEQ6-MII	0.30
6	SEQ6-MII	0.94	SEQ1-MII	0.42	PAR-MII	0.30
7	PAR-MII	0.94	SEQ2-MII	0.42	SEQ2-MII	0.30
Difference Between Rank 1 and 7		0		0.42		0.04

The trends discovered in Table 87 are as follows:

HOS2-LOFVC-INC1. The LOFVC in the STRUCTURAL module of the 7 OMS is the same. This indicates the performance of the STRUCTURAL module across the 7 OMS is the same.

HOS2-LOFVC-INC2. The values of the CO2 column in Table 87 shows that SEQ3-MII is ahead of the other OMS with a 0.17 difference compared with the OMS ranked in second place. As there is not much difference between the values of rankings 1 and 7 in the COST column (i.e. the max spread = 0.04), it is suggested that the CO2 module made the most 'effort' in making SEQ3-MII be ranked first in Table 84.

HOS2-LOFVC-INC3. SEQ2-MII has same performance as the other OMS in the STRUCTURAL module. However, it underperforms the other OMS in both the CO2 and the COST module. This is why it is ranked the lowest in Table 84. The uniqueness of the specific OMS order could be another reason for the SEQ2-MII to be ranked the lowest.

HOS2-LOFVC-INC4. SEQ1-MII is again ranked first in the COST column. As the difference between SEQ1-MII (1^{st}) and SEQ2-MII (7^{th}) is only 0.04, the 'outperformance' of SEQ1-MII in the COST module is considered to be indifferent.

By comparing the trends listed in subsections 5.5.1.1, 5.5.1.2 and 5.5.1.3, it is found that the trends found in each subsection are the same. This indicates that the 7 OMS have the same performance across the three individual modules in each of the evaluation methods.

5.5.2 Perspective of Sensitivity – HOS 2

In addition to the ranking of the 7 OMS based on the objective function value change in Table 84, the ranking based on their sensitivity performance is also part of the assessment for the 7 OMS. The sensitivity of the results of the 7 OMS are summarised and ranked in Table 88.

Table 88: Ranked 7 OMS based on the Global Spread Values (GSV) – HOS 2

Rank	ICE		ABC		INC	
	OMS	GSV	OMS	GSV	OMS	GSV
1	SEQ4-MII	11%	SEQ4-MII	0.12	SEQ3-MII	0.07
2	SEQ3-MII	12%	SEQ6-MII	0.13	SEQ6-MII	0.07
3	SEQ6-MII	12%	SEQ3-MII	0.13	SEQ4-MII	0.07
4	SEQ5-MII	15%	SEQ5-MII	0.15	SEQ1-MII	0.08
5	PAR-MII	15%	PAR-MII	0.15	SEQ2-MII	0.08
6	SEQ1-MII	16%	SEQ1-MII	0.16	SEQ5-MII	0.09
7	SEQ2-MII	16%	SEQ2-MII	0.16	PAR-MII	0.09

The 7 OMS are ranked from the lowest sensitivity to the highest. The following trends are found from Table 88:

HOS2-GSV1. The spread between the OMS ranked 1st and 7th is marginal in each evaluation method. For ICE, the spread is 5%; for ABC, the spread is 0.04; for INC, the spread is 0.02. This indicates that the results of the 7 OMS have a similar sensitivity performance in each evaluation method.

HOS2-GSV2. The top three ranked SEQ optimisation programmes have smaller values than the bottom three. This indicates that the results of SEQ3-MII, SEQ4-MII and SEQ6-MII are less sensitive to the change of the parameters than SEQ1-MII, SEQ2-MII and SEQ5-MII. It is suggested that the results of SEQ3-MII, SEQ4-MII and SEQ6-MII are considered to be more stable.

HOS2-GSV3. The top three ranked SEQ optimisation programmes optimised the CO2 module before the STRUCTURAL module while the bottom three optimised the STRUCTURAL module before the CO2 module. This is evidenced by Table 66. This could be the reason that SEQ3-MII, SEQ4-MII and SEQ6-MII are ranked higher than SEQ1-MII, SEQ2-MII and SEQ5-MII based on the sensitivity analysis.

In order to find out how the three individual modules influence the ranking of the 7 OMS based on their sensitivity performance, the global spread values (**GSV**) in ICE, ABC and INC are 'decomposed' into the local spread values (**LSV**) of the three individual modules respectively. The LSV of the 7 OMS for each module in each evaluation method will be investigated in the following subsections.

5.5.2.1 ICE – LSV – HOS 2

In order to assess the sensitivity performance of the three individual modules, a table containing the local spread values (LSV) of each module for the 7 OMS was created (Table 89). The local spread values of the 7 OMS based on the ICE method are ranked from the lowest to the highest in Table 89.

Table 89: LSV of each module based on ICE method – HOS 2

Rank	OMS	LSV (STRUCTURAL)	OMS	LSV (CO2)	OMS	LSV (COST)
1	SEQ1-MII	4%	SEQ3-MII	3%	SEQ4-MII	7%
2	SEQ2-MII	4%	SEQ4-MII	3%	SEQ1-MII	7%
3	SEQ3-MII	4%	SEQ6-MII	3%	SEQ3-MII	8%
4	SEQ4-MII	4%	SEQ5-MII	7%	SEQ5-MII	8%
5	SEQ5-MII	4%	PAR-MII	7%	PAR-MII	8%
6	SEQ6-MII	4%	SEQ2-MII	8%	SEQ2-MII	8%
7	PAR-MII	4%	SEQ1-MII	8%	SEQ6-MII	8%
Average		4%		6%		8%

The following trends are discovered:

HOS2-LSV-ICE1. The results of the STRUCTURAL module are less sensitive to the change of parameters, as this module has the lowest average LSV (4%) than the other two modules (6% and 8%). This also indicates that the performance of the 7 OMS in the STRUCTURAL module is more stable than their performance in the other modules. On the other hand, the results of the 7 OMS in the COST module are more sensitive to the change of parameters.

HOS2-LSV-ICE2. The STRUCTURAL module has the same performance across the 7 OMS, as the LSV of the 7 OMS is the same. The same trend can be found in the COST module as the difference in LSV between the 7 OMS is as small as 1%.

HOS2-LSV-ICE3. The top three ranked SEQ optimisation programmes have smaller values than the bottom three. This indicates that the results of SEQ3-MII, SEQ4-MII and SEQ6-MII in the CO2 module are less sensitive to the change of the parameters than SEQ1-MII, SEQ2-MII and SEQ5-MII. It is suggested that the results of SEQ3-MII, SEQ4-MII and SEQ6-MII are considered to be more stable in the CO2 module.

Analogous to the sensitivity analysis of the 33 case studies for each of the OMS in subsection 4.6.2, the spreads of the 33 case studies for each of the 7 OMS (HOS2) are ranked in Table 90. The following trends are discovered from Table 90:

HOS2-LSV-ICE4. For OAT, the single parameter of case study 8 is the most influential parameter for SEQ1-MII, SEQ3-MII, SEQ4-MII, SEQ5-MII, SEQ6-MII and PAR-MII; i.e. the Overhead cost. The most influential parameter for SEQ2-MII is the Geometry.

HOS2-LSV-ICE5. For TAT, the two parameters of case study 15 are the two most influential parameters for SEQ1-MII, SEQ2-MII, SEQ4-MII and PAR-MII, i.e. Geometry and Recycled content. The two most influential parameters for SEQ3-MII, SEQ5-MII and SEQ6-MII are Recycled content and Overhead cost. The two most influential parameters for each of the 7 OMS all contain the single-most influential parameters found in HOS2-LSV-ICE4.

The results of the 7 OMS will be analysed continuously based on the ABC method in the next subsubsection.

Table 90: Spread of each case study for the 7 OMS by the ICE method – HOS2

Method	Rank	CS No.	SEQ1-MII	CS No.	SEQ2-MII	CS No.	SEQ3-MII	CS No.	SEQ4-MII	CS No.	SEQ5-MII	CS No.	SEQ6-MII	CS No.	PAR-MII
OAT	1	8	38%	1	42%	8	40%	8	38%	8	40%	8	38%	8	39%
	2	1	38%	8	38%	7	21%	7	23%	1	35%	7	23%	1	34%
	3	7	23%	7	23%	1	19%	1	14%	7	22%	1	18%	7	23%
	4	3	12%	3	12%	3	10%	3	9%	3	12%	3	9%	3	13%
	5	6	0%	2	0%	2	0%	2	0%	2	0%	2	0%	6	0%
	6	2	0%	4	0%	4	0%	4	0%	4	0%	4	0%	2	0%
	7	4	0%	5	0%	5	0%	5	0%	5	0%	5	0%	4	0%
	8	5	0%	6	0%	6	0%	6	0%	6	0%	6	0%	5	0%
TAT	1	15	45%	15	47%	26	36%	26	35%	15	42%	26	36%	15	43%
	2	26	38%	26	40%	15	34%	15	33%	26	40%	15	34%	26	39%
	3	10	35%	10	35%	21	26%	21	26%	10	33%	21	26%	10	33%
	4	14	28%	14	29%	30	26%	30	26%	21	26%	30	26%	21	26%
	5	30	26%	21	26%	33	26%	33	26%	30	26%	33	26%	30	26%
	6	33	26%	30	26%	10	20%	10	19%	33	26%	10	20%	33	26%
	7	21	26%	33	26%	25	17%	25	17%	14	25%	14	17%	14	25%
	8	11	21%	13	23%	14	17%	14	16%	25	20%	25	17%	25	20%
	9	12	21%	12	22%	24	10%	16	9%	11	18%	11	10%	13	18%
	10	9	21%	11	21%	9	10%	22	9%	12	18%	12	10%	11	18%
	11	25	20%	9	21%	11	10%	23	9%	9	18%	9	10%	12	18%
	12	13	20%	25	20%	12	10%	24	9%	13	17%	13	9%	9	18%
	13	24	12%	16	12%	16	10%	20	8%	24	14%	16	9%	24	13%
	14	16	12%	22	12%	22	10%	29	8%	16	12%	22	9%	16	13%
	15	22	12%	23	12%	23	10%	32	8%	22	12%	23	9%	22	13%
	16	23	12%	24	12%	13	9%	13	8%	23	12%	24	9%	23	13%
	17	29	8%	20	8%	20	7%	11	8%	20	7%	20	8%	20	8%
	18	20	8%	29	8%	29	7%	12	8%	29	7%	29	8%	29	8%
	19	32	8%	32	8%	32	7%	9	8%	32	7%	32	8%	32	8%
	20	19	0%	17	0%	17	0%	17	0%	17	0%	17	0%	19	0%
	21	31	0%	18	0%	18	0%	18	0%	18	0%	18	0%	31	0%
	22	28	0%	19	0%	19	0%	19	0%	19	0%	19	0%	28	0%
	23	17	0%	27	0%	27	0%	27	0%	27	0%	27	0%	17	0%
	24	18	0%	28	0%	28	0%	28	0%	28	0%	28	0%	18	0%
	25	27	0%	31	0%	31	0%	31	0%	31	0%	31	0%	27	0%

5.5.2.2 ABC – LSV – HOS 2

The rankings of the 7 OMS in each module based on the ICE method have been analysed in the previous subsection. In this subsection, the rankings of the 7 OMS in each module based on the ABC method will be studied and discussed. The rankings of the 7 OMS for the individual modules are tabulated in Table 91.

Table 91: LSV of each module based on the ABC method – HOS 2

Rank	OMS	LSV (STRUCTURAL)	OMS	LSV (CO2)	OMS	LSV (COST)
1	SEQ1-MII	0.04	SEQ3-MII	0.03	SEQ4-MII	0.10
2	SEQ2-MII	0.04	SEQ4-MII	0.04	SEQ1-MII	0.10
3	SEQ3-MII	0.04	SEQ6-MII	0.04	SEQ3-MII	0.11
4	SEQ4-MII	0.04	SEQ5-MII	0.08	SEQ5-MII	0.11
5	SEQ5-MII	0.04	PAR-MII	0.08	PAR-MII	0.11
6	SEQ6-MII	0.04	SEQ2-MII	0.10	SEQ2-MII	0.11
7	PAR-MII	0.04	SEQ1-MII	0.10	SEQ6-MII	0.11
Average		0.04		0.06		0.11

The following trends are discovered:

HOS2-LSV-ABC1. The results of the STRUCTURAL module are less sensitive to the change of parameters, as this module has the lowest average LSV (0.04) than the other two modules (0.06 and 0.11). This also indicates that the performance of the 7 OMS in the STRUCTURAL module is more stable than their performance in the other modules. On the other hand, the results of the 7 OMS in the COST module are more sensitive to the change of parameters.

HOS2-LSV-ABC2. The STRUCTURAL module has the same performance across the 7 OMS, as the LSV of the 7 OMS is the same. The same trend can be found in the COST module as the difference in LSV between the 7 OMS is as small as 0.01.

HOS2-LSV-ABC3. The top three ranked SEQ optimisation programmes have smaller values than the bottom three. This indicates that the results of SEQ3-MII, SEQ4-MII and SEQ6-MII in the CO2 module are less sensitive to the change of the parameters than SEQ1-MII, SEQ2-MII and SEQ5-MII. It is suggested that the results of SEQ3-MII, SEQ4-MII and SEQ6-MII are considered to be more stable in the CO2 module.

HOS2-LSV-ABC4. For OAT, the single parameter of case study 8 is the most influential parameter for SEQ3-MII, SEQ4-MII, SEQ5-MII, SEQ6-MII and PAR-MII; i.e. the Overhead cost. The most influential parameter for SEQ1-MII and SEQ2-MII is the Geometry.

HOS2-LSV-ABC5. For TAT, the two parameters of case study 15 are the two most influential parameters for SEQ1-MII, SEQ2-MII, SEQ3-MII, SEQ5-MII and PAR-MII, i.e. Geometry and Recycled content. The two most influential parameters for SEQ4-MII and SEQ6-MII are Recycled content and Overhead cost. The two most influential parameters for each of the 7 OMS all contain the single-most influential parameters found in HOS2-LSV-ICE4.

The trends found in Table 92 are the same as those defined in HOS2-LSV-ICE4 and HOS2-LSV-ICE5 in subsubsection 5.5.2.1. To further study the trends of the 7 OMS, the results will be investigated based on the INC method in the next subsubsection.

Table 92: Spread of each case study for the 7 OMS by the ABC method – HOS2

Method	Rank	CS No.	SEQ1-MII	CS No.	SEQ2-MII	CS No.	SEQ3-MII	CS No.	SEQ4-MII	CS No.	SEQ5-MII	CS No.	SEQ6-MII	CS No.	PAR-MII
OAT	**1**	1	0.43	1	0.46	8	0.55	8	0.48	8	0.51	8	0.49	8	0.50
	2	8	0.41	8	0.42	7	0.30	7	0.27	1	0.32	7	0.28	1	0.32
	3	7	0.22	7	0.23	1	0.19	1	0.16	7	0.27	1	0.21	7	0.28
	4	3	0.07	3	0.07	3	0.01	3	0.03	3	0.03	3	0.03	3	0.04
	5	6	0.00	2	0.00	2	0.00	2	0.00	2	0.00	2	0.00	6	0.00
	6	2	0.00	4	0.00	4	0.00	4	0.00	4	0.00	4	0.00	2	0.00
	7	4	0.00	5	0.00	5	0.00	5	0.00	5	0.00	5	0.00	4	0.00
	8	5	0.00	6	0.00	6	0.00	6	0.00	6	0.00	6	0.00	5	0.00
TAT	**1**	15	0.43	15	0.46	15	0.41	26	0.39	15	0.43	26	0.41	15	0.44
	2	26	0.40	26	0.41	26	0.40	15	0.37	26	0.42	15	0.39	26	0.40
	3	10	0.33	10	0.33	21	0.37	21	0.34	21	0.35	21	0.34	21	0.35
	4	30	0.30	21	0.30	30	0.37	30	0.34	30	0.35	30	0.34	30	0.35
	5	33	0.30	30	0.30	33	0.37	33	0.34	33	0.35	33	0.34	33	0.35
	6	21	0.30	33	0.30	14	0.19	14	0.17	14	0.24	14	0.18	14	0.24
	7	14	0.28	14	0.29	13	0.14	25	0.15	10	0.23	25	0.15	10	0.23
	8	13	0.25	13	0.26	25	0.13	10	0.14	13	0.20	10	0.15	13	0.20
	9	9	0.22	12	0.22	10	0.12	13	0.12	9	0.16	13	0.12	9	0.15
	10	11	0.22	9	0.21	9	0.10	20	0.10	11	0.16	20	0.10	11	0.15
	11	12	0.22	11	0.21	11	0.10	29	0.10	12	0.16	29	0.10	12	0.15
	12	25	0.18	25	0.18	12	0.10	32	0.10	25	0.15	32	0.10	25	0.15
	13	24	0.14	24	0.14	20	0.10	24	0.10	24	0.14	9	0.10	24	0.14
	14	29	0.09	20	0.09	29	0.10	9	0.07	20	0.09	11	0.10	20	0.10
	15	20	0.09	29	0.09	32	0.10	11	0.07	29	0.09	12	0.10	29	0.10
	16	32	0.09	32	0.09	24	0.09	12	0.07	32	0.09	24	0.10	32	0.10
	17	16	0.07	16	0.07	16	0.01	16	0.03	16	0.03	16	0.03	16	0.04
	18	22	0.07	22	0.07	22	0.01	22	0.03	22	0.03	22	0.03	22	0.04
	19	23	0.07	23	0.07	23	0.01	23	0.03	23	0.03	23	0.03	23	0.04
	20	19	0.00	17	0.00	17	0.00	17	0.00	17	0.00	17	0.00	19	0.00
	21	31	0.00	18	0.00	18	0.00	18	0.00	18	0.00	18	0.00	31	0.00
	22	28	0.00	19	0.00	19	0.00	19	0.00	19	0.00	19	0.00	28	0.00
	23	17	0.00	27	0.00	27	0.00	27	0.00	27	0.00	27	0.00	17	0.00
	24	18	0.00	28	0.00	28	0.00	28	0.00	28	0.00	28	0.00	18	0.00
	25	27	0.00	31	0.00	31	0.00	31	0.00	31	0.00	31	0.00	27	0.00

5.5.2.3 INC – LSV – HOS 2

So far, the trends found in subsection 5.5.2.1 are the same as those found in this subsection though the actual values of each OMS are different. In order to see if the trends of the 7 OMS in each module continue to be the same for the INC method, the 7 OMS are ranked according to their sensitivity performance in each module based on this method. The rankings are tabulated in Table 93.

Table 93: LSV of each module based on the INC method – HOS 2

Rank	OMS	LSV (STRUCTURAL)	OMS	LSV (CO2)	OMS	LSV (COST)
1	SEQ1-MII	0.04	SEQ4-MII	0.04	SEQ3-MII	0.11
2	SEQ2-MII	0.04	SEQ6-MII	0.04	SEQ5-MII	0.11
3	SEQ3-MII	0.04	SEQ3-MII	0.04	SEQ2-MII	0.12
4	SEQ4-MII	0.04	SEQ5-MII	0.06	SEQ6-MII	0.12
5	SEQ5-MII	0.04	PAR-MII	0.06	PAR-MII	0.12
6	SEQ6-MII	0.04	SEQ2-MII	0.08	SEQ1-MII	0.13
7	PAR-MII	0.04	SEQ1-MII	0.08	SEQ4-MII	0.13
Average		0.04		0.05		0.12

The following trends are discovered:

HOS2-LSV-INC1. The results of the STRUCTURAL module are less sensitive to the change of parameters, as this module has the lowest average LSV (0.04) than the other two modules (0.05 and 0.12). This also indicates that the performance of the 7 OMS in the STRUCTURAL module is more stable than their performance in the other modules. On the other hand, the results of the 7 OMS in the COST module are more sensitive to the change of parameters.

HOS2-LSV-INC2. The STRUCTURAL module has the same performance across the 7 OMS, as the LSV of the 7 OMS is the same. The same trend can be found in the COST module as the difference of LSV between the 7 OMS is as small as 0.02.

HOS2-LSV-INC3. The top three ranked SEQ optimisation programmes have smaller values than the bottom three. This indicates that the results of SEQ3-MII, SEQ4-MII and SEQ6-MII in the CO2 module are less sensitive to the change of the parameters than SEQ1-MII, SEQ2-MII and SEQ5-MII. It is suggested that the results of SEQ3-MII, SEQ4-MII and SEQ6-MII are considered to be more stable in the CO2 module.

Table 94 shows the spreads of the 33 case studies for each of the 7 OMS. A number of noteworthy trends are found in Table 94:

HOS2-LSV-INC4. For OAT, the 7 OMS have the same single-most influential parameter, i.e. Geometry.

HOS2-LSV-INC5. For TAT, the two parameters of case study 10 are the two most influential parameters for all the 7 OMS, i.e. Geometry and Recycled content.

The general trends of the 7 OMS have been further analysis in this section. The overall general trends of the 7 OMS will then be summarised in the next section for HOS2.

Table 94: Spread of each case study for the 7 OMS by the INC method – HOS2

Method	Rank	CS No.	SEQ1-MII	CS No.	SEQ2-MII	CS No.	SEQ3-MII	CS No.	SEQ4-MII	CS No.	SEQ5-MII	CS No.	SEQ6-MII	CS No.	PAR-MII
OAT	1	1	0.42	1	0.44	1	0.15	1	0.20	1	0.37	1	0.22	1	0.37
	2	8	0.13	8	0.12	8	0.11	8	0.12	8	0.11	8	0.11	8	0.11
	3	7	0.12	7	0.11	7	0.09	7	0.11	7	0.10	7	0.10	7	0.10
	4	3	0.07	3	0.07	3	0.07	3	0.06	3	0.08	3	0.06	3	0.09
	5	6	0.00	2	0.00	2	0.00	2	0.00	2	0.00	2	0.00	6	0.00
	6	2	0.00	4	0.00	4	0.00	4	0.00	4	0.00	4	0.00	2	0.00
	7	4	0.00	5	0.00	5	0.00	5	0.00	5	0.00	5	0.00	4	0.00
	8	5	0.00	6	0.00	6	0.00	6	0.00	6	0.00	6	0.00	5	0.00
TAT	1	10	0.35	10	0.35	10	0.48	10	0.45	10	0.49	10	0.46	10	0.49
	2	15	0.24	15	0.22	11	0.45	11	0.40	11	0.38	11	0.40	11	0.38
	3	14	0.17	14	0.19	26	0.11	15	0.12	15	0.19	26	0.11	15	0.20
	4	9	0.16	12	0.18	25	0.09	26	0.11	14	0.17	15	0.11	14	0.17
	5	11	0.16	9	0.17	15	0.08	25	0.09	9	0.16	25	0.08	9	0.16
	6	12	0.16	11	0.17	16	0.07	14	0.07	12	0.16	14	0.08	12	0.16
	7	26	0.13	26	0.12	22	0.07	21	0.06	26	0.13	9	0.07	26	0.13
	8	25	0.10	25	0.10	23	0.07	30	0.06	25	0.11	12	0.07	25	0.11
	9	16	0.07	16	0.07	24	0.07	33	0.06	16	0.08	16	0.06	16	0.09
	10	22	0.07	22	0.07	14	0.05	9	0.06	22	0.08	22	0.06	22	0.09
	11	23	0.07	23	0.07	9	0.05	12	0.06	23	0.08	23	0.06	23	0.09
	12	30	0.06	13	0.05	12	0.05	16	0.06	24	0.08	24	0.05	24	0.07
	13	33	0.06	24	0.05	21	0.04	22	0.06	21	0.05	21	0.05	13	0.05
	14	21	0.06	21	0.05	30	0.04	23	0.06	30	0.05	30	0.05	21	0.05
	15	24	0.05	30	0.05	33	0.04	24	0.05	33	0.05	33	0.05	30	0.05
	16	29	0.03	33	0.05	13	0.03	13	0.03	13	0.04	20	0.03	33	0.05
	17	20	0.03	20	0.03	20	0.02	20	0.03	20	0.02	29	0.03	20	0.03
	18	32	0.03	29	0.03	29	0.02	29	0.03	29	0.02	32	0.03	29	0.03
	19	13	0.01	32	0.03	32	0.02	32	0.03	32	0.02	13	0.01	32	0.03
	20	19	0.00	17	0.00	17	0.00	17	0.00	17	0.00	17	0.00	19	0.00
	21	31	0.00	18	0.00	18	0.00	18	0.00	18	0.00	18	0.00	31	0.00
	22	28	0.00	19	0.00	19	0.00	19	0.00	19	0.00	19	0.00	28	0.00
	23	17	0.00	27	0.00	27	0.00	27	0.00	27	0.00	27	0.00	17	0.00
	24	18	0.00	28	0.00	28	0.00	28	0.00	28	0.00	28	0.00	18	0.00
	25	27	0.00	31	0.00	31	0.00	31	0.00	31	0.00	31	0.00	27	0.00

5.6 Summary of Holistic Optimisation Study 2

The lower engine mount has been optimised in this chapter with 7 MII optimisations. The results of the 7 OMS-MII were evaluated by the three methods: ICE, ABC and INC. The general trends based on different analysis methods were extracted. The overall trends of the 7 OMS-MII for the Holistic Optimisation Study 2 are summarised as follows:

HOS2-1. SEQ3-MII is suggested to be more stable than the other OMS. This is evidenced by the following general trends: HOS2-GT-ICE 2, HOS2-GT-ABC 3, HOS2-GT-INC 2.

HOS2-2. SEQ2-MII is suggested to be less stable than the other OMS. This is evidenced by the general trends defined in HOS2-GT-ICE 1, HOS2-GT-ABC 2, HOS2-GT-INC 1.

HOS2-3. The LOFVC in the STRUCTURAL module of the 7 OMS is the same. This indicates the performance of the STRUCTURAL module across the 7 OMS is the same. This is evidenced by the trends defined in HOS2-LOFVC-ICE1, HOS2-LOFVC-ABC1 and HOS2-LOFVC-INC1.

HOS2-4. It is suggested that the CO2 module is more influential in the 'Global' performance of the 7 OMS than the other two modules. This is evidenced by trends defined in HOS2-LOFVC-ICE2, HOS2-LOFVC-ABC2 and HOS2-LOFVC-INC2.

HOS2-5. The performance of the 7 OMS in the STRUCTURAL module is more stable than their performance in other modules. This is evidenced by the constant spread values of the STRUCTRAL module in Table 89, Table 91 and Table 93. The tables also indicate that the results of the COST and CO2 modules are more sensitive to the input parameters.

HOS2-6. The influential individual parameters for each of the 7 OMS are slightly different based on the three evaluation methods. This is evidenced by the trends defined in HOS2-LSV-ICE4, HOS2-LSV-ABC4 and HOS2-LSV-INC4. However, by comparing the trends through HOS2-LSV-ICE4, HOS2-LSV-ABC4 and HOS2-LSV-INC4, it is found that the Geometry is the most influential parameter for SEQ1-MII and SEQ2-MII; and the Overhead cost is the most influential parameter for SEQ3-MII, SEQ4-MII, SEQ5-MII, SEQ6-MII and PAR-MII. The other common top-ranked individual parameters for the 7 OMS are the recycled content and labour cost.

HOS2-7. The influential two parameters in each of the 7 OMS are different. This is evidenced by the trends defined in HOS2-LSV-ICE5, HOS2-LSV-ABC5 and HOS2-LSV-INC5. By comparing the trends through the points above, it is found that the two most influential parameters for each of the 7 OMS all contain the individual parameters defined in HOS2-6. This indicates that the results of the 7 OMS are more sensitive to the change of the Geometry and Overhead cost.

HOS2-8. The PAR-MII was proved to be "less efficiency" than the SEQ optimisation programmes, especially the top-ranked SEQ optimisation programmes such as SEQ1-MII, SEQ3-MII and SEQ5-MII.

5.7 Comparison of HOS1 to HOS2 Results

The purpose of this section is to compare the general results found in both HOS1 and HOS2 and discuss any major differences. At this point, it is important to remember that the two HOS utilised different components, i.e. a side impact beam for HOS1 and a lower engine mount for HOS2. The ideology behind choosing two significantly different components was to investigate the effects of optimisation trends identified. For this purpose, any two (or more) components could however have been selected. The reason for choosing these specific components was that while they do contain sufficient "variability" such as the difference in manufacturing methods between them, the "complexity" such as geometry remains appropriately simplistic. The latter enables conclusion of results and trends to be deduced and justified using logical engineering reasoning.

Apart from the components used in both HOS, the actual optimisation results and trends deduced also differed. SEQ5-MII was suggested as the best OMS for HOS1 while SEQ3-MII was suggested as the best for HOS2. The obvious explanation is that the two HOS used different components, so there will inherently be differences between the two studies, e.g. material, manufacturing method, geometry, etc. But there is another potential explanation which further underlines the importance of the OMS. The Table 95 shows the average change of objective function values (COFV) for SEQ3-MII and SEQ5-MII of the two HOSs respectively across all three evaluation methods. The difference between the values of SEQ3-MII and SEQ5-MII was calculated based on equation(5.2).

$$\%Difference = \frac{\left|(COFV_{SEQ3-MII}^{Average} - COFV_{SEQ5-MII}^{Average})\right|}{COFV_{SEQ5-MII}^{Average}} \tag{5.2}$$

Table 95 Comparison of Average COFV for SEQ3-MII and SEQ5-MII for both HOS

Evaluation Methods	HOS1			HOS2		
	SEQ3-MII	SEQ5-MII	%Difference	SEQ3-MII	SEQ5-MII	Difference
ICE	211%	223%	5%	143%	130%	10%
ABC	0.31	0.15	107%	0.62	0.69	10%
INC	1.55	1.63	5%	1.32	1.21	9%

From Table 95, it is found that most percentage COFV differences between SEQ3-MII and SEQ5-MII in each HOS are less than 10%. Although, the maximum difference was found to be 107% for the ABC evaluation method used in HOS1. This significant difference was also found to be related to the CO2 module of the two OMS, i.e. it is evidenced in Table 54. Moreover, the difference of module sequences between SEQ3-MII and SEQ5-MII was the CO2 module as evidenced in Table 46. Therefore, the significant difference could be caused by the uniqueness of the module sequence in that specific evaluation method (ABC). However, the general trend in Table 95 indicates that SEQ3-MII and SEQ5-MII in the two HOS respectively have similar performance (i.e. generally speaking, difference less 10%), although further HOS should be completed to clarify this postulation. For both HOS SEQ3-MII and SEQ5-MII are top-ranked across all three evaluation methods as e.g. evidenced by, Table 45 and Table 66. As before, it should be noted that this trend was observed based on the current two HOS only. It can therefore not rigorously be evidenced that either SEQ3-MII or SEQ5-MII will be the best OMS for other components or products. It therefore follows that additional components/ products should be studied to further assess the general trends.

During the post-processing of HOS1 and HOS2 the results from the 6 SEQs were divided into categories according to COFV. In HOS1, the 6 SEQs were categorised into two groups as defined in Table 46. In HOS2, the 6 SEQs were categorised into three groups as defined in Table 67. The two categories for the 6 SEQs in each HOS were both created based on the optimisation results. However, the category of HOS1 focused on the influence of sequence of COST module and CO2 module while the category of HOS2 focused on the influence of sequence of the STRUCTURAL module. The potential reason could be that a specific type of component/ product may be influenced by a specific sequence of a single module/ modules. This remains difficult to rigorously prove based on the current results/ trends.

6 Design of Experiments

In the first and second holistic optimisation studies (HOS), the 33 case studies of each of the 7 optimisation module sequences (OMS) varied 1-2 parameters at a time (i.e. OAT and TAT). The results of the 7 OMS were analysed based on the three evaluation methods: Individual Criterion Evaluation (ICE) method, the Absolute Criterion (ABC) method and the Incremental Criterion (INC) method. The extracted general trends from each analysis are summarised as the "trends list" in section 4.7 and section 5.6. For optimisation, in general, it is important to know the most influential parameters. This is the purpose of varying 1-2 parameters at a time to do the sensitivity analysis in subsection 4.6.2 and subsection 5.5.2. The ultimate aim of this chapter is to investigate the response from a much wider perspective by allowing "all" the parameters to be changed at a time (AAT). With a limited number of parameters, one of the most typical methods to do AAT is to use a metamodel, which will be built from data based on a Design of Experiment (DOE).

A DOE method is used to investigate the relationships between input variables/ parameters and the outputs of the process. The main idea of this chapter is to use a DOE method to build a response surface of the results to determine the relations between input parameters and the responses of the objective function. This method is different from what has been performed in chapter 4 and 5 as the analysis in those two chapters are based on output responses and model numbers. The model numbers will not form any axis of the 3D response surface meta-model based on the DOE.

The response surface will be created based on the results of the 7 OMS for the HOS1 and HOS2. The results of the 7 OMS, of course, are obtained based on the three evaluation methods. The Fit method used for the response surface for each of the 7 OMS is based on a Least Squares Regression (LSR). This method has been privileged over Kriging as it allows the computation of the ANOVA (Analysis of Variance) for assessing the influential input parameters on the responses. The LSR method will create a regression polynomial for the results of each OMS to produce a response surface. This surface contains the predicted output responses which (ideally) will have minimum deviation compared with the corresponding results of each OMS. As an example, the side view of a surface created by the LSR method and the original sample results are illustrated in Figure 50. The green line is the side view of the response surface created by the LSR method as defined in the legend box. The purple points are the original sample results.

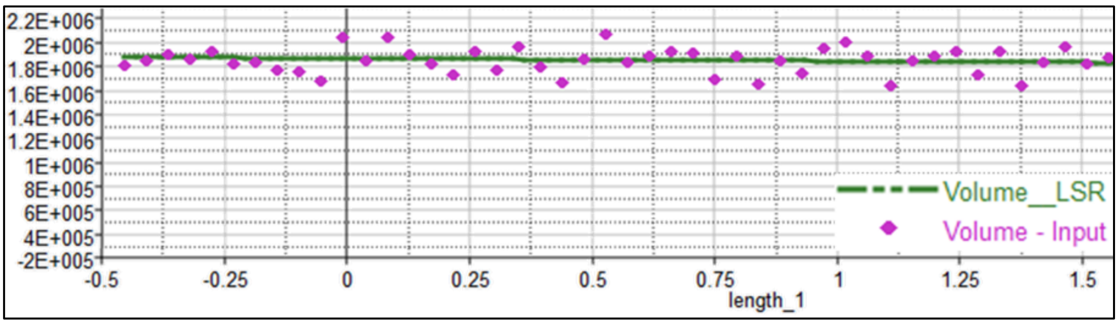

Figure 50: Example of surface created by LSR Fit method – Side view

For the results of the 7 OMS in HOS1 and HOS2, the LSR of the 3rd order (i.e. full cubic) is created, as it was observed that the trend had a slight non-linear bias. This is the maximum order for the current number of sample data points. The polynomials of the 4th or a higher order will require more samples than the current number of models. Furthermore, the 4th or higher order will usually not provide more accurate responses in most cases (Jin, Chen and Simpson, 2001).

Therefore, the framework of this chapter contains two major sections. The two sections will analyse the results of the 7 OMS in HOS1 and HOS2 respectively using a response surface method. Moreover, each section contains four subsections which will analyse the ICE, ABC and INC results and summarise the subsection respectively.

6.1 DOE – HOS1

In this section, the response surface will be created by the LSR method for each of the 7 OMS based on the ICE, ABC and INC results. The response surfaces will be assessed to find out the best response surface for the specific OMS with the smallest deviation, i.e. the tightest to the response data points. This will be done by investigating the percentage errors of 'Residual' and the R-Squares of the 'Diagnostics' for each of the 7 OMS. The most influential parameters for each of the 7 OMS will then be analysed based on the ANOVA. The ANOVA is a method to rank the influential parameters (Christensen and Bastien, 2016). The influential parameters obtained using this new method will be compared with those defined in section 4.7 through HOS1-9 and HOS1-10. The first subsection will study the results of the 7 OMS based on the ICE method.

6.1.1 Fit model based on ICE results – HOS1

As defined previously in chapter 4 and chapter 5, each of the 7 OMS contains 203 models. Therefore, each response surface created by the LSR method will also contain 203 predicted points. The deviations between the original 203 results and the corresponding predicted points are Residuals for which a percentage error can be calculated. In order to evaluate the fit quality of each response surface, the percent errors are processed based on the following aspects:

- Average percent error, the average value calculated based on the overall percent errors of each of the 7 OMS.
- Max-Positive percent error, the maximum percent error occurs between the surface and the original result above it.
- Max-Negative percent error, the maximum percent error occurs between the surface and the original result under it.

- Max-Spread, the difference between the Max-Positive percent error and Max-Negative percent error.

Based on the requirements listed above, the percent errors of the 7 OMS are processed in Table 96. From Table 96, the average percent errors of the 7 OMS are nearly the same, and the differences can be considered negligible. This indicates that the 7 response surfaces have the similar 'tightness' based on the average percent errors. However, from the Max-Positive and Max-Negative percent errors, it is found that the surface and the original result in SEQ2-MII have the largest deviation; while the PAR-MII has the smallest deviation. This is also evidenced by the values of the Max-Spread where PAR-MII has the smallest spread 2.43% and the SEQ2-MII has the largest spread 16.24%. This may indicate that the predicted points of the response surface for PAR-MII are closer to the original results. It is suggested that the PAR-MII has a tighter response surface than all other OMS. In order to see what the best and worst response surfaces look like, the response surfaces of SEQ2-MII and PAR-MII are created as illustrated in Figure 51.

Table 96: Processed percent errors of the 7 OMS – ICE – HOS1

Percent Error (%)	SEQ1-MII	SEQ2-MII	SEQ3-MII	SEQ4-MII	SEQ5-MII	SEQ6-MII	PAR-MII
Average	0.00	0.02	0.00	0.01	0.00	0.01	0.00
Max-Positive	1.42	4.27	1.75	2.67	3.02	4.24	1.43
Max-Negative	-2.55	-12.06	-0.85	-2.50	-2.14	-2.50	-1.00
Max-Spread	3.97	16.34	2.59	5.17	5.16	6.74	2.43

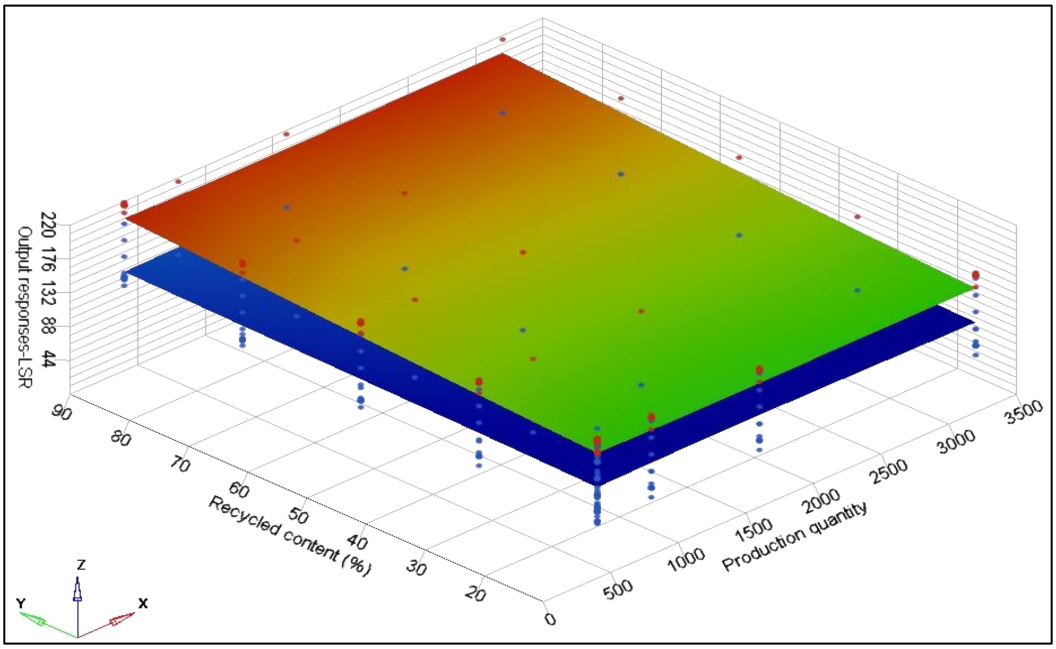

Figure 51: Response surface of SEQ2-MII and PAR-MII – ICE – HOS1

In order to obtain a clearer review of the tightness of the two surfaces, a side view of the response surfaces is created in Figure 52. From Figure 52, it is clear to see that the red points around the response surface of SEQ2-MII have larger deviations than the purple points around the response surface of PAR-MII.

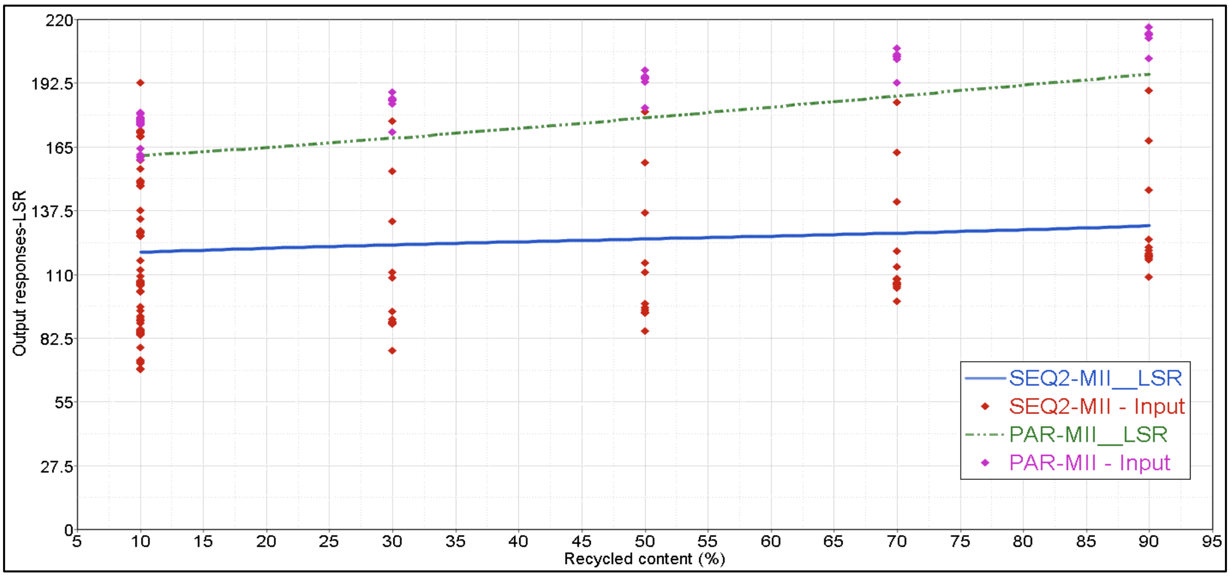

Figure 52: Side of the response surfaces (Y-Z plane) – ICE – HOS1

To further assess the accuracy of the LSR Fit for each of the 7 OMS, the R-Square values of each of the 7 OMS are investigated. The R-Square is used to measure the fit quality of the response surface. A perfect fit is achieved when R-Square equals to 1. However, good quality of the fit will not be able to reach 1 in practice. The Fit quality is categorised into four levels based on the range of the R-Square values (Jin, Chen and Simpson, 2001; HyperStudy, 2017):

- Perfect quality, R-Square = 1.
- Good quality, 0.92 < R-Square < 1
- Normal quality, 0.7 < R-Square < 0.92
- Bad quality, R-Square < 0.7

To assess the fit quality of the 7 response surfaces, the R-Square values of the 7 OMS are summarised in Table 97. According to Table 97, it can be observed that the R-Square values of each of the 7 OMS are all larger than 0.92, indicating that the fit quality of the 7 response surfaces are good to use and accurate

Table 97: R-Square values of the 7 OMS – ICE – HOS1

OMS names	SEQ1-MII	SEQ2-MII	SEQ3-MII	SEQ4-MII	SEQ5-MII	SEQ6-MII	PAR-MII
R-Square	0.995	0.998	0.991	0.997	0.937	0.997	0.997

As each of the 7 OMS has a good response surface, the next step is to investigate the influential parameter(s) for each of the 7 OMS based on the Mean Squares Percent (MSP) of the ANOVA. The MSP is used to assess whether a variable/ parameter is influential to the output responses (Kutner, 2005; Montgomery, 2009). A higher value of the MSP represents the specific parameter(s) is/ are more influential. The MSPs of each of the 7 OMS are ranked in descending order, for convenience, only the top three ranked MSPs and the corresponding parameters are tabulated in Table 98.

Table 98: Top ranked influential parameters for the 7 OMS – DOE – ICE – HOS1

Rank		1	2	3
SEQ1-MII	**Variables**	Recycled content (%), Maximum component CO_2 (kg/unit)	Geometry, Recycled content (%)	Geometry, Maximum component CO_2 (kg/unit)
	MSP	34.9	14.7	10.9
SEQ2-MII	**Variables**	Recycled content (%), Maximum component cost (GBP/unit)	Geometry, Recycled content (%)	Recycled content (%), Maximum component CO_2 (kg/unit)
	MSP	49.8	11.8	8.4
SEQ3-MII	**Variables**	Maximum component cost (GBP/unit), Maximum component CO_2 (kg/unit)	Recycled content (%), Maximum component cost (GBP/unit)	Production quantity
	MSP	15.3	10.4	9.2
SEQ4-MII	**Variables**	Maximum component cost (GBP/unit), Maximum component CO_2 (kg/unit)	Maximum component cost (GBP/unit)	Production quantity
	MSP	82.1	6.4	1.3
SEQ5-MII	**Variables**	Recycled content (%)	Recycled content (%), Maximum component cost (GBP/unit)	Recycled content (%), Maximum component CO_2 (kg/unit)
	MSP	35.8	28.6	17.6
SEQ6-MII	**Variables**	Production quantity	Maximum component cost (GBP/unit)	Geometry, Recycled content (%)
	MSP	14.5	13.7	8.7
PAR-MII	**Variables**	Geometry, Recycled content (%)	Geometry	Production quantity
	MSP	36.5	19.7	7.6

Based on Table 98, it is observed that the most influential parameters (ranked 1st) of each OMS are different apart from SEQ3-MII and SEQ4-MII. Although SEQ3-MII and SEQ4-MII have the same most influential parameters, the MSP values of the two OMS are significantly different, i.e. 66.8%. This indicates that different OMS demonstrate different sensitivity even they have the same influential parameters. Another trend obtained from Table 98 is that all of the top-ranked parameters do not contain the travel distance, labour cost and overhead cost. This indicates that the ICE results of the 7 OMS are less/ not sensitive to those three parameters. In order to further study the influential parameters of the 7 OMS with LSR method, the ABC results are investigated in the next subsection.

6.1.2 Fit model based on ABC results – HOS1

As demonstrated in subsection 6.1.1, the method to determine the fit quality of the response surfaces for the 7 OMS is to assess the R-Square value. Therefore, the R-Square values of the 7 OMS are summarised in Table 99. As defined in subsection 6.1.1, the fit quality is good if the R-Square value is between 0.92 and 1. Based on the R-Square values of the 7 OMS in Table 99, it shows that the 7 response surfaces have good fit quality.

Table 99: R-Square values of the 7 OMS – ABC – HOS1

OMS names	SEQ1-MII	SEQ2-MII	SEQ3-MII	SEQ4-MII	SEQ5-MII	SEQ6-MII	PAR-MII
R-Square	0.9989	0.9958	0.9981	0.9999	0.9377	0.9999	0.9998

To investigate the influential parameters of the 7 OMS based on the ABC results, the MSPs of each of the 7 OMS are ranked in descending order and tabulated in Table 100 with the same format as Table 98.

Table 100: Top ranked influential parameters for the 7 OMS – DOE – ABC – HOS1

Rank		1	2	3
SEQ1-MII	**Variables**	Geometry, Maximum component CO_2 (kg/unit)	Geometry, Recycled content (%)	Maximum component CO_2 (kg/unit), Travel Distance
	MSP	27.6	16.4	8.7
SEQ2-MII	**Variables**	Recycled content (%), Maximum component cost (GBP/unit)	Recycled content (%), Maximum component CO_2 (kg/unit)	Recycled content (%)
	MSP	73.2	3.9	3.8
SEQ3-MII	**Variables**	Geometry, Maximum component CO_2 (kg/unit)	Maximum component cost (GBP/unit), Maximum component CO_2 (kg/unit)	Maximum component cost (GBP/unit)
	MSP	37.1	22.3	12.7
SEQ4-MII	**Variables**	Geometry, Recycled content (%)	Recycled content (%)	Geometry
	MSP	54.4	37.1	2.9
SEQ5-MII	**Variables**	Recycled content (%)	Recycled content (%), Maximum component cost (GBP/unit)	Recycled content (%), Maximum component CO_2 (kg/unit)
	MSP	33.1	31.5	17.9
SEQ6-MII	**Variables**	Geometry, Recycled content (%)	Geometry	Recycled content (%)
	MSP	87.4	4.8	3.9
PAR-MII	**Variables**	Recycled content (%)	Geometry, Recycled content (%)	Geometry
	MSP	46.4	41.5	8.1

By observing Table 100, it is observed that different OMS demonstrate different sensitivity even they have the same influential parameters. This is evidenced by SEQ4-MII (MSP = 54.4%) and SEQ6-MII (MSP = 87.4%). In Table 100, it is also found that the production quantity is no longer top ranked. This may indicate that the ABC results of the 7 OMS are not sensitive to the production quantity. Moreover, the ABC results of the 7 OMS are not sensitive to the travel distance, labour cost and overhead cost as well. The similar method for the ABC results of the 7 OMS will be applied to the INC results of the 7 OMS in the next subsection.

6.1.3 Fit model based on INC results – HOS1

Analogue to subsection 6.1.1, the Fit quality of the response surfaces for the 7 OMS will be assessed by the R-Square values. The R-Square values of each of the 7 OMS are tabulated in Table 101.

Table 101: R-Square values of the 7 OMS – INC – HOS1

OMS names	SEQ1-MII	SEQ2-MII	SEQ3-MII	SEQ4-MII	SEQ5-MII	SEQ6-MII	PAR-MII
R-Square	0.9884	0.9885	0.9875	0.9990	0.9563	0.9981	0.9961

According to the R-Square values tabulated in Table 101, the 7 response surfaces of the 7 OMS have a good Fit quality, i.e. R-Square > 0.92. In order to investigate the influential parameters of the 7 OMS based on the INC results, the MSPs of each of the 7 OMS are ranked in descending order. Only the top three ranked parameters are tabulated in Table 102.

Table 102: Top ranked influential parameters for the 7 OMS – DOE – INC – HOS1

Rank		1	2	3
SEQ1-MII	**Variables**	Recycled content (%), Maximum component CO_2 (kg/unit)	Geometry, Recycled content (%)	Geometry, Maximum component cost (GBP/unit)
	MSP	21.3	11.9	6.9
SEQ2-MII	**Variables**	Recycled content (%), Maximum component cost (GBP/unit)	Geometry, Recycled content (%)	Recycled content (%)
	MSP	38.2	38.0	5.8
SEQ3-MII	**Variables**	Maximum component cost (GBP/unit), Maximum component CO_2 (kg/unit)	Recycled content (%), Maximum component CO_2 (kg/unit)	Recycled content (%), Maximum component cost (GBP/unit)
	MSP	13.8	10.7	10.0
SEQ4-MII	**Variables**	Maximum component cost (GBP/unit), Maximum component CO_2 (kg/unit)	Geometry, Recycled content (%)	Geometry
	MSP	59.3	17.8	6.5
SEQ5-MII	**Variables**	Recycled content (%)	Recycled content (%), Maximum component cost (GBP/unit)	Recycled content (%), Maximum component CO_2 (kg/unit)
	MSP	35.8	27.0	18.6
SEQ6-MII	**Variables**	Geometry, Recycled content (%)	Geometry	Recycled content (%)
	MSP	43.6	14.1	5.1
PAR-MII	**Variables**	Geometry	Recycled content (%)	Geometry, Recycled content (%)
	MSP	16.8	12.2	9.7

Based on Table 102, it is observed that different OMS demonstrate different sensitivity even they have the same influential parameters. This is evidenced by SEQ3-MII (MSP = 13.8%) and SEQ4-MII (MSP = 59.3%). In Table 102, it is also found that the INC results of the 7 OMS are not sensitive to the production quantity, travel distance, labour cost and overhead cost.

6.1.4 Summary of DOE – HOS1

In this section, the response surface method based on a DOE sampling technique was applied to the 7 OMS in order to investigate the influential parameters. The response surfaces of the 7 OMS were accurately created. After assessing the MSPs of each of the 7 OMS, the influential parameters of the 7 OMS can be ranked according to the level of influence. It is however observed that the most influential parameters for each of the 7 OMS differs according to the evaluation method used (i.e. ICE. ABC, INC). It is therefore difficult to identify the 'level of influence' of individual parameters consistently. The reason could be that the DOE analyses the sensitivity from another point of view, i.e. different from OAT and TAT in nature. On the other hand, the top three ranking parameters for all 7 OMS were:

- Geometry
- Recycled content

- Maximum component cost

The parameters listed above were the top three influential parameters across all three evaluation methods. The individual parameters' ranking inside the 'top three' were however not consistent across OMS and evaluation methods used. For each of the 7 OMS, those common influential parameters are geometry, Maximum component cost, Maximum component CO_2 and recycled content. The influential parameters in this section are the same as those summarised in section 4.7 through HOS1-9 to HOS1-11. This indicates that the influential parameters discovered by the DOE method concur with the influential parameters defined by 1-2 at a time method, i.e. OAT and TAT. To further assess the DOE method for analysing the influential parameters of the 7 OMS, the DOE method will be applied to the 7 OMS of HOS2 in the next section.

6.2 DOE – HOS2

The same method used for the HOS1 in section 6.1 will be applied to the results of the 7 OMS for HOS2 in this section. The response surface will be created by the LSR method for each of the 7 OMS according to the ICE, ABC and INC results. The fit quality of each response surface will be assessed with the R-Square values. If the fit quality of each response surface is good to use, then the Mean Square Percent (MSP) will be further used to investigate the most influential parameters of each of the 7 OMS. The results based on ICE, ABC and INC will be studied in three subsections respectively. This section only contains the analysis for ICE results (HOS2), the analysis for ABC and INC results can be found in Appendix – G. The general trends of each of those three analyses will then be compared and summarised in the final subsection of section 6.2.

6.2.1 Fit model based on ICE results – HOS2

As defined in section 6.1, each response surface created by the LSR method contains 203 predicted points. The deviation between the predicted points and the corresponding original sample results demonstrates how good the fit quality is, i.e. the smaller deviation, the better. The R-Square values of the 7 surfaces for the 7 OMS are summarised in Table 103. According to Table 103, all 7 R-Square values are lower than the corresponding values in Table 97. This indicates that the response surfaces based on ICE results of the 7 OMS for HOS1 have better Fit quality than the response surfaces for HOS2.

Table 103: R-Square values of the 7 OMS – ICE – HOS2

OMS names	SEQ1-MII	SEQ2-MII	SEQ3-MII	SEQ4-MII	SEQ5-MII	SEQ6-MII	PAR-MII
R-Square	0.8156	0.8337	0.7434	0.7296	0.8079	0.7454	0.8076

To investigate the influential parameters of the 7 OMS based on the ICE results, the MSP values of each of the 7 OMS are ranked in descending order, for convenience; the corresponding parameters are also included.

Table 104: Top ranked influential parameters for the 7 OMS – DOE – ICE – HOS2

Rank		1	2	3
SEQ1-MII	Variables	Production quantity	Recycled content (%)	Maximum component cost (GBP/unit)
	MSP	17.8	8.8	7.3
SEQ2-MII	Variables	Production quantity	Maximum component cost (GBP/unit)	Recycled content (%)
	MSP	17.4	7.2	5.8
SEQ3-MII	Variables	Production quantity	Recycled content (%)	Maximum component cost (GBP/unit)
	MSP	17.1	8.2	7.0
SEQ4-MII	Variables	Production quantity	Recycled content (%)	Maximum component cost (GBP/unit)
	MSP	18.0	7.8	7.4
SEQ5-MII	Variables	Production quantity	Recycled content (%)	Maximum component cost (GBP/unit)
	MSP	17.2	8.7	7.1
SEQ6-MII	Variables	Production quantity	Maximum component cost (GBP/unit)	Recycled content (%)
	MSP	17.4	7.2	6.4
PAR-MII	Variables	Production quantity	Recycled content (%)	Maximum component cost (GBP/unit)
	MSP	17.1	9.9	7.1

It is observed from Table 104 that the most influential parameters of the 7 OMS are the production quantity. Furthermore, the ICE results of the 7 OMS have nearly the same MSP values. This indicates that the results of the 7 OMS have the similar sensitivity to the change of production quantity. Another trend observed from Table 104 is the top three influential parameters of the 7 OMS are same, i.e. production quantity, recycled content and Maximum component cost. To investigate the influential parameters of the 7 OMS, the similar method is applied to the ABC and INC results in the Appendix – G.

6.2.2 Summary of DOE – HOS2

The DOE method was applied to the 7 OMS to investigate the influential parameters. The response surfaces for the 7 OMS were created with a feasible quality which is not as accurate as the fit quality obtained in HOS1 section 6.1. After assessing the MSP values of each of the 7 OMS it is found that the 'ranking' of parameter influence for the 7 OMS are identical across ICE and ABC results. This is not the case when using the INC evaluation method; although similarities do exist. Specifically, it can be seen that the most influential parameters across all 7OMS and 3 evaluation methods always include input Maximum component CO_2, production quantity and maximum component cost. By comparing this parameter ranking to those determined in subsection 5.6 through HOS2-6 and HOS2-7, it is found that only one of the influential parameters is the same, namely: geometry. One of the potential reasons could be that the DOE method is the 'extension' of the OAT and TAT. In this case, the DOE method analysed more possible combinations of the input parameters, i.e. 3 parameters at a time. This means the sensitivity analysis was implemented based on a larger amount of data which give more possibilities for parameters to show their influence. The second reason is simply that the DOE is different from OAT and TAT in nature.

6.3 Application of DOE for Holistic Optimisation Study

The Design of Experiments (DOE) was utilised in section 6.1 and section 6.2 to analyse all parameters at a time for the 7 Optimisation Module Sequences (OMS) in each Holistic Optimisation Study (HOS). Fit models based on the Least Square Regression (LSR) method were created for each of the 7 OMS. In this section, Fit models are used to optimise the components of the two HOS respectively.

The optimisation in this section will be conducted in a significantly different way to the ones completed in chapters 4 and 5. In HOS1 and HOS2 the optimisation results were generated using the 7 OMS separately. In this section DOE will be used to optimise two given scenarios for all 7 OMS simultaneously. Although this approach may seem controversial it can be used to 'reveal' the best optimisation 'compromise' across all 7 OMS.

Subsequently, the DOE based optimum solutions will be compared to the optimum solutions obtained from the holistic optimisation tool defined in chapter 3.

The results obtained so far have clearly indicated that the OMS is important and yields a significant variation in optimisation results, but these have been based on varying one or two parameters at a time: OAT and TAT. The metamodels created in this chapter enable further studies of the OMS influence by varying all parameters simultaneously (AAT) and can therefore be used to further analyse the importance of OMS. If the OMS is of 'low influence' then optimising for all 7 OMS simultaneously (using DOE) should provide a single solution which also optimises the individual OMS. By subsequently inserting this single solution into the individual holistic OMS tool (and completing optimisation runs) will reveal if the DOE based solution is indeed the optimum solution. If the holistic optimisation results show little difference to the DOE based results (for all 7 OMS) it is an indication that the OMS is of little influence, whereas 'significant' differences in results will indicate a high level of OMS influence.

6.3.1 DOE/ Fit model-based optimisation

The purpose of using the DOE based optimisation is to find the best 'compromise' across all 7 OMS by varying all parameters at a time.

The initial idea is to determine the best OMS for one of the input parameters. Using geometry as an example, for each of three input geometry which OMS is the best one? Before making any action to answer this question, the definition of the geometry parameter needs to be reiterated. The geometry parameter in HOS1 and HOS2 represents three changes of the internal design for each corresponding component. For HOS1, the internal design represents the dimensions of the cross-section of a side impact beam as defined in section 4.1. For HOS2, the internal design represents the size of the bottom curve and extra holes of a lower engine mount as defined in section 5.1. It should be noted that the slight change of the internal design does not change the 'original identity' of the components, i.e. a side impact beam and a lower engine mount. Now to answer the question above, a basic setup of the DOE based optimisation is illustrated in Table 105.

Table 105: The basic setup of the DOE based optimisation for the geometry

Input Parameters	**Optimiser**	**Fit models**	**Objectives**
Geometry	Multi-objective genetic algorithm	Based on ICE results	Maximising
Production Quantity			
Recycled Content (%)		Based on ABC results	Minimising
Maximum component cost (GBP/unit)			
Maximum component CO_2 (kg/unit)		Based on INC results	Maximising
Travel Distance (km)			
Labour Cost (GBP/hr)			
Overhead cost (GBP/MJ)			

As defined in Table 105, the DOE based optimisation is applied to the Fit models of the 7 OMS based on the three evaluation methods. The optimiser for the DOE based optimisation is the Multi-Objective Genetic Algorithm (MOGA) method. This optimisation method is the extension of the Genetic Algorithm (GA) as introduced in subsection 2.2.3. The MOGA mainly focus on the Multi-Objective Optimisation Problems (MOOP) where there are at least two objective functions to be optimised. Moreover, it is the only available optimiser for Fit models within HyperStudy. For this initial DOE based optimisation, the aim is to determine the best OMS for each of the three input geometries. Therefore, there will be three DOE based optimisations with fixed input geometry for each HOS. Furthermore, the optimum solutions of each DOE based optimisation are evaluated by the three evaluation methods: ICE, ABC and INC. After completing the DOE based optimisations in HyperStudy, the evaluated optimum solutions are assessed in the next two subsubsections.

6.3.1.1 DOE based optimisation with fixed geometry – HOS1

The DOE based optimum solutions of the 7 OMS based on the three evaluation methods for each input geometry are summarised and ranked in Table 106.

Table 106: Ranked DOE-based optimum solutions for all 7 OMS (Geometry fixed) – HOS1

Input Parameter	Rank	OMS	DOE based optimum solutions ICE	OMS	DOE based optimum solutions ABC	OMS	DOE based optimum solutions INC
Geometry 1	1	SEQ5-MII	159%	SEQ5-MII	0.1	SEQ5-MII	1.35
	2	PAR-MII	150%	SEQ1-MII	0.2	SEQ6-MII	1.31
	3	SEQ1-MII	140%	SEQ3-MII	0.2	SEQ1-MII	1.3
	4	SEQ3-MII	138%	SEQ6-MII	0.4	SEQ3-MII	1.29
	5	SEQ4-MII	118%	PAR-MII	0.4	PAR-MII	1.23
	6	SEQ6-MII	114%	SEQ4-MII	0.5	SEQ4-MII	1.19
	7	SEQ2-MII	57%	SEQ2-MII	0.9	SEQ2-MII	1.09
Geometry 2	1	SEQ5-MII	183%	SEQ5-MII	0.056	SEQ5-MII	1.3
	2	PAR-MII	167%	SEQ1-MII	0.062	PAR-MII	1.28
	3	SEQ3-MII	165%	SEQ2-MII	0.067	SEQ3-MII	1.24
	4	SEQ1-MII	156%	SEQ3-MII	0.092	SEQ1-MII	1.2
	5	SEQ4-MII	130%	PAR-MII	0.302	SEQ6-MII	1.02
	6	SEQ6-MII	126%	SEQ6-MII	0.425	SEQ4-MII	0.95
	7	SEQ2-MII	85%	SEQ4-MII	0.437	SEQ2-MII	0.74
Geometry 3	1	SEQ5-MII	191%	SEQ5-MII	0.08	SEQ5-MII	1.48
	2	SEQ1-MII	181%	SEQ2-MII	0.1	SEQ1-MII	1.47
	3	SEQ3-MII	157%	SEQ1-MII	0.3	SEQ6-MII	1.46
	4	PAR-MII	156%	SEQ3-MII	0.4	SEQ4-MII	1.37
	5	SEQ2-MII	135%	PAR-MII	0.4	SEQ3-MII	1.36
	6	SEQ4-MII	131%	SEQ6-MII	0.5	PAR-MII	1.28
	7	SEQ6-MII	113%	SEQ4-MII	0.6	SEQ2-MII	1.04

The DOE based optimum solutions are ranked according to the 'Objectives' defined in Table 105. For ICE and INC method, the DOE based optimum solutions are ranked in descending order; while for ABC method, the DOE based optimum solutions are ranked in ascending order. By observing Table 106, it is found that SEQ5-MII is the best OMS across all three input geometries and evaluation methods as it is consistently ranked first. For each of the three geometries, the difference between ranking 1st and 7th based on each evaluation method is significant:

- Geometry 1, difference based on ICE method is about 179%; 800% for ABC and 24% for INC.
- Geometry 2, 115% for ICE, 680% for ABC and 76% for INC.
- Geometry 3, 69% for ICE, 650% for ABC and 42% for INC.

This indicates the OMS is important and yields a significant variation in optimum results. It is also observed in Table 106 that as the input geometry changes, the optimum solutions for the 7 OMS based on three evaluation methods are varied. For instance, based on ICE method, the DOE based optimum solution of SEQ5-MII has 20% difference between Geometry 1 and Geometry 3. Based on ABC method, the difference of DOE based optimum solutions for SEQ5-MII between Geometry 1 and Geometry 2 are even larger, i.e. 79%. This indicates that a certain change of the geometry can give different 'levels' of influence on the optimum solutions based on different evaluation methods. Another trend observed in Table 106 is that the SEQ5-MII is always the best OMS regardless of the change of the geometry. However, this trend could be a coincidence for this specific case. More input geometries could be used for future studies to verify this trend. To determine the best OMS for each of the three geometries in HOS2, the DOE based optimum solutions of the 7 OMS based on the three evaluation methods will be assessed in the next subsubsection.

6.3.1.2 DOE based optimisation with fixed geometry – HOS2

The DOE based optimum solutions of the 7 OMS based on the three evaluation methods for each input geometry are summarised and ranked in Table 107.

Table 107: Ranked DOE-based optimum solutions for the 7 OMS (Geometry fixed) – HOS2

Input Parameter	Rank	OMS	DOE based optimum solutions - ICE	OMS	DOE based optimum solutions - ABC	OMS	DOE based optimum solutions - INC
Geometry 1	1	SEQ3-MII	405%	SEQ3-MII	0.40	SEQ3-MII	1.37
	2	PAR-MII	399%	PAR-MII	0.46	SEQ4-MII	1.28
	3	SEQ1-MII	392%	SEQ5-MII	0.47	SEQ5-MII	1.26
	4	SEQ5-MII	383%	SEQ4-MII	0.47	SEQ6-MII	1.26
	5	SEQ4-MII	382%	SEQ6-MII	0.48	SEQ1-MII	1.25
	6	SEQ6-MII	355%	SEQ1-MII	0.57	PAR-MII	1.23
	7	SEQ2-MII	355%	SEQ2-MII	0.60	SEQ2-MII	1.23
Geometry 2	1	SEQ3-MII	443%	SEQ3-MII	0.45	SEQ3-MII	1.00
	2	PAR-MII	427%	SEQ4-MII	0.49	SEQ4-MII	0.99
	3	SEQ4-MII	423%	SEQ6-MII	0.50	SEQ1-MII	0.97
	4	SEQ5-MII	415%	SEQ5-MII	0.55	SEQ6-MII	0.97
	5	SEQ1-MII	411%	PAR-MII	0.55	SEQ5-MII	0.95
	6	SEQ6-MII	389%	SEQ2-MII	0.72	PAR-MII	0.95
	7	SEQ2-MII	383%	SEQ1-MII	0.73	SEQ2-MII	0.93
Geometry 3	1	SEQ3-MII	541%	SEQ4-MII	1.29	SEQ1-MII	2.70
	2	SEQ4-MII	528%	SEQ6-MII	1.34	SEQ2-MII	2.49
	3	PAR-MII	511%	SEQ3-MII	1.43	SEQ5-MII	2.00
	4	SEQ5-MII	505%	SEQ5-MII	1.43	PAR-MII	1.98
	5	SEQ1-MII	476%	PAR-MII	1.46	SEQ4-MII	1.93
	6	SEQ6-MII	473%	SEQ1-MII	1.50	SEQ6-MII	1.84
	7	SEQ2-MII	469%	SEQ2-MII	1.53	SEQ3-MII	1.58

The DOE based optimum solutions are ranked according to the 'Objectives' defined in Table 105. For ICE and INC method, the DOE based optimum solutions are ranked in descending order; while for ABC method, the DOE based optimum solutions are ranked in ascending order. According to Table 107, it is observed that the SEQ3-MII is the best OMS across the Geometry 1 and Geometry 2 based on the three evaluation methods. However, the best OMS for Geometry 3 cannot be found directly based on the ranking. A method could be used to determine the best OMS for Geometry 3 is to calculate the average ranking for each OMS across all three evaluation methods. The method is further demonstrated in Table 108.

Table 108: Rankings of the 7 OMS based on evaluation methods for Geometry 3 – HOS2

OMS	ICE ranking	ABC ranking	INC ranking	Average rankings
SEQ1-MII	5	6	1	4
SEQ2-MII	7	7	2	5
SEQ3-MII	1	3	7	4
SEQ4-MII	2	1	5	3
SEQ5-MII	4	4	3	4
SEQ6-MII	6	2	6	5
PAR-MII	3	5	4	4

As evidenced in Table 108, the SEQ4-MII outperforms all other OMS as it has the smallest average ranking. Therefore, the SEQ4-MII is suggested to be the best OMS for Geometry 3.

6.3.1.3 Comparison between holistic optimisation programme and DOE based optimisation

In the previous two subsubsections, the DOE based optimisation also proved the importance of the OMS. However, the DOE based optimum solutions were obtained by fixing the geometry but varying other parameters. After all, this is a holistic optimisation. Hence, the DOE based optimisation needs to consider all parameters at a time to change which includes the geometry. In this subsubsection, the 7 OMS for HOS1 as an example, will be optimised by the DOE based optimisation. The aim is to assess whether the DOE based solution is indeed the optimum solution. After completing the DOE based optimisation for all input parameters, the best compromises across all 7 OMS and three evaluation methods for HOS1 are obtained. The DOE based optimum solutions of the 7 OMS using the three evaluation methods are tabulated in Table 109.

Table 109: DOE based optimum solutions across all 7 OMS and evaluation methods – HOS1

OMS names	DOE based Optimum Solution - ICE	DOE based Optimum Solution - ABC	DOE based Optimum Solution - INC
SEQ1-MII	123%	0.30	1.03
SEQ2-MII	44%	0.93	1.02
SEQ3-MII	116%	0.23	1.10
SEQ4-MII	106%	0.35	0.83
SEQ5-MII	146%	0.27	1.03
SEQ6-MII	82%	0.30	0.94
PAR-MII	117%	0.25	1.22

In Table 109, for each evaluation method, a single solution is provided by optimising all 7 OMS simultaneously using DOE method. This single solution consists of a set of input parameters. To compare the DOE based optimum solutions of the 7 OMS to the optimum solutions obtained by the individual holistic OMS tool defined in chapter 3, the single solution based on each evaluation method is needed. The input parameters for each single solution which produced the best compromise across all 7 OMS using the three evaluation methods are tabulated in Table 110.

Table 110: Parameters for the best compromises based on the three evaluation methods

Parameters	Values/ Index – ICE – HOS1	Values/ Index – ABC – HOS1	Values/ Index – INC – HOS1
Geometry	1	1	1
Production Quantity	400	3200	400
Recycled Content (%)	70	30	90
Max cost (GBP/unit)	2	10	6
Max CO2 (kg/unit)	1.5	1.5	1
Travel Distance	-1	1	1
Labour Cost (GBP/hr)	-1	-1	1
Overhead cost (GBP/MJ)	1	-1	-1

Within the DOE based optimisation, the value of each parameter in Table 110 has different meanings:

- The geometry uses 1, 2 and 3 as the index to represent the change of the geometry as defined previously in this subsection.
- The production quantity, recycled content, Maximum component cost and Maximum component CO_2 use the actual values as defined in subsection 3.5.1.
- The travel distance uses -1, 0 and 1 to represent the short, medium and long distance.
- The labour cost and overhead cost use -1, 0 and 1 to represent the lowest, medium and the highest cost.

The input parameters in Table 110 are inserted into the individual holistic OMS tool to generate the 'theoretical' optimum solutions. The generated optimum solutions are tabulated in Table 111 along with the DOE based optimum solutions and the average, maximum and minimum change of objective function values (COFV) defined in subsections 4.3, 4.4 and 4.5.

Table 111: Comparison between all types of optimum solutions – HOS1

Evaluation methods	OMS names	DOE based optimum solutions	Theoretical solutions	Average COFVs	Max COFVs	Min COFVs
ICE	SEQ1-MII	123%	236%	206%	241%	189%
	SEQ2-MII	44%	164%	110%	193%	69%
	SEQ3-MII	116%	236%	211%	242%	200%
	SEQ4-MII	106%	185%	106%	145%	94%
	SEQ5-MII	146%	236%	223%	238%	208%
	SEQ6-MII	82%	185%	108%	147%	96%
	PAR-MII	117%	153%	183%	217%	159%
ABC	SEQ1-MII	0.30	0.06	0.35	0.48	0.005
	SEQ2-MII	0.93	1.04	0.81	1.08	0.213
	SEQ3-MII	0.23	0.29	0.31	0.37	0.010
	SEQ4-MII	0.35	0.83	0.83	1.03	0.235
	SEQ5-MII	0.27	0.26	0.15	0.29	0.014
	SEQ6-MII	0.30	0.81	0.79	1.00	0.090
	PAR-MII	0.25	0.46	0.50	0.77	0.042
INC	SEQ1-MII	1.03	0.15	1.53	1.73	1.41
	SEQ2-MII	1.02	0.56	1.13	1.43	0.96
	SEQ3-MII	1.10	0.14	1.55	1.72	1.45
	SEQ4-MII	0.83	1.12	1.51	1.74	1.18
	SEQ5-MII	1.03	0.10	1.63	1.72	1.51
	SEQ6-MII	0.94	1.10	1.61	1.74	1.30
	PAR-MII	1.22	0.03	1.48	1.70	1.33

From Table 111, the following trends are observed:

- By comparing the DOE based optimum solutions to the theoretical optimum solutions, it is found that the corresponding optimum solutions of each of the 7 OMS are different; although some corresponding optimum solutions based on ABC method are very close. The average differences between the DOE based optimum solutions and the theoretical optimum solutions are significant based on the three evaluation methods: 109% for ICE, 117% for ABC and 906% for INC. This indicates the OMS is of high influence.

By comparing the theoretical optimum solutions with the average, maximum and minimum COFVs, trends are observed from the following aspects:

- For ICE method, most of the theoretical optimum solutions are larger than the corresponding average COFVs but less than the corresponding maximum COFVs. PAR-MII as a special case, its theoretical optimum solution (153%) is even smaller than the corresponding minimum COFV (159%). On the other hand, SEQ6-MII has a larger theoretical optimum solution (185%) than the corresponding maximum COFV (145%).
- For ABC method, the theoretical optimum solutions are close to the corresponding average COFVs but larger than the corresponding minimum COFVs. This indicates that the theoretical optimum solutions are not the best solutions as the optimum solutions based on ABC method are the smaller, the better.
- For INC method, all theoretical optimum solutions are smaller than the corresponding

minimum COFVs. This indicates that the theoretical solutions are not the best solutions as the optimum solution based on INC method is the larger, the better.

The trends listed above indicate the DOE based solutions are not the real optimum solutions. Moreover, the theoretical solutions obtained based on each single solution are also not the optimum solutions. However, the significant differences between holistic optimisation results and DOE based optimisation results indicates the high level of OMS influence. To further investigate whether the DOE based optimum solutions have the same trends as defined in section 4.7 and 5.6, the DOE based optimum solutions of the 7 OMS for HOS1 and HOS2 are ranked subsequently in the following two subsections.

6.3.2 DOE Application – HOS1

The DOE based optimum solutions of the 7 OMS will be investigated based on the ICE, ABC and INC evaluation methods respectively. The general trends will be extracted and compared with the trends found in chapter 4. The DOE based optimum solutions are ranked in a descending order respectively in Table 112.

Table 112: DOE based optimum solutions based on ICE, ABC and INC methods– HOS1

Rank	ICE		ABC		INC	
	OMS	DOE based optimum solution	OMS	DOE based optimum solution	OMS	DOE based optimum solution
1	SEQ5-MII	146%	SEQ3-MII	0.23	PAR-MII	1.22
2	SEQ1-MII	123%	PAR-MII	0.25	SEQ3-MII	1.10
3	PAR-MII	117%	SEQ5-MII	0.27	SEQ5-MII	1.03
4	SEQ3-MII	116%	SEQ1-MII	0.30	SEQ1-MII	1.03
5	SEQ4-MII	106%	SEQ6-MII	0.30	SEQ2-MII	1.02
6	SEQ6-MII	82%	SEQ4-MII	0.35	SEQ6-MII	0.94
7	SEQ2-MII	44%	SEQ2-MII	0.93	SEQ4-MII	0.83
Difference (%) Between Rank 1st and 7th		233%		76%		47%

The DOE based optimum solutions are ranked according to the 'Objectives' defined in Table 105. For ICE and INC method, the DOE based optimum solutions are ranked in descending order; while for ABC method, the DOE based optimum solutions are ranked in ascending order. By observing Table 112, the following General Trends (GT) are found:

DOE-HOS1-GT1. For the three evaluation methods, the 'outperformance' of the 1st ranked OMS is significant as the difference between ranking 1 and ranking 7 is 233% for ICE, 76% for ABC and 47% for INC. It is observed that the "outperformance" of SEQ5-MII illustrated by ICE method is more noticeable. The reason could be that the three evaluation methods are different in nature or the ICE method is more appropriate to analyse the 7 OMS.

DOE-HOS1-GT2. The PAR-MII is top three ranked in ICE, ABC and INC columns. As the difference between PAR-MII and other top three ranked OMS is less noticeable (i.e. 0.02 for ABC and 0.12 for INC), the PAR-MII is considered to be a high-performance OMS but not the best OMS.

DOE-HOS1-GT3. Despite the performance of the PAR-MII, the 6 SEQ optimisation programmes can be categorised into two groups as defined in Table 46 of subsection 4.3.1. This indicates that the SEQ1-MII, SEQ3-MII and SEQ5-MII are consistently outperform the SEQ2-MII, SEQ4-MII and SEQ6-MII. Moreover, this could be explained by the specific optimisation position of the COST module and CO2 module. The always SEQ1-MII, SEQ3-MII and SEQ5-MII optimises the COST module before the CO2 module. The SEQ2-MII, SEQ4-MII and SEQ6-MII always optimise the CO2 module before the COST module.

By comparing the general trends listed above with the trends defined in subsection 4.7, there are some common points. Despite the 'outperformance' of the PAR-MII, SEQ5-MII is suggested to be more stable than all other OMS. This is similar to HOS1-2 in subsection 4.7. The trend, for the 6 SEQ optimisation programmes, as defined in DOE-HOS1-GT3 is also the same as HOS1-3 in subsection 4.7. In order to see how the DOE based optimum solutions performance for the HOS2, the ranked DOE based optimum solutions will be investigated in the next section.

6.3.3 DOE Application – HOS2

Analogue to DOE application in section 6.3.2, the DOE based optimum solutions for the 7 OMS based on the three evaluation methods are ranked in descending order in Table 113.

Table 113: DOE based optimum solutions based on ICE, ABC and INC methods – HOS2

Rank	ICE		ABC		INC	
	OMS	DOE based optimum solution	OMS	DOE based optimum solution	OMS	DOE based optimum solution
1	SEQ3-MII	257%	SEQ3-MII	0.33	SEQ3-MII	1.07
2	PAR-MII	248%	SEQ4-MII	0.38	SEQ5-MII	1.04
3	SEQ5-MII	241%	SEQ6-MII	0.44	SEQ1-MII	1.03
4	SEQ4-MII	235%	PAR-MII	0.50	SEQ4-MII	0.97
5	SEQ1-MII	234%	SEQ5-MII	0.53	PAR-MII	0.94
6	SEQ6-MII	219%	SEQ2-MII	0.79	SEQ2-MII	0.91
7	SEQ2-MII	211%	SEQ1-MII	0.90	SEQ6-MII	0.89
Difference (%) Between Rank 1st and 7th		22%		63%		20%

The DOE based optimum solutions are ranked according to the 'Objectives' defined in Table 105. For ICE and INC method, the DOE based optimum solutions are ranked in descending order; while for ABC method, the DOE based optimum solutions are ranked in ascending order. From Table 113, the following trends are observed:

DOE-HOS2-GT1. The DOE based optimum solution of SEQ3-MII is consistently outperforms all other OMS. It is suggested that SEQ3-MII is more robust than all other OMS.

DOE-HOS2-GT2. The SEQ2-MII is consistently lower-ranked (6^{th} – 7^{th}) though it is not bottom-ranked all the time. This indicates the SEQ2-MII underperforms other OMS.

DOE-HOS2-GT3. For the three evaluation methods, the 'outperformance' is significant for the ABC method as the difference between ranking 1 and ranking 7 is 63% for ABC. However, the "outperformance" for ICE and INC method is not as significant as the ABC method as the difference between ranking 1, and ranking 7 is 22% for the ICE and 20% for the INC. The 'outperformance' of SEQ3-MII illustrated by ABC method is more noticeable. The reason could be the three evaluation methods are different in nature. It may also indicate that the ABC method is more appropriate to analyse the 7 OMS for HOS2.

By comparing the trends listed above with the general trends defined in subsection 5.6, it is found that DOE-HOS2-GT1 and DOE-HOS2-GT2 described the same trends as HOS2-1 and HOS2-2 in subsection 5.6.

Based on the comparison of trends found in this chapter, chapter 4 and chapter 5, it is found that the DOE based optimum solutions have common trends with the optimum solutions obtained by individual holistic OMS tool. This indicates that the DOE application introduced in this chapter also determined the importance and a high-level influence of OMS. Although the DOE based optimisation can provide a single solution for optimising all 7 OMS simultaneously, the DOE based solutions are not considered as the real optimum solutions.

7 Potential Improvements

Through the two Holistic Optimisation Studies (HOSs) completed in this thesis, it is found that both the 7 Optimisation Module Sequences (OMS) and the three evaluation methods are important and yield a significant variation in optimisation results. This was evidenced by the tables in each HOS, e.g. Table 45 indicates that the optimisation results of the 7 OMS based on the same evaluation method has a significant variation of 117%. Within this research, the very basic holistic optimisation tool has been built. For further study, the refinements and more detailed analysis should be added to make the results more feasible and relevant to industrial applications. In the following subsections suggested next step improvements to the three parametric modules will be discussed.

7.1 STRUCTURAL Module

For the STRUCTURAL module there are two aspects which should be improved: the database of template geometries and the structural optimisation capabilities, in order to make the results of the tool more feasible and relevant to industrial applications.

Expansion of template geometries could be as simple as adding, e.g. I-beam cross-sections but should ideally be parameterised in order to cater for any cross-section /geometry.

The current structural optimisation method is size optimisation. Although this is sufficient for some applications, e.g. sheet metal manufacturing (HOS1) it has limited use with other applications, e.g. casting (HOS2). To maximise the usability, flexibility and functionality of the tool additional structural optimisation methods such as shape optimisation and topology optimisation should be added. This improvement will make the tool and results more feasible and relevant to real-world industrial applications.

7.2 COST and CO2 Module

Both COST module and CO2 module have four parts: material, manufacturing, transport and end of life. A "full" life cycle analysis of a component/ product should include the 'in use phase' which for some applications is the highest contributor to the CO_2 footprint. The 'use phase' can, however, be very complicated to determine, and in most (automotive) applications it heavily depends on individual end-user behaviour. The following general points may be considered to calculate the CO_2 footprint and costs of the 'use phase':

1. Lifetime, how long the components/ products are normally used in real life.
2. Location, where the components/ products are going to be used.
3. Frequency, how often the components/ products are used.
4. Category, the type of the components/ products.

The first point is very straightforward. It gives the total time of the usage of components/ products which can be used to calculate the costs or CO_2 during that period. The second point indicates that there are different local consumption levels in the world, i.e. different fuel/ energy costs if the components/ products are transportation types. The third point shows the frequency that can be potentially used to calculate daily /monthly used cost and CO_2. For instance, an automotive product may need to consider how many kilometres per day the vehicle used. For a static product such as a fridge, hours per day may be considered as the frequency of usage. The last point indicates that the components/ products should be categorised into different groups in order to make the calculations easier, e.g. static type, mobile type, high-frequency type, low-frequency type, etc. Those groups can then further spread into more details, e.g. mobile type – automotive – family car – electric. With the points listed above, the improvement in terms of costs/ CO_2 of the 'use phase' could potentially be done. However, the improvement still needs additional calculations and case studies to further verify the corresponding programme.

7.3 Industrial Tool

Once all relevant improvements have been implemented to the three modules of the optimisation tool, the next step is further verification through actual industrial applications. Firstly, the industrial application should be optimised using the holistic optimisation tool to get the theoretical data. Secondly, the optimised industrial application should be manufactured, transported, used and disposal (or another end of life option) to get the practical data. By comparing the practical data with the theoretical data of the optimisation tool to find out the differences, i.e. the difference is significant or minor. After that, an 'improvement – verification' loop should be created. This is the way to move the current 'proof of concept' stage to a useful and usable industry tool. Once the optimisation tool has been verified, it can be applied to many areas: automation (i.e. less labour), the simplicity of calculations (CO_2 footprint and costs), usage guidance of a product (i.e. suggest the frequency of use to reduce potential costs and environmental impact), etc.

The costs of deploying such a tool in a practical context depend on the complexity of the geometry of components/ products. The complex geometry of a component/ product normally consumes more time (i.e. CPU time) and costs (e.g. cost to keep the corresponding equipment running). The benefits of using such a tool could be: optimisation becomes more efficiency, less model setup, etc. Moreover, results of the optimisation tool can be used to manufacture the optimised product. Of course, the tool needs to be applied at a very early stage. For instance, there are three (or maybe more) different designs. All the designs will be manufactured in different locations (i.e. country of production), e.g. cast in Germany, welded in the US or machined in China. The user can search the existed designs in the database or customise the designs by input the corresponding parameters in the optimisation tool. It should be noted that the tool is now updated (i.e. all improvements applied). The tool will then complete the holistic optimisation and extract realistic and highly credible data which can help the user to make an informed decision about which design to choose.

8 Conclusion

The ultimate aim of this research was to create a holistic optimisation tool to obtain the 'ideal' engineering product by determining the optimum 'compromise' between a number of key aspects: material, manufacturing, transportation, costs, CO_2 footprint, end of life, etc. After a critical review and analysis, the potential inputs and outputs of each aspects were summarised. Three parametric modules labelled, COST, CO2 and STRUCTURAL were subsequently programmed based on the above analyses. These three modules formed the basis for the creation of a series of holistic optimisation software programmes / tools obtained by varying the individual Optimisation Module Sequence (OMS) both sequentially and in parallel, leading to a total of 7 (OMS) programmes.

Furthermore, 3 different optimisation evaluation methods labelled ICE, ABC and INC were defined and implemented alongside the 7 OMS leading to a total of 21 optimisation software programmes.

These 21 programmes were subsequently used to complete a total of 231 case studies designed to explore, critically assess and evaluate the influence of the holistic optimisation approach. The case studies focused on two automotive components namely a side impact beam and a lower engine mount. The results yielded the identification of a number of 'local' trends, each of which were uniquely labelled according to the optimisation programme (OMS and optimisation evaluation methods) used in that specific context. Once all case studies were completed the 'local' trends from all 21 programmes were compared, and where appropriate 'combined' into 'global' trends:

According to the global trend HOS1-1 of subsection 4.7, the 7 OMS with Multi-Inner Iterations (OMS-MII) outperforms the corresponding 7 OMS with Single-Inner Iteration (OMS-SII) as the 7 OMS-MII are more robust than the 7 OMS-SII. Moreover, the 7 OMS-MII consume similar CPU time to the 7 OMS-SII. The trend above is not a surprise as, theoretically, an optimisation algorithm with multiple iterations is more likely to obtain a more optimised solution than a single iteration optimisation.

The evaluation results proved that the specific OMS order influences the performance of the sequential (SEQ) optimisation programmes. As stated in HOS1-3 of subsection 4.7, optimising the COST module before the CO2 module benefits the performance of the specific OMS such as SEQ1-MII, SEQ3-MII and SEQ5-MII. For the performance of each parametric module, the STRUCTURAL module has the same performance across all 7 OMS, and it is more stable than the other two modules. It is evidenced by the specific trends observed in each HOS, i.e. HOS1-5 to HOS1-8 of subsection 4.7 and HOS2-3 to HOS2-5 of subsection 5.6. It is also found that the OMS is important and yields a significant variation in optimisation results. This is especially true for SEQ5-MII of Holistic Optimisation Study 1 (HOS1) and SEQ3-MII of Holistic Optimisation Study 2 (HOS2), which were found to be the “best” OMS as they are more stable than all other OMS across the three evaluation methods for both HOS. This is evidenced by HOS1-2 of subsection 4.7 and HOS2-1 of subsection 5.6.

In the first two holistic optimisation studies, HOS1 and HOS2, a maximum of two input parameters were varied for any given model (i.e. OAT and TAT) to find the most influential parameter(s). According to HOS1-9 through HOS1-11 of subsection 4.7 and HOS2-6 through HOS2-7 of subsection 5.6, results of the 7 OMS of HOS1 and HOS2 are more sensitive to the change of two specific input parameters namely: the geometry and the recycled content. The vast majority of structural optimisation tools are heavily influenced by the input geometry, and in this context, it should be noted that the variation of input geometry merely represents “design variations” of a single structure as opposed to two (or more) significantly different structures. The attempt to use a parallel (PAR) approach for holistic optimisation proved to be “less efficient” than the sequential (SEQ) optimisation approach. This was evidenced by HOS1-4 of subsection 4.7 and HOS2-8 of subsection 5.6.

Following the OAT and TAT based holistic optimisation studies (HOS1 and HOS2) a design of experiments (DOE) based holistic optimisation study was completed. This was done in order to evaluate the 21 programmes from a much wider perspective by allowing “all” input parameters to change at a time (AAT). However, it was not a truly AAT perspective as the current number of models (i.e. 203 in total) can only afford a least square regression (LSR) polynomial of the 3rd order, i.e. analyse maximum 3 parameters at a time. Therefore, a suggestion for future study is to increase the number of models to afford a higher polynomial order and to get a true AAT perspective. Although it is not a complete AAT perspective, the DOE based optimisation with Multi-Objective Genetic Algorithm (MOGA) can be still applied to the two HOS to study the OMS influence. After completing the DOE based optimisation for all 7 OMS simultaneously, a solution was obtained. By subsequently inserting the DOE study solution into the 21-holistic optimisation programmes a significant spread in results was found. This substantiates previous findings indicating a high OMS influence upon optimisation results.

In summary, the holistic optimisation methods developed throughout this thesis were found to be powerful tools for optimising automotive engineering products, as they (theoretically) provide the “optimal compromise” between a number of significantly different, and often contradictory product aspects.

The additional scenarios should be explored in order to further explore the trends, recommendations and conclusions drawn in this thesis.

Reference

Aderoba, A. (1997) 'A Generalised Cost-Estimation Model for Job Shops'. *International Journal of Production Economics* 53 (3), 257-263

Afrinaldi,F.,Mat Saman,M.Z. (2008) 'the Evaluation Methods of Disassemblability for Automotive Components – a Review and Agenda for Future Research ' (26), 49-62

Amelia, L., Wahab, D. A., Che Haron, C. H., Muhamad, N., and Azhari, C. H. (2009) 'Initiating Automotive Component Reuse in Malaysia'. *Journal of Cleaner Production* 17 (17), 1572-1579

Amesweb.info, (2015) I-Beam - Sectional Properties Calculator [online] available from <http://www.amesweb.info/SectionalPropertiesTabs/SectionalPropertiesIbeam.aspx> [17 November 2015]

Anon (2006) *ISO 14040:2006 Environmental Management -- Life Cycle Assessment -- Principles and Framework*.: International Organization for Standardization

Ardakani, M., Noorossana, R., Niaki, S., and Lahijanian, H. (2009) Robust Parameter Design using the Weighted Metric method—the Case of 'the Smaller the Better'.: University of Zielona Gora Press

Arora, J. S. (1989) Introduction to Optimum Design. New York ; London: New York ; London : McGraw-Hill

Asadi, E., da Silva, M. G., Antunes, C. H., Dias, L., & Glicksman, L. (2014). Multi-objective optimization for building retrofit: A model using genetic algorithm and artificial neural network and an application. Energy and Buildings, 81, 444-456.

Ashby, M. (2009) 'Materials and the Environment'. *Materials Today* 12 (5), 51

Askar, S. and Tiwari, A. (2009) 'Multi-Objective Optimisation Problems: A Symbolic Algorithm for Performance Measurement of Evolutionary Computing Techniques'. in . ed. by Ehrgott, M., Fonseca, C., Gandibleux, X., Hao, J., and Sevaux, M.: Springer Berlin Heidelberg, 169-182

Balling, R. J., Briggs, R. R., and Gillman, K. (2006) 'Multiple Optimum Size/Shape/Topology Designs for Skeletal Structures using a Genetic Algorithm'. Journal of Structural

Engineering 132 (7), 1158-1165

Baumann, H. and Tillman, A. M. (2004) *The Hitch Hiker's Guide to LCA-an Orientation in Life Cycle Assessment Methodology and Application*. 1:7 edn. Sweden: Holmbergs i Malmo AB

Bendsøe, M. P. (1989) 'Optimal Shape Design as a Material Distribution Problem'. *Strutural and Multidisciplinary Optimization* (4), 193-202

Bendsøe, M. P. (2003) *Topology Optimization: Theory, Methods, and Applications*. Berlin; London: Berlin; London: Springer

Bogue, R. (2007) 'Design for Disassembly: A Critical twenty-first Century Discipline'. *Assembly Automation* 27 (4), 285-289

Bolton, W. (2006) Mechanical Science. 3rd edn. Oxford: Blackwell Pub, p.64.

Brief, P. (2012, July). Quality Function Deployment. Creative Industries Research Institute.

Browne, P. A. (2013) *Topology Optimization of Linear Elastic Structures*. [online] PhD thesis or dissertation: University of Bath

Burger, M., Hackl, B., and Ring, W. (2004) 'Incorporating Topological Derivatives into Level Set Methods'. *Journal of Computational Physics* 194 (1), 344-362

Cantor, B. (2007) *Automotive Engineering: Lightweight, Functional, and Novel Materials*. Boca Raton: Boca Raton: Taylor & Francis

Casado, L. G., Martinez, J. A., & García, I. (2001). Experiments with a new selection criterion in a fast interval optimization algorithm. Journal of Global Optimization, 19(3), 247-264.

Castro-Gutierrez, J. P. (2012) Multi-Objective Tools for the Vehicle Routing Problem with Time Windows.: University of Nottingham

Challis, V. J. (2010) 'A Discrete Level-Set Topology Optimization Code Written in Matlab'. *Structural and Multidisciplinary Optimization* 41 (3), 453-464

Christensen, J., Bastien, C. (2016) Nonlinear Optimization of Vehicle Safety Structures: Modeling of Structures Subjected to Large Deformations.

Cline, R. S. and Shapiro, J. M. (2000) Automobile Door Impact Beam.: Google Patents

Coello, C. A. (2000) 'An Updated Survey of GA-Based Multiobjective Optimization Techniques'. ACM Comput.Surv. 32 (2), 109-143

Coello, C. A. C. (1996) An Empirical Study of Evolutionary Techniques for Multiobjective Optimization in Engineering Design. [online] thesis or dissertation: Tulane University

Cohon, J. L. (2010). Multiobjective programming and planning. 1978. Academic, New York.

Collette, Y. and Siarry, P. (2003) Multiobjective Optimization.: Springer

Corley, H. (1980) 'A New Scalar Equivalence for Pareto Optimization'. Automatic Control, IEEE Transactions on 25 (4), 829-830

Corne, D. W., Knowles, J. D., & Oates, M. J. (2000, September). The Pareto envelope-based selection algorithm for multiobjective optimization. In International Conference on Parallel Problem Solving from Nature (pp. 839-848). Springer, Berlin, Heidelberg.

Court, A.W.,Culley,S.J.,McMahon,C.A., (ed.) (1993) *Ninth International Conference on Engineering Design*. 'The Information Requirements of Engineering Designs'. held August 17-19

Couture, D. (2016). Haversine. [online] Mathyourlife.github.io. Available at: http://mathyourlife.github.io/spouting-jibberish/Haversine/Haversine.html [Accessed 7 Jun. 2016].

Csendes, T. (2001). New subinterval selection criteria for interval global optimization. Journal of Global Optimization, 19(3), 307-327.

Davies, G. (2003) *Materials for Automobile Bodies*. Burlington: Burlington : Elsevier Science

Deb, K. (2000) 'An Efficient Constraint Handling Method for Genetic Algorithms'. Computer Methods in Applied Mechanics and Engineering 186 (2–4), 311-338

Deb, K. (2001). Multi-objective optimization using evolutionary algorithms (Vol. 16). John Wiley & Sons.

Deb, K. (2003) 'Unveiling Innovative Design Principles by Demonstrates of Multiple Conflicting Objectives'. Engineering Optimization 35 (5), 445-470

Deb, K. (2011) 'Multi-Objective Optimisation using Evolutionary Algorithms: An Introduction'. in . ed. by Wang, L., Ng, A. H. C., and Deb, K. : Springer London, 3-34

Deb, K. (2014). Multi-objective optimization. In Search methodologies (pp. 403-449). Springer US.

Deb, K., Agrawal, S., Pratap, A., & Meyarivan, T. (2000, September). A fast elitist non-dominated sorting genetic algorithm for multi-objective optimization: NSGA-II. In International Conference on Parallel Problem Solving From Nature (pp. 849-858). Springer, Berlin, Heidelberg.

Deb, K., Pratap, A., Agarwal, S., & Meyarivan, T. A. M. T. (2002). A fast and elitist multi-objective genetic algorithm: NSGA-II. IEEE transactions on evolutionary computation, 6(2), 182-197.

Deb, K., Thiele, L., Laumanns, M., & Zitzler, E. (2002, May). Scalable multi-objective optimization test problems. In Evolutionary Computation, 2002. CEC'02. Proceedings of the 2002 Congress on (Vol. 1, pp. 825-830). IEEE.

Desai, A. and Mital, A. (2003) 'Evaluation of Disassemblability to Enable Design for Disassembly in Mass Production'. *International Journal of Industrial Ergonomics* 32 (4), 265-281

Desai, A. and Mital, A. (2005) 'Incorporating Work Factors in Design for Disassembly in Product Design'. *Jnl of Manu Tech Mnagmnt* 16 (7), 712-732

Desai, A.,Mital, A. (2003) 'Review of Literature on Disassembly Algorithms and Design for Disassembly Guidelines for Product Design' 10 (3), 244-255

Dodge, Y. (2006) The Oxford Dictionary Of Statistical Terms. 1st edn. Oxford: Oxford University Press

Dowie-Bhamra, T. (2000) 'Design for Disassembly'. *Co-Design the Interdisciplinary Journal of Design and Contextual Studies*

Du, K. L., & Swamy, M. N. S. (2016). Ant colony optimization. In Search and Optimization by Metaheuristics (pp. 191-199). Springer International Publishing.

Dunning, P. (2011) *Introducing Loading Uncertainty in Level Set- Based Structural Topology Optimisation*.

Ec.europa.eu. (2016). Phases 1 and 2 (2005-2012) - European Commission. [online] Available at: http://ec.europa.eu/clima/policies/ets/pre2013/index_en.htm [Accessed 6 Nov. 2016].

Ehrgott, M. (2000) Multicriteria Optimization.: Springer-Verlag Berlin Heidelberg

Ehrgott, M. (2012) Vilfredo Pareto and Multi-Objective Optimization. Bielefeld

Engau, A. and Wiecek, M. (2007) 'Exact Generation of Epsilon-Efficient Solutions in Multiple Objective Programming'. OR Spectrum 29 (2), 335-350

Engau, A. and Wiecek, M. M. (2007) 'Generating Epsilon-Efficient Solutions in Multi-objective Programming'. European Journal of Operational Research 177 (3), 1566-1579

Fang, D., Liu, X., & Chen, W. (2014). Evaluation and Optimization of Two-Echelon Distribution Networks with the Aid of Simulate Anneal Arithmetic and Neighbourhood Search Methods. In ICLEM 2014: System Planning, Supply Chain Management, and Safety (pp. 871-877).

Fonseca, C. M., & Fleming, P. J. (1993, June). Genetic Algorithms for Multiobjective Optimization: Formulation Discussion and Generalization. In Icga (Vol. 93, No. July, pp. 416-423).

FOX, R. L. and SCHMIT, L. A. (1965) 'An Integrated Approach to Structural Synthesis and Analysis'. *AIAA Journal* 3 (6), 1104-1112

Gadd, K. (2011) TRIZ for Engineers : Enabling Inventive Problem Solving [online] . Hoboken, NJ, USA: John Wiley & Sons. available from <http://site.ebrary.com/lib/coventry/docDetail.action?docID=10510618&ppg=1>

Gao, L., Zhou, Y., Li, X., Pan, Q., and Yi, W. (2015) 'Multi-Objective Optimization Based Reverse Strategy with Differential Evolution Algorithm for Constrained Optimization Problems'. Expert Systems with Applications 42 (14), 5976-5987

Gendreau, M., & Potvin, J. Y. (2014). Tabu search. In Search methodologies (pp. 243-263). Springer US.

Gerrard, J. and Kandlikar, M. (2007) 'Is European End-of-Life Vehicle Legislation Living Up to Expectations? Assessing the Impact of the ELV Directive on ‘green’ Innovation and Vehicle Recovery'. *Journal of Cleaner Production* 15 (1), 17-27

Giudice, F. and Fargione, G. (2007) *Disassembly Planning of Mechanical Systems for Service and Recovery: A Genetic Algorithms Based Approach*.: - Springer US

Glover, F. (1989). Tabu search—part I. ORSA Journal on computing, 1(3), 190-206.

Glover, F., & Laguna, M. (2013). Tabu Search∗. In Handbook of Combinatorial Optimization (pp. 3261-3362). Springer New York.

Glover, F., & Taillard, E. (1993). A user's guide to tabu search. Annals of operations research, 41(1), 1-28.

Go, T. F., Wahab, D. A., Rahman, M. N. A., Ramli, R., and Azhari, C. H. (2011) 'Disassemblability of End-of-Life Vehicle: A Critical Review of Evaluation Methods'. *Journal of Cleaner Production* 19 (13), 1536-1546

Goldberg, D. E. and Samtani, M. P. (1986) 'Engineering Optimization Via Genetic Algorithm'. *ASCE Structural Division*, 471-482

Grierson, D. E. and Pak, W. H. (1993) 'Optimal Sizing, Geometrical and Topological Design using a Genetic Algorithm'. *Structural Optimization* 6 (3), 151-159

Groover, M. P., 1939- (2011) *Principles of Modern Manufacturing*. 4th ed., SI version. edn. Hoboken, N.J.: Hoboken, N.J.: John Wiley

Gungor, A. and Gupta, S. M. (1997) 'An Evaluation Methodology for Disassembly Processes'. *Computers & Industrial Engineering* 33 (1–2), 329-332

Gupta, S. M. and McLean, C. R. (1996) 'Disassembly of Products'. *Computers and Industrial Engineering* 31, 225-228

Hajela, P., Lee, E., and Lin, C. -. (1993) 'Genetic Algorithms in Structural Topology Optimization' 227, 117-133

Holistic Optimization (2016) available from <https://adexa.com/wp-content/uploads/2016/05/Holistic-Optimization.pdf> [7 January 2016]

Horn, J., Nafpliotis, N., & Goldberg, D. E. (1994, June). A niched Pareto genetic algorithm for multiobjective optimization. In Evolutionary Computation, 1994. IEEE World Congress on Computational Intelligence., Proceedings of the First IEEE Conference on (pp. 82-87).

Houck, C. R., Joines, J., & Kay, M. G. (1995). A genetic algorithm for function optimization: a

Matlab implementation. Ncsu-ie tr, 95(09).

Hyperstudy (2017) available from <https://altairhyperworks.com/hwhelp/Altair/2017/help/hst/hst.htm?singularities_in_a_fit_matrix.htm> [4 March 2017]

Ilgin, M. A. and Gupta, S. M. (2010) 'Environmentally Conscious Manufacturing and Product Recovery (ECMPRO): A Review of the State of the Art'. *Journal of Environmental Management* 91 (3), 563-591

Jada, R. (2016). WHAT'S IN YOUR NETWORK. [online] Wiyn15.blogspot.co.uk. Available at: http://wiyn15.blogspot.co.uk/ [Accessed 6 Jun. 2016].

Jia, S. J., Yi, J., Yang, G. K., Du, B., and Zhu, J. (2013) 'A Multi-Objective Optimisation Algorithm for the Hot Rolling Batch Scheduling Problem'. International Journal of Production Research 51 (3), 667-681

Jin, R., Chen, W., and Simpson, T. W. (2001) 'Comparative Studies of Metamodelling Techniques Under Multiple Modelling Criteria'. *Structural and Multidisciplinary Optimization* 23 (1), 1-13

Joines, J. A., Gupta, D., Gokce, M. A., King, R. E., & Kay, M. G. (2002, December). Supply chain multi-objective simulation optimization. In Simulation Conference, 2002. Proceedings of the Winter (Vol. 2, pp. 1306-1314). IEEE.

Kirkpatrick, S., Gelatt, C. D., & Vecchi, M. P. (1983). Optimization by simulated annealing. science, 220(4598), 671-680.

Knowles, J. D., & Corne, D. W. (2000). Approximating the nondominated front using the Pareto archived evolution strategy. Evolutionary computation, 8(2), 149-172.

Koffler, C., Krinke, S., Schebek, L., and Buchgeister, J. (2008) 'Volkswagen slimLCI: A Procedure for Streamlined Inventory Modelling within Life Cycle Assessment of Vehicles'. *International Journal of Vehicle Design* 46 (2), 172-188

Kongar, E. and Gupta, S. M. (2006) 'Disassembly Sequencing using Genetic Algorithm'. *International Journal of Advanced Manufacturing Technology* 30 (5), 497-506

Konz, R., J. (2009) 'End-of-Life Vehicle (ELV) Directive: The Road to Responsible Disposal'. *Minnesota Journal of International Law* 18 (2), 431-457

Kroll, E., T.A.Hanft (1998) 'Quantitative Evaluation of Product Disassembly for Recycling' 10 (1), 1-14

Kutner, M. H. (2005) *Applied Linear Statistical Models*. 5th ed., International ed.. edn. Boston, Mass. ; London: Boston, Mass. ; London : McGraw-Hill

Lambert, A. J. D. and Gupta, S. M. (2005) *Disassembly Modeling for Assembly, Maintenance, Reuse, and Recycling*. Boca Raton, FL ; London: Boca Raton, FL ; London : CRC Press

Lee, J. Y. (2010) 'Multi-Objective Optimisation using the Bees Algorithm'

Lee, S.G.,S.W.Lye, M.K.Khoo (2001) 'A Multi-Objective Methodology for Evaluating Product End-of-Life Options and Disassembly' 18 (2), 148-156

Li, S., & Yuncheng, W. (2015). A Modified Cut-Peak Function Method for Global Optimization. In Advances in Global Optimization (pp. 51-56). Springer International Publishing.

Liao, T., Socha, K., de Oca, M. A. M., Stützle, T., & Dorigo, M. (2014). Ant colony optimization for mixed-variable optimization problems. IEEE Transactions on Evolutionary Computation, 18(4), 503-518.

Liao, T., Stützle, T., de Oca, M. A. M., & Dorigo, M. (2014). A unified ant colony optimization algorithm for continuous optimization. European Journal of Operational Research, 234(3), 597-609.

Lim, T. S. and Lee, D. G. (2002) 'Mechanically Fastened Composite Side-Door Impact Beams for Passenger Cars Designed for Shear-Out Failure Modes'. Composite Structures 56 (2), 211-221

LIN, C. Y. and HAJELA, P. (1992) 'Genetic Algorithms in Optimization Problems with Discrete and Integer Design Variables'. *Engineering Optimization* 19 (4), 309-327

Low & High Pressure Diecasting | Choosing A Pressure Casting (2017) available from <https://www.mrt-castings.co.uk/pressure-diecasting-methods.html> [10 October 2017]

Mallick, P. K. (2010) *Materials, Design and Manufacturing for Lightweight Vehicles*.: Oxford : Woodhead

Markót, M. C., Fernández, J., Casado, L. G., & Csendes, T. (2006). New interval methods for constrained global optimization. Mathematical Programming, 106(2), 287-318.

Mat Saman, M. Z. and Blount, G. (2008) 'The DFEL Value Methodology: A Tool for Design-for-Environment in Automotive Industry'. *Jurnal Mekanikal* (27), 23-41

Mat Saman,M.Z.,Blount, G. (2006) 'End of Life Vehicles Recovery: Process Description, its Impact and Direction of Research
'. *Jurnal Mekanikal* 21, 40-52

Mathieux, F., Froelich, D., and Moszkowicz, P. (2008) 'ReSICLED: A New Recovery-Conscious Design Method for Complex Products Based on a Multicriteria Assessment of the Recoverability'. *Journal of Cleaner Production* 16 (3), 277-298

Mayyas, A. T., Qattawi, A., Mayyas, A. R., and Omar, M. (2013) 'Quantifiable Measures of Sustainability: A Case Study of Materials Selection for eco-Lightweight Auto-Bodies'. *Journal of Cleaner Production* 40 (0), 177-189

Messac, A., Sundararaj, G. J., Tappeta, R. V., and Renaud, J. E. (2000) 'Ability of Objective Functions to Generate Points on Nonconvex Pareto Frontiers'. AIAA Journal 38 (6), 1084-1091

Michell, A. G. M. (1904) 'LVIII. the Limits of Economy of Material in Frame-Structures'. *Philosophical Magazine Series 6* 8 (47), 589-597

Miettinen, K. (1998) Nonlinear Multiobjective Optimization.: Springer US

Mildenberger, U. and Khare, A. (2000) 'Planning for an Environment-Friendly Car'. *Technovation* 20 (4), 205-214

Mohd Fadzli Abdollah, Rafidah Hassan (2013) 'Preliminary Design of Side Door Impact Beam for Passenger Cars using Aluminium Alloy' 5 (2180-1053), 11-18

Moncayo-Martínez, L. A. and Zhang, D. Z. (2011) 'Multi-Objective Ant Colony Optimisation: A Meta-Heuristic Approach to Supply Chain Design'. International Journal of Production Economics 131 (1), 407-420

Monmasson, E., Idkhajine, L., Cirstea, M. N., Bahri, I., Tisan, A., & Naouar, M. W. (2011). FPGAs in industrial control applications. IEEE Transactions on Industrial informatics, 7(2), 224-243.

Montgomery, D. C. (2009) *Design and Analysis of Experiments*. 7th ed., international student version.. edn. Hoboken, N.J.: Hoboken, N.J. : Wiley

Nandi, A. K., Chakraborty, D., and Vaz, W. (2015) 'Design of a Comfortable Optimal Driving Strategy for Electric Vehicles using Multi-Objective Optimization'. Journal of Power Sources 283 (0), 1-18

Nunes, B. and Bennett, D. (2008) *Environmental Threats and their Impacts on the Automotive Industry*.

Ohsaki, M. (1995) 'Genetic Algorithm for Topology Optimization of Trusses'. *Computers & Structures* 57 (2), 219-225

Omar, M. A. (2011) *Automotive Body Manufacturing Systems and Processes* [online] . Hoboken, NJ, USA: John Wiley & Sons. available from <http://site.ebrary.com/lib/coventry/docDetail.action?docID=10510465&ppg=1>

Östlin, J., Sundin, E., and Björkman, M. (2009) 'Product Life-Cycle Implications for Remanufacturing Strategies'. *Journal of Cleaner Production* 17 (11), 999-1009

Pennington, D. W., Potting, J., Finnveden, G., Lindeijer, E., Jolliet, O., Rydberg, T., and Rebitzer, G. (2004) 'Life Cycle Assessment Part 2: Current Impact Assessment Practice'. *Environment International* 30 (5), 721-739

Qi, X., Tielin, S., and Michael, Y. W. (2010) 'A Level Set Based Shape and Topology Optimization Method for Maximizing the Simple Or Repeated Rst Eigenvalue of Structure Vibration.'. *Structural and Multidisciplinary Optimization* 43 (4), 473-485

Rajan, S. D. (1995) 'Sizing, Shape, and Topology Design Optimization of Trusses using Genetic Algorithm'. *Journal of Structural Engineering* 121 (10), 1480

Rajeev, S. and Krishnamoorthy, C. (1992) 'Discrete Optimization of Structures using Genetic Algorithms'. *Journal of Structural Engineering* 118 (5), 1233-1250

Rangaiah, G. P. (Ed.). (2016). Multi-objective optimization: techniques and applications in chemical engineering (Vol. 5). World Scientific.

Ravi, N., Liu, J., & Chakradhar, S. T. (2014). U.S. Patent No. 8,793,674. Washington, DC: U.S. Patent and Trademark Office.

Reeves, C. R. (1995). A genetic algorithm for flowshop sequencing. Computers & operations research, 22(1), 5-13.

Rowley, J. (2017) *Design For Six Sigma–Quality Function Deployment And The House Of Quality* [online] available from <https://4squareviews.com/2012/11/19/design-for-six-sigma-quality-function-deployment-and-the-house-of-quality/> [16 May 2016]

Roy, R., Kelvesjo, S., Forsberg, S., and Rush, C. (2001) 'Quantitative and Qualitative Cost Estimating for Engineering Design'. *Journal of Engineering Design* 12 (2), 147-162

Roy, R., Souchoroukov, P., and Griggs, T. (2008) 'Function-Based Cost Estimating'. *International Journal of Production Research* 46 (10), 2621-2650

Roy, R., Souchoroukov, P., and Shehab, E. (2011) *Detailed Cost Estimating in the Automotive Industry: Data and Information Requirements* [online] . available from <http://www.sciencedirect.com/science/article/pii/S0925527311002350>

Sakamoto, J. and Oda, J. (eds.) (1993) *34th Structures, Structural Dynamics and Materials Conference*. 'A Technique of Optimal Layout Design for Truss Structures using Genetic Algorithm ': -American Institute of Aeronautics and Astronautics

Sakundarini, N., Taha, Z., Abdul-Rashid, S. H., and Ghazila, R. A. R. (2013) 'Optimal Multi-Material Selection for Lightweight Design of Automotive Body Assembly Incorporating Recyclability'. *Materials & Design* 50 (0), 846-857

Save, M., Prager, W., and Warner, W. H. (1986) *Structural Optimization Volume 1: Optimality Criteria*.

Scheuring, J. F., Bras, B., and Kok-Meng Lee (eds.) (1994) *Computer Integrated Manufacturing and Automation Technology, 1994., Proceedings of the Fourth International Conference on*. 'Effects of Design for Disassembly on Integrated Disassembly and Assembly Processes'

Science Note – Eco Audit, CES EduPack 2016. Cambridge, United Kingdom: Granta Design Limited

Shrestha, S. M. and Ghaboussi, J. (1998) 'Evolution of Optimum Structural Shapes using Genetic Algorithm'. *Journal of Structural Engineering* 124 (11), 1331

Singh, K. (2011) Engineering Mathematics through Applications. 2nd ed. edn. Basingstoke: Basingstoke: Palgrave Macmillan

Sofia Börjesson (1994) 'What Kind of Activity-based Information does Your Purpose Require?'. *Int Jrnl of Op & Prod Mnagemnt* 14 (12), 79-99

Soh, C. K. and Yang, J. (1996) 'Fuzzy Controlled Genetic Algorithm Search for Shape Optimization'. *Journal of Computing in Civil Engineering* 10 (2), 143

Souchoroukov, P. (2004) *Improvement of Cost Estimating Internal Practice.* [online] PhD thesis or dissertation: School of Applied Sciences

Srinivas, N., & Deb, K. (1994). Muiltiobjective optimization using nondominated sorting in genetic algorithms. Evolutionary computation, 2(3), 221-248.

Stidsen, T., Andersen, K. A., & Dammann, B. (2014). A branch and bound algorithm for a class of biobjective mixed integer programs. Management Science, 60(4), 1009-1032.

Sturrus, P., Lewis, L. A., and Johnson, R. (1992) Impact Beam.: Google Patents

Sun, F., Wang, T., & Lu, W. (2008, September). A data association method based on simulate anneal arithmetic for mobile robot SLAM. In Automation and Logistics, 2008. ICAL 2008. IEEE International Conference on (pp. 425-430). IEEE.

Sundin, E. (2004) *Product and Process Design for Successful Remanufacturing*. [online] thesis or dissertation. Sweden: Department of Mechanical Engineering, Linköping University

T. F. Go, D. A. Wahab, M. N.A. Rahman and R. Ramli (2010) 'A Design Framework for End-of-Life Vehicles Recovery: Optimization of Disassembly Sequence using Genetic Algorithms' 6 (4), 350-356

Takeuchi, S. and Saitou, K. (eds.) (2005) *Assembly and Task Planning: From Nano to Macro Assembly and Manufacturing, 2005. (ISATP 2005). the 6th IEEE International Symposium on*. 'Design for Product Embedded Disassembly Sequence'

Tang, H. (2010) - *Latest Advances in Joining Technologies for Automotive Body Manufacturing*.

Tempelman, E. (2011) 'Multi-Parametric Study of the Effect of Materials Substitution on Life Cycle Energy use and Waste Generation of Passenger Car Structures'. *Transportation Research Part D: Transport and Environment* 16 (7), 479-485

Thota, J. (2016). Lecture 13: Loads & Boundary Conditions. [online] Available at https://faculty.unlv.edu/jagadeep/ME741/Lectures/Lecture%2013.pdf [Accessed 5 Jun. 2016]

Tseng, H., Chang, C., and Li, J. (2008) 'Modular Design to Support Green Life-Cycle Engineering'. *Expert Systems with Applications* 34 (4), 2524-2537

Vanderbilt, D., & Louie, S. G. (1984). A Monte Carlo simulated annealing approach to optimization over continuous variables. Journal of computational physics, 56(2), 259-271.

Vasant, P. and M, K. (2016) *Handbook Of Research On Holistic Optimization Techniques In The Hospitality, Tourism, And Travel Industry*. IGI Global, 2016

Veness, C. (2016). Calculate distance and bearing between two Latitude/Longitude points using haversine formula in JavaScript. [online] Movable-type.co.uk. Available at: http://www.movable-type.co.uk/scripts/latlong.html [Accessed 7 Jun. 2016].

Vilà, M., & Pereira, J. (2014). A branch-and-bound algorithm for assembly line worker assignment and balancing problems. Computers & Operations Research, 44, 105-114.

Wang, F. S., & Jang, H. J. (2000). Parameter estimation of a bioreaction model by hybrid differential evolution. In Evolutionary Computation, 2000. Proceedings of the 2000 Congress on (Vol. 1, pp. 410-417). IEEE.

Wei, P., Wang, M. Y., and Xing, X. (2010) 'A Study on X-FEM in Continuum Structural Optimization using a Level Set Model'. *Computer-Aided Design* 42 (8), 708-719

Whitley, D. (1994). A genetic algorithm tutorial. Statistics and computing, 4(2), 65-85.

Whitley, D. (2014). An executable model of a simple genetic algorithm. Foundations of genetic algorithms, 2(1519), 45-62.

Wilson, R. B., Shapiro, J. M., and Cline, R. S. (1989) Automotive Vehicle Door and Bar Reinforcement.: Google Patents

Winter, D. (2013) *Dupont Develops Plastic Side-Impact Door Beam* [online] available from <http://wardsauto.com/industry/dupont-develops-plastic-side-impact-door-beam> [28 March 2015]

Witik, R. A., Payet, J., Michaud, V., Ludwig, C., and Månson, J. E. (2011) 'Assessing the Life Cycle Costs and Environmental Performance of Lightweight Materials in Automobile Applications'. *Composites Part A: Applied Science and Manufacturing* 42 (11), 1694-1709

Wu, S. and Chow, P. (1995) 'Integrated Discrete and Configuration Optimization of Trusses using Genetic Algorithms'. *Computers & Structures* 55 (4), 695-702

Zhang, Y., Zhu, P., and Chen, G. (2007) 'Lightweight Design of Automotive Front Side Rail Based on Robust Optimisation'. *Thin-Walled Structures* 45 (7–8), 670-676

Zicai, W., Tong, Z., & Hongwei, W. (1999). Simulated Annealing Algorithm Based on Chaotic Variable [J]. Control and Decision, 4.

Zitzler, E., & Thiele, L. (1999). Multiobjective evolutionary algorithms: a comparative case study and the strength Pareto approach. IEEE transactions on Evolutionary Computation, 3(4), 257-271.

Zwolinski, P., Lopez-Ontiveros, M., and Brissaud, D. (2006) 'Integrated Design of Remanufacturable Products Based on Product Profiles'. Journal of Cleaner Production 14 (15–16), 1333-1345

Bibliography

A.A., L., D.A., W., S., A., and C.H., C. H. (2013) 'A Review on End-of-Life Vehicle Design Process and Management'. *Journal of Applied Sciences* 13, 654-662

Alting, L. (1995) 'Life Cycle Engineering and Design'. *CIRP Annals - Manufacturing Technology* 44 (2), 569-580

Anon- *Comparative Life Cycle Assessment (LCA) of Passenger Seats and their Impact on Different Vehicle Models*.

Anon(2005) 'Life Cycle Assessment'. *Automotive Industries* 185 (2), 8-8

Anon(2009) 'Briefs'. *Advanced Materials & Processes* 167 (10), 10-12

Anon(2010) *Environmental Management - the ISO 14000 Family of International Standards*. 2nd edn: iso.org

Azapagic, A. (1999) 'Life Cycle Assessment and its Application to Process Selection, Design and Optimisation'. *Chemical Engineering Journal* 73 (1), 1-21

Azapagic, A. and Clift, R. (1999) 'Life Cycle Assessment and Multiobjective Optimisation'. *Journal of Cleaner Production* 7 (2), 135-143

Azapagic, A. and Clift, R. (1999) 'The Application of Life Cycle Assessment to Process Optimisation'. *Computers & Chemical Engineering* 23 (10), 1509-1526

Baskin, D. M., Reed, D. B., Seel, T. N., Hunt, M. N., Oenkal, M., Takacs, Z., and Vollmer, A. B. (2008) *A Case Study in Structural Optimization of an Automotive Body-in-White Design*.: SAE International

Bennett, J. A. and Nelson, M. F. (1979) *An Optimization Capability for Automotive Structures*.: SAE International

Blume, T. and Walther, M. (2013) 'The End-of-Life Vehicle Ordinance in the German Automotive Industry – Corporate Sense Making Illustrated'. *Journal of Cleaner Production* 56 (0), 29-38

Boothroyd, G. and Alting, L. (1992) 'Design for Assembly and Disassembly'. *CIRP Annals -*

Manufacturing Technology 41 (2), 625-636

Calvo, P. R. (2013) *Design Optimization of Hybrid Body-in-White*.: SAE International

Camp, C., Pezeshk, S., and Cao, G. (1998) 'Optimized Design of Two-Dimensional Structures using a Genetic Algorithm'. *Journal of Structural Engineering* 124 (5), 551

Chang-Koon Choi and Hyuk-Chun Noh (2000) 'Stochastic Analysis of Shape Imperfection in Rc Cooling Tower Shells'. *Journal of Structural Engineering* 126 (3), 417

Coates,G.,Rahimifard,S. (ed.) (2006) *13th CIPR International Conference on Life Cycle Engineering.* 'Cost Models for Increased Value Recovery from End-of-Life Vehicles'. held May 31st at City campus of the Katholieke Universiteit Leuven

Court, A. W. (1997) 'The Relationship between Information and Personal Knowledge in New Product Development'. *International Journal of Information Management* 17 (2), 123-138

David, E. and Kopac, J. (2012) 'Hydrolysis of Aluminum Dross Material to Achieve Zero Hazardous Waste'. *Journal of Hazardous Materials* 209–210 (0), 501-509

David, E. and Kopac, J. (2013) 'Aluminum Recovery as a Product with High Added Value using Aluminum Hazardous Waste'. *Journal of Hazardous Materials* 261 (0), 316-324

Detwiler, D., Ekhande, S., and Kistner, M. (1996) *Computer Aided Structural Optimization of Automotive Body Structure*.: SAE International

Deutz, P., McGuire, M., and Neighbour, G. (2013) 'Eco-Design Practice in the Context of a Structured Design Process: An Interdisciplinary Empirical Study of UK Manufacturers'. *Journal of Cleaner Production* 39 (0), 117-128

Du, J., Han, W., and Peng, Y. (2010) 'Life Cycle Greenhouse Gases, Energy and Cost Assessment of Automobiles using Magnesium from Chinese Pidgeon Process'. *Journal of Cleaner Production* 18 (2), 112-119

Edwards,C.,Bhamra,T.,Rahimifard,S. (ed.) (2006) *The 13th CIRP International Conference on Life Cycle Engineering*. 'A Design Framework for End-of-Life Vehicle Recovery'

Erbatur, F., Hasançebi, O., Tütüncü, İ., and Kılıç, H. (2000) 'Optimal Design of Planar and

Space Structures with Genetic Algorithms'. *Computers & Structures* 75 (2), 209-224

Eskandari, M., Najafizadeh, A., Kermanpur, A., and Karimi, M. (2009) 'Potential Application of Nanocrystalline 301 Austenitic Stainless Steel in Lightweight Vehicle Structures'. *Materials & Design* 30 (9), 3869-3872

Fischer, R., Klein, M., and Wulf, C. (2011) *Process Improvements in Structural Optimization and NVH.*: The Automotive Research Association of India

Foley, C. M. and Schinler, D. (2003) 'Automated Design of Steel Frames using Advanced Analysis and Object-Oriented Evolutionary Computation'. *Journal of Structural Engineering* 129 (5), 648

Gaidajis, G., Angelakoglou, K., Botsaris, P. N., and Filippidou, F. (2011) 'Analysis of the Recycling Potential of used Automotive Oil Filters using the Life Cycle Assessment Approach'. *Resources, Conservation and Recycling* 55 (11), 986-994

Go, T. F., Wahab, D. A., Rahman, M. N. A., Ramli, R., and Hussain, A. (2012) 'Genetically Optimised Disassembly Sequence for Automotive Component Reuse'. *Expert Systems with Applications* 39 (5), 5409-5417

Gu, L. and Yang, R. J. (2003) *Recent Applications on Reliability-Based Optimization of Automotive Structures.*: SAE International

Güngör, A. (2006) 'Evaluation of Connection Types in Design for Disassembly (DFD) using Analytic Network Process'. *Computers & Industrial Engineering* 50 (1–2), 35-54

Hayalioglu, M. S. (2000) 'Optimum Design of Geometrically Non-Linear elastic–plastic Steel Frames Via Genetic Algorithm'. *Computers & Structures* 77 (5), 527-538

Hodkinson, R. and Fenton, J. (2000) '7 - Lightweight Construction Materials and Techniques'. in *Lightweight Electric/Hybrid Vehicle Design*. ed. by Hodkinson, R. and Fenton, J. Oxford: Butterworth-Heinemann, 173-198

Hongwei, Z., Xiaokai, C., and Yi, L. (2008) *Topology Optimization of Hybrid Electric Vehicle Frame using Multi-Loading Cases Optimization.*: SAE International

Jenkins, W. M. (1997) 'On the Application of Natural Algorithms to Structural Design Optimization'. *Engineering Structures* 19 (4), 302-308

Jovane, F., Alting, L., Armillotta, A., Eversheim, W., Feldmann, K., Seliger, G., and Roth, N. (1993) 'A Key Issue in Product Life Cycle: Disassembly'. *CIRP Annals - Manufacturing Technology* 42 (2), 651-658

Kiani, M., Motoyama, K., Rais-Rohani, M., and Shiozaki, H. (2014) 'Joint Stiffness Analysis and Optimization as a Mechanism for Improving the Structural Design and Performance of a Vehicle'. *Proceedings of the Institution of Mechanical Engineers, Part D: Journal of Automobile Engineering*

Kopp, G., Beeh, E., Schšll, R., Kobilke, A., Stra§burger, P., and Krieschera, M. (2012) 'New Lightweight Structures for Advanced Automotive Vehicles–Safe and Modular'. *Procedia - Social and Behavioral Sciences* 48 (0), 350-362

Kroll, E. and Carver, B. S. (1999) 'Disassembly Analysis through Time Estimation and Other Metrics'. *Robotics and Computer-Integrated Manufacturing* 15 (3), 191-200

Kuo, T. C. (2000) 'Disassembly Sequence and Cost Analysis for Electromechanical Products'. *Robotics and Computer-Integrated Manufacturing* 16 (1), 43-54

Laxman, S., Iyengar, R. M., and Morgans, S. (2009) *Achieving Light-Weight Design of Automotive Bodies with Advanced High Strength Steels Via Structural Optimization*.: SAE International

Lee, D. and Han, C. (2009) 'CAE (Computer Aided Engineering) Driven Durability Model Verification for the Automotive Structure Development'. *Finite Elements in Analysis and Design* 45 (5), 324-332

LEE, K. and NIKOLAIDIS, E. (1992; 1992) 'Identification of Flexible Joints in Vehicle Structures'. *AIAA Journal* 30 (2), 482-489

Lee, K. W., Chong, T. H., and Park, G. (2003) 'Development of a Methodology for a Simplified Finite Element Model and Optimum Design'. *Computers & Structures* 81 (14), 1449-1460

Liu, Q., Lin, Y., Zong, Z., Sun, G., and Li, Q. (2013) 'Lightweight Design of Carbon Twill Weave Fabric Composite Body Structure for Electric Vehicle'. *Composite Structures* 97 (0), 231-238

Luh, G. and Lin, C. (2009) 'Structural Topology Optimization using Ant Colony Optimization Algorithm'. *Applied Soft Computing* 9 (4), 1343-1353

Luttropp, C. (1998) 'Design for Disassembly: A New Element in Product Development' 6 (6), 30-40

Ma, Z., Wang, H., Kikuchi, N., Pierre, C., and Raju, B. (2003) *Substructure Design using a Multi-Domain Multi-Step Topology Optimization Approach*.: SAE International

Mårtensson, P. (2014) *Cost and Weight Effective Composite Design of Automotive Body Structures*.

Mayyas, A. T., Qattawi, A., Mayyas, A. R., and Omar, M. A. (2012) 'Life Cycle Assessment-Based Selection for a Sustainable Lightweight Body-in-White Design'. *Energy* 39 (1), 412-425

Mayyas, A., Qattawi, A., Omar, M., and Shan, D. (2012) 'Design for Sustainability in Automotive Industry: A Comprehensive Review'. *Renewable and Sustainable Energy Reviews* 16 (4), 1845-1862

McGlothlin, S. and Kroll, E. (eds.) (1995) *Electronics and the Environment, 1995. ISEE., Proceedings of the 1995 IEEE International Symposium on*. 'Systematic Estimation of Disassembly Difficulties: Application to Computer Monitors'

Mergenthaler, W., Stadler, W., Wilbertz, H., and Zimmer, N. (1995) 'Optimizing Automotive Manufacturing Sequences using Simulated Annealing and Genetic Algorithms'. *Control Engineering Practice* 3 (4), 569-573

Michalos, G., Makris, S., Papakostas, N., Mourtzis, D., and Chryssolouris, G. (2010) 'Automotive Assembly Technologies Review: Challenges and Outlook for a Flexible and Adaptive Approach'. *CIRP Journal of Manufacturing Science and Technology* 2 (2), 81-91

Mital, A.,Desai, A. (2007) 'A Structured Approach to New Product Design, Development and Manufacture Part II: Putting the Product Together (Assembly) and Disposal (Disassembly)' 14 (1), 23-32

Mok, H. S., Kim, H. J., and Moon, K. S. (1997) 'Disassemblability of Mechanical Parts in Automobile for Recycling'. *Computers & Industrial Engineering* 33 (3–4), 621-624

Muhl, E., Charpentier, P., and Chaxel, F. (2003) 'Optimization of Physical Flows in an Automotive Manufacturing Plant: Some Experiments and Issues'. *Engineering*

Applications of Artificial Intelligence 16 (4), 293-305

Nicholson, A. L., Olivetti, E. A., Gregory, J. R., Field, F. R., and Kirchain, R. E. (eds.) (2009) *Sustainable Systems and Technology, 2009. ISSST '09. IEEE International Symposium on*. 'End-of-Life LCA Allocation Methods: Open Loop Recycling Impacts on Robustness of Material Selection Decisions'

Obradovic, J., Boria, S., and Belingardi, G. (2012) 'Lightweight Design and Crash Analysis of Composite Frontal Impact Energy Absorbing Structures'. *Composite Structures* 94 (2), 423-430

Pakalapati, V., Katkar, V., and Babar, R. (2011) *CAE Based â€˜Multi Objective Optimization Approach for Spot Weld Connections Layoutâ€™ in Automotive Structure*.: SAE International

Qin, S. and Wu, B. (2011) 'Effect of Self-Glazing on Reducing the Radioactivity Levels of Red Mud Based Ceramic Materials'. *Journal of Hazardous Materials* 198 (0), 269-274

Rais-Rohani, M., Solanki, K. N., Acar, E., and Eamon, C. D. (2010) 'Shape and Sizing Optimisation of Automotive Structures with Deterministic and Probabilistic Design Constraints'. *International Journal of Vehicle Design* 54 (4), 309-338

Raugei, M., El Fakir, O., Wang, L., Lin, J., and Morrey, D. (2014) 'Life Cycle Assessment of the Potential Environmental Benefits of a Novel Hot Forming Process in Automotive Manufacturing'. *Journal of Cleaner Production* 83 (0), 80-86

Rebitzer, G., Ekvall, T., Frischknecht, R., Hunkeler, D., Norris, G., Rydberg, T., Schmidt, W. -., Suh, S., Weidema, B. P., and Pennington, D. W. (2004) 'Life Cycle Assessment: Part 1: Framework, Goal and Scope Definition, Inventory Analysis, and Applications'. *Environment International* 30 (5), 701-720

Rehman, S. and Guenov, M. D. (1998) 'A Methodology for Modelling Manufacturing Costs at Conceptual Design'. *Computers & Industrial Engineering* 35 (3–4), 623-626

Rush, C. and Roy, R. (2001) 'Expert Judgement in Cost Estimating: Modelling the Reasoning Process'. *Concurrent Engineering* 9 (4), 271-284

Sakai, S., Yoshida, H., Hiratsuka, J., Vandecasteele, C., Kohlmeyer, R., Rotter, V., Passarini, F., Santini, A., Peeler, M., Li, J., Oh, G., Chi, N., Bastian, L., Moore, S., Kajiwara, N., Takigami, H., Itai, T., Takahashi, S., Tanabe, S., Tomoda, K., Hirakawa, T., Hirai, Y., Asari, M., and Yano, J. (2014) 'An International Comparative Study of End-of-Life Vehicle (ELV) Recycling Systems'. *Journal of Material Cycles and Waste Management* 16 (1), 1-20

Saman, M. Z. M., Zakuan, N., and Blount, G. (2012) 'Design for End-of-Life Value Framework for Vehicles Design and Development Process'. *Journal of Sustainable Development* 5 (2), 95

SATHYA GANGADHARAN, EFSTRATIOS NIKOLAIDIS, and RAPHAEL HAFTKA (1990; 1990) 'Probabilistic System Identification of Two Flexible Joint Models'. in *31st Structures, Structural Dynamics and Materials Conference*. ed. by Anon: American Institute of Aeronautics and Astronautics

Seitz, M. A. (2007) 'A Critical Assessment of Motives for Product Recovery: The Case of Engine Remanufacturing'. *Journal of Cleaner Production* 15 (11–12), 1147-1157

Shehab, E. M. and Abdalla, H. S. (2006) 'A Cost-Effective Knowledge-Based Reasoning System for Design for Automation'. *Proceedings of the Institution of Mechanical Engineers, Part B: Journal of Engineering Manufacture* 220 (5), 729-743

Shepperd, M. and Schofield, C. (1997) 'Estimating Software Project Effort using Analogies'. *Software Engineering, IEEE Transactions on* 23 (11), 736-743

Shimoda, M. (2011) 'Free-Form Optimization Method for Designing Automotive Shell Structures' 4 (1), 42-54

Subramoniam, R., Huisingh, D., and Chinnam, R. B. (2009) 'Remanufacturing for the Automotive Aftermarket-Strategic Factors: Literature Review and Future Research Needs'. *Journal of Cleaner Production* 17 (13), 1163-1174

Tamaki, Y. (1999) 'Research into Achieving a Lightweight Vehicle Body Utilizing Structure Optimizing Analysis: Aim for a Lightweight and High and Rigid Vehicle Body'. *JSAE Review* 20 (4), 558-561

Tan, X., Mu, Z., Wang, S., Zhuang, H., Cheng, L., Wang, Y., and Gu, B. (2011) 'Study on Whole-Life Cycle Automotive Manufacturing Industry CO2 Emission Accounting Method and Application in Chongqing'. *Procedia Environmental Sciences* 5 (0), 167-172

Tang, D. and Qian, X. (2008) 'Product Lifecycle Management for Automotive Development

Focusing on Supplier Integration'. *Computers in Industry* 59 (2–3), 288-295

Tempelman, E. (2014) 'Chapter 18 - Lightweight Materials, Lightweight Design?'. in *Materials Experience: Fundamentals of Materials and Design*. ed. by Karana, E., Pedgley, O., and Rognoli, V. Boston: Butterworth-Heinemann, 247-258

Teresko, J. (2005) 'Green Machines'. *Industry Week/IW* 254 (2), 40-45

Tian, J. and Chen, M. (2014) 'Sustainable Design for Automotive Products: Dismantling and Recycling of End-of-Life Vehicles'. *Waste Management* 34 (2), 458-467

Tonn, B. E., Schexnayder, S. M., Peretz, J. H., Das, S., and Waidley, G. (2003) 'An Assessment of Waste Issues Associated with the Production of New, Lightweight, Fuel-Efficient Vehicles'. *Journal of Cleaner Production* 11 (7), 753-765

Tsai, Y. and Chang, Y. (2004) 'Function-Based Cost Estimation Integrating Quality Function Deployment to Support System Design'. *International Journal of Advanced Manufacturing Technology* 23 (7), 514-522

Veerakamolmal, P. and Gupta, S. M. (1999) 'Analysis of Design Efficiency for the Disassembly of Modular Electronic Products'. *Journal of Electronics Manufacturing* 9 (1), 79

Vermeulen, I., Van Caneghem, J., Block, C., Baeyens, J., and Vandecasteele, C. (2011) 'Automotive Shredder Residue (ASR): Reviewing its Production from End-of-Life Vehicles (ELVs) and its Recycling, Energy Or Chemicals' Valorisation'. *Journal of Hazardous Materials* 190 (1–3), 8-27

Wang, H., Ma, Z., Kikuchi, N., Pierre, C., and Raju, B. (2004) *Multi-Domain Multi-Step Topology Optimization for Vehicle Structure Crashworthiness Design*.: SAE International

Wei, F., Zhang, Y., Lv, F., Chu, P. K., and Ye, Z. (2011) 'Extraction of Organic Materials from Red Water by Metal-Impregnated Lignite Activated Carbon'. *Journal of Hazardous Materials* 197 (0), 352-360

Wenzel, H., Hauschild, M. Z., Jorgensen, J., and Alting, L. (eds.) (1994) *Electronics and the Environment, 1994. ISEE 1994., Proceedings., 1994 IEEE International Symposium on*. 'Environmental Tools in Product Development'

Wu, C. (2012) 'Product-Design and Pricing Strategies with Remanufacturing'. *European*

Journal of Operational Research 222 (2), 204-215

Wu, S. and Chow, P. (1995) 'Steady-State Genetic Algorithms for Discrete Optimization of Trusses'. *Computers & Structures* 56 (6), 979-991

Yildiz, A. R. (2013) 'Comparison of Evolutionary-Based Optimization Algorithms for Structural Design Optimization'. *Engineering Applications of Artificial Intelligence* 26 (1), 327-333

Yu, J. and Li, Y. (2006) 'Structure Representation for Concurrent Analysis of Product Assembly and Disassembly'. *Expert Systems with Applications* 31 (4), 705-714

Zhang, T., Chu, J., Wang, X., Liu, X., and Cui, P. (2011) 'Development Pattern and Enhancing System of Automotive Components Remanufacturing Industry in China'. *Resources, Conservation and Recycling* 55 (6), 613-622

Zhu, P., Pan, F., Chen, W., and Viana, F. A. C. (2013) 'Lightweight Design of Vehicle Parameters Under Crashworthiness using Conservative Surrogates'. *Computers in Industry* 64 (3), 280-289

Ziout, A., Azab, A., and Atwan, M. (2014) 'A Holistic Approach for Decision on Selection of End-of-Life Products Recovery Options'. *Journal of Cleaner Production* 65 (0), 497-516

Appendix – A

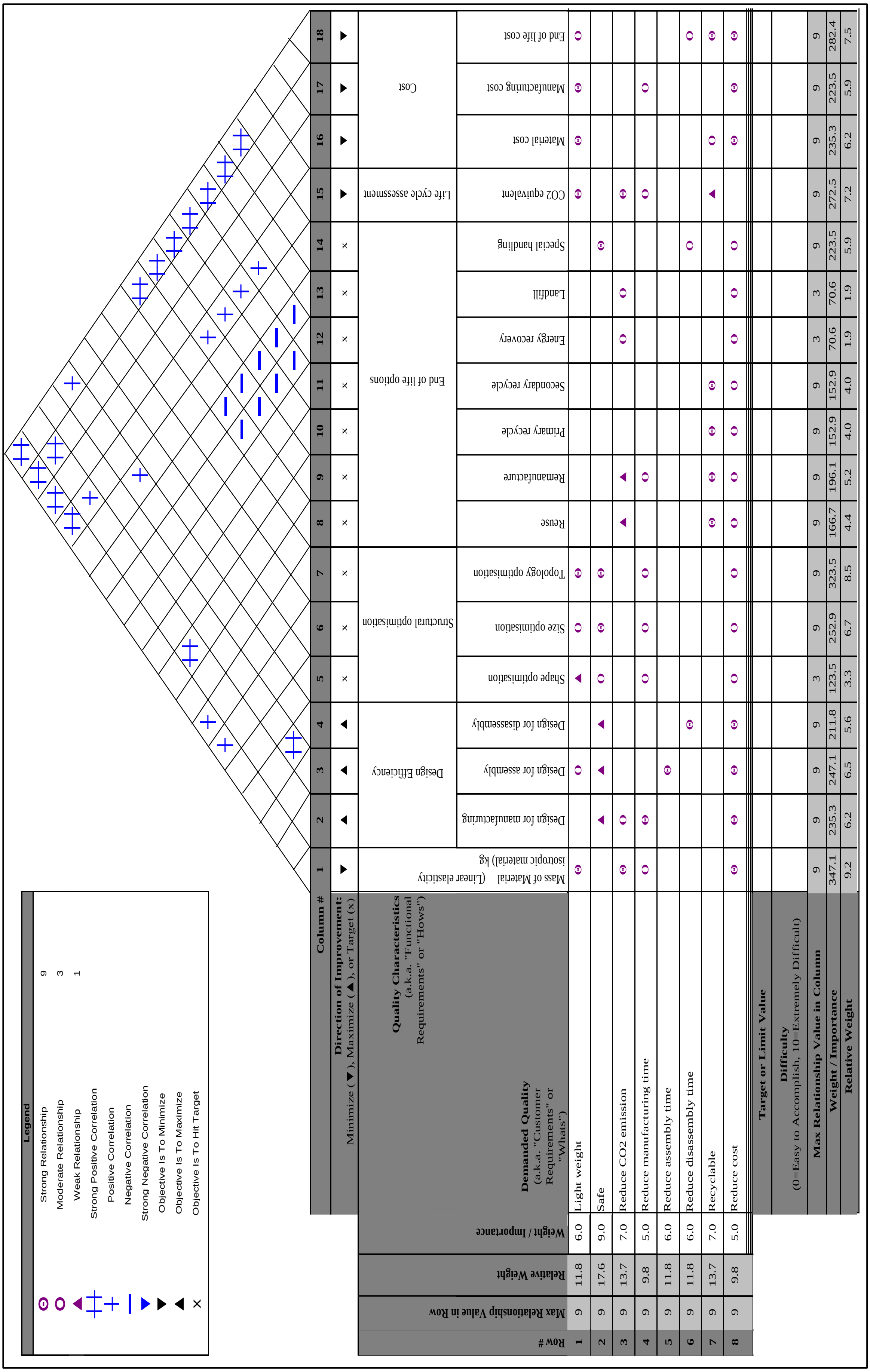

Figure 53: Full QFD for product

Appendix – B

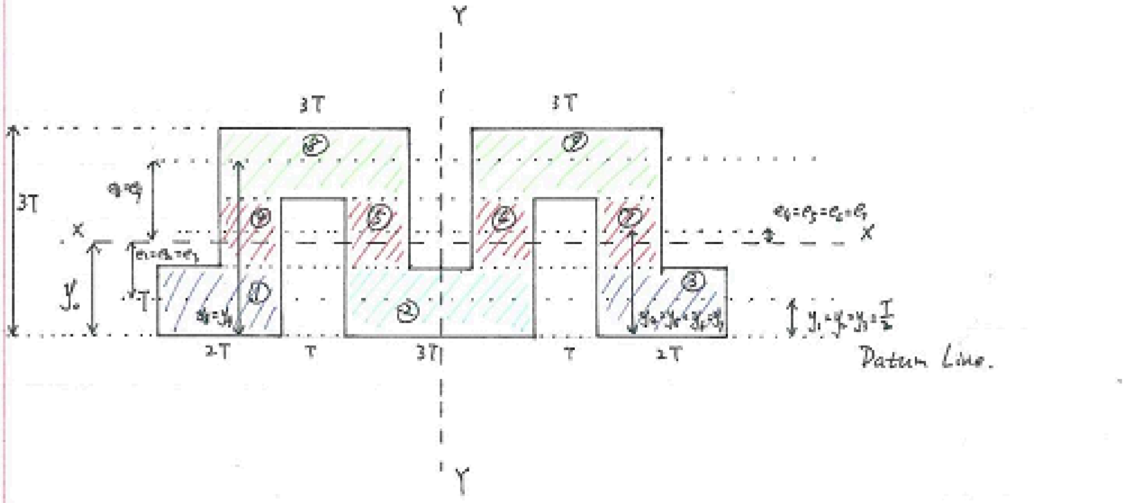

For I_{xx}:

$$y_o = \frac{\Sigma A_i y_i}{\Sigma A_i}$$

$$= (A_1y_1 + \cdots + A_9y_9) \div (A_1 + \cdots + A_9)$$

$$= (2T\times T\times \tfrac{T}{2}\times 2 + T\times T\times \tfrac{3T}{2}\times 4 + 3T\times T\times \tfrac{5T}{2}\times 2 + 3T\times T\times \tfrac{T}{2}) \div (T\times 2T\times 2 + T\times T\times 4$$

$$+ 3T\times T\times 3)$$

$$= 24.5T^3 \div 17T^2$$

$$= \frac{49T}{34}$$

$\therefore\ e_1 = e_2 = e_3 = \frac{16}{17}T$; $e_4 = e_5 = e_6 = e_7 = \frac{T}{17}$; $e_8 = e_9 = \frac{18T}{17}$

$$\therefore\ I_{xx} = \Sigma \frac{1}{12} b_i d_i^3 + A_i e_i^2$$

$$= (\tfrac{1}{12}\times 2T\times T^3 + 2T\times T\times(\tfrac{16}{17}T)^2)\times 2 + (\tfrac{1}{12}\times 3T\times T^3 + 3T\times T\times(\tfrac{16}{17}T)^2)$$

$$+ (\tfrac{1}{12}\times T\times T^3 + T\times T\times(\tfrac{T}{17})^2)\times 4 + (\tfrac{1}{12}\times 3T\times T^3 + 3T\times T\times(\tfrac{18}{17}T)^2)\times 2$$

$$= \frac{T^4}{3} + \frac{16^2}{17^2}T^4 + \frac{T^4}{4} + \frac{3\times 16^2}{17^2}T^4 + \frac{T^4}{3} + \frac{4T^4}{17^2} + \frac{T^4}{2} + \frac{6\times 18^2}{17^2}T^4$$

$$= \frac{2929}{204}T^4$$

For I_{yy}:

$x_o = 4.5T$ $\quad\therefore\ e_1 = e_3 = \frac{7T}{2}$; $e_4 = e_7 = 3T$; $e_5 = e_6 = T$; $e_2 = 0$; $e_8 = e_9 = 2T$

$$\therefore\ I_{yy} = \Sigma \frac{1}{12} d_i b_i^3 + A_i e_i^2$$

$$= (\tfrac{1}{12}\times T\times(2T)^3 + T\times 2T\times(\tfrac{7T}{2})^2)\times 2 + (\tfrac{1}{12}\times T\times T^3 + T\times T\times(3T)^2)\times 2 + (\tfrac{1}{12}\times T\times T^3 + T\times T\times(T)^2)\times 2$$

$$+ (\tfrac{1}{12}\times T\times(3T)^3 + T\times 3T\times 0) + (\tfrac{1}{12}\times T\times(3T)^3 + T\times 3T\times(2T)^2)\times 2$$

$$= \frac{1217}{12}T^4$$

Figure 54: Hand calculation for second moment of areas

Appendix – C

Case Study No.	Model No.	Geometry	Production Quantity	Recycled Content (%)	Max cost (GBP/unit)	Max CO_2 (kg/unit)	Origin Continents	Destination Continents	Origin Location	Destination Location	Travel Distance	Labour Cost (GBP/hr)	Overhead cost (GBP/MJ)	Approach
1	1	a	400	10	10	1.5	Europe	NorthAmerica	Coventry,UK	Coventry,USA	Long	Medium	Medium	Sequential
	2	b	400	10	10	1.5	Europe	NorthAmerica	Coventry,UK	Coventry,USA	Long	Medium	Medium	Sequential
	3	c	400	10	10	1.5	Europe	NorthAmerica	Coventry,UK	Coventry,USA	Long	Medium	Medium	Sequential
2	4	a	800	10	10	1.5	Europe	NorthAmerica	Coventry,UK	Coventry,USA	Long	Medium	Medium	Sequential
	5	a	1600	10	10	1.5	Europe	NorthAmerica	Coventry,UK	Coventry,USA	Long	Medium	Medium	Sequential
	6	a	3200	10	10	1.5	Europe	NorthAmerica	Coventry,UK	Coventry,USA	Long	Medium	Medium	Sequential
3	7	a	400	30	10	1.5	Europe	NorthAmerica	Coventry,UK	Coventry,USA	Long	Medium	Medium	Sequential
	8	a	400	50	10	1.5	Europe	NorthAmerica	Coventry,UK	Coventry,USA	Long	Medium	Medium	Sequential
	9	a	400	70	10	1.5	Europe	NorthAmerica	Coventry,UK	Coventry,USA	Long	Medium	Medium	Sequential
	10	a	400	90	10	1.5	Europe	NorthAmerica	Coventry,UK	Coventry,USA	Long	Medium	Medium	Sequential
4	11	a	400	10	8	1.5	Europe	NorthAmerica	Coventry,UK	Coventry,USA	Long	Medium	Medium	Sequential
	12	a	400	10	6	1.5	Europe	NorthAmerica	Coventry,UK	Coventry,USA	Long	Medium	Medium	Sequential
	13	a	400	10	4	1.5	Europe	NorthAmerica	Coventry,UK	Coventry,USA	Long	Medium	Medium	Sequential
	14	a	400	10	2	1.5	Europe	NorthAmerica	Coventry,UK	Coventry,USA	Long	Medium	Medium	Sequential
5	15	a	400	10	10	1	Europe	NorthAmerica	Coventry,UK	Coventry,USA	Long	Medium	Medium	Sequential
	16	a	400	10	10	0.5	Europe	NorthAmerica	Coventry,UK	Coventry,USA	Long	Medium	Medium	Sequential
6	17	a	400	10	10	1.5	Asia	Asia	Chennai, India	Shanghai, China	Short	Medium	Medium	Sequential
	18	a	400	10	10	1.5	Asia	Australia	Chennai, India	Melbourne, Australia	Medium	Medium	Medium	Sequential
	19	a	400	10	10	1.5	Asia	Europe	Chennai, India	Munich, Germany	Long	Medium	Medium	Sequential
7	20	a	400	10	10	1.5	SouthAmerica	Asia	São Paulo, Brazil	Shanghai, China	Long	Lowest	Medium	Sequential
	21	a	400	10	10	1.5	NorthAmerica	Asia	Houston,Texas, US	Shanghai, China	Long	Medium	Medium	Sequential
	22	a	400	10	10	1.5	Europe	Asia	Copenhagen, Denmark	Shanghai, China	Long	Highest	Medium	Sequential
8	23	a	400	10	10	1.5	NorthAmerica	Europe	Toronto,Canada	Munich, Germany	Long	Medium	Lowest	Sequential
	24	a	400	10	10	1.5	NorthAmerica	Europe	Houston,Texas, US	Munich, Germany	Long	Medium	Medium	Sequential
	25	a	400	10	10	1.5	Asia	Europe	Tokyo,Japan	Munich, Germany	Long	Medium	Highest	Sequential

Figure 55: Case study list

9	26	b	800	10	10	1.5	Europe	NorthAmerica	Coventry,UK	Coventry,USA	Long	Medium	Medium	Sequential	Part 2
	27	b	1600	10	10	1.5	Europe	NorthAmerica	Coventry,UK	Coventry,USA	Long	Medium	Medium	Sequential	
	28	b	3200	10	10	1.5	Europe	NorthAmerica	Coventry,UK	Coventry,USA	Long	Medium	Medium	Sequential	
	29	c	800	10	10	1.5	Europe	NorthAmerica	Coventry,UK	Coventry,USA	Long	Medium	Medium	Sequential	
	30	c	1600	10	10	1.5	Europe	NorthAmerica	Coventry,UK	Coventry,USA	Long	Medium	Medium	Sequential	
	31	c	3200	10	10	1.5	Europe	NorthAmerica	Coventry,UK	Coventry,USA	Long	Medium	Medium	Sequential	
10	32	b	800	30	10	1.5	Europe	NorthAmerica	Coventry,UK	Coventry,USA	Long	Medium	Medium	Sequential	
	33	b	800	50	10	1.5	Europe	NorthAmerica	Coventry,UK	Coventry,USA	Long	Medium	Medium	Sequential	
	34	b	800	70	10	1.5	Europe	NorthAmerica	Coventry,UK	Coventry,USA	Long	Medium	Medium	Sequential	
	35	b	800	90	10	1.5	Europe	NorthAmerica	Coventry,UK	Coventry,USA	Long	Medium	Medium	Sequential	
	36	c	800	30	10	1.5	Europe	NorthAmerica	Coventry,UK	Coventry,USA	Long	Medium	Medium	Sequential	
	37	c	800	50	10	1.5	Europe	NorthAmerica	Coventry,UK	Coventry,USA	Long	Medium	Medium	Sequential	
	38	c	800	70	10	1.5	Europe	NorthAmerica	Coventry,UK	Coventry,USA	Long	Medium	Medium	Sequential	
	39	c	800	90	10	1.5	Europe	NorthAmerica	Coventry,UK	Coventry,USA	Long	Medium	Medium	Sequential	
11	40	b	800	10	8	1.5	Europe	NorthAmerica	Coventry,UK	Coventry,USA	Long	Medium	Medium	Sequential	Part 2
	41	b	800	10	6	1.5	Europe	NorthAmerica	Coventry,UK	Coventry,USA	Long	Medium	Medium	Sequential	
	42	b	800	10	4	1.5	Europe	NorthAmerica	Coventry,UK	Coventry,USA	Long	Medium	Medium	Sequential	
	43	b	800	10	2	1.5	Europe	NorthAmerica	Coventry,UK	Coventry,USA	Long	Medium	Medium	Sequential	
	44	c	800	10	8	1.5	Europe	NorthAmerica	Coventry,UK	Coventry,USA	Long	Medium	Medium	Sequential	
	45	c	800	10	6	1.5	Europe	NorthAmerica	Coventry,UK	Coventry,USA	Long	Medium	Medium	Sequential	
	46	c	800	10	4	1.5	Europe	NorthAmerica	Coventry,UK	Coventry,USA	Long	Medium	Medium	Sequential	
	47	c	800	10	2	1.5	Europe	NorthAmerica	Coventry,UK	Coventry,USA	Long	Medium	Medium	Sequential	
12	48	b	800	10	10	1	Europe	NorthAmerica	Coventry,UK	Coventry,USA	Long	Medium	Medium	Sequential	
	49	b	800	10	10	0.5	Europe	NorthAmerica	Coventry,UK	Coventry,USA	Long	Medium	Medium	Sequential	
	50	c	800	10	10	1	Europe	NorthAmerica	Coventry,UK	Coventry,USA	Long	Medium	Medium	Sequential	
	51	c	800	10	10	0.5	Europe	NorthAmerica	Coventry,UK	Coventry,USA	Long	Medium	Medium	Sequential	
13	52	b	800	10	10	1.5	Asia	Australia	Chennai, India	Melbourne, Australia	Medium	Medium	Medium	Sequential	Part 2
	53	b	800	10	10	1.5	Asia	Europe	Chennai, India	Munich, Germany	Long	Medium	Medium	Sequential	
	54	c	800	10	10	1.5	Asia	Australia	Chennai, India	Melbourne, Australia	Medium	Medium	Medium	Sequential	
	55	c	800	10	10	1.5	Asia	Europe	Chennai, India	Munich, Germany	Long	Medium	Medium	Sequential	
14	56	b	800	10	10	1.5	NorthAmerica	Asia	Houston,Texas, US	Shanghai, China	Long	Medium	Medium	Sequential	
	57	b	800	10	10	1.5	Europe	Asia	Copenhagen, Denmark	Shanghai, China	Long	Highest	Medium	Sequential	
	58	c	800	10	10	1.5	NorthAmerica	Asia	Houston,Texas, US	Shanghai, China	Long	Medium	Medium	Sequential	
	59	c	800	10	10	1.5	Europe	Asia	Copenhagen, Denmark	Shanghai, China	Long	Highest	Medium	Sequential	

15	60	b	800	10	10	1.5	NorthAmerica	Europe	Houston,Texas, US	Munich, Germany	Long	Medium	Medium	Sequential	Part 2
	61	b	800	10	10	1.5	Asia	Europe	Tokyo,Japan	Munich, Germany	Long	Medium	Highest	Sequential	
	62	c	800	10	10	1.5	NorthAmerica	Europe	Houston,Texas, US	Munich, Germany	Long	Medium	Medium	Sequential	
	63	c	800	10	10	1.5	Asia	Europe	Tokyo,Japan	Munich, Germany	Long	Medium	Highest	Sequential	
16	64	a	800	30	10	1.5	Europe	NorthAmerica	Coventry,UK	Coventry,USA	Long	Medium	Medium	Sequential	Part 2
	65	a	800	50	10	1.5	Europe	NorthAmerica	Coventry,UK	Coventry,USA	Long	Medium	Medium	Sequential	
	66	a	800	70	10	1.5	Europe	NorthAmerica	Coventry,UK	Coventry,USA	Long	Medium	Medium	Sequential	
	67	a	800	90	10	1.5	Europe	NorthAmerica	Coventry,UK	Coventry,USA	Long	Medium	Medium	Sequential	
	68	a	1600	30	10	1.5	Europe	NorthAmerica	Coventry,UK	Coventry,USA	Long	Medium	Medium	Sequential	
	69	a	1600	50	10	1.5	Europe	NorthAmerica	Coventry,UK	Coventry,USA	Long	Medium	Medium	Sequential	
	70	a	1600	70	10	1.5	Europe	NorthAmerica	Coventry,UK	Coventry,USA	Long	Medium	Medium	Sequential	
	71	a	1600	90	10	1.5	Europe	NorthAmerica	Coventry,UK	Coventry,USA	Long	Medium	Medium	Sequential	
	72	a	3200	30	10	1.5	Europe	NorthAmerica	Coventry,UK	Coventry,USA	Long	Medium	Medium	Sequential	
	73	a	3200	50	10	1.5	Europe	NorthAmerica	Coventry,UK	Coventry,USA	Long	Medium	Medium	Sequential	
	74	a	3200	70	10	1.5	Europe	NorthAmerica	Coventry,UK	Coventry,USA	Long	Medium	Medium	Sequential	
	75	a	3200	90	10	1.5	Europe	NorthAmerica	Coventry,UK	Coventry,USA	Long	Medium	Medium	Sequential	
17	76	a	800	10	8	1.5	Europe	NorthAmerica	Coventry,UK	Coventry,USA	Long	Medium	Medium	Sequential	Part 2
	77	a	800	10	6	1.5	Europe	NorthAmerica	Coventry,UK	Coventry,USA	Long	Medium	Medium	Sequential	
	78	a	800	10	4	1.5	Europe	NorthAmerica	Coventry,UK	Coventry,USA	Long	Medium	Medium	Sequential	
	79	a	800	10	2	1.5	Europe	NorthAmerica	Coventry,UK	Coventry,USA	Long	Medium	Medium	Sequential	
	80	a	1600	10	8	1.5	Europe	NorthAmerica	Coventry,UK	Coventry,USA	Long	Medium	Medium	Sequential	
	81	a	1600	10	6	1.5	Europe	NorthAmerica	Coventry,UK	Coventry,USA	Long	Medium	Medium	Sequential	
	82	a	1600	10	4	1.5	Europe	NorthAmerica	Coventry,UK	Coventry,USA	Long	Medium	Medium	Sequential	
	83	a	1600	10	2	1.5	Europe	NorthAmerica	Coventry,UK	Coventry,USA	Long	Medium	Medium	Sequential	
	84	a	3200	10	8	1.5	Europe	NorthAmerica	Coventry,UK	Coventry,USA	Long	Medium	Medium	Sequential	
	85	a	3200	10	6	1.5	Europe	NorthAmerica	Coventry,UK	Coventry,USA	Long	Medium	Medium	Sequential	
	86	a	3200	10	4	1.5	Europe	NorthAmerica	Coventry,UK	Coventry,USA	Long	Medium	Medium	Sequential	
	87	a	3200	10	2	1.5	Europe	NorthAmerica	Coventry,UK	Coventry,USA	Long	Medium	Medium	Sequential	
18	88	a	800	10	10	1	Europe	NorthAmerica	Coventry,UK	Coventry,USA	Long	Medium	Medium	Sequential	t 2
	89	a	800	10	10	0.5	Europe	NorthAmerica	Coventry,UK	Coventry,USA	Long	Medium	Medium	Sequential	
	90	a	1600	10	10	1	Europe	NorthAmerica	Coventry,UK	Coventry,USA	Long	Medium	Medium	Sequential	
	91	a	1600	10	10	0.5	Europe	NorthAmerica	Coventry,UK	Coventry,USA	Long	Medium	Medium	Sequential	
	92	a	3200	10	10	1	Europe	NorthAmerica	Coventry,UK	Coventry,USA	Long	Medium	Medium	Sequential	
	93	a	3200	10	10	0.5	Europe	NorthAmerica	Coventry,UK	Coventry,USA	Long	Medium	Medium	Sequential	

19	**94**	a	800	10	10	1.5	Asia	Australia	Chennai, India	Melbourne, Australia	Medium	Medium	Medium	Sequential	
	95	a	800	10	10	1.5	Asia	Europe	Chennai, India	Munich, Germany	Long	Medium	Medium	Sequential	
	96	a	1600	10	10	1.5	Asia	Australia	Chennai, India	Melbourne, Australia	Medium	Medium	Medium	Sequential	
	97	a	1600	10	10	1.5	Asia	Europe	Chennai, India	Munich, Germany	Long	Medium	Medium	Sequential	
	98	a	3200	10	10	1.5	Asia	Australia	Chennai, India	Melbourne, Australia	Medium	Medium	Medium	Sequential	
	99	a	3200	10	10	1.5	Asia	Europe	Chennai, India	Munich, Germany	Long	Medium	Medium	Sequential	
20	**100**	a	800	10	10	1.5	NorthAmerica	Asia	Houston,Texas, US	Shanghai, China	Long	Medium	Medium	Sequential	Part 2
	101	a	800	10	10	1.5	Europe	Asia	Copenhagen, Denmark	Shanghai, China	Long	Highest	Medium	Sequential	
	102	a	1600	10	10	1.5	NorthAmerica	Asia	Houston,Texas, US	Shanghai, China	Long	Medium	Medium	Sequential	
	103	a	1600	10	10	1.5	Europe	Asia	Copenhagen, Denmark	Shanghai, China	Long	Highest	Medium	Sequential	
	104	a	3200	10	10	1.5	NorthAmerica	Asia	Houston,Texas, US	Shanghai, China	Long	Medium	Medium	Sequential	
	105	a	3200	10	10	1.5	Europe	Asia	Copenhagen, Denmark	Shanghai, China	Long	Highest	Medium	Sequential	
21	**106**	a	800	10	10	1.5	NorthAmerica	Europe	Houston,Texas, US	Munich, Germany	Long	Medium	Medium	Sequential	
	107	a	800	10	10	1.5	Asia	Europe	Tokyo,Japan	Munich, Germany	Long	Medium	Highest	Sequential	
	108	a	1600	10	10	1.5	NorthAmerica	Europe	Houston,Texas, US	Munich, Germany	Long	Medium	Medium	Sequential	
	109	a	1600	10	10	1.5	Asia	Europe	Tokyo,Japan	Munich, Germany	Long	Medium	Highest	Sequential	Part 2
	110	a	3200	10	10	1.5	NorthAmerica	Europe	Houston,Texas, US	Munich, Germany	Long	Medium	Medium	Sequential	
	111	a	3200	10	10	1.5	Asia	Europe	Tokyo,Japan	Munich, Germany	Long	Medium	Highest	Sequential	
22	**112**	a	400	30	8	1.5	Europe	NorthAmerica	Coventry,UK	Coventry,USA	Long	Medium	Medium	Sequential	
	113	a	400	30	6	1.5	Europe	NorthAmerica	Coventry,UK	Coventry,USA	Long	Medium	Medium	Sequential	
	114	a	400	30	4	1.5	Europe	NorthAmerica	Coventry,UK	Coventry,USA	Long	Medium	Medium	Sequential	
	115	a	400	30	2	1.5	Europe	NorthAmerica	Coventry,UK	Coventry,USA	Long	Medium	Medium	Sequential	
	116	a	400	50	8	1.5	Europe	NorthAmerica	Coventry,UK	Coventry,USA	Long	Medium	Medium	Sequential	
	117	a	400	50	6	1.5	Europe	NorthAmerica	Coventry,UK	Coventry,USA	Long	Medium	Medium	Sequential	
	118	a	400	50	4	1.5	Europe	NorthAmerica	Coventry,UK	Coventry,USA	Long	Medium	Medium	Sequential	
	119	a	400	50	2	1.5	Europe	NorthAmerica	Coventry,UK	Coventry,USA	Long	Medium	Medium	Sequential	
	120	a	400	70	8	1.5	Europe	NorthAmerica	Coventry,UK	Coventry,USA	Long	Medium	Medium	Sequential	
	121	a	400	70	6	1.5	Europe	NorthAmerica	Coventry,UK	Coventry,USA	Long	Medium	Medium	Sequential	
	122	a	400	70	4	1.5	Europe	NorthAmerica	Coventry,UK	Coventry,USA	Long	Medium	Medium	Sequential	
	123	a	400	70	2	1.5	Europe	NorthAmerica	Coventry,UK	Coventry,USA	Long	Medium	Medium	Sequential	Part 2
	124	a	400	90	8	1.5	Europe	NorthAmerica	Coventry,UK	Coventry,USA	Long	Medium	Medium	Sequential	
	125	a	400	90	6	1.5	Europe	NorthAmerica	Coventry,UK	Coventry,USA	Long	Medium	Medium	Sequential	
	126	a	400	90	4	1.5	Europe	NorthAmerica	Coventry,UK	Coventry,USA	Long	Medium	Medium	Sequential	
	127	a	400	90	2	1.5	Europe	NorthAmerica	Coventry,UK	Coventry,USA	Long	Medium	Medium	Sequential	

23	128	a	400	30	10	1	Europe	NorthAmerica	Coventry,UK	Coventry,USA	Long	Medium	Medium	Sequential	Part 2
	129	a	400	30	10	0.5	Europe	NorthAmerica	Coventry,UK	Coventry,USA	Long	Medium	Medium	Sequential	
	130	a	400	50	10	1	Europe	NorthAmerica	Coventry,UK	Coventry,USA	Long	Medium	Medium	Sequential	
	131	a	400	50	10	0.5	Europe	NorthAmerica	Coventry,UK	Coventry,USA	Long	Medium	Medium	Sequential	
	132	a	400	70	10	1	Europe	NorthAmerica	Coventry,UK	Coventry,USA	Long	Medium	Medium	Sequential	
	133	a	400	70	10	0.5	Europe	NorthAmerica	Coventry,UK	Coventry,USA	Long	Medium	Medium	Sequential	
	134	a	400	90	10	1	Europe	NorthAmerica	Coventry,UK	Coventry,USA	Long	Medium	Medium	Sequential	
	135	a	400	90	10	0.5	Europe	NorthAmerica	Coventry,UK	Coventry,USA	Long	Medium	Medium	Sequential	
24	136	a	400	30	10	1.5	Asia	Australia	Chennai, India	Melbourne, Australia	Medium	Medium	Medium	Sequential	Part 2
	137	a	400	30	10	1.5	Asia	Europe	Chennai, India	Munich, Germany	Long	Medium	Medium	Sequential	
	138	a	400	50	10	1.5	Asia	Australia	Chennai, India	Melbourne, Australia	Medium	Medium	Medium	Sequential	
	139	a	400	50	10	1.5	Asia	Europe	Chennai, India	Munich, Germany	Long	Medium	Medium	Sequential	
	140	a	400	70	10	1.5	Asia	Australia	Chennai, India	Melbourne, Australia	Medium	Medium	Medium	Sequential	
	141	a	400	70	10	1.5	Asia	Europe	Chennai, India	Munich, Germany	Long	Medium	Medium	Sequential	
	142	a	400	90	10	1.5	Asia	Australia	Chennai, India	Melbourne, Australia	Medium	Medium	Medium	Sequential	
	143	a	400	90	10	1.5	Asia	Europe	Chennai, India	Munich, Germany	Long	Medium	Medium	Sequential	
25	144	a	400	30	10	1.5	NorthAmerica	Asia	Houston,Texas, US	Shanghai, China	Long	Medium	Medium	Sequential	Part 2
	145	a	400	30	10	1.5	Europe	Asia	Copenhagen, Denmark	Shanghai, China	Long	Highest	Medium	Sequential	
	146	a	400	50	10	1.5	NorthAmerica	Asia	Houston,Texas, US	Shanghai, China	Long	Medium	Medium	Sequential	
	147	a	400	50	10	1.5	Europe	Asia	Copenhagen, Denmark	Shanghai, China	Long	Highest	Medium	Sequential	
	148	a	400	70	10	1.5	NorthAmerica	Asia	Houston,Texas, US	Shanghai, China	Long	Medium	Medium	Sequential	
	149	a	400	70	10	1.5	Europe	Asia	Copenhagen, Denmark	Shanghai, China	Long	Highest	Medium	Sequential	
	150	a	400	90	10	1.5	NorthAmerica	Asia	Houston,Texas, US	Shanghai, China	Long	Medium	Medium	Sequential	
	151	a	400	90	10	1.5	Europe	Asia	Copenhagen, Denmark	Shanghai, China	Long	Highest	Medium	Sequential	
26	152	a	400	30	10	1.5	NorthAmerica	Europe	Houston,Texas, US	Munich, Germany	Long	Medium	Medium	Sequential	
	153	a	400	30	10	1.5	Asia	Europe	Tokyo,Japan	Munich, Germany	Long	Medium	Highest	Sequential	
	154	a	400	50	10	1.5	NorthAmerica	Europe	Houston,Texas, US	Munich, Germany	Long	Medium	Medium	Sequential	
	155	a	400	50	10	1.5	Asia	Europe	Tokyo,Japan	Munich, Germany	Long	Medium	Highest	Sequential	
	156	a	400	70	10	1.5	NorthAmerica	Europe	Houston,Texas, US	Munich, Germany	Long	Medium	Medium	Sequential	
	157	a	400	70	10	1.5	Asia	Europe	Tokyo,Japan	Munich, Germany	Long	Medium	Highest	Sequential	
	158	a	400	90	10	1.5	NorthAmerica	Europe	Houston,Texas, US	Munich, Germany	Long	Medium	Medium	Sequential	
	159	a	400	90	10	1.5	Asia	Europe	Tokyo,Japan	Munich, Germany	Long	Medium	Highest	Sequential	

27	**160**	a	400	10	8	1	Europe	NorthAmerica	Coventry,UK	Coventry,USA	Long	Medium	Medium	Sequential	Part 2
	161	a	400	10	8	0.5	Europe	NorthAmerica	Coventry,UK	Coventry,USA	Long	Medium	Medium	Sequential	
	162	a	400	10	6	1	Europe	NorthAmerica	Coventry,UK	Coventry,USA	Long	Medium	Medium	Sequential	
	163	a	400	10	6	0.5	Europe	NorthAmerica	Coventry,UK	Coventry,USA	Long	Medium	Medium	Sequential	
	164	a	400	10	4	1	Europe	NorthAmerica	Coventry,UK	Coventry,USA	Long	Medium	Medium	Sequential	
	165	a	400	10	4	0.5	Europe	NorthAmerica	Coventry,UK	Coventry,USA	Long	Medium	Medium	Sequential	
	166	a	400	10	2	1	Europe	NorthAmerica	Coventry,UK	Coventry,USA	Long	Medium	Medium	Sequential	
	167	a	400	10	2	0.5	Europe	NorthAmerica	Coventry,UK	Coventry,USA	Long	Medium	Medium	Sequential	
28	**168**	a	400	10	8	1.5	Asia	Australia	Chennai, India	Melbourne, Australia	Medium	Medium	Medium	Sequential	Part 2
	169	a	400	10	8	1.5	Asia	Europe	Chennai, India	Munich, Germany	Long	Medium	Medium	Sequential	
	170	a	400	10	6	1.5	Asia	Australia	Chennai, India	Melbourne, Australia	Medium	Medium	Medium	Sequential	
	171	a	400	10	6	1.5	Asia	Europe	Chennai, India	Munich, Germany	Long	Medium	Medium	Sequential	
	172	a	400	10	4	1.5	Asia	Australia	Chennai, India	Melbourne, Australia	Medium	Medium	Medium	Sequential	
	173	a	400	10	4	1.5	Asia	Europe	Chennai, India	Munich, Germany	Long	Medium	Medium	Sequential	
	174	a	400	10	2	1.5	Asia	Australia	Chennai, India	Melbourne, Australia	Medium	Medium	Medium	Sequential	
	175	a	400	10	2	1.5	Asia	Europe	Chennai, India	Munich, Germany	Long	Medium	Medium	Sequential	
29	**176**	a	400	10	8	1.5	NorthAmerica	Asia	Houston,Texas, US	Shanghai, China	Long	Medium	Medium	Sequential	Part 2
	177	a	400	10	8	1.5	Europe	Asia	Copenhagen, Denmark	Shanghai, China	Long	Highest	Medium	Sequential	
	178	a	400	10	6	1.5	NorthAmerica	Asia	Houston,Texas, US	Shanghai, China	Long	Medium	Medium	Sequential	
	179	a	400	10	6	1.5	Europe	Asia	Copenhagen, Denmark	Shanghai, China	Long	Highest	Medium	Sequential	
	180	a	400	10	4	1.5	NorthAmerica	Asia	Houston,Texas, US	Shanghai, China	Long	Medium	Medium	Sequential	
	181	a	400	10	4	1.5	Europe	Asia	Copenhagen, Denmark	Shanghai, China	Long	Highest	Medium	Sequential	
	182	a	400	10	2	1.5	NorthAmerica	Asia	Houston,Texas, US	Shanghai, China	Long	Medium	Medium	Sequential	
	183	a	400	10	2	1.5	Europe	Asia	Copenhagen, Denmark	Shanghai, China	Long	Highest	Medium	Sequential	
30	**184**	a	400	10	8	1.5	NorthAmerica	Europe	Houston,Texas, US	Munich, Germany	Long	Medium	Medium	Sequential	
	185	a	400	10	8	1.5	Asia	Europe	Tokyo,Japan	Munich, Germany	Long	Medium	Highest	Sequential	
	186	a	400	10	6	1.5	NorthAmerica	Europe	Houston,Texas, US	Munich, Germany	Long	Medium	Medium	Sequential	
	187	a	400	10	6	1.5	Asia	Europe	Tokyo,Japan	Munich, Germany	Long	Medium	Highest	Sequential	
	188	a	400	10	4	1.5	NorthAmerica	Europe	Houston,Texas, US	Munich, Germany	Long	Medium	Medium	Sequential	
	189	a	400	10	4	1.5	Asia	Europe	Tokyo,Japan	Munich, Germany	Long	Medium	Highest	Sequential	
	190	a	400	10	2	1.5	NorthAmerica	Europe	Houston,Texas, US	Munich, Germany	Long	Medium	Medium	Sequential	
	191	a	400	10	2	1.5	Asia	Europe	Tokyo,Japan	Munich, Germany	Long	Medium	Highest	Sequential	

31	192	a	400	10	10	1	Asia	Australia	Chennai, India	Melbourne, Australia	Medium	Medium	Medium	Sequential	Part 2
	193	a	400	10	10	1	Asia	Europe	Chennai, India	Munich, Germany	Long	Medium	Medium	Sequential	
	194	a	400	10	10	0.5	Asia	Australia	Chennai, India	Melbourne, Australia	Medium	Medium	Medium	Sequential	
	195	a	400	10	10	0.5	Asia	Europe	Chennai, India	Munich, Germany	Long	Medium	Medium	Sequential	
32	196	a	400	10	10	1	NorthAmerica	Asia	Houston,Texas, US	Shanghai, China	Long	Medium	Medium	Sequential	
	197	a	400	10	10	1	Europe	Asia	Copenhagen, Denmark	Shanghai, China	Long	Highest	Medium	Sequential	
	198	a	400	10	10	0.5	NorthAmerica	Asia	Houston,Texas, US	Shanghai, China	Long	Medium	Medium	Sequential	
	199	a	400	10	10	0.5	Europe	Asia	Copenhagen, Denmark	Shanghai, China	Long	Highest	Medium	Sequential	
33	200	a	400	10	10	1	NorthAmerica	Europe	Houston,Texas, US	Munich, Germany	Long	Medium	Medium	Sequential	
	201	a	400	10	10	1	Asia	Europe	Tokyo,Japan	Munich, Germany	Long	Medium	Highest	Sequential	
	202	a	400	10	10	0.5	NorthAmerica	Europe	Houston,Texas, US	Munich, Germany	Long	Medium	Medium	Sequential	
	203	a	400	10	10	0.5	Asia	Europe	Tokyo,Japan	Munich, Germany	Long	Medium	Highest	Sequential	Part 2

Appendix – D

Table 114: Case studies and corresponding parameters analysed in each case study

Methods	Case Study	Parameters
OAT	1	Geometry
	2	Production Quantity
	3	Recycled Content
	4	Maximum component cost
	5	Maximum component CO_2
	6	Travel Distance
	7	Labour Cost
	8	Overhead Cost
TAT	9	Geometry and Production Quantity
	10	Geometry and Recycled Content
	11	Geometry and Maximum component cost
	12	Geometry and Maximum component CO_2
	13	Geometry and Travel Distance
	14	Geometry and Labour Cost
	15	Geometry and Overhead Cost
	16	Production Quantity and Recycled Content
	17	Production Quantity and Maximum component cost
	18	Production Quantity and Maximum component CO_2
	19	Production Quantity and Travel Distance
	20	Production Quantity and Labour Cost
	21	Production Quantity and Overhead Cost
	22	Recycled Content and Maximum component cost
	23	Recycled Content and Maximum component CO_2
	24	Recycled Content and Travel Distance
	25	Recycled Content and Labour Cost
	26	Recycled Content and Overhead Cost
	27	Maximum component CO_2 and Maximum component cost
	28	Maximum component cost and Travel Distance
	29	Maximum component cost and Labour Cost
	30	Maximum component cost and Overhead Cost
	31	Maximum component CO_2 and Travel Distance
	32	Maximum component CO_2 and Labour Cost
	33	Maximum component CO_2 and Overhead Cost

Appendix – E

9.1.1 Results based on the average change of the objective function values

The average COFV across the 203 models of each of the 7 OMS is calculated based on Equation (4.1). The 7 OMS are ranked from the lowest COFV to the highest average COFV in Table 115.

Table 115: The ranked 7 OMS based on the average COFV – ABC – HOS 1

Rank	OMS	Objective function value changes (Average – ABC)
1	SEQ5-MII	0.15
2	SEQ3-MII	0.31
3	SEQ1-MII	0.35
4	PAR-MII	0.50
5	SEQ6-MII	0.79
6	SEQ2-MII	0.81
7	SEQ4-MII	0.83

The following trends are observed from Table 115:

HOS1-Avg-ABC 1. The 7 OMS can be categorised into 3 Groups based on the range of the average COFV of each OMS. The three groups of OMS are tabulated in Table 116, which for convenience also contains the specific OMS order and the range of average COFV.

Table 116: The 7 OMS grouped by the range of average COFV – ABC -HOS 1

Group D				
OMS Name	**SEQ1-MII**	**SEQ3-MII**	**SEQ5-MII**	**Range of objective function value change**
Module Sequence	STRUCTURAL	COST	COST	**Below 0.4**
	COST	CO2	STRUCTURAL	
	CO2	STRUCTURAL	CO2	
Group E				
OMS Name	**SEQ2-MII**	**SEQ4-MII**	**SEQ6-MII**	**Above 0.7**
Module Sequence	STRUCTURAL	CO2	CO2	
	CO2	COST	STRUCTURAL	
	COST	STRUCTURAL	COST	
Group F				
OMS Name	**PAR-MII**			**Between 0.4 and 0.7**
Module Sequence	Parallel			

HOS1-Avg-ABC 2. The SEQ1-MII, SEQ3-MII and SEQ5-MII (in Group D) have a smaller average COFV than the OMS in the other groups which indicates that the OMS in Group D outperform the OMS in the other two groups.

HOS1-Avg-ABC 3. The three OMS in Group D optimise the COST module before the CO2 module compared to the OMS orders of the other OMS. This trend is also found in section 4.3. It is also suggested that this is the reason SEQ1-MII, SEQ3-MII and SEQ5-MII outperform SEQ2-MII, SEQ4-MII and SEQ6-MII.

HOS1-Avg-ABC 4. SEQ5-MII has the smallest average COFV while the SEQ4-MII has the largest average COFV. This indicates that the results of SEQ5-MII outperform the other 6 OMS while the results of SEQ4-MII underperform the other OMS.

HOS1-Avg-ABC 5. The PAR-MII has a ‘medium’ level performance which is the same as discovered in section 4.3.

The general trends of the 7 OMS based on the average COFV are nearly the same as the trends found in subsection 4.3.1. To further analyse the trends of the 7 OMS based on the ABC method, the maximum COFV for each OMS is studied in the next subsection.

9.1.2 Results based on the minimum change of the objective function values

Similar to the maximum COFV, the minimum COFV is the minimum value of the 203 COFVs for each of the 7 OMS. The 7 OMS are ranked based on the minimum COFVs in Table 117, i.e. from the lowest to the highest.

Table 117: The ranked 7 OMS based on the minimum COFV – ABC – HOS 1

Rank	OMS	Objective function value changes (Minimum – ABC)
1	SEQ1-MII	0.005
2	SEQ3-MII	0.010
3	SEQ5-MII	0.014
4	PAR-MII	0.042
5	SEQ6-MII	0.090
6	SEQ2-MII	0.213
7	SEQ4-MII	0.235

The following trends are found from Table 117:

HOS1-Min-ABC 1. The 7 OMS can be categorised into 3 Groups based on the range of the minimum COFV of each OMS. The three groups are the same as the groups defined in Table 116 although the ranking of the top three OMS is slightly different.

HOS1-Min-ABC 2. SEQ1-MII, SEQ3-MII and SEQ5-MII have smaller minimum COFV than the other OMS. It indicates that the results of these three OMS are closer to the absolute optimum solution than the results of other OMS.

HOS1-Min-ABC 3. SEQ1-MII, SEQ3-MII and SEQ5-M optimise the COST module before the CO2 module compared to the orders of the other OMS. This trend is also found in section 4.3. It is also suggested that this is the reason SEQ1-MII, SEQ3-MII and SEQ5-MII outperform SEQ2-MII, SEQ4-MII and SEQ6-MII.

HOS1-Min-ABC 4. SEQ5-MII has the smallest minimum COFV while the SEQ4-MII has the largest. This indicates that the results of SEQ5-MII outperform the other 6 OMS while the results of SEQ4-MII underperform the other OMS. This is same as the trend found in subsection 9.

HOS1-Min-ABC 5. The PAR-MII is still ranked in the middle of the SEQ optimisation programmes which indicates it has a ‘medium’ level COFV. This is same as the trend discovered in section 4.3.

9.1.3 Results based on the average spreads of objective function value change

The average spread of COFV for each of the 7 OMS is calculated based on Equation (4.2) as defined in subsection 4.3.4. The 7 OMS are ranked based on the average spread of COFV in Table 118, i.e. from the lowest to the highest.

Table 118: The average spreads of the 7 OMS – ABC – HOS 1

Rank	OMS	Average Spreads – ABC
1	SEQ3-MII	0.06
2	SEQ5-MII	0.06
3	SEQ1-MII	0.06
4	PAR-MII	0.13
5	SEQ4-MII	0.15
6	SEQ6-MII	0.18
7	SEQ2-MII	0.22

The ranking of the 7 OMS in Table 118 shows the following trends:

HOS1-ASp-ABC 1. The top three ranked OMS have the same value which indicates that the results of these three OMS have the same sensitivity to the change of input parameter(s).

HOS1-ASp-ABC 2. The OMS ranked from the 4th to 7th have larger average spreads which indicates that the results of these four OMS are more sensitive to the change of input parameter(s) than SEQ1-MII, SEQ3-MII and SEQ5-MII.

HOS1-ASp-ABC 3. For the 6 SEQ optimisation programmes, the results of SEQ1-MII, SEQ3-MII and SEQ5-MII are more stable than those of SEQ2-MII, SEQ4-MII and SEQ6-MII. This can be explained by their different OMS orders as defined in HOS1-Min-ABC 3 of subsection 9.1.2.

The PAR-MII shows different sensitivity compared to its ranking in Table 49. The results of the PAR-MII based on the ABC method are less sensitive to the change of input parameter(s) than its results evaluated by the ICE method. That the two evaluation methods are different in nature could be the reason to explain that difference.

9.1.4 Summary of the general trends – ABC – HOS 1

The results analysis of the 7 OMS is based the ABC method in this section. It is found that most of the general trends of the 7 OMS are same as those found in section 4.3. However, some of the trends are slightly different, as the ABC method is different from the ICE method in nature. The General Trends of the 7 OMS based on the ABC method are summarised as follows:

HOS1-GT-ABC 1. The 7 OMS are categorised into three groups based on their overall performance. As defined in subsection 9, Group D contains SEQ1-MII, SEQ3-MII and SEQ5-MII; Group E contains SEQ2-MII, SEQ4-MII and SEQ6-MII; Group F contains PAR-MII.

HOS1-GT-ABC 2. The three OMS in Group D are suggested to be more stable and robust than those in Groups E and F. This is evidenced by the general trends found in subsections 4.4.1, and subsections 9.1.1, 9.1.2, 9.1.3 in Appendix – E.

HOS1-GT-ABC 3. For the SEQ optimisation programmes in Group D and E, SEQ1-MII, SEQ3-MII and SEQ5-MII in Group D always optimise the COST module before the CO2 module; while the OMS in Group E always optimise the CO2 module before the COST module. This is suggested to be the reason why the OMS in Group D outperform those in Group E.

HOS1-GT-ABC 4. SEQ2-MII is the most sensitive of the 7 OMS. However, it is considered to be indifferent as the COFV of SEQ2-MII is consistently lower than SEQ1-MII, SEQ3-MII, SEQ5-MII and PAR-MII.

HOS1-GT-ABC 5. SEQ5-MII is suggested to be the most stable and robust of the OMS. This is also found in subsection 4.3.5, i.e. HOS1-GT-ICE 4.

HOS1-GT-ABC 6. The PAR-MII shows a consistent 'medium' performance in this section. This is evidenced by the ranking of PAR-MII in Table 115, Table 50, Table 117 and Table 118.

As defined above, nearly all the general trends found in section 4.3.5 are verified in this subsection. The next section will continue to analyse the results of the 7 OMS based on the INC method. The extracted general trends will be compared with the trends discovered in this section and in section 4.3.

Appendix – F

9.1.5 Results based on the average change of the objective function values

The average COFV of each of the 7 OMS based on the INC method is calculated by Equation (4.1). The 7 OMS are ranked based on the average COFV in Table 119, from the highest to the lowest.

Table 119: The ranked 7 OMS based on the average COFV – INC – HOS1

Rank	OMS	Objective function value changes (Average – INC)
1	SEQ5-MII	1.63
2	SEQ6-MII	1.61
3	SEQ3-MII	1.55
4	SEQ1-MII	1.53
5	SEQ4-MII	1.51
6	PAR-MII	1.48
7	SEQ2-MII	1.13

According to the ranking of the 7 OMS in Table 119, the following trends are found:

HOS1-Avg-INC 1. SEQ2-MII is ranked 7th and its average COFV is much lower than the average COFV SEQ5-MII, i.e. about 44%. This indicates that SEQ2-MII underperforms the other OMS based on the average COFV.

HOS1-Avg-INC 2. The 6 SEQ optimisation programmes cannot be categorised into three groups as defined in subsection 4.3.1. This indicates that no further trends can be found based on the average COFVs and the OMS orders.

SEQ5-MII outperforms the other OMS but the difference of the average COFV between SEQ5-MII and PAR-MII (0.15) is even less than the difference between PAR-MII and SEQ2-MII (0.35). This indicates that the performance of the OMS ranked from the 1st to 6th is not significantly different.

9.1.6 Results based on the minimum change of objective function values

The minimum COFV of each OMS is summarised and ranked from the highest to the lowest in Table 120.

Table 120: The ranked 7 OMS based on the minimum COFV – INC – HOS1

Rank	OMS	Objective function value changes (Minimum – INC)
1	SEQ5-MII	1.51
2	SEQ3-MII	1.45
3	SEQ1-MII	1.41
4	PAR-MII	1.33
5	SEQ6-MII	1.30
6	SEQ4-MII	1.18
7	SEQ2-MII	0.96

The following trends are obtained from Table 120:

HOS1-Min-INC 1. SEQ2-MII still underperforms the other OMS as it is ranked 7th in Table 120.

HOS1-Min-INC 2. SEQ5-MII outperforms the other OMS as it has the highest minimum COFV.

HOS1-Min-INC 3. The ranking of the 7 OMS in Table 120 is nearly the same as in Table 45 and Table 115. This indicates that SEQ1-MII, SEQ3-MII and SEQ5-MII outperform SEQ2-

MII, SEQ4-MII and SEQ6-MII.

HOS1-Min-INC 4. SEQ1-MII, SEQ3-MII and SEQ5-MII always optimise the COST module before the CO2 module; while SEQ2-MII, SEQ4-MII and SEQ6-MII always optimise the CO2 module before the COST module. This trend indicates how the pattern of the OMS order influences the performance of the 7 OMS. This trend was also found in Table 45 and Table 115.

HOS1-Min-INC 5. The PAR-MII is now ranked 4th in the middle of the 7 OMS. However, its minimum COFV is still lower than the values of SEQ1-MII, SEQ3-MII and SEQ5-MII. This is the same trend as that found in Table 45 and Table 115.

9.1.7 Results based on average spreads of the objective function value change

The average spread of the COFV for each of the 7 OMS is calculated by Equation (4.2). The 7 OMS are ranked in Table 121 based on the average spread, from the lowest to the highest.

Table 121: The average spreads of the 7 OMS – INC – HOS1

Rank	OMS	Average Spreads – INC
1	SEQ5-MII	0.05
2	SEQ1-MII	0.05
3	SEQ3-MII	0.05
4	PAR-MII	0.08
5	SEQ6-MII	0.08
6	SEQ4-MII	0.09
7	SEQ2-MII	0.10

The trends observed from Table 121 are summarised below:

HOS1-ASp-INC 1. The top three ranked OMS have the same value which indicates that the results of these three OMS have the same sensitivity to the change of input parameter(s). This was also discovered in HOS1-ASp-ABC 1 in subsection 9.1.4.

HOS1-ASp-INC 2. The OMS ranked from 4th to 7th have larger average spreads which indicates that the results of these four OMS are more sensitive to the change of input parameter(s) than SEQ1-MII, SEQ3-MII and SEQ5-MII.

HOS1-ASp-INC 3. For the 6 SEQ optimisation programmes, the results of SEQ1-MII, SEQ3-MII and SEQ5-MII are more stable than the results of SEQ2-MII, SEQ4-MII and SEQ6-MII. This can be explained by their different OMS orders as defined in HOS1-Min-ABC 3 of subsection 9.1.2.

The PAR-MII has same value as SEQ6-MII which indicates that the results sensitivity of these two OMS is the same.

9.1.8 Summary of general trends – INC – HOS 1

The overall general trends of the 7 OMS based on the INC method are summarised in this section as follows:

HOS1-GT-INC 1. The overall performance of SEQ1-MII, SEQ3-MII and SEQ5-MII is suggested to outperform SEQ2-MII, SEQ4-MII and SEQ6-MII. This is evidenced by the overall ranking of SEQ1-MII, SEQ3-MII and SEQ5-MII being consistently higher than SEQ2-MII, SEQ4-MII and SEQ6-MII in Table 119, Table 51, Table 120, and Table 121. This was also discovered in the previous two sections (section 4.3 and 4.4).

HOS1-GT-INC 2. SEQ5-MII is suggested to be more stable and robust than the other OMS. This is evidenced by the following general trends: HOS1-Avg-INC 1, HOS1-Min-INC 1 and HOS1-ASp-INC 1.

HOS1-GT-INC 3. SEQ1-MII, SEQ3-MII and SEQ5-MII always optimise the COST module before the CO2 module; while SEQ2-MII, SEQ4-MII and SEQ6-MII always optimise the CO2 module before the COST module. This is suggested to be the reason why the SEQ optimisation programmes have a different performance.

HOS1-GT-INC 4. SEQ2-MII is the most sensitive of the 7 OMS. However, it is considered to be indifferent as the COFV of SEQ2-MII is consistently lower than the other OMS in this section.

The PAR-MII shows different performance based on the analysis of different types of COFV. However, the PAR-MII in each subsection is consistently ranked at the bottom of the 7 OMS, i.e. the best ranking is 4th. Therefore, the PAR-MII is not considered to be a high-performance OMS based on the INC method.

Appendix – G

9.1.9 Fit model based on ABC results – HOS2

By applying the LSR method to the ABC results of the 7 OMS, the R-Square values are extracted and summarised in Table 122. The R-Square values of the 7 OMS in Table 122 are similar to the values in Table 103, i.e. they are feasible but not represent the good Fit quality as defined in subsection 6.1.1.

Table 122: R-Square values of the 7 OMS – ABC – HOS2

OMS names	SEQ1-MII	SEQ2-MII	SEQ3-MII	SEQ4-MII	SEQ5-MII	SEQ6-MII	PAR-MII
R-Square	0.8911	0.8923	0.7382	0.7687	0.8039	0.7769	0.8041

To determine which parameter is the most influential parameter of each of the 7 OMS, the top three MSP values for the 7 OMS are ranked and tabulated in Table 123.

Table 123: Top ranked influential parameters for the 7 OMS – DOE – ABC – HOS2

Rank		1	2	3
SEQ1-MII	Variables	Production quantity	Recycled content (%)	Maximum component cost (GBP/unit)
	MSP	20.5	8.6	8.4
SEQ2-MII	Variables	Production quantity	Maximum component cost (GBP/unit)	Production quantity, Recycled content (%)
	MSP	20.6	8.5	5.4
SEQ3-MII	Variables	Production quantity	Maximum component cost (GBP/unit)	Recycled content (%)
	MSP	17.7	7.3	7.3
SEQ4-MII	Variables	Production quantity	Recycled content (%)	Maximum component cost (GBP/unit)
	MSP	19.8	8.8	8.2
SEQ5-MII	Variables	Production quantity	Recycled content (%)	Maximum component cost (GBP/unit)
	MSP	18.0	9.1	7.4
SEQ6-MII	Variables	Production quantity	Recycled content (%)	Maximum component cost (GBP/unit)
	MSP	18.9	8.2	7.8
PAR-MII	Variables	Production quantity	Recycled content (%)	Maximum component cost (GBP/unit)
	MSP	19.0	8.3	7.8

By observing Table 123, the most influential parameters of the 7 OMS are the production quantity. Furthermore, the ICE results of the 7 OMS have nearly the same MSP values. This indicates that the results of the 7 OMS have the similar sensitivity to the change of production quantity. Another trend is the top three influential parameters of the 7 OMS are same, i.e. production quantity, recycled content and Maximum component cost. The general trends indicated above are the same as the trends observed in Table 104. To further investigate the influential parameters for the 7 OMS, the INC results are studied in the next subsection.

9.1.10 Fit model based on INC results – HOS2

Similar to the subsection 0, the fit quality of the response surfaces for the 7 OMS will be assessed by the R-Square values. The R-Square values of each of the 7 OMS are summarised in Table 124. The Fit quality of the

7 OMS based on the R-Square values is similar to the Fit quality defined in Table 103 and Table 122.

Table 124: R-Square values of the 7 OMS – INC – HOS2

OMS names	SEQ1-MII	SEQ2-MII	SEQ3-MII	SEQ4-MII	SEQ5-MII	SEQ6-MII	PAR-MII
R-Square	0.8681	0.8899	0.7751	0.7881	0.8752	0.8130	0.8744

In order to investigate the influence of the parameters for each of the 7 OMS, the MSP values are ranked in descending order, and for convenience, the corresponding parameters are also tabulated in Table 125.

Table 125: Top ranked influential parameters for the 7 OMS – DOE – INC – HOS2

Rank		1	2	3
SEQ1-MII	Variables	Production quantity	Recycled content (%)	Maximum component cost (GBP/unit)
	MSP	12.8	6.7	4.9
SEQ2-MII	Variables	Production quantity	Recycled content (%)	Geometry
	MSP	11.8	5.9	5.0
SEQ3-MII	Variables	Geometry, Recycled content (%)	Geometry, Maximum component cost (GBP/unit)	Recycled content (%)
	MSP	27.5	21.4	7.8
SEQ4-MII	Variables	Geometry, Recycled content (%)	Geometry, Maximum component cost (GBP/unit)	Production quantity
	MSP	20.4	14.0	8.7
SEQ5-MII	Variables	Geometry, Recycled content (%)	Production quantity	Recycled content (%)
	MSP	21.3	9.2	8.2
SEQ6-MII	Variables	Geometry, Recycled content (%)	Geometry, Maximum component cost (GBP/unit)	Production quantity
	MSP	23.8	14.7	7.6
PAR-MII	Variables	Geometry, Recycled content (%)	Recycled content (%)	Production quantity
	MSP	21.4	9.6	9.0

According to Table 125, the most influential parameters (i.e. ranked 1st) for each of the 7 OMS are different. The most influential parameter for SEQ1-MII and SEQ2-MII is production quantity. This is the same as the trend observed in Table 104 and Table 123. However, the most influential parameters for all other OMS in Table 125 are the geometry and recycled content. In order to compare and assess the influential parameters observed in subsections 0, 9.1.9 and 9.1.10, a summary of this section is created subsequently.

Appendix – H

Country fuel costs				British Pound to US Dollar foreign exchange rate (0.64 : 1) was taken on 21/08/2015											
	Electricity cost - commercial		Electricity cost - domestic		Gasoline		Diesel		LPG		Kerosene		Domestic		Commercial	
	GBP/MJ	GBP/MJ	GBP/MJ	GBP/MJ	GBP/m3		GBP/m3		GBP/m3		GBP/MJ		GBP/m3		GBP/kg	
World	0.0192	0.0256	0.0320	0.0320	833.1584	833.1584	780.6656	780.6656	381.3504	482.2976	0.0147	0.0147	613.9904	676.9088	0.3916	0.4299
Europe	0.0256	0.0256	0.0384	0.0384	1277.6320	1277.6320	1235.3600	1235.3600	663.9872	684.1280	0.0147	0.0147	847.0976	855.3216	0.4897	0.4947
Former USSR	0.0064	0.0128	0.0064	0.0256	660.0128	660.0128	631.5520	631.5520	296.2176	387.0080	0.0147	0.0147	388.1472	535.5904	0.2364	0.3262
North America	0.0192	0.0192	0.0192	0.0192	640.2240	640.2240	673.3760	673.3760	279.8720	391.3088	0.0147	0.0147	691.4048	697.3248	0.4453	0.4489
South America	0.0192	0.0192	0.0256	0.0256	762.6816	762.6816	598.1952	598.1952	333.4016	466.1504	0.0147	0.0147	460.6208	630.6560	0.2802	0.3837
Asia	0.0192	0.0192	0.0192	0.0256	824.3520	824.3520	705.3952	705.3952	350.8352	483.2256	0.0147	0.0147	501.0112	617.4528	0.3451	0.4160
Oceania	0.0256	0.0384	0.0384	0.0640	915.5136	915.5136	961.3056	961.3056	400.2112	559.5648	0.0147	0.0147	546.0992	728.2048	0.3326	0.4435
Middle East	0.0192	0.0192	0.0192	0.0320	382.6880	382.6880	332.6912	332.6912	178.0352	213.3312	0.0147	0.0147	306.9504	355.8976	0.1911	0.2209
Australia	0.0256	0.0448	0.0384	0.0704	889.6000	889.6000	1004.8000	1004.8000	388.8832	543.7248	0.0147	0.0147	524.2432	738.9888	0.3193	0.4500
Austria	0.0256	0.0256	0.0448	0.0448	1158.4000	1158.4000	1158.4000	1158.4000	695.4496	695.4496	0.0147	0.0147	822.5984	822.5984	0.5043	0.5043
Belgium	0.0192	0.0192	0.0448	0.0448	1337.6000	1337.6000	1267.2000	1267.2000	536.1664	536.1664	0.0147	0.0147	739.1168	739.1168	0.4606	0.4606
Brazil	0.0192	0.0192	0.0320	0.0320	889.6000	889.6000	652.8000	652.8000	388.8832	543.7248	0.0147	0.0147	524.2432	738.9888	0.3193	0.4500
Canada	0.0064	0.0128	0.0128	0.0192	844.8000	844.8000	787.2000	787.2000	369.2992	516.3456	0.0147	0.0147	859.0144	859.0144	0.5231	0.5231
China	0.0064	0.0128	0.0128	0.0192	876.8000	876.8000	819.2000	819.2000	383.2896	535.9040	0.0147	0.0147	516.6976	728.3584	0.3147	0.4436
Czech Republic	0.0256	0.0256	0.0384	0.0384	1235.2000	1235.2000	1196.8000	1196.8000	548.3520	548.3520	0.0147	0.0147	802.8544	802.8544	0.3547	0.3547
Denmark	0.0192	0.0192	0.0704	0.0704	1292.8000	1292.8000	1209.6000	1209.6000	1053.1840	1053.1840	0.0147	0.0147	1301.2224	1301.2224	0.5797	0.5797
Finland	0.0192	0.0192	0.0384	0.0384	1331.2000	1331.2000	1248.0000	1248.0000	581.9328	813.6320	0.0147	0.0147	953.6512	953.6512	0.5807	0.5807
France	0.0192	0.0192	0.0320	0.0320	1222.4000	1222.4000	1139.2000	1139.2000	754.6368	754.6368	0.0147	0.0147	815.5392	815.5392	0.4827	0.4827
Germany	0.0256	0.0256	0.0576	0.0576	1254.4000	1254.4000	1203.2000	1203.2000	628.4288	628.4288	0.0147	0.0147	728.0832	728.0832	0.4503	0.4503
Greece	0.0256	0.0256	0.0320	0.0320	1318.4000	1318.4000	1331.2000	1331.2000	735.4880	735.4880	0.0147	0.0147	1099.2768	1099.2768	0.5194	0.5194
Hungary	0.0256	0.0256	0.0384	0.0384	1177.6000	1177.6000	1222.4000	1222.4000	682.3936	682.3936	0.0147	0.0147	960.0000	960.0000	0.4678	0.4678
Iceland	0.0128	0.0128	0.0192	0.0192	1273.6000	1273.6000	1318.4000	1318.4000	556.7488	778.4256	0.0147	0.0147	750.5344	1057.9776	0.4571	0.6443
India	0.0064	0.0128	0.0128	0.0192	800.0000	800.0000	550.4000	550.4000	349.7152	488.9600	0.0147	0.0147	471.4432	664.5632	0.2871	0.4047
Ireland	0.0256	0.0256	0.0448	0.0448	1292.8000	1292.8000	1267.2000	1267.2000	678.0416	678.0416	0.0147	0.0147	927.1232	927.1232	0.7249	0.7249
Italy	0.0320	0.0320	0.0512	0.0512	1459.2000	1459.2000	1395.2000	1395.2000	649.3184	649.3184	0.0147	0.0147	1218.8480	1218.8480	0.5618	0.5618
Japan	0.0320	0.0320	0.0512	0.0512	1280.0000	1280.0000	1030.4000	1030.4000	559.5456	782.3360	0.0147	0.0147	692.6976	692.6976	0.6089	0.6089
South Korea	0.0128	0.0128	0.0192	0.0192	1152.0000	1152.0000	1043.2000	1043.2000	503.5904	704.1024	0.0147	0.0147	817.2736	817.2736	0.5861	0.5861
Mexico	0.0192	0.0192	0.0192	0.0192	550.4000	550.4000	544.0000	544.0000	240.6080	336.4032	0.0147	0.0147	596.6656	596.6656	0.3634	0.3634
Netherlands	0.0192	0.0192	0.0448	0.0448	1491.2000	1491.2000	1248.0000	1248.0000	651.8720	911.4240	0.0147	0.0147	768.0000	768.0000	0.4379	0.4379
New Zealand	0.0192	0.0192	0.0384	0.0384	1132.8000	1132.8000	793.6000	793.6000	495.2000	692.3712	0.0147	0.0147	713.8752	713.8752	0.4347	0.4347
Norway	0.0128	0.0128	0.0256	0.0256	1619.2000	1619.2000	1504.0000	1504.0000	675.4304	675.4304	0.0147	0.0147	1126.2720	1126.2720	0.6859	0.6859
Poland	0.0192	0.0192	0.0320	0.0320	1113.6000	1113.6000	1107.2000	1107.2000	461.3120	461.3120	0.0147	0.0147	819.1040	819.1040	0.4990	0.4990
Portugal	0.0256	0.0256	0.0448	0.0448	1376.0000	1376.0000	1209.6000	1209.6000	709.3760	709.3760	0.0147	0.0147	1092.6336	1092.6336	0.6990	0.6990
Russia	0.0000	0.0128	0.0064	0.0256	633.6000	633.6000	640.0000	640.0000	276.9792	387.2576	0.0147	0.0147	373.3824	526.3296	0.2274	0.3205
Slovakia	0.0320	0.0320	0.0384	0.0384	1267.2000	1267.2000	1184.0000	1184.0000	617.9840	617.9840	0.0147	0.0147	768.0000	768.0000	0.4422	0.4422
South Africa	0.0064	0.0192	0.0128	0.0256	883.2000	883.2000	908.8000	908.8000	386.0864	539.8144	0.0147	0.0147	520.4672	733.6768	0.3170	0.4468
Spain	0.0192	0.0192	0.0448	0.0448	1120.0000	1120.0000	1120.0000	1120.0000	655.4112	655.4112	0.0147	0.0147	795.2640	795.2640	0.4814	0.4814
Sweden	0.0128	0.0128	0.0384	0.0384	1344.0000	1344.0000	1382.4000	1382.4000	852.1216	852.1216	0.0147	0.0147	1342.8096	1342.8096	0.9337	0.9337
Switzerland	0.0192	0.0192	0.0384	0.0384	1203.2000	1203.2000	1318.4000	1318.4000	762.4704	762.4704	0.0147	0.0147	705.5552	705.5552	0.4712	0.4712
Turkey	0.0256	0.0256	0.0320	0.0320	1625.6000	1625.6000	1491.2000	1491.2000	807.7312	807.7312	0.0147	0.0147	1230.0928	1230.0928	0.7870	0.7870
United Kingdom (UK)	0.0256	0.0256	0.0384	0.0384	1388.8000	1388.8000	1452.8000	1452.8000	769.4336	769.4336	0.0147	0.0147	714.7584	714.7584	0.4353	0.4353
United States	0.0192	0.0192	0.0192	0.0192	620.8000	620.8000	672.0000	672.0000	271.3792	379.4304	0.0147	0.0147	691.0912	691.0912	0.4511	0.4511

Figure 56: Country fuel costs

County energy costs

	Electricity cost - commercial		Electricity cost - domestic		Gasoline		Diesel		LPG		Kerosene		oil Domestic		Oil Commercial	
	GBP/MJ	GBP/MJ	GBP/MJ	GBP/MJ	GBP/MJ	GBP/MJ	GBP/MJ	GBP/MJ	GBP/MJ	GBP/MJ	GBP/MJ	GBP/MJ	GBP/MJ	GBP/MJ	GBP/MJ	GBP/MJ
World	0.0205	0.0224	0.0314	0.0346	0.0237	0.0237	0.0205	0.0205	0.0147	0.0186	0.0147	0.0147	0.0160	0.0179	0.0090	0.0096
Europe	0.0237	0.0237	0.0390	0.0390	0.0365	0.0365	0.0326	0.0326	0.0256	0.0262	0.0147	0.0147	0.0224	0.0224	0.0109	0.0115
Former USSR	0.0038	0.0141	0.0058	0.0230	0.0186	0.0186	0.0166	0.0166	0.0115	0.0147	0.0147	0.0147	0.0102	0.0141	0.0051	0.0077
North America	0.0205	0.0205	0.0192	0.0205	0.0186	0.0186	0.0179	0.0179	0.0109	0.0154	0.0147	0.0147	0.0179	0.0186	0.0102	0.0102
South America	0.0160	0.0179	0.0224	0.0262	0.0218	0.0218	0.0160	0.0160	0.0128	0.0179	0.0147	0.0147	0.0122	0.0166	0.0064	0.0090
Asia	0.0192	0.0224	0.0179	0.0250	0.0237	0.0237	0.0186	0.0186	0.0134	0.0186	0.0147	0.0147	0.0134	0.0160	0.0077	0.0096
Oceania	0.0230	0.0403	0.0390	0.0659	0.0262	0.0262	0.0256	0.0256	0.0154	0.0218	0.0147	0.0147	0.0141	0.0192	0.0077	0.0102
Middle East	0.0179	0.0224	0.0224	0.0307	0.0109	0.0109	0.0090	0.0090	0.0070	0.0083	0.0147	0.0147	0.0083	0.0096	0.0045	0.0051
Australia	0.0237	0.0422	0.0390	0.0710	0.0256	0.0256	0.0262	0.0262	0.0147	0.0211	0.0147	0.0147	0.0141	0.0192	0.0070	0.0102
Austria	0.0269	0.0269	0.0448	0.0448	0.0333	0.0333	0.0307	0.0307	0.0269	0.0269	0.0147	0.0147	0.0218	0.0218	0.0115	0.0115
Belgium	0.0224	0.0224	0.0442	0.0442	0.0384	0.0384	0.0333	0.0333	0.0205	0.0205	0.0147	0.0147	0.0192	0.0192	0.0102	0.0102
Brazil	0.0173	0.0173	0.0288	0.0288	0.0256	0.0256	0.0173	0.0173	0.0147	0.0211	0.0147	0.0147	0.0141	0.0192	0.0070	0.0102
Canada	0.0070	0.0128	0.0115	0.0211	0.0243	0.0243	0.0205	0.0205	0.0141	0.0198	0.0147	0.0147	0.0224	0.0224	0.0122	0.0122
China	0.0077	0.0115	0.0134	0.0198	0.0250	0.0250	0.0218	0.0218	0.0147	0.0205	0.0147	0.0147	0.0134	0.0192	0.0070	0.0102
Czech Republic	0.0256	0.0256	0.0352	0.0352	0.0352	0.0352	0.0314	0.0314	0.0211	0.0211	0.0147	0.0147	0.0211	0.0211	0.0083	0.0083
Denmark	0.0186	0.0186	0.0672	0.0672	0.0371	0.0371	0.0320	0.0320	0.0403	0.0403	0.0147	0.0147	0.0346	0.0346	0.0134	0.0134
Finland	0.0186	0.0186	0.0358	0.0358	0.0378	0.0378	0.0326	0.0326	0.0224	0.0314	0.0147	0.0147	0.0250	0.0250	0.0134	0.0134
France	0.0205	0.0205	0.0314	0.0314	0.0352	0.0352	0.0301	0.0301	0.0288	0.0288	0.0147	0.0147	0.0218	0.0218	0.0109	0.0109
Germany	0.0262	0.0262	0.0582	0.0582	0.0358	0.0358	0.0314	0.0314	0.0243	0.0243	0.0147	0.0147	0.0192	0.0192	0.0102	0.0102
Greece	0.0237	0.0237	0.0320	0.0320	0.0378	0.0378	0.0352	0.0352	0.0282	0.0282	0.0147	0.0147	0.0288	0.0288	0.0115	0.0115
Hungary	0.0237	0.0237	0.0358	0.0358	0.0339	0.0339	0.0320	0.0320	0.0262	0.0262	0.0147	0.0147	0.0250	0.0250	0.0109	0.0109
Iceland	0.0096	0.0109	0.0160	0.0179	0.0365	0.0365	0.0346	0.0346	0.0211	0.0301	0.0147	0.0147	0.0198	0.0282	0.0102	0.0147
India	0.0083	0.0128	0.0141	0.0211	0.0230	0.0230	0.0147	0.0147	0.0134	0.0186	0.0147	0.0147	0.0122	0.0173	0.0064	0.0090
Ireland	0.0275	0.0275	0.0467	0.0467	0.0371	0.0371	0.0333	0.0333	0.0262	0.0262	0.0147	0.0147	0.0243	0.0243	0.0166	0.0166
Italy	0.0314	0.0314	0.0493	0.0493	0.0416	0.0416	0.0365	0.0365	0.0250	0.0250	0.0147	0.0147	0.0320	0.0320	0.0128	0.0128
Japan	0.0346	0.0346	0.0493	0.0493	0.0365	0.0365	0.0269	0.0269	0.0218	0.0301	0.0147	0.0147	0.0179	0.0179	0.0141	0.0141
South Korea	0.0102	0.0102	0.0166	0.0166	0.0326	0.0326	0.0275	0.0275	0.0192	0.0269	0.0147	0.0147	0.0218	0.0218	0.0134	0.0134
Mexico	0.0205	0.0205	0.0160	0.0160	0.0160	0.0160	0.0141	0.0141	0.0090	0.0128	0.0147	0.0147	0.0160	0.0160	0.0083	0.0083
Netherlands	0.0205	0.0205	0.0422	0.0422	0.0429	0.0429	0.0326	0.0326	0.0250	0.0352	0.0147	0.0147	0.0205	0.0205	0.0102	0.0102
New Zealand	0.0166	0.0166	0.0410	0.0410	0.0326	0.0326	0.0211	0.0211	0.0192	0.0269	0.0147	0.0147	0.0186	0.0186	0.0096	0.0096
Norway	0.0102	0.0102	0.0243	0.0243	0.0461	0.0461	0.0397	0.0397	0.0262	0.0262	0.0147	0.0147	0.0294	0.0294	0.0154	0.0154
Poland	0.0192	0.0192	0.0339	0.0339	0.0320	0.0320	0.0294	0.0294	0.0179	0.0179	0.0147	0.0147	0.0218	0.0218	0.0115	0.0115
Portugal	0.0262	0.0262	0.0461	0.0461	0.0390	0.0390	0.0320	0.0320	0.0275	0.0275	0.0147	0.0147	0.0288	0.0288	0.0160	0.0160
Russia	0.0026	0.0147	0.0045	0.0250	0.0179	0.0179	0.0166	0.0166	0.0109	0.0147	0.0147	0.0147	0.0096	0.0141	0.0051	0.0070
Slovakia	0.0301	0.0301	0.0410	0.0410	0.0365	0.0365	0.0314	0.0314	0.0237	0.0237	0.0147	0.0147	0.0205	0.0205	0.0102	0.0102
South Africa	0.0083	0.0173	0.0141	0.0282	0.0250	0.0250	0.0237	0.0237	0.0147	0.0205	0.0147	0.0147	0.0134	0.0192	0.0070	0.0102
Spain	0.0224	0.0224	0.0422	0.0422	0.0320	0.0320	0.0294	0.0294	0.0250	0.0250	0.0147	0.0147	0.0211	0.0211	0.0109	0.0109
Sweden	0.0160	0.0160	0.0397	0.0390	0.0384	0.0384	0.0365	0.0365	0.0326	0.0326	0.0147	0.0147	0.0352	0.0352	0.0211	0.0211
Switzerland	0.0211	0.0211	0.0397	0.0397	0.0346	0.0346	0.0346	0.0346	0.0294	0.0294	0.0147	0.0147	0.0186	0.0186	0.0109	0.0109
Turkey	0.0262	0.0262	0.0326	0.0326	0.0467	0.0467	0.0390	0.0390	0.0314	0.0314	0.0147	0.0147	0.0326	0.0326	0.0179	0.0179
United Kingdom (UK)	0.0237	0.0237	0.0390	0.0390	0.0397	0.0397	0.0384	0.0384	0.0294	0.0294	0.0147	0.0147	0.0186	0.0186	0.0096	0.0096
United States	0.0211	0.0211	0.0211	0.0211	0.0179	0.0179	0.0179	0.0179	0.0102	0.0147	0.0147	0.0147	0.0179	0.0179	0.0102	0.0102

Figure 57 Country energy costs

Energy conversion factors		
Conversion factor	MJ/litre	MJ/kg
Oil	38	44
Diesel	38	44
Gasoline	35	45
Kerosene	35	43.8
LPG	26	42.5

County labor costs			
	Median Labour Cost GBP/h		Median Labour Cost GBP/h
World	3.53	Greece	0.03
Europe	0.02	Hungary	0.03
Former USSR	0.03	Iceland	0.03
North America	0.01	India	0.01
South America	0.02	Ireland	0.01
Asia	0.02	Italy	0.03
Oceania	0.02	Japan	0.03
Middle East	0.03	South Korea	0.03
Australia	0.02	Mexico	0.01
Austria	0.03	Netherlands	0.02
Belgium	0.03	New Zealand	0.02
Brazil	0.02	Norway	0.02
Canada	0.02	Poland	0.01
China	0.01	Portugal	0.02
Czech Republic	0.01	Russia	0.03
Denmark	0.03	Slovakia	0.00
Finland	0.02	South Africa	0.03
France	0.02	Spain	0.01
Germany	0.02	Sweden	0.02
United Kingdom (UK)	0.03	Switzerland	0.01
United States	0.03	Turkey	0.02

Available transport options and associated environmental		
	Transport energy (MJ/kg/m)	CO_2 footprint, source (kg/MJ)
Sea freight	3.00E-08	0.071
River / canal freight	4.00E-08	0.071
Rail freight	1.00E-08	0.071
32 tonne truck	3.00E-08	0.071
14 tonne truck	3.00E-08	0.071
Light goods vehicle	3.00E-08	0.071
Air freight - long haul	4.00E-08	0.067
Air freight - short haul	3.00E-08	0.067
Helicopter - Eurocopter AS 350	4.00E-08	0.067

Available joining and finishing processes and associated environmental burden				
	Process	Energy (MJ/unit)	CO_2/unit)	Unit
Joining	Adhesives, cold curing	9.9	1.9	m^2
	Adhesives, heat curing	27	4.7	m^2
	Fasteners, large	0.071	0.0052	-
	Fasteners, small	0.028	0.0021	-
	Welding, electric	2.4	0.17	m
	Welding, gas	1.7	0.091	m
	Construction	0.1	0.0075	kg
Finishing	Painting	12	0.98	m^2
	Electroplating	89	4.8	m^2
	Baked coating	21	1.1	m^2
	Powder coating	76	4.1	m^2

Overview of downcycling techniques	
Technique	Applicable Materials
Reprocessing	Metals
	Thermoplastic polymers & thermoplastic elastomers (TPEs)
Comminution	Ceramics, glasses, natural materials (organic & inorganic), thermoset plastics & elastomers
Metal recovery	Electrical components: Batteries, PCBs…

Value of recycled material and manufacturing scrap		
Generic material type	**Price of recycled material**	**Value of Production Scrap**
Metal (ferrous)	0.93	0.49
Metal (non-ferrous)	0.65	0.31
Metal (precious)	1	0.9
Metal (other)	0.65	0.31

Summary of end of life options

End of life option	Applicable materials
Landfill	All non-toxic materials
Combust (for energy recovery)	All organic-based materials with a heat of combustion value >5 MJ/kg
Downcycle	All
Recycle	All unfilled: metals / glasses / thermoplastics /TPEs
	Particulate filled thermoplastics
	Particulate & whisker reinforced metals
	(All ceramics / thermosets / elastomers / natural organic / natural inorganic materials and all fiber reinforced materials are marked as non-recyclable)
Re-manufacture	All
Reuse	All
None	All

Transport factors								
Factor	**Desctiption**	**Unit**	**Air freight**	**Ocean freight**	**Rail freight**	**Truck freight**	**River/canal freight**	**Helicopter**
CMD	**Critical Minimum Density**	kg/m3	167	20	20	267	20	200
SD	**Switch Distance**	m	0	0	1301810	0	0	0
T1	**Correction Factor**	%	70%	93%	100%	100%	93%	100%
T2	**Fixed Cost**	£/(kg*m)	6.4000E-06	2.5600E-05	6.6001E-01	6.6001E-01	6.3155E-01	6.3155E-01
T3	**Variable Cost**	£/(kg*m)	1.9200E-05	1.9200E-05	6.4022E-01	6.4022E-01	6.7338E-01	6.7338E-01

Summary of collection and sorting energies associated with each end of life option

	Collection Energy H_c (MJ/kg)	Primary Sorting Energy H_{ps} (MJ/kg)	Secondary Sorting Energy H_{ss} (MJ/kg)
Landfill	0.2	-	-
Combustion	0.2	0.3	-
Downcycle	0.2	0.3	-
Recycle	0.2	-	0.5
Re-engineer	0.2	-	-
Reuse	0.2	-	-
None	-	-	-

Energy conversion factors		
Process	**Energy carrier**	**Conversion factor**
		%
Adhesives, cold curing	Electricity cost - commercial	33%
Adhesives, heat curing	Electricity cost - commercial	33%
Construction	Electricity cost - commercial	33%
Fasteners, large	Electricity cost - commercial	33%
Fasteners, small	Electricity cost - commercial	33%
Welding, electric	Electricity cost - commercial	33%
Welding, gas	Oil Commercial	100%
Electro-plating	Electricity cost - commercial	33%
Baked coatings	Electricity cost - commercial	33%
Painting	Electricity cost - commercial	33%
Powder coating	Electricity cost - commercial	33%
Coarse machining	Electricity cost - commercial	33%
Fine machining	Electricity cost - commercial	33%
Grinding	Electricity cost - commercial	33%
Cutting and trimming	Electricity cost - commercial	33%
Non-conventional machining	Electricity cost - commercial	33%

Use phase: Mobile mode				
Fuel and vehicle type	**Energy**	**Energy equivalence,**	**CO2 footprint,**	**Cost, source (GBP/MJ)**
	(MJ/kg.m)	**source (MJ/MJ)**	**source (kg/MJ)**	
Diesel - ocean shipping	3.00E-08	1	0.071	Country specific
Diesel - coastal shipping	4.00E-08	1	0.071	
Diesel - rail	1.00E-08	1	0.071	
Diesel - heavy goods vehicle	3.00E-08	1	0.071	
Diesel - light goods vehicle	3.00E-08	1	0.071	
Diesel - family car	3.00E-08	1	0.071	
Electric - family car	4.00E-08	Country specific	Country specific	Country specific
Electric - rail	3.00E-08	Country specific	Country specific	
Gasoline - hybrid family car	4.00E-08	1	0.071	Country specific
Gasoline - family car	4.00E-08	1	0.071	
Gasoline - super sports and SUV	3.00E-08	1	0.071	
Kerosene - long haul aircraft	3.00E-08	1	0.067	Country specific
Kerosene - short haul aircraft	1.00E-08	1	0.067	
Kerosene - helicopter (Eurocopter AS 350)	1.00E-08	1	0.067	
LPG - family car	4.00E-08	1	0.058	Country specific

Country energy mix and associated environmental footprint							
Country	Data based on OECD** countries	Fossil fuel		Nuclear	Renewables	Energy equivalence (MJ/MJ)	CO_2 footprint (kg/MJ)
		Proportion *	Efficiency	Proportion *	Proportion*		
World	-	0.67	0.36	0.15	0.19	2.18	0.131
Europe	Yes	0.53	0.33	0.27	0.2	2.07	0.113
Former USSR	-	0.65	0.33	0.18	0.17	2.32	0.14
North America	Yes	0.66	0.33	0.18	0.16	2.34	0.141
Latin America	-	0.27	0.33	0.02	0.71	1.55	0.058
Asia	-	0.8	0.33	0.04	0.17	2.62	0.172
Pacific	Yes	0.65	0.33	0.25	0.1	2.32	0.14
Middle East	-	0.97	0.33	0	0.03	2.96	0.208
Australia		0.92	0.33	0	0.08	2.87	0.198
Austria		0.33	0.33	0	0.67	1.66	0.07
Belgium		0.39	0.33	0.54	0.06	1.8	0.084
Brazil		0.1	0.33	0.03	0.87	1.2	0.021
Canada		0.24	0.38	0.16	0.6	1.39	0.045
China		0.83	0.33	0.02	0.15	2.68	0.178
Czech Republic		0.64	0.32	0.31	0.05	2.36	0.142
Denmark		0.78	0.33	0	0.22	2.58	0.168
Finland		0.44	0.33	0.28	0.28	1.9	0.095
France		0.1	0.4	0.78	0.12	1.14	0.017
Germany		0.61	0.38	0.26	0.13	1.99	0.114
Greece		0.86	0.37	0	0.14	2.47	0.166
Hungary		0.58	0.33	0.38	0.05	2.18	0.125
Iceland		0	0.33	0	1	1	0
India		0.81	0.27	0.03	0.17	3.19	0.213
Ireland		0.9	0.33	0	0.1	2.82	0.193
Italy		0.81	0.45	0	0.19	1.99	0.128
Japan		0.61	0.43	0.28	0.11	1.81	0.101
Korea		0.62	0.39	0.37	0.01	1.97	0.112
Mexico		0.8	0.38	0.04	0.16	2.3	0.149
Netherlands		0.87	0.44	0.04	0.1	2.1	0.14
New Zealand		0.35	0.33	0	0.65	1.71	0.076
Norway		0.01	0.33	0	0.99	1.01	0.001
Poland		0.96	0.36	0	0.04	2.72	0.19
Portugal		0.66	0.33	0	0.34	2.35	0.143
Russia		0.66	0.32	0.16	0.18	2.41	0.147
Slovak Republic		0.27	0.33	0.57	0.16	1.54	0.057
South Africa		0.94	0.37	0.04	0.02	2.59	0.18
Spain		0.6	0.39	0.2	0.2	1.94	0.11
Sweden		0.03	0.33	0.47	0.5	1.06	0.006
Switzerland		0.02	0.33	0.43	0.55	1.03	0.003
Turkey		0.75	0.43	0	0.25	1.99	0.123
United Kingdom		0.75	0.43	0.19	0.06	1.99	0.124
United States		0.71	0.36	0.19	0.1	2.26	0.14

Appendix – I

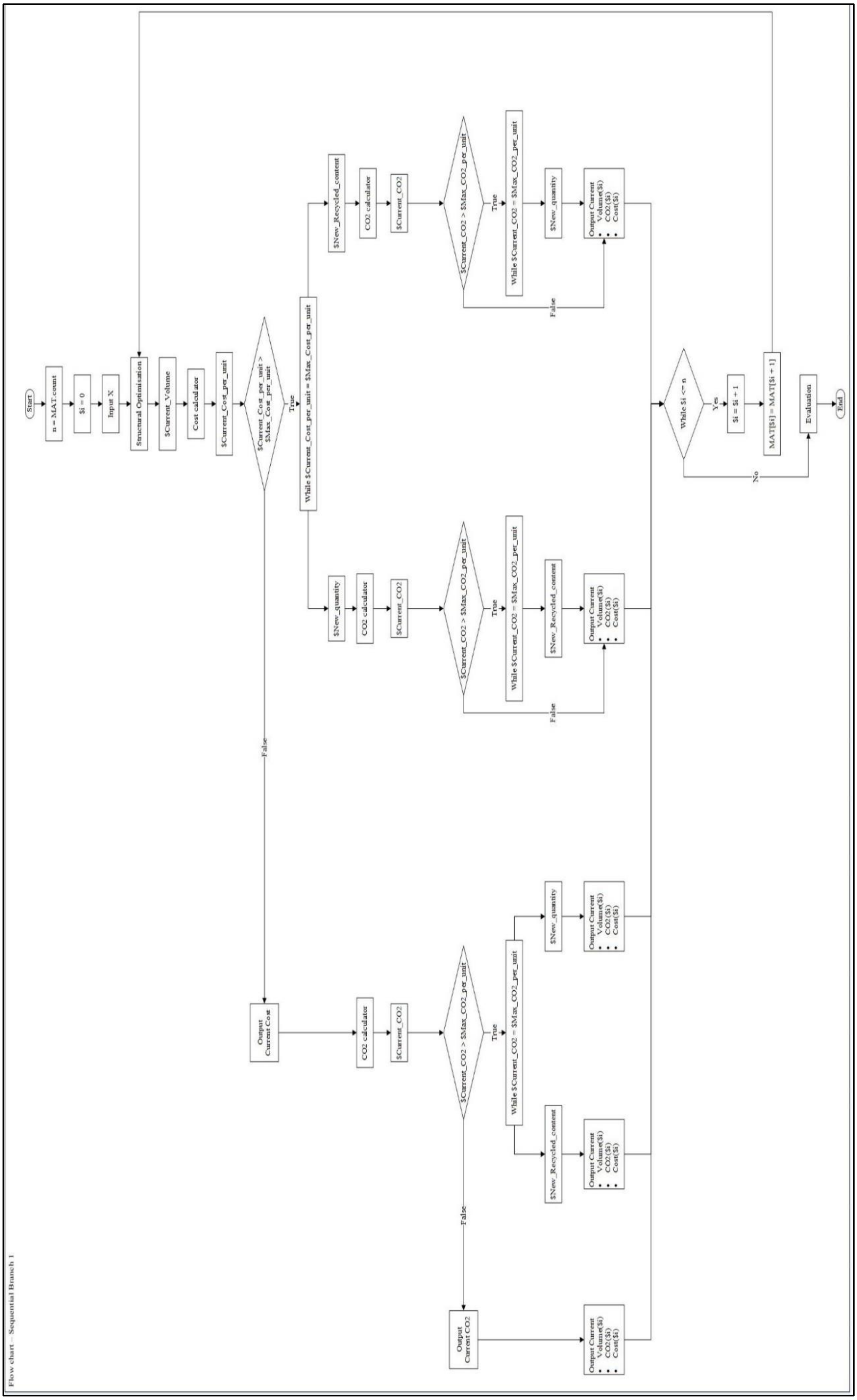

Figure 58: Example of holistic optimisation flowchart

Appendix – J

```
Pseudo Code

X = Initial Inputs
n = The maximum iteration number
    ($MAT.count)
$i = The current iteration number
$Min_thickness = The lower bound of thickness
Set $Max_CO2_per_unit
Set $Max_Cost_per_unit

•  Start
•  Set n
•  Set $i = 0
•  Input X
•  Call function of structural optimisation (FEA & Size_Opti)
•  Get the current $Volume
•  Call function of Cost calculator
•  Get the $Current_Cost_per_unit
•  If $Current_Cost_per_unit > $Max_Cost_per_unit
•        Two suggestions: $New_quantity and $New_Recycled_content
•
•        Route One: Calculate $New_quantity When $Current_Cost_per_unit = $Max_Cost_per_unit
•        Pass the current $MAT, $Volume and $New_quantity to the function of CO2
•        Calculate the $Current_CO2
•        If the $Current_CO2 > $Max_Cost_per_unit
•        Calculate the $New_Recycled_content when $Current_CO2 = $Max_CO2_per_unit
•        If the $Current_CO2 <= $Max_Cost_per_unit
•        Output the $Current_CO2
•        Output the current Volume($i), CO2($i) and Cost($i) of Route One (Per Unit)
•        End Route One
•
•        Route Two: Caculate $New_Recycled_content When $Current_Cost_per_unit = $Max_Cost_per_unit
•        Pass the current $MAT, $Volume and $New_Recycled_content to the function of CO2
•        Calculate the $Current_CO2
•        If the $Current_CO2 > $Max_CO2_per_unit
•        Calculate the $New_quantity when $Current_CO2 = $Max_CO2_per_unit
•        If the $Current_CO2 <= $Max_Cost_per_unit
•        Output the current Volume($i), CO2($i) and Cost($i) of Route Two (Per Unit)
•        End Route Two
•  If $Current_Cost_per_unit <= $Max_Cost_per_unit
•        Output the $Current_Cost_per_unit
•        Call function CO2 calculator
•        Calculate the $Current_CO2
•        If the $Current_CO2 > $Max_Cost_per_unit
•        Calculate the $New_quantity when $Current_CO2 = $Max_CO2_per_unit
•        Calculate the $New_Recycled_content when $Current_CO2 = $Max_CO2_per_unit
•        If the $Current_CO2 <= $Max_Cost_per_unit
•        Output the $Current_CO2
•        Output the current Volume($i), CO2($i) and Cost($i) of Route One (Per Unit)
•  While $i < n,
•  $i = $i + 1
•  MAT[$i] = MAT[$i + 1]
•  New iteration
•  If $i => n,
•  End While
•  Evaluation
•  End
```

Figure 59: Pseudo code for optimisation algorithm

Appendix – K

Method	Rank	CS No.	SEQ1-MII	CS No.	SEQ2-MII	CS No.	SEQ3-MII	CS No.	SEQ4-MII	CS No.	SEQ5-MII	CS No.	SEQ6-MII	CS No.	PAR-MII
OAT	**1**	6	150%	6	147%	6	179%	6	167%	6	167%	6	164%	6	167%
	2	7	118%	7	115%	7	147%	7	135%	7	135%	7	133%	7	135%
	3	3	116%	3	114%	3	143%	3	130%	3	133%	3	129%	3	133%
	4	8	112%	8	109%	8	141%	8	128%	8	129%	8	126%	8	129%
	5	2	105%	2	104%	2	135%	2	122%	2	123%	2	121%	2	123%
	6	4	105%	4	104%	4	135%	4	122%	4	123%	4	121%	4	123%
	7	5	105%	5	104%	5	135%	5	122%	5	123%	5	121%	5	123%
	8	1	87%	1	83%	1	126%	1	115%	1	106%	1	112%	1	106%
TAT	**1**	24	161%	24	158%	24	187%	24	175%	24	178%	24	172%	24	178%
	2	28	150%	31	147%	31	179%	31	167%	19	167%	31	164%	28	167%
	3	19	150%	19	147%	19	179%	19	167%	28	167%	19	164%	31	167%
	4	31	150%	28	147%	28	179%	28	167%	31	167%	28	164%	19	167%
	5	25	122%	25	120%	13	164%	13	155%	13	140%	13	150%	13	140%
	6	13	120%	13	115%	25	149%	25	137%	25	140%	25	135%	25	139%
	7	22	116%	22	114%	16	143%	16	130%	16	133%	23	129%	22	133%
	8	16	116%	16	114%	22	143%	22	130%	23	133%	16	129%	16	133%
	9	23	116%	23	114%	23	143%	23	130%	22	133%	22	129%	23	133%
	10	26	113%	26	111%	20	142%	20	129%	26	131%	20	126%	26	130%
	11	29	112%	20	109%	29	142%	29	129%	20	129%	29	126%	20	129%
	12	20	112%	29	109%	32	142%	32	129%	29	129%	32	126%	29	129%
	13	32	112%	32	109%	26	140%	26	128%	32	129%	26	125%	32	129%
	14	17	105%	18	104%	18	135%	27	122%	17	123%	18	121%	17	123%
	15	18	105%	27	104%	27	135%	18	122%	18	123%	27	121%	18	123%
	16	27	105%	17	104%	17	135%	17	122%	27	123%	17	121%	27	123%
	17	33	103%	21	100%	21	132%	10	120%	21	120%	21	117%	21	120%
	18	30	103%	30	100%	33	132%	30	120%	30	120%	30	117%	30	120%
	19	21	103%	33	100%	30	132%	21	120%	33	120%	33	117%	33	120%
	20	10	91%	10	86%	10	130%	33	120%	10	111%	10	116%	10	111%
	21	14	84%	14	79%	14	128%	14	118%	14	104%	14	114%	14	103%
	22	9	78%	12	73%	9	122%	9	112%	9	97%	9	108%	11	97%
	23	11	78%	9	72%	12	122%	11	112%	11	97%	11	108%	12	97%
	24	12	78%	11	72%	11	122%	12	112%	12	97%	12	108%	9	97%
	25	15	75%	15	70%	15	119%	15	110%	15	95%	15	105%	15	95%

Figure 60: Average COFV of each case study for the 7 OMS by ICE method – HOS2

Method	Rank	CS No.	SEQ1-MII	CS No.	SEQ2-MII	CS No.	SEQ3-MII	CS No.	SEQ4-MII	CS No.	SEQ5-MII	CS No.	SEQ6-MII	CS No.	PAR-MII
OAT	**1**	6	0.51	6	0.52	6	0.15	6	0.31	6	0.29	6	0.32	6	0.29
	2	7	0.71	7	0.73	7	0.53	7	0.57	7	0.59	7	0.61	7	0.59
	3	3	0.77	3	0.79	8	0.62	8	0.66	8	0.68	8	0.70	8	0.68
	4	8	0.78	8	0.81	3	0.69	3	0.70	3	0.71	3	0.72	3	0.71
	5	2	0.84	2	0.86	2	0.70	2	0.74	2	0.74	2	0.75	4	0.75
	6	4	0.84	4	0.86	4	0.70	4	0.74	4	0.74	4	0.75	5	0.75
	7	5	0.84	5	0.86	5	0.70	5	0.74	5	0.74	5	0.75	2	0.75
	8	1	1.05	1	1.09	1	0.79	1	0.82	1	0.90	1	0.86	1	0.91
TAT	**1**	24	0.39	24	0.39	24	0.08	24	0.22	24	0.17	24	0.23	24	0.17
	2	28	0.51	19	0.52	19	0.15	19	0.31	19	0.29	19	0.32	28	0.29
	3	19	0.51	28	0.52	28	0.15	28	0.31	28	0.29	28	0.32	19	0.29
	4	31	0.51	31	0.52	31	0.15	31	0.31	31	0.29	31	0.32	31	0.29
	5	25	0.69	25	0.71	13	0.40	13	0.52	25	0.61	13	0.53	25	0.62
	6	29	0.76	16	0.79	25	0.59	25	0.61	13	0.65	25	0.64	13	0.65
	7	20	0.76	23	0.79	20	0.61	20	0.65	29	0.66	20	0.68	20	0.66
	8	32	0.76	22	0.79	29	0.61	29	0.65	20	0.66	29	0.68	29	0.66
	9	22	0.77	32	0.80	32	0.61	32	0.65	32	0.66	32	0.68	32	0.66
	10	16	0.77	20	0.80	16	0.69	23	0.70	22	0.71	22	0.72	22	0.71
	11	23	0.77	29	0.80	22	0.69	16	0.70	23	0.71	16	0.72	16	0.71
	12	26	0.80	26	0.83	23	0.69	22	0.70	16	0.71	23	0.72	23	0.71
	13	17	0.84	18	0.86	17	0.70	26	0.73	26	0.74	17	0.75	26	0.75
	14	18	0.84	27	0.86	18	0.70	17	0.74	18	0.74	18	0.75	17	0.75
	15	27	0.84	17	0.86	27	0.70	18	0.74	27	0.74	27	0.75	18	0.75
	16	33	0.87	21	0.90	26	0.72	27	0.74	17	0.74	26	0.77	27	0.75
	17	30	0.87	30	0.90	21	0.75	33	0.77	21	0.79	21	0.80	21	0.79
	18	21	0.87	33	0.90	30	0.75	21	0.77	30	0.79	30	0.80	30	0.79
	19	13	0.95	13	0.95	33	0.75	30	0.77	33	0.79	33	0.80	33	0.79
	20	10	1.03	10	1.08	14	0.76	14	0.79	10	0.89	14	0.84	10	0.89
	21	14	1.12	14	1.16	10	0.81	10	0.81	14	0.92	10	0.86	14	0.92
	22	11	1.16	12	1.21	11	0.84	11	0.86	11	0.98	11	0.91	12	0.99
	23	12	1.16	11	1.21	12	0.84	12	0.86	12	0.98	12	0.91	11	0.99
	24	9	1.16	9	1.21	9	0.84	9	0.86	9	0.98	9	0.91	9	0.99
	25	15	1.20	15	1.24	15	0.88	15	0.89	15	1.02	15	0.95	15	1.02

Figure 61: Average COFV of each case study for the 7 OMS by ABC method – HOS2

Method	Rank	CS No.	SEQ1-MIII	CS No.	SEQ2-MIII	CS No.	SEQ3-MIII	CS No.	SEQ4-MIII	CS No.	SEQ5-MIII	CS No.	SEQ6-MIII	CS No.	PAR-MIII
OAT	**1**	6	1.39	6	1.36	6	1.52	6	1.46	6	1.45	6	1.43	6	1.45
	2	7	1.16	3	1.15	3	1.34	7	1.25	3	1.27	3	1.24	3	1.27
	3	3	1.15	7	1.15	7	1.33	3	1.24	7	1.25	7	1.23	7	1.25
	4	8	1.15	8	1.14	8	1.32	8	1.23	8	1.24	8	1.22	8	1.24
	5	2	1.10	2	1.10	2	1.28	2	1.19	2	1.20	2	1.19	2	1.20
	6	4	1.10	4	1.10	4	1.28	4	1.19	4	1.20	4	1.19	4	1.20
	7	5	1.10	5	1.10	5	1.28	5	1.19	5	1.20	5	1.19	5	1.20
	8	1	0.88	1	0.86	1	1.20	1	1.08	1	1.01	1	1.07	1	1.01
TAT	**1**	24	1.43	24	1.41	24	1.56	24	1.50	24	1.51	24	1.48	24	1.51
	2	28	1.39	28	1.36	19	1.52	19	1.46	19	1.45	31	1.43	28	1.45
	3	19	1.39	19	1.36	28	1.52	31	1.46	28	1.45	19	1.43	19	1.45
	4	31	1.39	31	1.36	31	1.52	28	1.46	31	1.45	28	1.43	31	1.45
	5	25	1.18	25	1.17	13	1.38	13	1.30	25	1.29	13	1.26	25	1.29
	6	26	1.16	26	1.16	25	1.35	25	1.26	26	1.28	25	1.25	26	1.28
	7	22	1.15	16	1.15	26	1.34	26	1.25	16	1.27	26	1.24	16	1.27
	8	16	1.15	22	1.15	16	1.34	23	1.24	22	1.27	23	1.24	23	1.27
	9	23	1.15	23	1.15	22	1.34	16	1.24	23	1.27	16	1.24	22	1.27
	10	29	1.13	20	1.12	23	1.34	22	1.24	20	1.22	22	1.24	20	1.22
	11	20	1.13	29	1.12	20	1.30	20	1.21	29	1.22	20	1.20	29	1.22
	12	32	1.13	32	1.12	29	1.30	29	1.21	32	1.22	29	1.20	32	1.22
	13	13	1.12	21	1.11	32	1.30	32	1.21	21	1.21	32	1.20	21	1.21
	14	33	1.11	30	1.11	21	1.29	21	1.20	30	1.21	21	1.19	30	1.21
	15	30	1.11	33	1.11	33	1.29	30	1.20	33	1.21	30	1.19	33	1.21
	16	21	1.11	17	1.10	30	1.29	33	1.20	17	1.20	33	1.19	27	1.20
	17	17	1.10	18	1.10	17	1.28	17	1.19	18	1.20	17	1.19	18	1.20
	18	18	1.10	27	1.10	18	1.28	18	1.19	27	1.20	18	1.19	17	1.20
	19	27	1.10	13	1.06	27	1.28	27	1.19	13	1.19	27	1.19	13	1.18
	20	10	0.81	10	0.80	10	1.19	10	1.05	10	0.99	10	1.04	10	0.99
	21	14	0.79	14	0.77	14	1.17	14	1.04	14	0.93	14	1.02	14	0.93
	22	15	0.77	15	0.76	15	1.16	15	1.03	15	0.92	15	1.02	15	0.92
	23	11	0.77	11	0.75	12	1.15	12	1.02	12	0.91	12	1.01	12	0.91
	24	9	0.76	9	0.74	9	1.15	9	1.02	9	0.91	9	1.01	9	0.91
	25	12	0.76	12	0.74	11	1.10	11	0.97	11	0.88	11	0.97	11	0.88

Figure 62: Average COFV of each case study for the 7 OMS by INC method – HOS2